OSU/NREL REPORT 99-01

TECHNICAL AND USER'S MANUAL FOR THE
FAST_AD ADVANCED DYNAMICS CODE

Two-Bladed Tilting and Teetering Hub Version
Three-Blade Rigid Hub Version

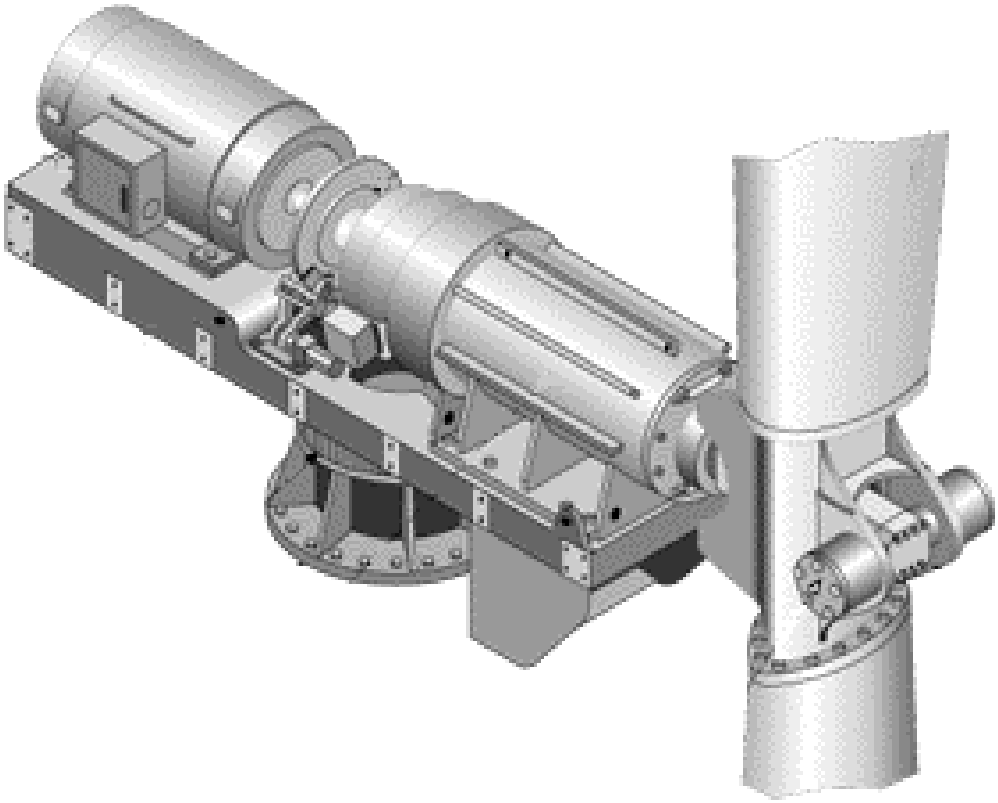

Prepared by

R.E. Wilson, S.N. Walker, and P. Heh

OREGON STATE UNIVERSITY
Department of Mechanical Engineering
Oregon State University
Corvallis, Oregon 97331-6001

May 1999

Prepared under NREL subcontract number XCX-6-1674-01

NOTICE

This report was prepared as an account of work sponsored by the National Renewable Energy Laboratory, a Division of Midwest Research Institute, in support of its Contract No. DE-AC02-83-CH10093 with the United States Department of Energy. Neither the National Renewable Energy Laboratory, the United States Government, nor the United States Department of Energy, nor any of their employees, no any of their contractors, subcontractors, or their employees, makes any warranty, express or implied, or assumes any legal liability or responsibility for the accuracy, completeness or usefulness of any information, apparatus, product or process disclosed, or represents that its use would not infringe privately owned rights.

TABLE OF CONTENTS

NOTICE i

TABLE OF CONTENTS ii

LIST OF FIGURES iv

LIST OF TABLES vi

1.0 FORWARD 1

2.0 KINETICS / KINEMATICS FOR A TWO-BLADED HAWT 2
- 2.1 Theory 3
- 2.2 Mechanical Elements 3
- 2.3 Geometry and Coordinate Systems 4
- 2.4 Blade and Tower Deflections 14
- 2.5 Kinematics 18
- 2.6 Kinetics 23
- 2.7 Generalized Active Forces 27
  - 2.7.1 Aerodynamic Loading 27
  - 2.7.2 Elastic Restoring Forces 29
  - 2.7.3 Drive Train Loading 30
- 2.8 Wind Model 35
- 2.9 Numerical Solution Technique 38
- 2.10 References 40

3.0 CONFIGURATION/NOMENCLATURE USED FOR A THREE-BLADED HAWT . 41
- 3.1 Overview 41

4.0 AeroDyn AERODYNAMICS 43
- 4.1 Theory 43
- 4.2 Kinematics 49
- 4.3 Yaw and Tilt 50
- 4.4 Dynamic Stall 51
- 4.5 References for AeroDyn 52

5.0 PROGRAM INPUT FILES 53

6.0 DESCRIPTION OF CODE INPUTS 55
- 6.1 General Inputs 55

6.2 Degree of Freedom Switches 57

6.3 Initial Conditions 59
6.4 Machine Parameters 60
6.5 Mass and Inertia 61
6.6 Drive Train Parameters 62
6.7 Tower Parameters 63
6.8 Tower Distributed Parameters 64
6.9 Tilt, Yaw and Teeter Parameters 65
6.10 Blade Parameters 67
6.11 Blade Sectional Data 68
6.12 Mode Shapes 69
6.13 Format of Output File 70
6.14 YawDyn/AeroDyn Parameter Input 71
6.15 Possible Output Quantities 75
6.16 References 77

7.0 PROGRAM OUTPUT FILES 78

8.0 EXAMPLE CASE STUDIES 80

9.0 CALCULATED OPERATIONS OF THE AWT-27 USING FAST_AD; 84
9.1 Introduction 84
9.2 FAST_AD Code 84
9.3 Modeling the AWT-27 88
9.4 Simulation of Inflow 97
9.5 Results 105
9.6 Discussion 155
9.7 Acknowledgments 161
9.8 References 162

APPENDIX A: CASE STUDY SAMPLE INPUT FILES 163
A.1 Steady Wind 163
A.2 Turbulent Wind 169
A.3 3D Turbulence Input Data File 170
A.4 user2.inp Automatic Input File 172
A.5 Sample Airfoil Data File 173

APPENDIX B: OUTPUT FILES 175
B.1 awt.sum 175
B.2 awt.out 178

B.3 gfosub.opt 179

APPENDIX C: MODE SHAPES 182

LIST OF FIGURES

Figure 2.1. Coordinate System Formed by Unit Vector Sets without tilt. 6
Figure 2.2. Tower Bending and Location of Tower Top 10
Figure 2.3. Orientation of Delta-3 Angle 10
Figure 2.4. Orientation of Local Blade Structural Twist Angle 11
Figure 2.5. Orientation of Blade Flapwise and Edgewise Bending Angles 12
Figure 2.6. Blade Bending in Flapwise Direction 13
Figure 2.7. Variation of Shaft Speed with Torque 31
Figure 2.8. Turbine Drive Train as Modeled in FAST_AD 33
Figure 2.9. Tower Shadow 36
Figure 2.10. Wind Shear 39
Figure 2.11. Variable Wind Angle (Top View of Turbine) 39
Figure 4.1. Rotor Geometry and Coordinates, for a Yawing, Non-Tilting Rotor 44
Figure 4.2. Velocity Diagram for a Blade element with Coning 46
Figure 4.3. Ideal Thrust Coefficient vs. Axial Induction.. 48
Figure 9.1. Lift Coefficient, CL versus attack angle. 93
Figure 9.2. Drag Coefficient, CD versus attack angle. 94
Figure 9.3. Thrust Coefficient, Ct versus attack angle. 95
Figure 9.4. Power Curve Comparison between FAST_AD and Field Data. 96
Figure 9.5. PSD and Histogram of Windspeed in u Component (Blade 1). 99
Figure 9.6. PSD and Histogram of Windspeed in v Component (Blade 1). 100
Figure 9.7. PSD and Histogram of Windspeed in w Component (Blade 1). 101
Figure 9.8. PSD and Histogram of Windspeed in u Component (Blade 2). 102
Figure 9.9. PSD and Histogram of Windspeed in v Component (Blade 2). 103
Figure 9.10. PSD and Histogram of Windspeed in w Component (Blade 2). 104
Figure 9.11. Rainflow Count of Blade Root Edgewise Bending Moment (low turb). 108
Figure 9.12. Rainflow Count of Blade Root Edgewise Bending Moment (med turb). 109
Figure 9.13. Rainflow Count of Blade Root Edgewise Bending Moment (high turb). 110
Figure 9.14. Rainflow Count of Blade Root Flapwise Bending Moment (low turb). 111
Figure 9.15. Rainflow Count of Blade Root Flapwise Bending Moment (med turb). 112
Figure 9.16. Rainflow Count of Blade Root Flapwise Bending Moment (high turb). 113
Figure 9.17. Rainflow Count of Shaft Torque (low turbulence). 114
Figure 9.18. Rainflow Count of Shaft Torque (medium turbulence). 115
Figure 9.19. Rainflow Count of Shaft Torque (high turbulence). 116
Figure 9.20. Rainflow Count of Teeter Angle (low turbulence). 117
Figure 9.21. Rainflow Count of Teeter Angle (medium turbulence). 118
Figure 9.22. Rainflow Count of Teeter Angle (high turbulence). 119
Figure 9.23. Rainflow Count of Yaw Angle (low turbulence). 120
Figure 9.24. Rainflow Count of Yaw Angle (medium turbulence). 121

Figure 9.25. Rainflow Count of Yaw Angle (high turbulence). 122
Figure 9.26. Rainflow Count of Blade Root Edgewise Bending Moment (low turb). 124
Figure 9.27. Rainflow Count of Blade Root Edgewise Bending Moment (med turb) 125
Figure 9.28. Rainflow Count of Blade Root Edgewise Bending Moment (high turb) 126
Figure 9.29. Rainflow Count of Blade Root Flapwise Bending Moment (low turb). 127
Figure 9.30. Rainflow Count of Blade Root Flapwise Bending Moment (med turb) 128
Figure 9.31. Rainflow Count of Blade Root Flapwise Bending Moment (high turb). 129
Figure 9.32. Rainflow Count of Shaft Torque (low turbulence). 130
Figure 9.33. Rainflow Count of Shaft Torque (medium turbulence). 131
Figure 9.34. Rainflow Count of Shaft Torque (high turbulence). 132
Figure 9.35. Rainflow Count of Teeter Angle (low turbulence). 133
Figure 9.36. Rainflow Count of Teeter Angle (medium turbulence). 134
Figure 9.37. Rainflow Count of Teeter Angle (high turbulence). 135
Figure 9.38. Rainflow Count of Yaw Angle (low turbulence). 136
Figure 9.39. Rainflow Count of Yaw Angle (medium turbulence). 137
Figure 9.40. Rainflow Count of Yaw Angle (high turbulence). 138
Figure 9.41. Rainflow Count of Blade Root Edgewise Bending Moment (low turb). 140
Figure 9.42. Rainflow Count of Blade Root Edgewise Bending Moment (med turb). 141
Figure 9.43. Rainflow Count of Blade Root Edgewise Bending Moment (high turb). 142
Figure 9.44. Rainflow Count of Blade Root Flapwise Bending Moment (low turb). 143
Figure 9.45. Rainflow Count of Blade Root Flapwise Bending Moment (med turb). 144
Figure 9.46. Rainflow Count of Blade Root Flapwise Bending Moment (high turb). 145
Figure 9.47. Rainflow Count of Shaft Torque (low turbulence). 146
Figure 9.48. Rainflow Count of Shaft Torque (medium turbulence). 147
Figure 9.49. Rainflow Count of Shaft Torque (high turbulence). 148
Figure 9.50. Rainflow Count of Teeter Angle (low turbulence). 149
Figure 9.51. Rainflow Count of Teeter Angle (medium turbulence). 150
Figure 9.52. Rainflow Count of Teeter Angle (high turbulence). 151
Figure 9.53. Rainflow Count of Yaw Angle (low turbulence). 152
Figure 9.54. Rainflow Count of Yaw Angle (medium turbulence). 153
Figure 9.55. Rainflow Count of Yaw Angle (high turbulence). 154
Figure 9.56. Rotor RPM and Shaft Torque during Start-up at 12.5 m/s Wind Speed. 157
Figure 9.57. Rotor RPM and Shaft Torque during Start-up at 18 m/s Wind Speed. 158
Figure 9.58. Rotor RPM and Shaft Torque during Fast Stop at 12.5 m/s Wind Speed. 160

LIST OF TABLES

Table 2.1. Coordinate System Locations 4
Table 2.2. Time Varying Angles and Displacements 8
Table 2.3. Other Angles Used in Program 9
Table 2.4. Position Vectors Used in Program 9
Table 3-1 Comparison between Two and Three Bladed Models 41
Table 7.1. Output Variables for “.OUT” File 79
Table 8.1. Turbine Specifications 80
Table 8.2. Blade Parameters 81
Table 8.3. Tower Parameters 81
Table 8.4. Line-by-Line Description of Automatic Input File 83
Table 9.1. FAST_AD Degrees of Freedom, 2 Blade Option 85
Table 9.2. AWT-27 Turbine Specifications 88
Table 9.3. AWT-27 Drive Train 90
Table 9.4. Angle-of-Attack Range of Zero Torque Contribution 91
Table C.1. Input File modes.inp 182
Table C.2. Output File MODES 184

1.0 FORWARD

The FAST_AD Code is the result of the marriage of three distinct codes; the FAST2 Code for two-bladed horizontal axis wind turbines (HAWT); FAST3 code for three-bladed HAWT; and the AeroDyn aerodynamics subroutines for HAWT. While combining these three codes, changes were made in the computational loops and in the kinematic calculations of the FAST codes. These changes resulted in a code, FAST_AD, that runs very quickly, so that the code is indeed, ***fast***. This document covers the features of each code and outlines the operating procedure for the code.

Section two deals with the kinetics and kinematics for a two-bladed HAWT. Section three addresses the configuration and nomenclature for the three-bladed HAWT operation. In section four, the AeroDyn aerodynamics as used in FAST_AD is described. Sections five, six, seven, and eight describe the program input files, description of code inputs, program output files and example case studies respectively. In section nine, comparisons of the simulation results for two case studies; one with steady wind conditions and the other with turbulent wind conditions are shown.

2.0 KINETICS / KINEMATICS FOR A TWO-BLADED HAWT

The dynamic response of a two-bladed, horizontal axis wind turbine can be modeled by the FAST_AD code. This model relates six rigid bodies (earth, nacelle, base plate, armature, hub, and gears) and four flexible bodies (tower, two blades, and drive shaft) through 15 degrees of freedom. Accounted for in the degrees of freedom are tower flexibility (4 DOF), blade teetering (1 DOF), blade flexibility (6 DOF), nacelle yaw (1 DOF), nacelle tilt (1 DOF), and variable generator speed (2 DOF). The degrees of freedom are further described below.

The first and second degrees of freedom arise from the first mode flapwise bending motion of each blade. The third and fourth degrees of freedom originate from the second bending mode. Blade edgewise motion accounts for the fifth and sixth degrees of freedom. Motion of the blades is along the local principal axes.

The seventh degree of freedom accounts for teeter motion of the blades about a pin located on the hub. Teeter motion can be restricted by dampers or springs, or a combination of both.

The eighth degree of freedom accounts for variations in rotor speed. This degree of freedom can model a motor for start-up, a brake for shut-down, or an induction generator. The ninth degree of freedom accounts for the optional drive train flexibility associated with torsional loading between the generator and hub.

The tenth degree of freedom accounts for the nacelle yaw motion, which can be free or fixed with a torsional yaw spring. A yaw tracking control can be implemented with the fixed yaw version. The rotor can be either upwind or downwind with the rotor providing yaw loads. Tower and nacelle aerodynamic loads are not included.

The eleventh and twelfth degrees of freedom originate from the first bending mode of the tower in the longitudinal and transverse directions. The thirteenth and fourteenth degrees model the second bending mode in the same directions. The fifteenth degree of freedom (the most recent addition) is nacelle tilt. The amount of tilt can be restricted with springs or dampers or a combination of both.

2.1 Theory

Kane's method is used to set up equations of motion that can be solved by numerical integration. This method greatly simplifies the equations before they are ever written by considering components of the equations where many terms do not show up. These equations are easier to solve than those developed using methods of Newton or Lagrange and have fewer terms, reducing computation time.

The following sections cover the steps that lead to the equations of motion. First, the various rigid bodies in the system are defined, as well as the coordinate systems used to relate them. These are used to formulate expressions for velocity, and then acceleration. Next, aerodynamic, elastic, and drive train loading are described along with the wind model. Finally, the method of solution is outlined.

2.2 Mechanical Elements

FAST_AD models a horizontal axis wind turbine with six rigid and three flexible bodies. The earth is rigidly attached to a flexible tower which can bend in two directions, described by two modes in each direction. The top of the tower is fixed to a base plate, which supports a yaw bearing and nacelle. The yaw bearing allows everything atop the tower to rotate as the wind direction changes. The nacelle houses the generator and gearbox, and the entire assembly can be allowed to tilt. The low speed shaft connects the gearbox to the rotor. The rotor consists of a hub, one or more blades, and possibly tip brakes. A teeter hinge may be included between the rotor and the low speed shaft, and can be offset by a delta-3 angle. The hub supports two blades, each of which can be coned and can have aerodynamic pitch and twist. The blades are flexible and have properties that can vary along their length. Each blade can be structurally pre-twisted, but no torsional freedom is allowed. Bending can occur in the plane of the rotor (defined by one vibration mode), or out of the rotor plane (defined by two modes of vibration).

2.3 Geometry and Coordinate Systems

Coordinate systems formed by orthogonal sets of unit vectors define reference frames that are each fixed to a rigid body. Each system represents a change in angular orientation from the previous system. These coordinate systems, along with the bodies they are fixed to, are listed in Table 2.1 and illustrated in Figure 2.1. (A body is denoted by a script uppercase character, a point is denoted by a normal uppercase character, and a vector is represented by a bold character.)

Table 2.1. Coordinate System Locations

Unit Vector Set	Fixed in Body	Description of Coordinate System
a	E	Inertial coordinates, fixed to earth
b	B	Tower top coordinates, system, fixed to base plate
d	N	Yaw coordinates, fixed to nacelle
c	N	Tilt coordinates, fixed to nacelle
e	H	Azimuth coordinates, fixed to low speed shaft
g	R	Delta-3 coordinates, fixed to rotor assembly
f	R	Teeter coordinates, fixed to rotor assembly
i	R	Coning coordinates, fixed to rotor assembly
j	S	Local blade coordinates, fixed to local blade element

Once a complete set of coordinate systems have been defined, expressions can be translated to any system by coordinate transformations. The coordinate systems listed in Table 2.1 and shown in Figure 2.1 establish several reference frames which can be related by the following transformations. Most of the transformation matrices represent a rigid body rotation about one of the local coordinate axes. For example, the difference in orientation between coordinates **e** and **g** is the delta-3 angle. The transformation from inertial (**a**) to tower top (**b**) coordinates contains rotations in two directions, representing the total tower top rotation. Note that the coordinate systems are basically in alphabetical order, except that **d** and **c** and **g** and **f** are out of order, and there is no **h**.

From Inertial to Tower Top:

$$\begin{bmatrix} \mathbf{a}_1 \\ \mathbf{a}_2 \\ \mathbf{a}_3 \end{bmatrix} = \begin{bmatrix} c\theta_7 & -s\theta_7 & 0 \\ s\theta_7 c\theta_8 & c\theta_7 c\theta_8 & -s\theta_8 \\ s\theta_7 s\theta_8 & c\theta_7 s\theta_8 & c\theta_8 \end{bmatrix} \begin{bmatrix} \mathbf{b}_1 \\ \mathbf{b}_2 \\ \mathbf{b}_3 \end{bmatrix}$$

where:

c = cosine of angle

s = sine of angle

θ_7 = longitudinal angle of tower top slope

θ_8 = lateral angle of tower top slope

From Tower Top to Yaw:

$$\begin{bmatrix} \mathbf{b}_1 \\ \mathbf{b}_2 \\ \mathbf{b}_3 \end{bmatrix} = \begin{bmatrix} cq_6 & 0 & sq_6 \\ 0 & 1 & 0 \\ -sq_6 & 0 & cq_6 \end{bmatrix} \begin{bmatrix} \mathbf{d}_1 \\ \mathbf{d}_2 \\ \mathbf{d}_3 \end{bmatrix}$$

where q_6 = yaw angle

From Yaw to Tilt:

$$\begin{bmatrix} \mathbf{d}_1 \\ \mathbf{d}_2 \\ \mathbf{d}_3 \end{bmatrix} = \begin{bmatrix} cq_5 & -sq_5 & 0 \\ sq_5 & cq_5 & 0 \\ 0 & 0 & 1 \end{bmatrix} \begin{bmatrix} \mathbf{c}_1 \\ \mathbf{c}_2 \\ \mathbf{c}_3 \end{bmatrix}$$

where q_5 = tilt angle of shaft

From Tilt to Azimuth:

$$\begin{bmatrix} \mathbf{c}_1 \\ \mathbf{c}_2 \\ \mathbf{c}_3 \end{bmatrix} = \begin{bmatrix} 1 & 0 & 0 \\ 0 & cq_4 & -sq_4 \\ 0 & sq_4 & cq_4 \end{bmatrix} \begin{bmatrix} \mathbf{e}_1 \\ \mathbf{e}_2 \\ \mathbf{e}_3 \end{bmatrix}$$

where q_4 = azimuth angle

Figure 2.1. Coordinate System Formed by Unit Vector Sets without tilt.

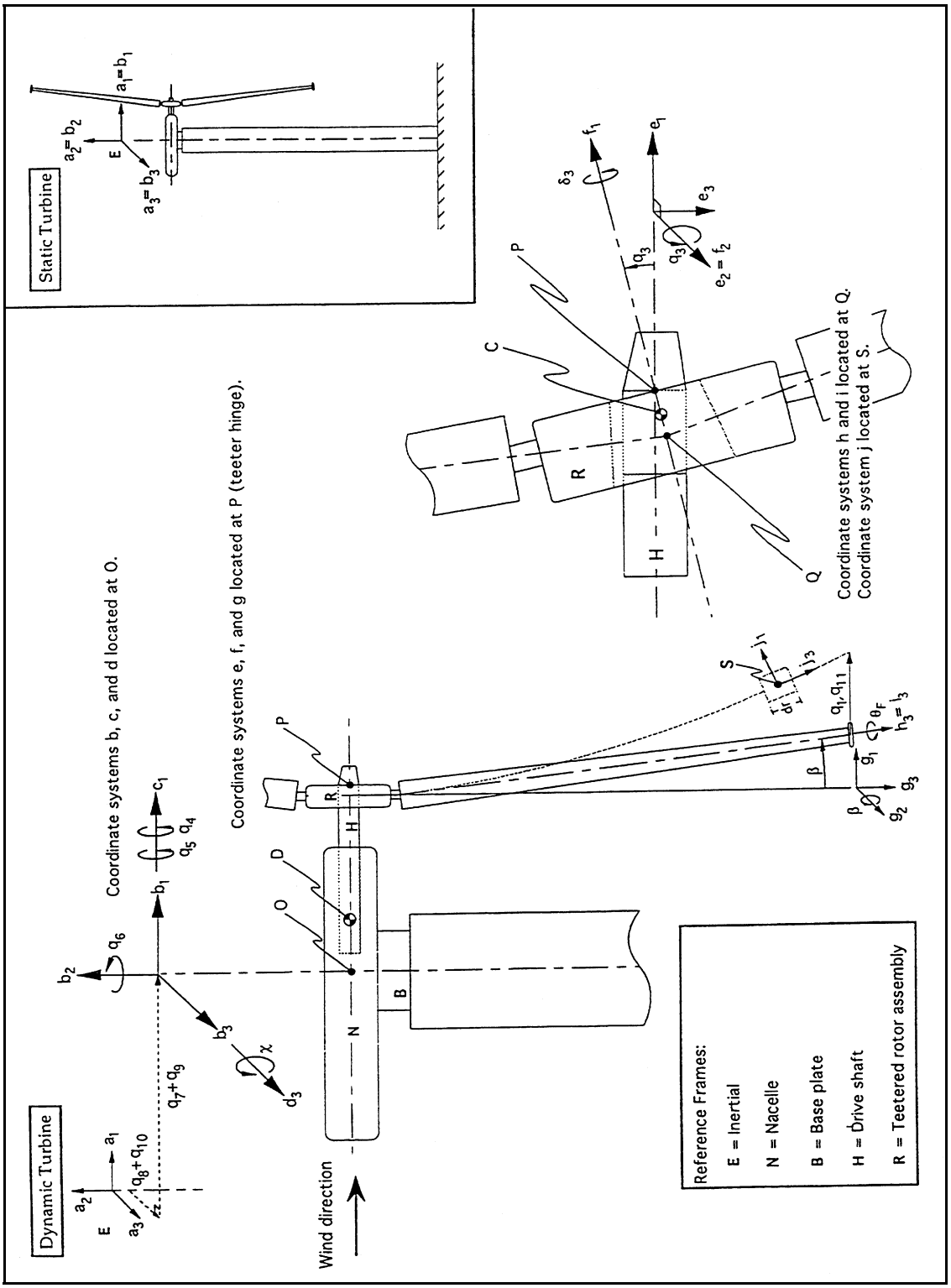

From Azimuth to Delta-3: $$\begin{bmatrix} \mathbf{e}_1 \\ \mathbf{e}_2 \\ \mathbf{e}_3 \end{bmatrix} = \begin{bmatrix} 1 & 0 & 0 \\ 0 & c\delta_3 & -s\delta_3 \\ 0 & s\delta_3 & c\delta_3 \end{bmatrix} \begin{bmatrix} \mathbf{g}_1 \\ \mathbf{g}_2 \\ \mathbf{g}_3 \end{bmatrix}$$ where δ_3 = delta-3 angle

From Delta-3 to Teeter: $$\begin{bmatrix} \mathbf{g}_1 \\ \mathbf{g}_2 \\ \mathbf{g}_3 \end{bmatrix} = \begin{bmatrix} cq_3 & 0 & sq_3 \\ 0 & 1 & 0 \\ -sq_3 & 0 & cq_3 \end{bmatrix} \begin{bmatrix} \mathbf{f}_1 \\ \mathbf{f}_2 \\ \mathbf{f}_3 \end{bmatrix}$$ where q_3 = teeter angle

From Teeter to Coning: $$\begin{bmatrix} \mathbf{f}_1 \\ \mathbf{f}_2 \\ \mathbf{f}_3 \end{bmatrix} = \begin{bmatrix} c\beta & 0 & s\beta \\ 0 & 1 & 0 \\ -s\beta & 0 & c\beta \end{bmatrix} \begin{bmatrix} \mathbf{i}_1 \\ \mathbf{i}_2 \\ \mathbf{i}_3 \end{bmatrix}$$ where β = coning angle

From Elastic to Local:

$$\begin{bmatrix} \mathbf{i}_1 \\ \mathbf{i}_2 \\ \mathbf{i}_3 \end{bmatrix} = \left[\begin{pmatrix} c\xi & 0 & s\xi \\ 0 & 1 & 0 \\ -s\xi & 0 & c\xi \end{pmatrix} \cdot \begin{pmatrix} 1 & 0 & 0 \\ 0 & c\eta & s\eta \\ 0 & -s\eta & c\eta \end{pmatrix} \right] \begin{bmatrix} \mathbf{j}_1 \\ \mathbf{j}_2 \\ \mathbf{j}_3 \end{bmatrix}$$

where ξ = local out-of-plane blade bending angle, and

η = local in-plane bending angle

Of the angles shown in the previous transformations, some are time-varying degrees of freedom and some are fixed over time. There are 15 degrees of freedom for the two-bladed machine which are used in formulating the equations of motion. Table 2.2 lists all 15 variables and a description of each. These variables are used to describe all of the motion that the wind turbine model exhibits.

Table 2.2. Time Varying Angles and Displacements

Variable	Description
q_1	Blade 1 flapwise tip displacement for mode 1
q_2	Blade 2 flapwise tip displacement for mode 1
q_3	Teeter angle
q_4	Azimuth angle, rotor side
q_5	Tilt angle
q_6	Yaw angle
q_7	Longitudinal tower top displacement for mode 1
q_8	Latitudinal tower top displacement for mode 1
q_9	Longitudinal tower top displacement for mode 2
q_{10}	Latitudinal tower top displacement for mode 2
q_{11}	Blade 1 flapwise tip displacement for mode 2
q_{12}	Blade 2 flapwise tip displacement for mode 2
q_{13}	Blade 1 edgewise tip displacement for mode 1
q_{14}	Blade 2 edgewise tip displacement for mode 1
q_{15}	Azimuth angle, generator site

Blade 1 is at an azimuth angle of q_4 and a teeter angle of q_3. In order to locate blade 2, an azimuth angle of $q_4 + \pi$ is used. However, rotating the azimuth angle also rotates the teeter axis, so in order to have the teeter remain in the proper orientation, the opposite sign is used.

Other important angles used in the above transformations are listed in Table 2.3. The tower top rotations are time varying since they are related to the tower freedom through the shape of the deflected tower, as shown in Figure 2.2. The delta-3 angle, shown in Figure 2.3, orients the teeter hinge so that teeter is no longer perpendicular to the unconed blade axis. Blades can be coned, or angled downwind slightly, as indicated by the coning angle, β. The previous three angles are all used to define the geometry of the wind turbine and are constant. The blade structural pre-twist is represented by θ_s and orients the

local axes of flapwise and edgewise bending. The out-of-plane rotation of the local blade element is ξ, while the in-plane blade element rotation is η. The previous three angles vary along the blade so that each blade segment has a different orientation. These are shown in Figures 2.4, 2.5, and 2.6.

Table 2.3. Other Angles Used in Program

Angle	Description
θ_7	Longitudinal tower top rotation angle
θ_8	Latitudinal tower top rotation angle
δ_3	Delta-3 angle (teeter hinge orientation)
β	Coning angle
θs	Structural pre-twist angle
ξ	Local blade out-of-plane rotation
η	Local blade in-plane rotation

Note that the coordinate systems are defined to be right-handed and all angular rotations are positive.

Some position vectors are used to define the wind turbine model. The magnitudes and directions of these vectors are listed in Table 2.4. These distances will be used in the kinematics expressions.

Table 2.4. Position Vectors Used in Program

Variable	Direction	Description
H_s	$\mathbf{a}_2$	Height of rigid base of tower
H_H	$\mathbf{a}_2$	Height of flexible portion of tower
D_N	$\mathbf{c}_1$	Distance from tower top to teeter axis
D_{NM1}	$\mathbf{c}_1$	Distance from tower top to nacelle center of mass
D_{NM2}	$\mathbf{c}_2$	Distance from tower top to nacelle center of mass
R_U	$-\mathbf{g}_1$	Distance from teeter pin to blade axis intersection
R_{UM}	$-\mathbf{g}_1$	Distance from teeter pin to hub center of mass

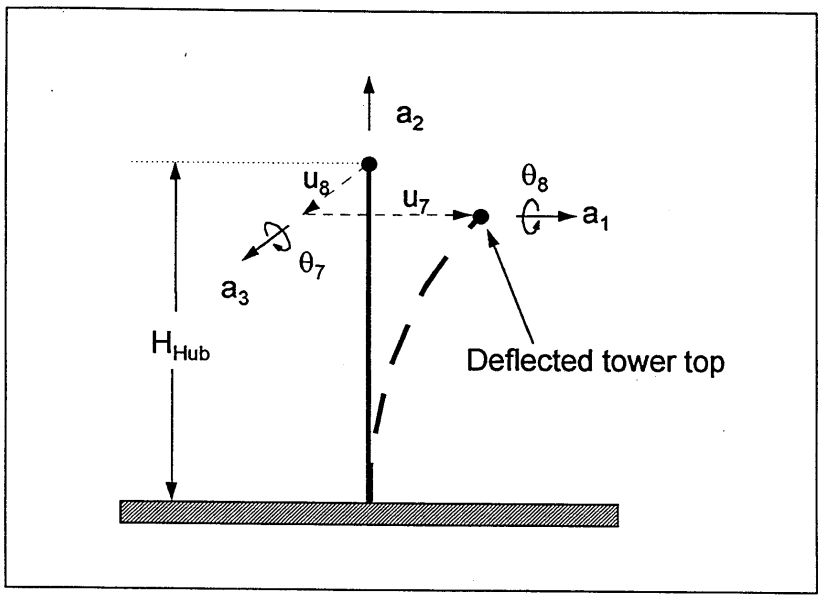

R	$\mathbf{i}_3$	Distance from blade axis intersection to local blade element

Figure 2.2.Tower Bending and Location of Tower Top

Figure 2.3.Orientation of Delta-3 Angle

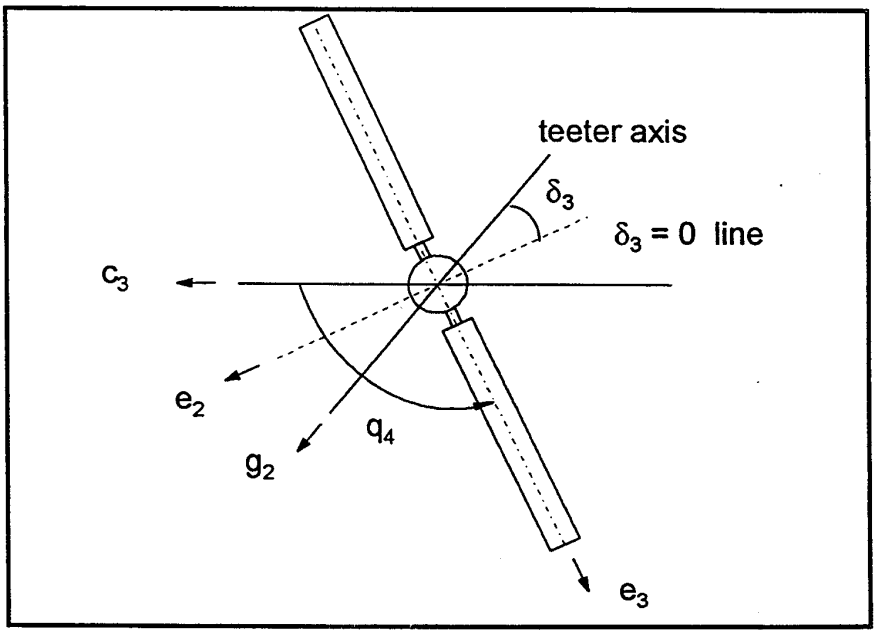

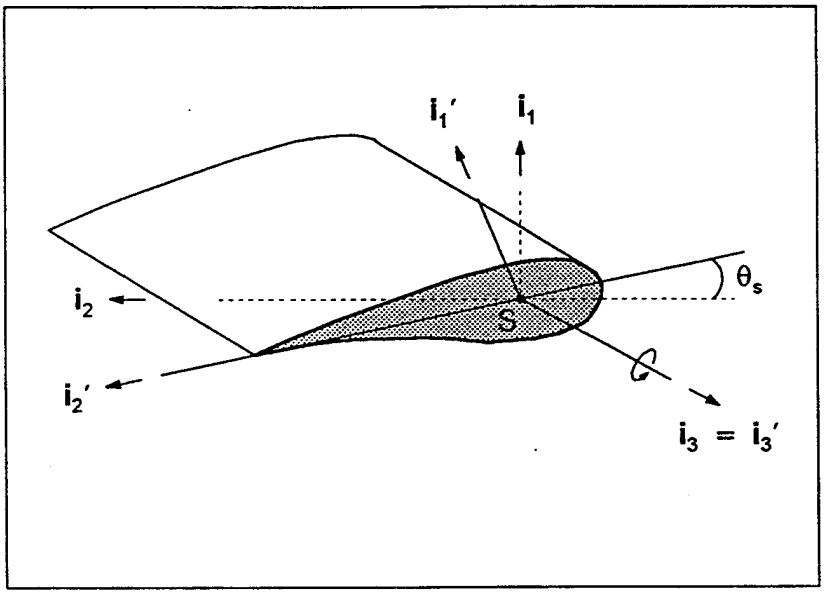

Figure 2.4.Orientation of Local Blade Structural Twist Angle

Finally, several points on the system are important in writing the equations of motion. These are listed in Table 2.5 and defined in Figure 2.1. These points are attached to a rigid body in one or more reference frames. For example, point O is the origin for both the tower top coordinates and the yaw coordinates.

Table 2.5. Points on the System

Point	Description
O	Tower top
P	Teeter hinge
Q	Intersection of blade inertia axes
S	Location of local blade segment
D	Mass center of nacelle
C	Mass center of hub

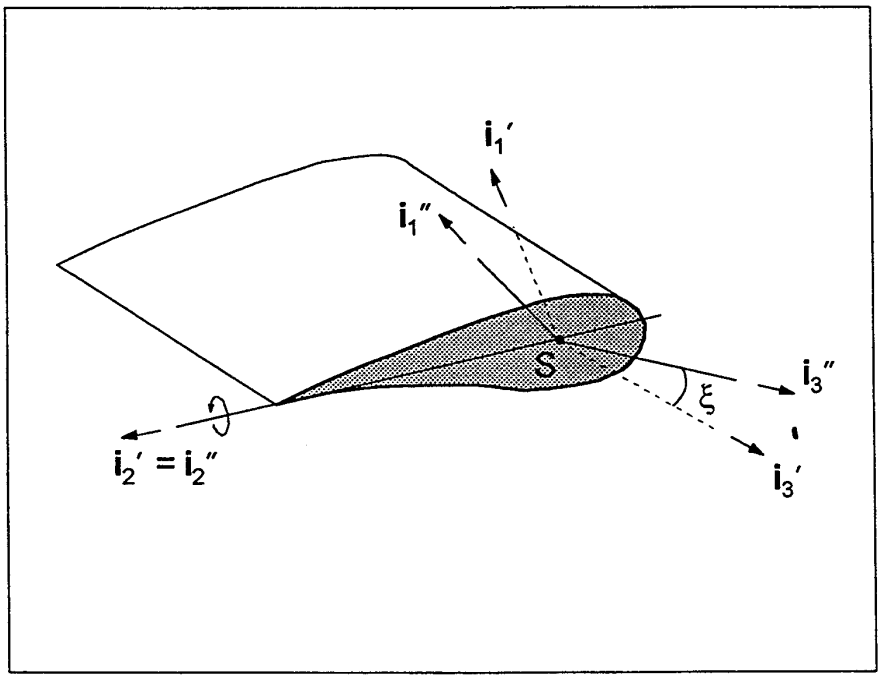

(a) Blade Flapwise Bending Angle

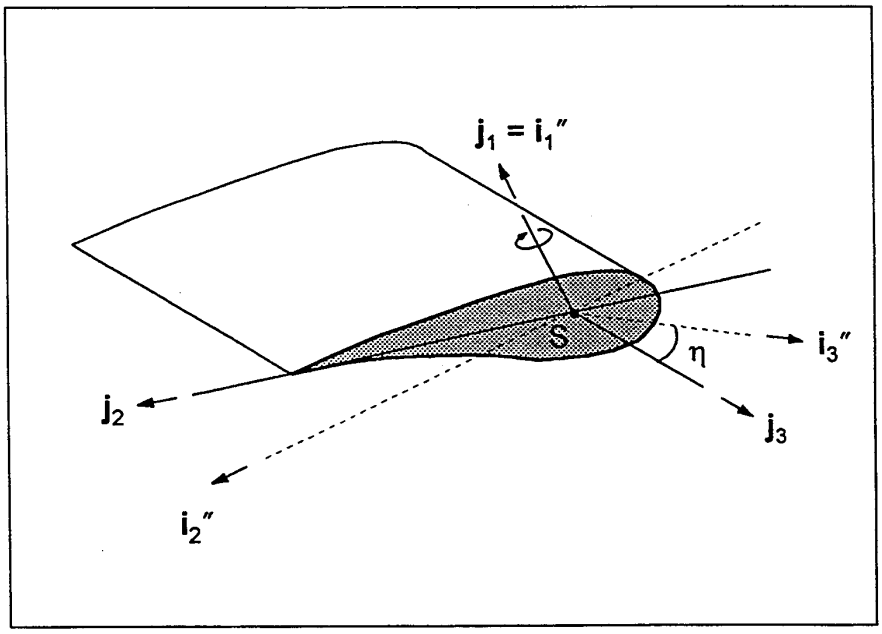

(b) Blade Edgewise Bending Angle

Figure 2.5.Orientation of Blade Flapwise and Edgewise Bending Angles

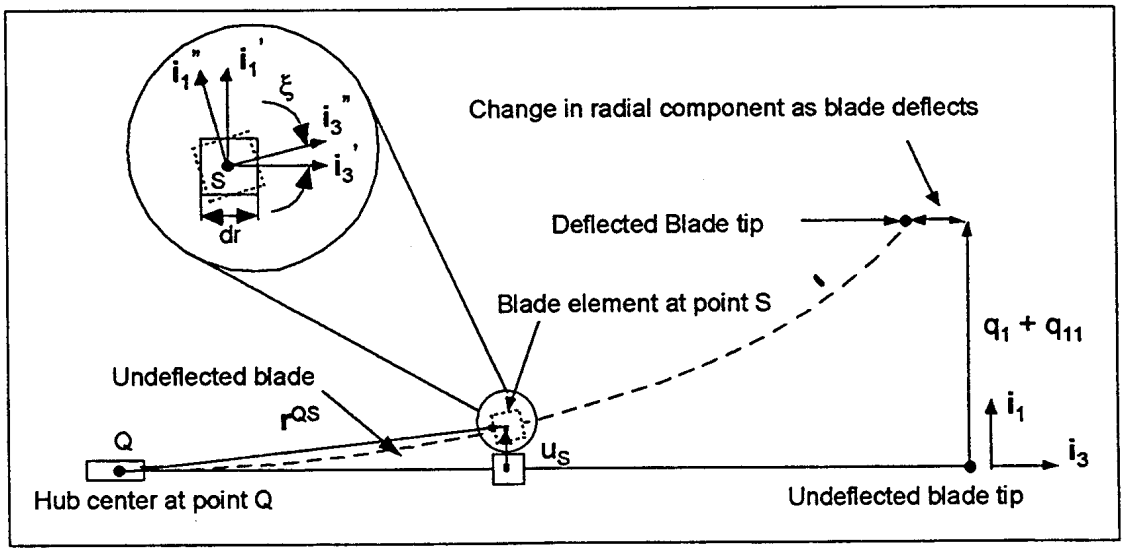

Figure 2.6.Blade Bending in Flapwise Direction

2.4 Blade and Tower Deflections

The treatment of flexible bodies in rigid-body dynamics requires an approximation so that the general deflection can be represented by only a few degrees of freedom. Both blades and tower can be treated as cantilever beams, fixed at one end to either the hub or the earth, and free at the other end. Both have point masses attached at the free end, either the tip brakes or the nacelle. The deflection of a cantilever beam can be represented as a linear combination of the known shapes of the first several normal vibration modes. For a flexible beam represented by only one vibration mode, the displacement anywhere on the flexible body is given as a product of the end displacement and a function which represents the normalized shape of the mode. This method is used to represent bending in two directions, and more than one mode can be used to give greater accuracy. Specifically, the tower deflection in both longitudinal and lateral directions is modeled by up to two modes, which requires two degrees of freedom in each direction to scale the shape functions. The blade deflection in the out-of-plane direction is also modeled with up to two vibration modes, requiring two degrees of freedom for each blade. The in-plane deflection of the blade is modeled with only one mode since the flexibility in this direction is much lower. This requires a total of three degrees of freedom (and mode shapes) for each blade.

The blades are treated as flexible beams fixed at the hub and free at the tip. Because the blade can have some structural pre-twist, defining the deflection in two directions which change along the twisted blade can be quite complicated. A better method is to define the total blade curvature as the combination of curvature in each direction, oriented by the structural pre-twist. This curvature is resolved into in-plane and out-of-plane components which are then integrated twice to get the deflection shape. Let f_1 and f_2 be the flapwise mode shapes for the non-pre-twisted blade, and g be the edgewise mode shape for the non-pretwisted blade. For this discussion let q_1 represent the first flapwise tip deflection, q_2 be the second flapwise tip deflection, and q_3 be the edgewise tip deflection. Note that for blade 1, q_1, q_2, and q_3 become q_1, q_{11}, and q_{13}; and for blade 2 they become q_2, q_{12}, and q_{14}. The local curvature in the flapwise direction is

$$q_1(t)\, f_1''(z) \;+\; q_2(t)\, f_2''(z) \;,$$

while the local edgewise curvature is

$$q_3(t)\, g''(z) \;,$$

where z is the coordinate along the blade. If the local pre-twist angle is $\theta_o(z)$, then the local coordinate system can be transformed back to the system fixed at the blade root. The out-of-plane curvature is

$$u'' \;=\; \cos\theta_o \{q_1(t)\, f_1''(z) + q_2(t)\, f_2''(z)\} \;-\; \sin\theta_o \{q_3(t)\, g''(z)\} \;,$$

while the in-plane curvature is

$$v'' \;=\; \sin\theta_o \{q_1(t)\, f_1''(z) + q_2(t)\, f_2''(z)\} \;+\; \cos\theta_o \{q_3(t)\, g''(z)\} \;.$$

These can be represented by twisted shape functions, as follows:

$$u'' \;=\; q_1\, \phi_1'' \;+\; q_2\, \phi_2'' \;+\; q_3\, \phi_3''$$

$$v'' \;=\; q_1\, \psi_1'' \;+\; q_2\, \psi_2'' \;+\; q_3\, \psi_3''$$

where

$$\phi_1'' \;=\; \cos\theta_o\, f_1''(z) \;,$$

$$\phi_2'' \;=\; \cos\theta_o\, f_2''(z) \;,$$

$$\phi_3'' \;=\; -\sin\theta_o\, g''(z) \;,$$

$$\psi_1'' \;=\; \sin\theta_o\, f_1''(z) \;,$$

$$\psi_2'' \;=\; \sin\theta_o\, f_2''(z) \;, \text{ and}$$

$$\psi_3'' \;=\; \cos\theta_o\, g''(z) \;.$$

These functions can be integrated twice with respect to z, the coordinate along the blade, to get the overall mode shapes for in-plane and out-of-plane bending. The deflection of the blade in each direction can then be written as

$$u(z,t) = \sum_{i=1}^{3} q_i(t)\,\phi_i(z)$$

$$v(z,t) = \sum_{i=1}^{3} q_i(t)\,\psi_i(z)\ , \qquad i = 1..3$$

Because the bending blade stays the same length, the distance from the root to the local segment along the blade changes. This shortening can be expressed as

$$w(z,t) = -\frac{1}{2}\int_0^z \left((u')^2 + (v')^2\right) d\varsigma$$

or, in terms of the above functions,

$$w = -\frac{1}{2}\sum_{i=1}^{3}\sum_{j=1}^{3} s_{ij}\,q_i\,q_j \qquad s_{ij} = \int_0^z \left(\phi_i'\,\phi_j' + \psi_i'\,\psi_j'\right) dz$$

The current position of the local blade segment as it is vibrating can now be expressed in root-fixed coordinates as

$$\mathbf{u}(z,t) = u(z,t)\,\mathbf{i}_1 + v(z,t)\,\mathbf{i}_2 + \left(r(z) + w(z,t)\right)\mathbf{i}_3$$

where the vector **u** is the vector position of the local blade segment, $\mathbf{i}_3$ is along the blade, $\mathbf{i}_1$ is in the out-of-plane direction, $\mathbf{i}_2$ is in the in-plane direction, and r(z) is the distance along the undeformed blade to the current blade segment.

Components of the longitudinal and lateral displacement of the tower top are shown in Figure 2.6. These displacements include contributions from the first and second mode shapes in both the longitudinal, $\mathbf{a}_1$, and lateral, $\mathbf{a}_3$, directions. They are related to the tower degrees of freedom as follows:

$$u_7 = q_7 + q_9$$

$$u_8 = q_8 + q_{10}$$

where u_7 is the total tower top displacement in longitudinal direction and u_8 is the total tower top displacement in the lateral direction. The corresponding tower top rotation angles are given by:

$$\theta_7 = -(\alpha_7 q_7 + \alpha_9 q_9)$$

$$\theta_8 = \alpha_8 q_8 + \alpha_{10} q_{10}$$

where θ_7 is a rotation about $\mathbf{a}_3$, θ_8 is a rotation about $\mathbf{a}_1$, and the α's are the first derivatives of the mode shapes:

$$\alpha_7 = \frac{\partial \phi_{1T}}{\partial h} \qquad \alpha_9 = \frac{\partial \phi_{2T}}{\partial h}$$

$$\alpha_8 = \frac{\partial \phi_{1T}}{\partial h} \qquad \alpha_{10} = \frac{\partial \phi_{2T}}{\partial h}$$

where ϕ_{1T} and ϕ_{2T} represent the first and second tower bending mode shapes, which are shown in Appendix C.

2.5 Kinematics

Once the dynamic system is defined as a series of rigid body reference frames related by several degrees of freedom, the kinematics of the system can be expressed. Vectors from any of the above coordinate systems can be used, since they are easily transformed to a common coordinate system. The accelerations of points in the system can be expressed using velocities and angular velocities, which must first be computed.

The angular velocities can be written between neighboring reference frames and then summed. Note that the angular velocities are vectors that relate the reference frame represented by the left superscript to the reference frame represented by the right superscript. The angular velocity of the base plate in the inertial frame is given by

$$^{E}\omega^{B} = \dot{\theta}_8 \, \mathbf{a}_1 - \dot{\theta}_7 \, \mathbf{a}_3$$

The angular velocity of the nacelle relative to the base plate depends on the yaw rate and tilt rate

$$^{B}\omega^{N} = \dot{q}_6 \, \mathbf{d}_2 + \dot{q}_5 \, \mathbf{d}_3$$

The rotor speed relates the nacelle to the shaft reference frame:

$$^{N}\omega^{H} = \dot{q}_4 \, \mathbf{e}_1$$

The rotor is related to the shaft reference frame by the teeter rate.

$$^{H}\omega^{R} = \dot{q}_3 \, \mathbf{g}_2$$

Once the individual angular velocities are written, they can be combined to get the angular motion of each reference frame in relation to the inertial frame.

$$ {}^{E}\boldsymbol{\omega}^{N} = {}^{E}\boldsymbol{\omega}^{B} + {}^{B}\boldsymbol{\omega}^{N} $$

$$ {}^{E}\boldsymbol{\omega}^{H} = {}^{E}\boldsymbol{\omega}^{N} + {}^{N}\boldsymbol{\omega}^{H} $$

$$ {}^{E}\boldsymbol{\omega}^{R} = {}^{E}\boldsymbol{\omega}^{H} + {}^{H}\boldsymbol{\omega}^{R} $$

The angular velocity of the rotor in the inertial frame can be expressed by substituting the first two expressions above into the last one:

$$ {}^{E}\boldsymbol{\omega}^{R} = \dot{\theta}_8\, \mathbf{a}_1 - \dot{\theta}_7\, \mathbf{a}_3 + \dot{q}_6\, \mathbf{d}_2 + \dot{q}_5\, \mathbf{d}_3 + \dot{q}_4\, \mathbf{e}_1 + \dot{q}_3\, \mathbf{g}_2 $$

These angular velocities can now be used with the geometry of the structure to express the velocity of various points of interest. Velocities are also vectors, but they describe the motion of a point, the right superscript, in a particular reference frame, the left superscript. The velocity of the tower top in the inertial frame is:

$$ {}^{E}\mathbf{v}^{O} = (\dot{q}_7 + \dot{q}_9)\, \mathbf{a}_1 + (\dot{q}_8 + \dot{q}_{10})\, \mathbf{a}_3 $$

The velocity of the teeter hinge at the end of the low speed shaft can be related to the tower top velocity as follows:

$$ {}^{E}\mathbf{v}^{P} = {}^{E}\mathbf{v}^{O} + {}^{E}\boldsymbol{\omega}^{N} \times \mathbf{r}^{OP} $$

$$ \mathbf{r}^{OP} = D_N\, \mathbf{c}_1 $$

where the points O and P are fixed in reference frame N, $\mathbf{r}^{OP}$ is the vector that connects the points, and D_N is the distance from tower top to teeter hinge.

The velocities of point Q can be expressed in a similar manner,

$$ {}^{E}\mathbf{v}^{Q} = {}^{E}\mathbf{v}^{P} + {}^{E}\boldsymbol{\omega}^{R} \times \mathbf{r}^{PQ} $$

$$ \mathbf{r}^{PQ} = -R_U \, \mathbf{g}_1 $$

where points Q and P are fixed in the rotor frame, separated by the distance R_U.

The velocity of an individual blade segment is related to the velocity of a point on the rotor as follows

$$ {}^{E}\mathbf{v}^{S} = {}^{E}\mathbf{v}^{S_r} + {}^{R}\mathbf{v}^{S} + {}^{E}\boldsymbol{\omega}^{R} \times \mathbf{r}^{QS_r} $$

where S_r is the location of point S if it were fixed to the rotor (as if the blade was not flapping). Effectively, the motion of the segment away from its current position is added to the motion of the current position.

$$ {}^{E}\mathbf{v}^{S_r} = {}^{E}\mathbf{v}^{Q} + {}^{E}\boldsymbol{\omega}^{R} \times \mathbf{r}^{QS_r} $$

$$ \mathbf{r}^{QS_r} = r \, \mathbf{i}_3 $$

$$ {}^{R}\mathbf{v}^{S} = \dot{\mathbf{u}} $$

$$ \mathbf{r}^{QS} = \mathbf{u} $$

where γ is the blade length from the root to the corresponding segment, and **u** describes the location of the deflected blade segment and as discussed in the previous section.

These expressions can be combined to get the velocity of a blade segment in the inertial reference frame:

$$
\begin{aligned}
{}^{E}\mathbf{v}^{S} = {} & (\dot{q}_7 + \dot{q}_9)\,\mathbf{a}_1 + (\dot{q}_8 + \dot{q}_{10})\,\mathbf{a}_3 + (\dot{\theta}_8\,\mathbf{a}_1 - \dot{\theta}_7\,\mathbf{a}_3 + \dot{q}_6\,\mathbf{d}_2 + \dot{q}_5\,\mathbf{d}_3) \times D_N\,\mathbf{c}_1 \\
& - (\dot{\theta}_8\,\mathbf{a}_1 - \dot{\theta}_7\,\mathbf{a}_3 + \dot{q}_6\,\mathbf{d}_2 + \dot{q}_5\,\mathbf{d}_3 + \dot{q}_4\,\mathbf{e}_1 + \dot{q}_3\,\mathbf{g}_2) \times R_U\,\mathbf{g}_1 \\
& + (\dot{\theta}_8\,\mathbf{a}_1 - \dot{\theta}_7\,\mathbf{a}_3 + \dot{q}_6\,\mathbf{d}_2 + \dot{q}_5\,\mathbf{d}_3 + \dot{q}_4\,\mathbf{e}_1 + \dot{q}_3\,\mathbf{g}_2) \times r\,\mathbf{i}_3 \\
& + (\dot{\theta}_8\,\mathbf{a}_1 - \dot{\theta}_7\,\mathbf{a}_3 + \dot{q}_6\,\mathbf{d}_2 + \dot{q}_5\,\mathbf{d}_3 + \dot{q}_4\,\mathbf{e}_1 + \dot{q}_3\,\mathbf{g}_2) \times \mathbf{u} + \dot{\mathbf{u}}
\end{aligned}
$$

Many of the terms in this expression contain the first time derivative of a degree of freedom multiplied by a vector. This can be more easily expressed in terms of the coefficients of these degree of freedom rates and the portion left over.

$$
{}^{E}\mathbf{v}^{S} = \sum_{r=1}^{15} {}^{E}\mathbf{v}_r^{S}\,\dot{q}_r + {}^{E}\mathbf{v}_t^{S}
$$

where ${}^{E}\mathbf{v}_r^{S}$ is the coefficient of the time derivative of the rth degree of freedom and ${}^{E}\mathbf{v}_t^{S}$ contains all of the terms that are not of this form. Notice that these coefficients are vectors and can contain the degrees of freedom but not their time derivatives. In this case,

$$
{}^{E}\mathbf{v}_3^{S} = \mathbf{g}_2 \times (-R_U\,\mathbf{g}_1 + r\,\mathbf{i}_3 + \mathbf{u}) \text{ , and}
$$

$$
{}^{E}\mathbf{v}_7^{S} = \mathbf{a}_1 - \alpha_7\,\mathbf{a}_3 \times (D_N\,\mathbf{c}_1 - R_U\,\mathbf{g}_1 + r\,\mathbf{i}_3 + \mathbf{u}) \text{ .}
$$

The vector coefficients are called partial velocities. The dot product of these coefficient with the equations of motion produces a greatly simplified system of equations, which is the main advantage of Kane's method.

The equation for the angular motion of the rotor frame can be put into a similar form:

$$
{}^{E}\omega^{R} = \sum_{r=1}^{15} {}^{E}\omega_r^{R}\,\dot{q}_r + {}^{E}\omega_t^{R} \text{ ,}
$$

$$
\begin{aligned}
{}^{E}\omega_3^{R} &= \mathbf{g}_2 \text{ ,} \\
{}^{E}\omega_6^{R} &= \mathbf{d}_2 \text{ ,} \\
{}^{E}\omega_7^{R} &= -\,\alpha_7\,\mathbf{a}_3 \text{ , and} \\
{}^{E}\omega_t^{R} &= 0
\end{aligned}
$$

where

The velocities of points C and D can be expressed similarly to velocities of points Q and P, respectively; only the distances are different.

$$\mathbf{r}^{PC} = -R_{UM}\,\mathbf{g}_1$$

$$\mathbf{r}^{OD} = D_{NM1}\,\mathbf{c}_1 + D_{NM2}\,\mathbf{c}_2$$

where R_{UM} is the distance from teeter hinge to the mass center of the hub and D_{NM1} and D_{NM2} is the distance from the yaw axis-tilt axis intersection in $\mathbf{c}_1$ and $\mathbf{c}_2$ directions to the mass center of the nacelle.

The acceleration is the time derivative of the velocity. The time derivative of the velocity in the above simplified form is:

$$^{E}\mathbf{a}^{S} = \sum_{r=1}^{15} {}^{E}\mathbf{v}_r^{S}\,\ddot{q}_r + \sum_{r=1}^{15} \frac{d}{dt}\,{}^{E}\mathbf{v}_r^{S}\,\dot{q}_r + \frac{d}{dt}\,{}^{E}\mathbf{v}_t^{S}$$

Notice that the second and third terms contain only first time derivatives of the degrees of freedom, so this expression is already in the desired form if

$$^{E}\mathbf{a}_t^{S} = \sum_{r=1}^{15} \frac{d}{dt}\,{}^{E}\mathbf{v}_r^{S}\,\dot{q}_r + \frac{d}{dt}\,{}^{E}\mathbf{v}_t^{S}$$

Once the accelerations are expressed, we need to consider the forces acting on the system.

2.6 Kinetics

Once expressions for the accelerations and external forces are determined, these can be combined to form the equations of motion. These can be put into Newton's Second Law, $\mathbf{F} = m\mathbf{a}$, or $\mathbf{F} - m\mathbf{a} = 0$. Kane has simplified these vector equations by taking components in the direction of the partial velocities defined in the previous section. Each partial velocity produces a scalar equation related to a single degree of freedom of the form

$$F_r + F_r^* = 0 , \qquad r = 1,2,\ldots,15$$

where

$$F_r = \sum_i {}^E\mathbf{v}_r^S \cdot \mathbf{F}_i \qquad \text{i = sum over all external forces}$$

$$F_r^* = \sum_i {}^E\mathbf{v}_r^S \cdot (-m_i \mathbf{a}_i) \qquad \text{i = sum over each body in the system with mass}$$

These quantities are called generalized active forces and generalized inertia forces, respectively. The generalized active forces include all external forces acting on the body, such as aerodynamic forces, gravity, drive train forces, and forces due to the elastic bending of the blades and tower. These are detailed in sections 2.6.1 through 2.6.3.

The generalized inertia forces include all effects of linearly and angularly accelerating mass. There will be some contribution from all bodies that have mass, including the tower, nacelle, hub, and blades. These can be summed to get the total generalized inertia force:

$$F_r^*|_{Total} = F_r^*|_{Tower} + F_r^*|_{Nacelle} + F_r^*|_{Hub} + F_r^*|_{Blades}$$

The hub contains all mass in the rotor assembly except that contained in the blades and tip brakes. The contribution to inertia forces from the hub mass, m_{Hub}, is given by:

$$F_r^* \big|_{Hub} = - {}^E\mathbf{v}_r^C \cdot m_{Hub}\, {}^E\mathbf{a}^C - {}^E\boldsymbol{\omega}_r^R \cdot \left[\mathbf{I}_{Hub} \cdot {}^E\boldsymbol{\alpha}^R + {}^E\boldsymbol{\omega}^R \times \mathbf{I}_{Hub} \cdot {}^E\boldsymbol{\omega}^R \right]$$

where ${}^E\mathbf{v}_r^C$ is the partial velocity of the hub mass center for the rth degree of freedom, ${}^E\mathbf{a}^C$ is the acceleration of the hub mass center, ${}^E\omega_r^R$ is the partial angular velocity of the rotor for the rth degree of freedom, and ${}^E\alpha^R$ is the angular acceleration of the rotor assembly, all in the inertial reference frame. The inertia matrix of the hub about its mass center, $\mathbf{I}_{Hub}$, is determined from the inertia of the hub about the teeter axis.

The nacelle mass includes everything on top of the tower that yaws except the rotor assembly. The mass of individual components is described in terms of the total mass, the location of the mass center, and the total inertia of the components about the yaw axis. The rotational inertia of the gears and other internal mechanisms is neglected. The generalized inertia forces for the nacelle assembly is given by an equation similar to that for the hub:

$$F_r^* \big|_{Nacelle} = - {}^E\mathbf{v}_r^D \cdot m_{Nacelle}\, {}^E\mathbf{a}^D - {}^E\boldsymbol{\omega}_r^N \cdot \left[\mathbf{I}_{Nacelle} \cdot {}^E\boldsymbol{\alpha}^N + {}^E\boldsymbol{\omega}^N \times \mathbf{I}_{Nacelle} \cdot {}^E\boldsymbol{\omega}^N \right]$$

where ${}^E\mathbf{v}_r^D$ is the partial velocity of the nacelle mass for the rth degree of freedom, ${}^E\mathbf{a}^D$ is the acceleration of the nacelle mass center, ${}^E\omega_r^N$ is the partial angular velocity of the nacelle for the rth degree of freedom, and ${}^E\alpha^N$ is the angular acceleration of the nacelle assembly, all in the inertial reference frame. The inertia matrix of the nacelle about its mass center, $\mathbf{I}_{Nacelle}$, is determined from the inertia of the nacelle about the yaw axis.

Contributions from the flexible tower to the generalized inertia forces depend on its distributed mass. The generalized inertia force for the entire tower is the integral of the inertia force for each tower segment. If μ_{Tower} is the mass per unit length of the local tower segment, the generalized inertia forces are given by

$$F_r^* \big|_{Tower} = - \int_0^H \mu_{Tower}\, {}^E\mathbf{v}_r^T \cdot {}^E\mathbf{a}^T \, dz$$

where T is the current tower element, ${}^{E}\mathbf{v}_r^T$ is the partial velocity of the current tower element for the rth degree of freedom, and ${}^{E}\mathbf{a}^T$ is the acceleration of the tower element. The velocity of the tower element is given by

$$ {}^{E}\mathbf{v}^T = (\dot{q}_7\,\phi_{1T} + \dot{q}_9\,\phi_{2T})\,\mathbf{a}_1 + (\dot{q}_8\,\phi_{1T} + \dot{q}_{10}\,\phi_{2T})\,\mathbf{a}_3 = \Sigma\ {}^{E}\mathbf{v}_r^T\,\dot{q}_r $$

so that the partial velocities become

$$ {}^{E}\mathbf{v}_7^T = \phi_{1T}\,\mathbf{a}_1 \qquad {}^{E}\mathbf{v}_8^T = \phi_{1T}\,\mathbf{a}_3 $$

$$ {}^{E}\mathbf{v}_9^T = \phi_{2T}\,\mathbf{a}_1 \qquad {}^{E}\mathbf{v}_{10}^T = \phi_{2T}\,\mathbf{a}_3 $$

where ϕ's are the tower shape functions which vary with z, the location of the current element, T. The acceleration of T is just the time derivative of the velocity,

$$ {}^{E}\mathbf{a}^T = \frac{d\ {}^{E}\mathbf{v}^T}{dt} = \sum_{r=7}^{10} {}^{E}\mathbf{v}_r^T\,\ddot{q}_r $$

Notice that the partial velocities are constant over time. This expression can be substituted into the generalized inertia force equation,

$$ F_r^*\big|_{Tower} = -\sum_{r=7}^{10} \int_0^H \mu_{Tower}\ {}^{E}\mathbf{v}_r^T \cdot {}^{E}\mathbf{v}_r^T\,\ddot{q}_r\,dz $$

When the above expressions for the partial velocities are substituted into this equation, the terms involving $\mathbf{a}_1 \cdot \mathbf{a}_3$ go to zero. The others are of the form:

$$ F_7^*\big|_{Tower} = -\int_0^H \mu_{Tower}\,\phi_{1T}\,\phi_{1T}\,dz\,\ddot{q}_7 - \int_0^H \mu_{Tower}\,\phi_{1T}\,\phi_{2T}\,dz\,\ddot{q}_9 $$

Notice that because of orthogonality of the first two modes the second term will also go to zero.

The flexible blades contribute to the generalized inertia forces in a similar manner.

$$F_r^* \big|_{Blades} = - \int_0^{RT} \mu_{Blade} \, {}^E\mathbf{v}_r^{S1} \cdot {}^E\mathbf{a}^{S1} \, dr_1 - \int_0^{RT} \mu_{Blade} \, {}^E\mathbf{v}_r^{S2} \cdot {}^E\mathbf{a}^{S2} \, dr_2$$

where S_1 and S_2 are the local blade elements for blades 1 and 2, respectively, R_T is the distance to the blade tip, and μ_{Blade} is the mass of the local blade element. This can be simplified in a manner similar to the tower equations, but the equations are still quite lengthy.

All of the above expressions are combined to give a complete set of expressions for the generalized inertia forces. Once the generalized active forces are found, these can be combined to give the complete equations of motion, which can then be solved numerically.

2.7 Generalized Active Forces

The generalized active forces are composed of several different types of forces acting on the wind turbine. These include aerodynamic forces, gravity, drive train forces, and elastic restoring forces of the flexible bodies. The total contribution to the active forces is given by:

$$F_r|_{Total} = F_r|_{Aero} + F_r|_{Gravity} + F_r|_{Drive} + F_r|_{Elastic}$$

Each of these forces are described in the sections that follow.

2.7.1 Aerodynamic Loading

The major loading on the wind turbine blades is due to the aerodynamic forces of lift and drag. For a unit span of the blade, the incremental lift and drag forces are

$$L = \frac{1}{2} \rho W^2 c C_L$$

$$D = \frac{1}{2} \rho W^2 c C_D$$

where ρ is the ambient air density, c is the local blade chord length, C_L and C_D are the local sectional lift and drag coefficients, and W is the speed of the air relative to the blade. The local relative wind speed W contains contributions from the local wind, the rigid body motion of the blade due to rotation about the drive shaft, teeter and yaw axes, the flexible body motion of the blades and tower, and a contribution due to induction. The induced velocity is determined using strip theory wherein the local force on the blades due to lift is equated to the momentum flux. The blade force is based on the flow relative to the blade and contains the induced velocity explicitly in the W^2 term and also contains the induced velocity implicitly in

the lift coefficient and in the various trigonometric functions that are used to obtain the component of the blade force in the direction of the momentum flux.

The momentum flux through a segment of the rotor disk is obtained using the Momentum Equation. Whereas the blade force involves the flow relative to the blade, the momentum flux is determined in an inertial reference frame. The induced velocity appears both explicitly and implicitly in the momentum flux as well as in the blade force so that the induction must be solved for using iteration. A significant amount of computing time is used to determine the local induction at each time step.

The iteration process can include or neglect the effects of the tangential component of the induced velocity. The effects of turbulence are included in iteration in the AeroDyn code.

When the induction is determined, the aerodynamic force per unit span transmitted to the blade is

$$\mathbf{f}_A = [L\cos\phi + D\sin\phi]\,\mathbf{i}_1 + [-L\sin\phi + D\cos\phi]\,\mathbf{i}_2$$

where ϕ is the relative inflow angle of the blades. Note that there is no $\mathbf{i}_3$ component in the above equation.

The total aerodynamic generalized active force is then determined from the integral along the span

$$F_{r|Aero} = \int_0^R {}^E\mathbf{v}_r^{S1} \cdot \mathbf{f}_A \, dr_1 + \int_0^R {}^E\mathbf{v}_r^{S2} \cdot \mathbf{f}_A \, dr_2$$

where subscripts 1 and 2 refer to the blade number. The aerodynamic forces on the tower and nacelle could be included in a similar manner, but not have been accounted for in this study.

The lift and drag coefficients in the above equations are based on airfoil data in the form of either a curve fit or table which gives the variation with the local angle of attack, α, and the thickness.

Dynamic stall can also be accounted for in the calculation of aerodynamic forces. Dynamic stall occurs when the airfoil section is near stall. A rapid change in angle of attack causes a vortex to be shed over the top surface of the airfoil, producing an extra lift followed by a rapid decrease in lift until the stall

point is reached. In this case, the lift and drag are functions of the time rate of change of angle of attack as well as α.

2.7.2 Elastic Restoring Forces

The bending of flexible, elastic bodies produces forces which tend to restore the bodies to their undeflected position. The generalized active forces based on these restoring forces can be computed from the potential energy V, of a bent beam as follows:

$$F_{r|Elastic} = \frac{\partial V}{\partial q_r}$$

For the tower, the potential energy of bending is expressed as

$$V_{Tower} = \frac{1}{2}\left(k_{7\,7}\, q_7^2 + k_{8\,8}\, q_8^2\right) + \frac{1}{2}\left(k_{9\,9}\, q_9^2 + k_{10\,10}\, q_{10}^2\right)$$

where $k_{7\,7}$, $k_{8\,8,}$ $k_{9\,9}$, and $k_{10\,10}$ are tower stiffness terms given by:

$$k_{7\,7} = k_{8\,8} = \int_0^H \sigma_{Tower}\left(\phi_{1T}''\right)^2 dz - \int_0^H m_{Tower}\, g\left(\phi_{1T}'\right)^2 dz$$

$$k_{9\,9} = k_{10\,10} = \int_0^H \sigma_{Tower}\left(\phi_{2T}''\right)^2 dz - \int_0^H m_{Tower}\, g\left(\phi_{2T}'\right)^2 dz$$

where σ_{Tower} is the local tower stiffness, g is the gravitational constant, and m_{Tower} is the mass of everything above current tower element, including part of the tower, the nacelle, and the rotor.

For each blade, the potential energy expression is similar. Again, let the flapwise modes be represented by q_1 and q_2 and the edgewise mode be q_3.

$$V_{Blade\ 1} = k_{1\,1}\, q_1^2 + 2\, k_{1\,2}\, q_1\, q_2 + k_{2\,2}\, q_2^2 + k_{3\,3}\, q_3^2$$

where

$$k_{ij} = \int_0^R \frac{EI_{Flap}}{2} f_i'' f_j'' \, dr \qquad \begin{array}{l} i = 1, 2 \\ j = 1, 2 \end{array}$$

$$k_{33} = \int_0^R \frac{EI_{Edge}}{2} (g'')^2 \, dr$$

where EI_{Flap} is the flapwise blade stiffness, EI_{Edge} is the edgewise blade stiffness, and f's and g's are the blade deflections defined in section 2.3. Note that for blade 1, q_1, q_2, and q_3 become q_1, q_{11}, and q_{13}; and for blade 2 they become q_2, q_{12}, and q_{14}.

2.7.3 Drive Train Loading

There are four options available for modeling variations in shaft rotational speed. These include constant RPM, induction generator, start-up, and shut-down. Each are available by changing the variable, IZD(4), in the main input file. Additionally, drive shaft flexibility may be included with all these options except the constant RPM case.

Significant drive train loads can occur during starting and stopping operations. During start-up, the rotor starts as a result of the generator acting as a motor. During this time, the drive shaft, particularly the low speed shaft, acts as a torsional spring and may cause large torsional oscillations.

For start-up, the shaft speed and torque can be modeled by three curve fits over the motor side of the curve shown in Figure 2.7. Currently, the motor is modeled as a constant until the operating rpm is approached. Input constants include motor start-up torque, Q_0, slope of linear region curve, C_e, and the synchronous RPM, Ω_0, all of which are shown for the generator side of the shaft in Figure 2.7. The code, as delivered, has a constant motor start-up torque. Any changes must be recoded in the GNTORQ subroutine.

Figure 2.7. Variation of Shaft Speed with Torque

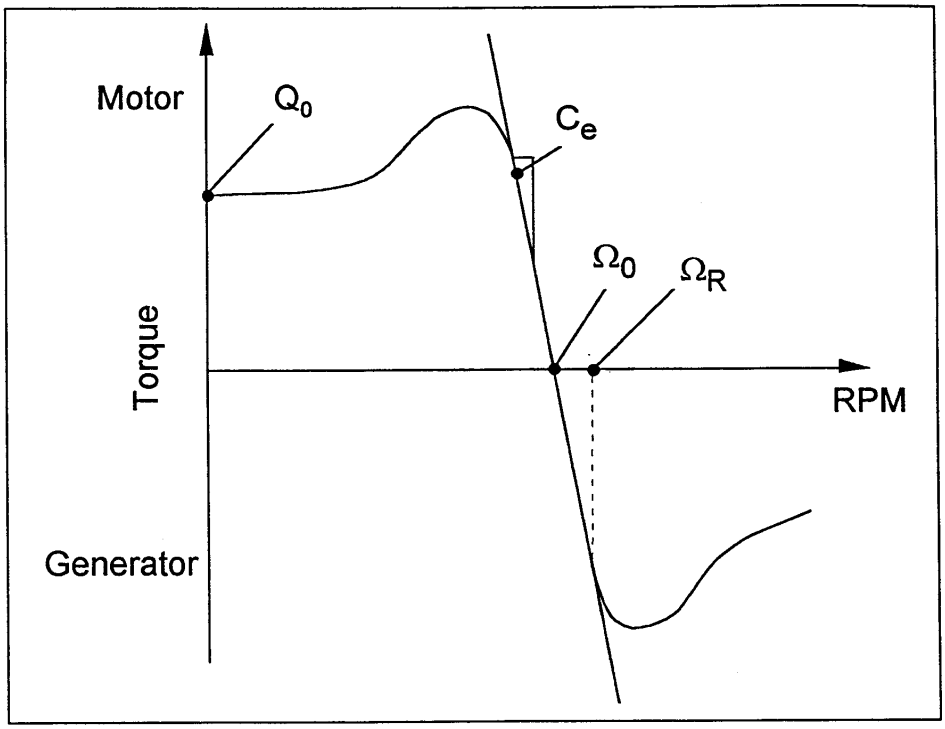

For shut-down or braking of the rotor, the torque is modeled over the negative, linear region of Figure 2.7, and is given by:

$$T_{Brake} = -\,\mathrm{sign}(\dot{q}_{15})\left[1 - 0.2\left(\frac{\dot{q}_{15}}{\Omega_0}\right)^2\right]Q_B$$

where:

sign ( ) = Gives the algebraic sign of quantity in parenthesis, returns only +1 or -1.

Q_B = Mechanical brake torque (specified by user in main input file).

Induction generators are commonly used in wind turbines because of their ability to control the rotor during start-up and shut-down. For the induction generator option, the torque is given by:

$$T_{Gen} + T_{Electrical} + T_{Losses}$$

where:

$$T_{Electrical} = c_e n^2 (\dot{q}_{15} - \Omega_0)$$

$$T_{Losses} = n\left[T_{Fixed}\left(\frac{\dot{q}_{15}}{\Omega_0}\right) + T_{Variable}\left(\frac{\dot{q}_{15} - \Omega_0}{\Omega_R - \Omega_0}\right)^2\right]$$

$$T_{Fixed} = f\left(\frac{1}{\eta_{Gen}} - 1\right)\frac{P_{Rated}}{n\Omega_R}$$ (T_{Fixed} is specified in main input file by QFL.)

$$T_{Variable} = (1 - f)\left(\frac{1}{\eta_{Gen}} - 1\right)\frac{P_{Rated}}{n\Omega_R}$$ ($T_{Variable}$ is specified in main input file by QVL.)

f = Fixed loss factor

η_{Gen} = Maximum generator efficiency (specified by user in main input file)

P_{Rated} = Generator rated power output

For cases involving a flexible drive shaft, the drive train between the rotor and generator is modeled as a single equivalent shaft characterized by a linear torsional spring, k_D, and a linear torsional damper, c_D. The equivalent drive shaft is massless and is modeled as an equivalent low speed shaft as shown in Figure 2.8. The torque is then given by:

$$T_{shaft} = k_D (q_4 - q_{15}) + c_D (\dot{q}_4 - \dot{q}_{15})$$

where:

k_D and c_D are constants (specified by the user in the main input file)

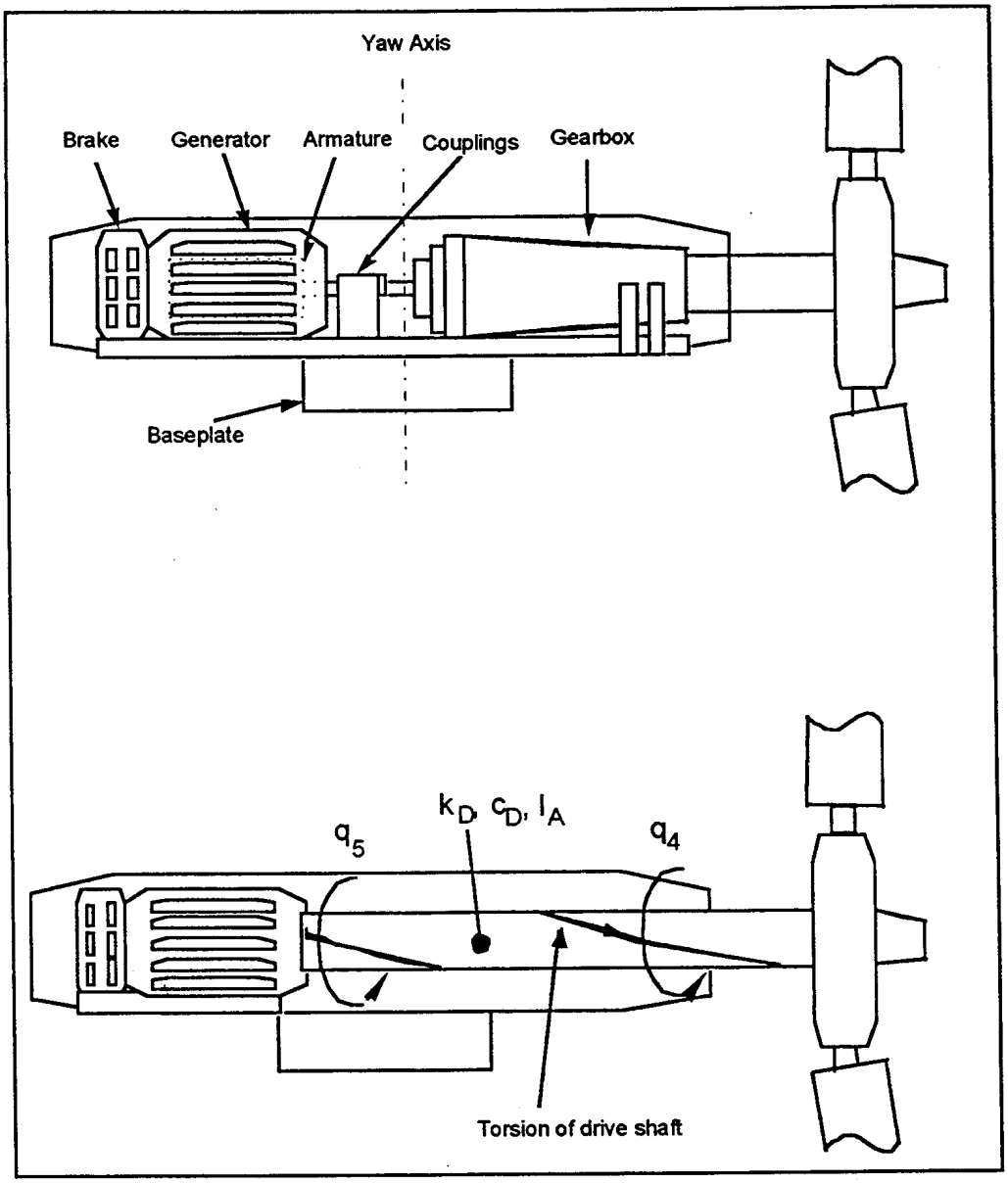

Figure 2.8.Turbine Drive Train as Modeled in FAST_AD

The generator armature, rotor brake, and other significant rotational inertias on the high speed shaft are lumped together in the sum of inertias, I_A. The equation for the fifteenth degree of freedom is then given by:

$$\ddot{q}_{15} = \frac{\eta_{GB}\, T_{Shaft} - T_{Gen}}{n^2\, I_A}$$

where:

η_{GB} = gearbox efficiency (specified by user in main input file)

n = gearbox step-up ratio (specified by user in main input file)

I_A = overall generator inertia (specified by user in main input file)

T_{Gen} = takes on value appropriate to motor start-up, induction generator, or shut-down

2.8 Wind Model

The wind applied to the turbine is made up of a deterministic portion and a stochastic part. The mean wind is uniform and steady, coming from a prescribed direction which can vary over time. This steady wind input is then modified to include the effects of tower shadow, if the rotor is downwind from the tower, and wind shear, to account for the earth's boundary layer. Finally, if turbulence is considered, it is added to this steady wind. The final local wind vector is used to determine the relative velocity over a particular blade segment.

If the tower is upwind of the rotor, its wake affects the aerodynamic loads on the blades. The wind velocity seen by the blades is reduced as they pass through the wake once per revolution. This acts as a forcing function with a once per revolution frequency, which may excite any component of the system that has a natural frequency near this. The tower shadow or wake is treated as a reduction in wind velocity of the form:

$$V = V_o [1 - \varepsilon \cos(\pi y/L)]$$

where V is the lower velocity in the wake, V_o is the free stream velocity, ε is the velocity deficit in the center of the wake, y is the horizontal distance from the center of the wake, and L is the width of the wake. The shape of the wake is shown in Figure 2.9. The parameters are determined by equating the drag force on the tower with the momentum loss between the uniform upwind stream and the deficit in the downstream wind. The center velocity deficit is based on the tower diameter, d, and the drag coefficient of the tower, C_D, as:

$$\varepsilon = \frac{2}{3}\left(1 - \sqrt{1 - \frac{3\,C_D\,d}{L}}\right)$$

This expression for the velocity deficit is only applied when the blade is in the wake region.

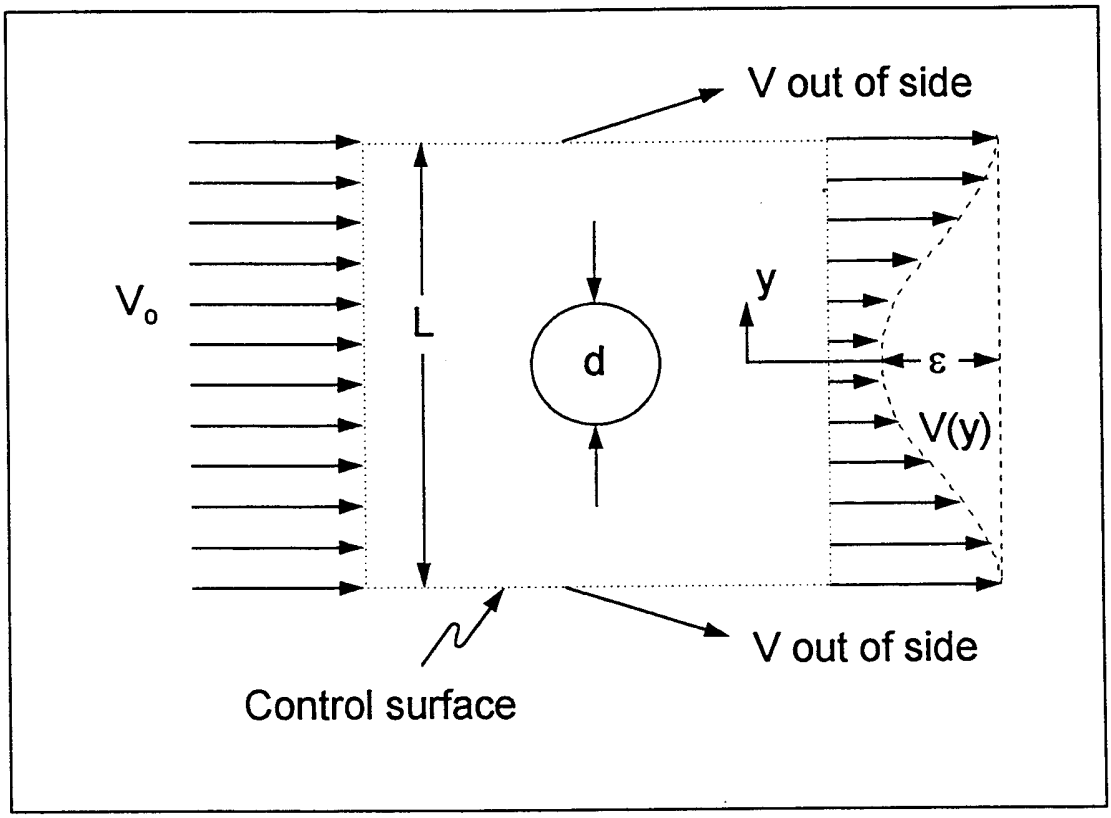

Figure 2.9.Tower Shadow

Wind shear occurs when the wind velocity decreases with height near the ground because of the earth's boundary layer. The velocity profile of the wind inside this boundary layer is assumed to have a shape given by a power law expression, with the mean wind velocity at the hub height specified. The wind speed at the current location is given by

$$V + V_o [1 + z/H]^{\eta}$$

where V_o is the mean wind velocity at the hub height, z is the vertical distance from the hub (up is positive), H is the hub height, and η is the power law component, usually between 0.1 and 0.2, with 0.2 indicating rougher terrain. The velocity profile of the wind is shown in Figure 2.10.

Turbulence in the wind can be accounted for by one of two different methods. First, a two-dimensional turbulence model can be used, such as the Veers Full Field Turbulence Code. This gives a rotationally sampled turbulence component for each blade at one point on the blade. Each value represents the change in wind velocity due to turbulence. These values are superimposed on the steady component of the wind which accounts for the tower shadow and wind shear. In order to account for varying wind direction, a specified wind direction can be combined with the two-dimensional turbulence simulation. This is shown in Figure 2.11.

Another method of account for wind turbulence is to generate a full three-dimensional field of turbulent wind values and interpolate between them to get values at a particular location. In this case, the array of turbulence values is read in initially and interpolated to give three components of wind once the current blade segment location is known. The turbulence filed accounts for varying wind direction and can also include wind shear.

2.9 Numerical Solution Technique

The numerical solution to the equations of motion is computed at each time step. Once the equations of motion for the 15 degrees of freedom are formulated from $F_r + F_r^* = 0$, they can be put into the form

$$\sum_s C_{rs}\,\ddot{q}_s + f_r(\dot{q},q) = 0$$

where C_{rs} are the known coefficients of the accelerations and f_r are functions containing lower order terms. This can also be expressed in a matrix form:

$$\begin{bmatrix} C_{11} & C_{12} & \cdots & \cdots & \cdots & C_{1\,15} \\ C_{21} & & & \vdots & & \vdots \\ \vdots & & & \vdots & & \vdots \\ \vdots & & \cdots & C_{rs} & \cdots & \vdots \\ \vdots & & & \vdots & & \vdots \\ \vdots & & & \vdots & & \vdots \\ C_{15\,1} & \cdots & \cdots & \cdots & \cdots & C_{15\,15} \end{bmatrix} \begin{Bmatrix} \ddot{q}_1 \\ \ddot{q}_2 \\ \vdots \\ \ddot{q}_s \\ \vdots \\ \ddot{q}_{14} \\ \ddot{q}_{15} \end{Bmatrix} = \begin{Bmatrix} -f_1(\dot{q}_1, q_1) \\ -f_2(\dot{q}_2, q_2) \\ \vdots \\ -f_r(\dot{q}_r, q_r) \\ \vdots \\ -f_{14}(\dot{q}_{14}, q_{14}) \\ -f_{15}(\dot{q}_{15}, q_{15}) \end{Bmatrix}$$

This matrix equation can be solved for the accelerations using a matrix inversion method, in this case Gauss elimination. The resulting differential equations can be solved with a fourth-order Adams-Bashforth predictor and an Adams-Mounton corrector. Since this method is not self-starting, a fourth-order Runge-Kutta method is used for the first four time steps. The predictor method is used to estimate the lower order terms that make up the functions on the right side of the equations. These are used to form the above matrix equation which is solved for the accelerations. These are used to improve the estimate

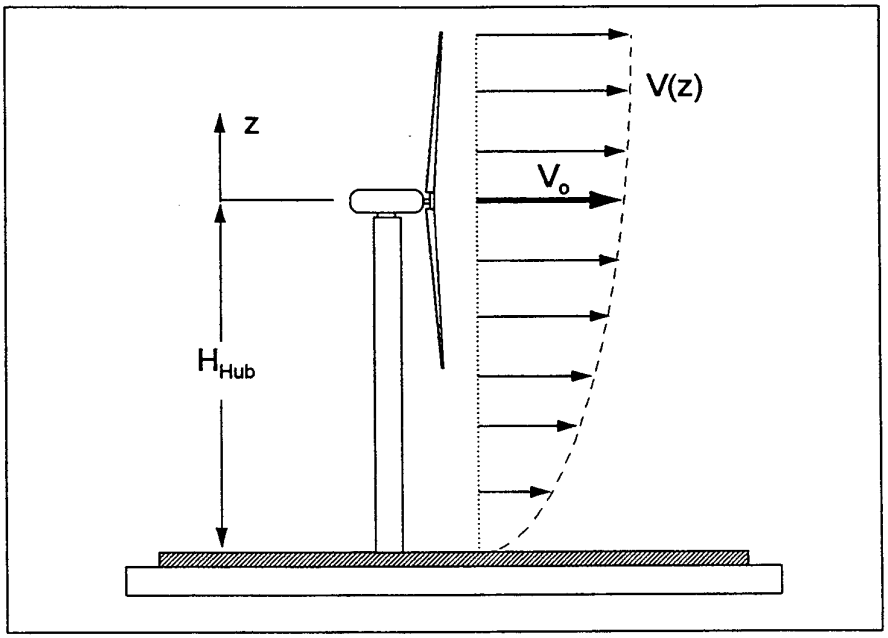

made by the predictor. After several iterations, the corrector is used to make a final estimate, and a final

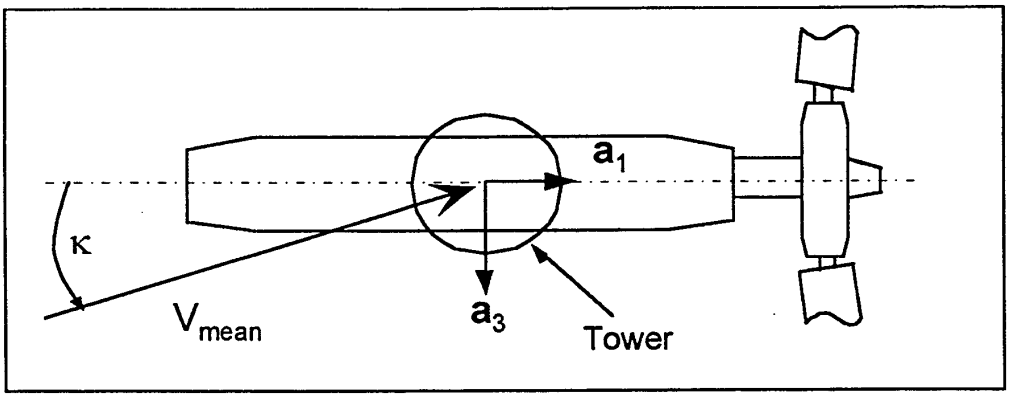

determination of the acceleration is made. This gives the final solution for this time step.

Figure 2.10.Wind Shear

Figure 2.11.Variable Wind Angle (Top View of Turbine)

2.10 References

1. Kane, T. R. and Levinson, D. A., *Dynamics: Theory and Applications*, McGraw-Hill Book Co., New York, 1985.

2. Harman, C. R., "PROPX: Definitions, Derivatives, and Data Flow," M. S. Project, Oregon State University, Corvallis, OR, August 1994.

3. Veers, P. S., "Modeling Stochastic Wind Loads on Vertical Axis Wind Turbines," SAND83-1909, Sandia National Laboratory, September 1984.

3.0 CONFIGURATION AND NOMENCLATURE USED FOR A THREE-BLADED HAWT

3.1 Overview

The FAST_AD code can model a three-bladed horizontal axis wind turbine (HAWT) with 16 degrees of freedom (DOF). The first three DOF are the blade flapwise tip motion for the first mode. The fourth DOF is for the rotor azimuth angle, while DOF five is the generator azimuth angle. These DOF account for variable rpm and drive shaft flexibility, respectively. The sixth DOF is yaw. The seventh thru tenth DOF account for tower motion, two longitudingal modes and two lateral modes. The eleventh, twelfth, and thirteenth DOF give the tip displacement for each blade for the second flapwise mode. The last three DOF, fourteen, fifteen, and sixteen are for the blade edgewise tip displacement for the first edgewise mode.

Table 3-1 below compares the degrees of freedom and their identification for the two and three blade operation of FAST_AD. It is to be noted that nacelle tilt and teeter are available only during two blade operation.

Table 3-1 Comparison between Two and Three Bladed Models

Two Blades	Three Blades	Description
q_1	q_1	Blade 1 flapwise tip displacement for mode 1
q_2	q_2	Blade 2 flapwise tip displacement for mode 1
	q_3	Blade 3 flapwise tip displacement for mode 1
q_3		Teeter angle (only available for two bladed turbines)
q_4	q_4	Azimuth angle, rotor side
q_5		Nacelle tilt angle
	q_5	Azimuth angle, generator side (three blades)

q_6	q_6	**Yaw angle**
Two Blades	**Three Blades**	**Description**
q_7	q_7	**Longitudinal tower top displacement for mode 1**
q_8	q_8	**Latitudinal tower top displacement for mode 1**
q_9	q_9	**Longitudinal tower top displacement for mode 2**
q_{10}	q_{10}	**Latitudinal tower top displacement for mode 1**
q_{11}	q_{11}	**Blade 1 flapwise tip displacement for mode 2**
q_{12}	q_{12}	**Blade 2 flapwise tip displacement for mode 2**
	q_{13}	**Blade 3 flapwise tip displacement for mode 2**
q_{13}	q_{14}	**Blade 1 edgewise tip displacement**
q_{14}	q_{15}	**Blade 2 edgewise tip displacement**
	q_{16}	**Blade 3 edgewise tip displacement**
q_{15}		**Azimuth angle, generator side (two blades)**

4.0 AeroDyn AERODYNAMICS

4.1 Theory

Strip theory, modified to include the effects of wake expansion, tip loss, yaw and dynamic stall is used in the AeroDyn subroutine. Strip theories, in various forms, have been the standard method of design and design analysis. The reasons are both positive and negative. On the positive side, strip theories are easy to program, inexpensive to run, and readily adaptable to any size computer. Strip theories have also met with modest success in load prediction. One source of error in load prediction has been airfoil data, and the uncertainties in airfoil data are frequently large enough to mask the inaccuracies of the theory. The lack of measurements of flow field variables is, in fact, one of the negative reasons for use of strip theory.

With an almost complete lack of flow field measurements, there is little data to evaluate the shortcomings of strip theory. Vortex analysis, both fixed and free wake, have been developed for research applications; however, the complexity, cost, and run times have prevented any wide-scale deployment of more sophisticated analysis methods.

The foremost assumption in strip theory is that individual streamtubes or strips can be analyzed independently of the rest of the flow. Such an assumption works well for cases where the circulation distribution over the blade is relatively uniform so that most of the vorticity is shed at the blade root and the blade tip. The use of partial span pitch control on HAWTs introduces a discontinuity in the circulation and appreciable vorticity can be shed near the junction between the main blade and tip. For such geometries, strip theory may not be able to account for the interaction between the shed vorticity and adjacent blade sections. Fortunately, partial span pitch control is employed to spill power when operating above rated wind speed. At high wind speeds, the induced velocity is relatively small. Thus, while calculation errors will exist when using strip theory methods to analyze partial span pitch control sections, the errors will occur when the induced velocities are small. The ultimate evaluation of the accuracy of strip theory will depend upon the acquisition of flow field and loading data for a blade with partial span pitch control under operating conditions that include large pitch deflections of the tips.

The second assumption associated with the development of strip theory is to neglect spanwise flow. Strip theory does not predict any induced flows along the blades; however, when the blades are inclined to the plane perpendicular to the axis of rotation such as occurs when the blade has a coning angle, the wind has a component which is directed along the span of the blade. This component is neglected and two-dimensional flow is assumed to occur over the blade section. Airfoil data is taken from two-dimensional section test data. Figure 4.1 shows the geometry to be used. Note that r is measured along the blade rather than radially.

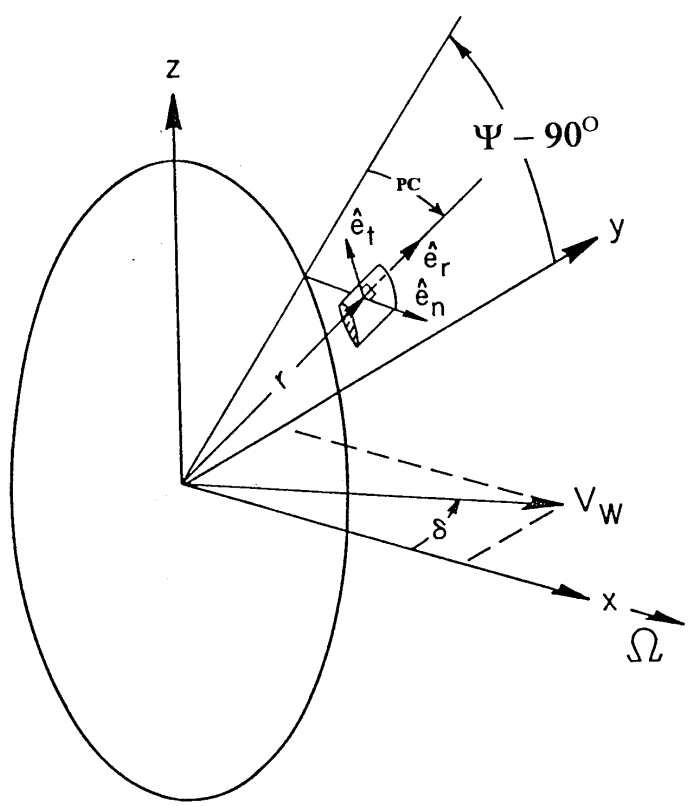

Figure 4.1.Rotor Geometry and Coordinates, for a Yawing, Non-Tilting Rotor

The next assumption is a key to the use of strip theory in load analysis. This assumption is that flow conditions vary in the direction of blade rotation (Figure 4.1). With this assumption, the "strip" to be analyzed is a polar segment positioned at distance r from the axis of rotation. The wind speed, V_w, is assumed to be variable in time and space and the wind is not assumed to be aligned with the axis of rotation so that the yaw angle, δ, must be included in the analysis; however, the for the initial analysis, we shall ignore the yaw angle.

Momentum and moment of momentum control volume relations are used to obtain relations for the induced axial and tangential velocities.

For the streamwise force, the momentum flux in a direction normal to the blade through a polar segment is

$$C_{T_L} \frac{1}{2} \rho V^2 r\cos^3 PC \, dr \, d\psi \tag{4.1}$$

Here C_{T_L} is the local thrust coefficient.

The normal force due to lift on a rotor with B blades of chord c is

$$Bc \frac{1}{2} \rho W^2 C_L \cos\phi dr \left(\frac{d\psi}{2\pi} \right) \tag{4.2}$$

where the last factor is the fraction of time spent in the polar segment.

Equating the momentum flux to the blade force

$$C_{T_L} = \left(\frac{Bc}{r} \right) \left(\frac{W}{V} \right)^2 \frac{C_L \cos\phi}{2\pi\cos^3 PC} \tag{4.3}$$

Figure 4.2 illustrates the velocity components for a blade element with coning.

The moment of momentum for a polar segment can be expressed as

$$\rho V(1 - a)\, a' \Omega^2 r^3 \cos^4 PC\, dr\; F\, d\psi \tag{4.4}$$

where F is the tip loss factor. The tip loss factor F is the ratio of the average value of circulation to the local value of circulation at the blades. The blade torque due to lift is

$$Bc\, \frac{1}{2}\, \rho W^2 C_L \sin\phi\; r\cos PC\, dr \left(\frac{d\psi}{2\pi} \right) \tag{4.5}$$

Equating these two expressions and expressing W in terms of ϕ one obtains

$$\frac{a'}{1 + a'} = \frac{Bc}{8\pi r}\, \frac{\quad}{Fc} \tag{4.6}$$

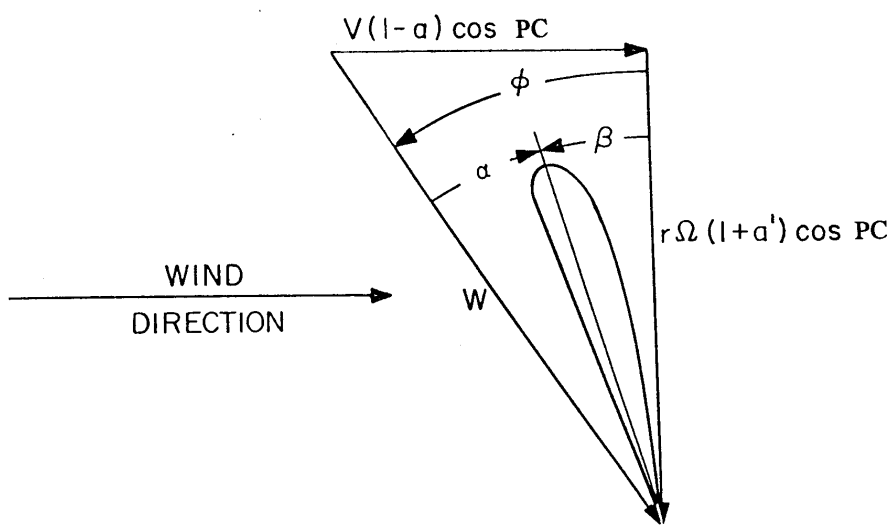

Figure 4.2.Velocity Diagram for a Blade element with Coning

For values of a ≤ 0.2 the thrust coefficient is written $C_{T_L} = 4aF(1-a)$* so that Eq. (4.4) becomes

$$\frac{a}{1-a} = \frac{Bc}{8\pi rF} \frac{C_L \cos\phi}{\sin^2\phi \cos PC} \tag{4.7}$$

Dividing Eqs. (4.6) by (4.7) shows that the induced velocity is perpendicular to the relative velocity at the rotor. Accordingly we can replace Eq. (4.6) with

$$a'(1+a') = a(1-a)\ v^2/(r\Omega)^2 \tag{4.8}$$

which is simple to program and retains the proper orientation of the induced velocity. For values of a ≥ 0.2, the local thrust coefficient is given by

$$C_{T_L} = C_{T_L}\Big|_{a_c} + \frac{\partial C_{T_L}}{\partial a}\Big|_{a_c} (a - a_c) \tag{4.9}$$

where $a_c = 0.2$. Figure 4.3 shows the thrust coefficient theory and data.

The equations used to determine the induced velocities are

$$a'(1+a') = a(1-a)\ (V/r\Omega)^2 \tag{4.10}$$

$$C_{T_L} = \frac{Bc}{2\pi r}\left(\frac{W}{V}\right)^2 \frac{C_L \cos\phi}{\sin^2\phi \cos PC} \tag{4.11}$$

$$C_{T_L} = \begin{cases} 4a(1-a) & a < 0.2 \\ 0.16 + 2.40a & a > 0.2 \end{cases} \tag{4.12}$$

$$C_L = C_L(\alpha) \tag{4.13}$$

---

*The current AeroDyn code uses 4aF(1-aF).

$$\alpha = \phi - \beta + \Delta\alpha_e \tag{4.14}$$

$$\tan\phi = \frac{V(1-a)}{r\Omega(1+a')} \tag{4.15}$$

An expression for the tip loss factor, F, is needed to solve Eqs. (4.10) through 4.15).

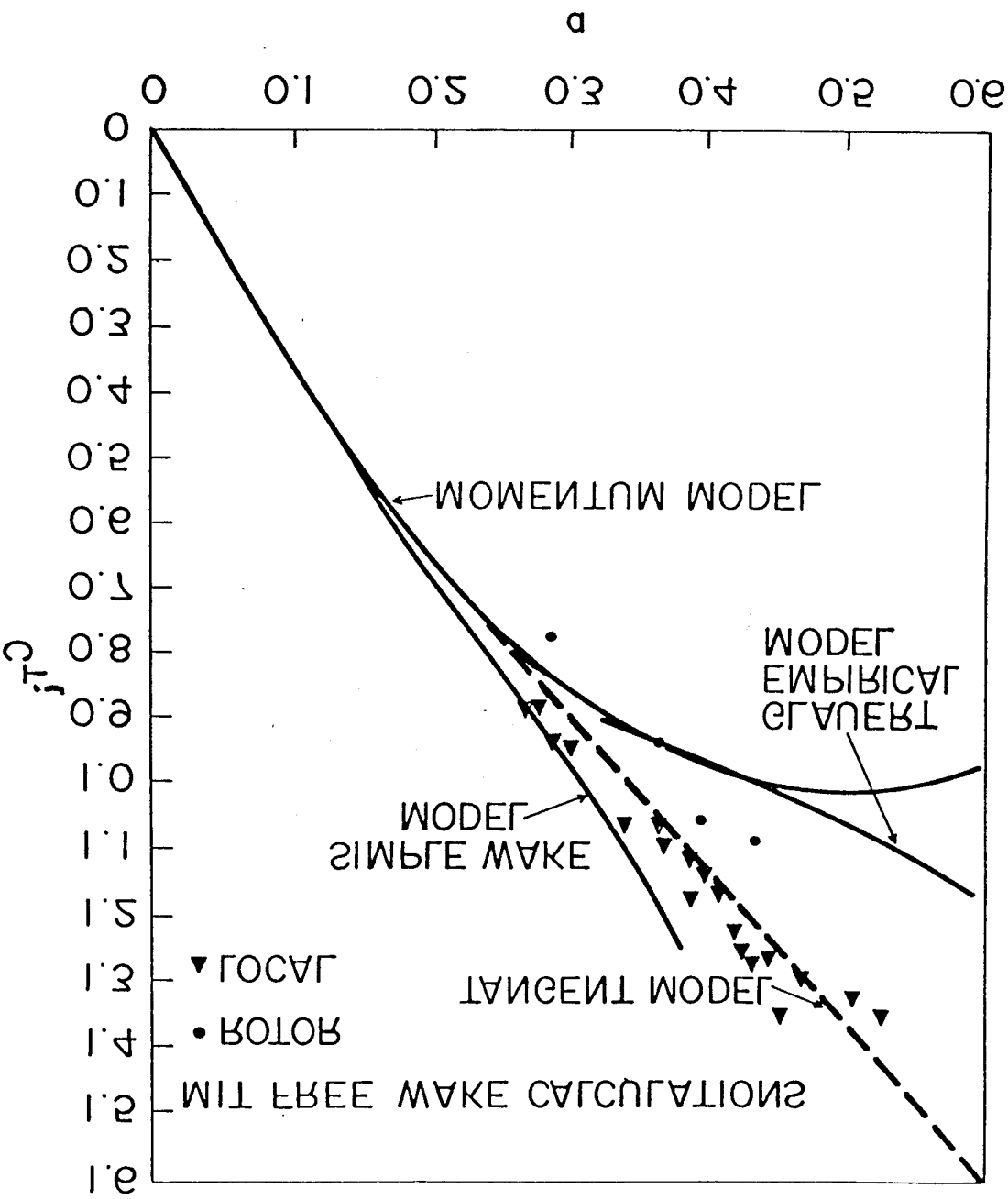

Figure 4.3. Ideal Thrust Coefficient vs. Axial Induction.
Free Wake Calculations Obtained from MIT.

4.2 Kinematics

The velocities used in the AeroDyn aerodynamics code as programmed in the FAST_AD code are the result of resolving all velocities into normal and tangential components. These components includes contributions from:

- the wind, including tower shadow, wind shear and turbulence
- rigid body motion of the nacelle (due to tilt, yaw and tower motions)
- rigid body teeter motion (for two blade machines only)
- flexible body motion of the blades with edgewise and flapwise directions

The authors of the report believe that while the effects of blade motion should be included in all calculations of the blade forces during iteration for induced velocities, the effects of blade motion should not be included in the momentum of the wind in the stream tube. As to the inclusion of the turbulence in the calculation of induced velocities, we believe that the turbulence should not be included in the calculation of induced velocity for either the blade force or the stream tube momentum. The reason for this belief is that the turbulence that produces the cyclic loads is not coherent over the rotor with a scale less than a rotor radius, and the fact that a continuous wake on the order of rotor diameters is required to produce an equilibrium wake. Thus we believe that the actual effects of turbulence are closer to the frozen wake situation and hope that future versions of AeroDyn contain a frozen wake option.

4.3 Yaw and Tilt

When the rotor yaws, the axial induction is affected by both the change in flow velocities relative to the blades and the fact that the rotor wake is deflected. The former changes are accounted for in the kinematics of the flow, the later change, the so-called skewed-wake correction is accounted by multiplying the axial induction factor by $1 + \varepsilon$ where

$$e = 0.7363(r / R)\cos^{-2}(d / 2)\sin d \sin y$$

where δ is the yaw angle and ψ is the blade azimuth angle.

It is noted that the correction changes linearly with the distance from the yaw axis ($r\sin\psi$) and linearly with yaw angle (at small angles). The $\cos^{-2}(\delta/2)$ term could be deleted as it has a singularity and does not contribute significantly until the yaw angle is well beyond the range of application. Up to yaw angles of 45°, the variation of the correction factor with yaw angle is linear with a maximum error of 5%. The use of the skewed-wake correction is quite prevalent and has been tested extensively in comparisons with test data by the developers of the AeroDyn code. At this time, the skewed-wake correction is the most accurate method available for the modeling of a yawed flow.

In the case of the two-bladed rotor in the FAST_AD code, the nacelle may tilt as well as yaw. For the tilting rotor, the aerodynamic restoring moment arises from the use of the skewed-wake applied at an angle between the rotor axis and the incoming flow, rather than the yaw angle. Although less tested than the use of the skewed-wake factor for yawed flow, the use of this factor as employed in the AeroDyn code is the best available method for analysis of tilting rotor aerodynamics.

4.4 Dynamic Stall

The lift coefficient, C_L , to be used in determining the axial and angular induced velocities is norminally a function of the angle of attack. As such, the lift coefficient is obtained from interpolation in a tabular array of lift coefficients as a function of the angle of attack. The AeroDyn code requires a tabular input of lift and drag coefficients for stations along the blade. Wind turbines operate at high angles of attack, well beyond the linear range usually associated with aircraft. Additionally, the effects of wind variation due to turbulence, tower shadow, wind shear as well as relative velocity changes cause by yaw, tilt, tower motion and teeter, blade motion can cause large and rapid change in the angle of attack. Under such conditions the aerodynamic forces have been observed to vary with the rate of change of the angle of attack and the history of the lift. Using the response of airfoil circulation to step inputs (actually approximated by an exponential), the AeroDyn code uses a convolution integral to determine the lift and drag coefficients in a continuously changing flow field. The AeroDyn code permits the user to have the dynamic stall calculations either on or off.

The dynamic stall subroutines of AeroDyn have been extensively tested via comparisons with field data. The listed references in section 4.5 document the development and validation of the AeroDyn code, particularly the dynamic stall portion of the code.

4.5 References for AeroDyn

1. Hansen, A.C., 1992, "Yaw Dynamics of Horizontal Axis Wind Turbines: Final Report." National Renewable Energy Laboratory, NREL Technical Report, TP 442-4822.

2. Hansen, A.C., C. P. Buterfield and X. Cui, 1990, "Yaw Loads and Motions of Horizontal Axis Wind Turbines." Journal of Solar Energy Engineering. Vol. 112, No. 4. Pp. 310-314.

3. Hansen, A.C., C. P. Buterfield and X. Cui, 1990, "Yaw Loads and Motions of Horizontal Axis Wind Turbines." Journal of Solar Energy Engineering. Vol. 112, No. 4. Pp. 310-314.

4. Hansen, A.C. and X. Cui, 1989, "Analyses and Observations of Wind Turbines Yaw Dynamics." Journal of Solar Energy Engineering. Vol. 111, No. 4. Pp. 367-371.

5. Hansen, A.C. and A.D. Wright, 1991, "A Comparison of Combined Experiment Flap Load Predictions by the FLAP and YawDyn Codes." Tenth ASME Wind Energy Symposium, Houston, TX.

6. Hansen, A.C., 1993, "Structural Response to Unsteady and Stall Aerodynamics." 1993 DOE Wind Energy Program Review Meeting, Golden, CO.

7. Hansen, A.C., Butterfield, C.P., 1993 Aerodynamics of Horizontal-Axis Wind Turbines. Annual Review of Fluid Mechanics, 1993. Palo Alto, Annual Reviews, Inc.

8. Leishman, J.G., Beddoes, T.S., 1989. A Semi-Empirical Model for Dynamic Stall. Journal of the American Helicopter Society. 34(3): 3-17.

9. Peters, D.A., HaQuang. N., 1988. Dynamic Inflow for Practical Applications. Journal of the American Helicopter Society. 33(4):64-68.

10. Hansen, A.C. and D.J. Laino, "User's Guide, YawDyn and AeroDyn for ADAMS® ." ME Department, University of Utah, Salt Lake City, UT. prepared for the National Renewable Energy Laboratory, Golden, CO, August 1998.

5.0 PROGRAM INPUT FILES

The code uses a main input file to describe the wind turbine's operating parameters and basic geometry. Depending on the options chosen in the main input file, additional input data files may be necessary. Sample input and data files are provided in Appendix A for the sample cases described in Section 8. Descriptions of the individual inputs to the main input file are provided in Section 6.0.

The main input file has a simple text format that can be read by most editors and imported into many word processing applications. Each line in the input file is divided into three sections: number, variable, and description. The number section contains the value assigned to the variable. Numbers of up to seven significant digits can be input, and must be separated from other sections by a space, tab, or comma. The variable section contains the name of the variable assigned to the numerical value which is used by the program. The description section of the line contains a brief description of the numerical value as a reminder to the user of its purpose. This section also contains the physical units of the numerical value, where appropriate. A sample line from the input file divided into its sections is shown below.

```
10.        VWIND        - MEAN WIND VELOCITY UPSTREAM AT HUB HEIGHT (m/s)
 ⇑          ⇑                          ⇑
Number    Variable                  Description
```

Note that only the number is read by the computer, the rest of the line is only a comment.

Near the end of the input file, there are tables that describe the blade characteristics. Six columns of data are required in this section, each of which must be separated from the other by a space, tab, or comma. There is also a table for the tower characteristics which requires four columns of data.

Note that there are no blank lines in the input file. The program reads each line of the input file in sequential order, and if any lines are inserted or deleted, data will be read incorrectly. This should never be done unless the code is changed to accept such a format.

Note also that lines containing section or file titles may be altered to suite the user. These lines are ignored by the program when the input data is read in, but should not be deleted for the same reasons mentioned in the previous paragraph. Two examples title lines from the input file are shown below:

```
---------- INPUT WITH MODE AND ADJUSTMENTS -----------

---------- DEGREE OF FREEDOM SWITCHES ----------------------
```

6.0 DESCRIPTION OF CODE INPUTS

The definitions and physical locations of some of the inputs to the main input file are not as obvious as others, so a brief description of each is given below. For inputs that require only a one or zero, a value of one indicates the desire to have that option and a value of zero indicates the opposite (i.e., 1 = yes or 0 = no). A section of the input called YAWDYN/AERODYN parameter inputs uses the inputs TRUE or FALSE. Units and reference to descriptive figures are also given where applicable.

6.1 General Inputs

NRSTRT (dimensionless) - Number of revolutions before turbulence and recording. This tells the program how many revolutions to wait before outputting data to files. It also causes a delay in including the effects of turbulence. A delay of at least three revolutions is advisable to allow the transient effects associated with starting from rest to become steady state.

TMAX (seconds) - The program stops running when TMAX has been exceeded. If turbulence effects are included, the program will terminate at the end of the turbulence file if there are less lines of data in it than the maximum time that is set by this parameter.

DT (seconds) - Step for numerical integration. Care should be taken in choosing a small enough value for DT, as the numerical solution will become unstable and cause an overflow error if DT is too large. Typical values of DT are less than 0.01 seconds. If two dimensional turbulence effects are included, DT should agree with the time incrementation in the turbulence file.

NTSKIP (dimensionless) - Number of time steps to skip for output (0 = none). Allows user to pre-filter the data and save only a portion of the output. Useful if a very small time step is required.

VWIND (m/s) - Mean wind velocity upstream of the rotor at the height of the hub.

ETA (dimensionless) - Wind shear power law exponent used to describe the roughness of the surrounding terrain at the wind turbine site. Typical values range from 0.1 to 0.2 with the higher value indicating rougher terrain. ETA is used in calculating the increase in wind speed with height due to the planetary boundary layer.

RHO (kg/m^3) - The ambient air density at the site elevation.

6.2 Degree of Freedom Switches

IZ(1) (yes or no) - Switch for including the first flapwise blade bending mode.

IZ(11) (yes or no) - Switch for including the second flapwise blade bending mode. Including this gives more accurate predictions of the blade vibration. This should not be used without IZ(1).

IZ(13) (yes or no) - Switch for first edgewise bending mode.

IZ(3) (yes or no) - Switch to include rotor teetering. If this option is off, teeter can be set to a non-zero, fixed angle.

IZD(4) (yes or no) - Switch to include the effects of a variable rotor rotational speed. 0 = constant RPM, 1 = induction generator, 2 = start-up, 3 = shut-down. Note that the two-dimensional turbulence option and the variable speed option can't be used together.

IZD(15) (yes or no) - Switch to include flexibility of the drive train. This models the drive train between the generator and rotor as a lumped torsion spring.

IZD(5) (yes or no) - Switch to include nacelle tilt.

IZ (6) (yes or no) - Switch for yaw degree of freedom. If this option is off, yaw can be set to a non-zero, fixed angle.

IZ (7) (yes or no) - Switch for first tower bending mode. All mode shapes are in Appendix D.

IZ (9) (yes or no) - Switch for second tower bending mode. This should not be used without IZ(7), and used only when added accuracy is required for tower motion.

ISHAD (yes or no) - Switch for tower shadow. This models the loss in wind speed at the rotor due to tower interference. Note that tower shadow is applicable only to turbines whose blades are down wind of the tower.

ISHR (yes or no) - Switch for wind shear. This models the effects of the planetary boundary layer on the mean wind.

ITRB2D (yes or no) - Switch to include the effects of two dimensional turbulence. This models the effects of turbulence on the local wind and requires a turbulence data file generated by the Veers' Turbulence Code [3]. The time increment of the data file should be the same as DT. Note that this turbulence option and the variable speed option can not be used together.

ITRB3D (yes or no) - Switch to include three dimensional turbulence field. A binary turbulence data file is required for each velocity component.

IDYNST (yes or no) - Switch for dynamic stall. This models dynamic stall with the Gormont Model. This option can not be used with the airfoil data file.

IWNDIR (yes or no) - Switch for varying wind direction for 2D turbulence. This option requires an input data file and can only be used with ITRB2D = 1. A sample data file is shown in Appendix A.4.

6.3 Initial Conditions

Z(1) (m) - Initial flapwise blade tip displacement (see Figure 2.1). Note that by specifying values for initial conditions close to the steady state conditions, the numerical solution technique will converge FAST_ADer and shorten computational time. This is especially useful when making repetitive runs.

Z(13) (m) - Initial edgewise blade tip displacement (see Figure 2.1).

Z(3) (deg) - Initial or fixed teeter angle (see Figure 2.1).

Z(4) (deg) - Initial azimuth angle for blade 1 (see Figure 2.1).

ZD(4) (RPM) - Steady state angular velocity (see Figure 2.1).

Z(5) (deg) - Fixed or initial tilt angle (see Figure 2.1).

Z(6) (deg) - Initial or fixed yaw angle (see Figure 2.1).

Z(7) (m) - Initial longitudinal tower displacement (see Figure 2.1).

Z(8) (m) - Initial lateral tower displacement (see Figure 2.1).

6.4 Machine Parameters

RT (m) - Blade tip radius (see Figure 2.1).

RH (m) - Blade hub radius (see Figure 2.1).

THETA (deg) - Blade collective pitch for partial-span aileron control devices (see Figure 2.1).

RRGAP (dimensionless) - Location of end of gap between blade and partial-span aileron control devices (see Figure 2.1).

RLU (m) - Underslung length (see Figure 2.1).

RLUM (m) - Distance to hub mass center from teeter pin (see Figure 2.1).

DN (m) - Distance from yaw axis to rotor/teeter pin (see Figure 2.1).

DNM1 (m) - Distance to nacelle mass center from yaw axis d1 (see Figure 2.1).

DNM2 (m) - Distance to nacelle mass center from yaw axis d2 (see Figure 2.1).

HH (m) - Hub height above ground level (see Figure 2.1).

HS (m) - Tower rigid base height (see Figure 2.1).

DELTA3 (deg) - Teeter pin orientation angle (see Figure 2.1).

BETA(1) (deg) - Blade one coning angle (see Figure 2.1).

BETA(2) (deg) - Blade two coning angle (see Figure 2.1).

6.5 Mass and Inertia

XMNAC (kg) - Nacelle mass.

XMHUB (kg) - Hub mass.

TIPM(1) (kg) - Blade one aerodynamic tip brake mass (see Figure 2.1).

TIPM(2) (kg) - Blade two aerodynamic tip brake mass (see Figure 2.1).

HTINER (kg - m^2) - Nacelle moment of inertia about tilt axis.

HSINER (kg - m^2) - Generator moment of inertia.

HYINER (kg - m^2) - Nacelle moment of inertia about yaw axis.

HINER (kg - m^2) - Hub moment of inertia about teeter axis.

6.6 Drive Train Parameters

ETAGB (dimensionless) - Gearbox efficiency.

ETAGEN (dimensionless) - Generator efficiency.

OMEGR (RPM) - Rated speed for induction generator (see Figure 2.7).

OMEG0 (RPM) - Initial induction generator speed for producing electricity (see Figure 2.7).

CINGEN ((N-m)/(r/s)) - Induction generator slope constant for generator side of turbine (see Figure 2.7).

YN (dimensionless) - Gearbox ratio.

QFL (N-m) - Fixed loss constant.

QVL (N-m) - Variable loss constant.

QBRAKE (N/m) - Mechanical brake torque value.

QMOTOR (N-m) - Motor start-up torque for generator side of turbine (see Figure 2.7).

ZKDRV ((N-m)/rad) - Drive train torsional spring constant.

CDRV ((N-m)/s) - Drive train torsional damper constant.

6.7 Tower Parameters

CTWR (%) - Tower structural damping in percent of critical.

EL (dimensionless) - Tower shadow width/rotor radius. Tower shadow width is L in Figure 2.9.

EPP (dimensionless) - Tower shadow velocity deficit. This varies from 0 to 1 and is shown as ε in Figure 2.9.

TWRMT1 (dimensionless) - Tower mass tuner for 1st mode.

TWRMT2 (dimensionless) - Tower mass tuner for 2nd mode.

TWRST1 (dimensionless) - Tower stiffness tuner for 1st mode.

TWRST2 (dimensionless) - Tower stiffness tuner for 2nd mode.

NXTWR (dimensionless) - Number of tower increments.

N2 (dimensionless) - Number of input stations to specify tower geometry.

AMSTWR (dimensionless) - Factor to adjust tower mass.

STFLNG (dimensionless) - Factor to adjust longitudinal stiffness.

STFLAT (dimensionless) - Factor to adjust lateral stiffness.

6.8 Tower Distributed Parameters

RAD (dimensionless) - Fractional height along tower of the following parameters:

MASS (kg/m) - Mass per unit length of tower section.

LONG STIF (Nm^2) - Longitudinal tower stiffness.

LAT STIF (Nm^2) - Lateral tower stiffness.

6.9 Tilt, Yaw and Teeter Parameters

ZKYAW ((N-m)/rad) - Yaw spring constant.

ZCYAW ((N-m)/(rad/s) - Yaw damper constant.

ZKTILT ((N-m)/rad) - Tilt spring constant.

ZCTILT ((N-m)/(rad/s)) - Tilt damper.

TILTSTOP1 (deg) - Tilt soft stop angle.

TILTSTOP2 (deg) - Tilt hard stop angle.

QKTSTOP1 ((N-m)/rad) - Nacelle soft stop stiffness.

QKTSTOP2 ((N-m)/rad) - Nacelle hard stop stiffness.

COULMB (Nm) - Coulomb teeter damping moment at teeter hinge.

ITSPDM (dimensionless) - Teeter damper type. Choices are: 0 = no teeter damper, 1 = linear damper, 3 = user's function. Option 3 requires modification of the source code.

CTEET ((N-m)/(rad/s)) - Teeter damper constant.

ZKTEET(1) (N-m) - First teeter spring coefficient for cubic curve fit.

ZKTEET(2) ((N-m)/rad) - Second teeter spring coefficient for cubic curve fit.

ZKTEET(3) ((N-m)/rad^2) - Third teeter spring coefficient for cubic curve fit.

QCTEET (deg) - Angle where teeter damper begins (see Figure 2.1).

QKTEET (deg) - Angle where teeter spring begins (see Figure 2.1).

TSTOP (deg) - Teeter stop angle (see Figure 2.1).

6.10 Blade Parameters

CBLDF (N-sec) - Flapwise blade structural damping.

CBLDE (N-sec) - Edgewise blade structural damping.

CDATIPN (m^2) - Drag due to tip brakes at normal operation (Cd * flat plate drag area).

CDATIPB (m^2) - Drag due to tip brakes at braking (Cd * flat plate drag area).

IAIRFO (0, 1, 2, or 3) - Blade airfoil choice. Choices are as follows: 0 = Table look up, 1 = NASA LS-1 laminar flow airfoil, 2 = NACA 23000, 3 = NACA xxxxx experimental. Option 0 requires a airfoil data file. An example of this file is provided in Appendix A.5.

NR (dimensionless) - Number of increments along blade for integration of forces. The more increments, the more accurate the integral, but longer the computational time. A good compromise for NR is 20.

N1 (dimensionless) - Number of rows of data in blade sectional data per blade.

STFFAC(1), (2) - Factor to adjust blade flapwise stiffness in blade sectional data.

STEFAC(1), (2) - Factor to adjust blade edgewise stiffness in blade sectional data.

AMSFAC(1), (2) - Factor to adjust blade mass per unit length in blade sectional data.

CHDFAC(1), (2) - Factor to adjust blade chord in blade sectional data.

TWIFAC(1), (2) - Factor to adjust blade aerodynamic twist angle in blade sectional data.

TWSFAC(1), (2) - Factor to adjust blade structural twist angle in blade sectional data.

6.11 Blade Sectional Data

RAD (dimensionless) - Fractional location along turbine blade of following parameters:

CHORD (m) - Length of airfoil section from the leading edge to trailing edge.

THICK (dimensionless) - Maximum thickness of the airfoil/chord length.

AERO TWIST (deg) - Blade aerodynamic twist angle.

MASS (kg/m) - Mass per unit length of blade section.

FLAP STIFF (Nm^2) - Blade flapwise stiffness.

STRUC TWIST (deg) - Blade structural twist angle.

EDGEW STIFF (Nm^2) - Blade edgewise stiffness.

6.12 Mode Shapes

PC(1,1-6) (dimensionless) - Coefficients of polynomial equation used to model first flapwise mode shape of blade.

PC(2,1-6) (dimensionless) - Coefficients of polynomial equation used to model second flapwise mode shape of blade.

PC(3,1-6) (dimensionless) - Coefficients of polynomial equation used to model first edgewise mode shape of blade.

PC(4,1-6) (dimensionless) - Coefficients of polynomial equation used to model first mode shape of tower.

PC(5,1-6) (dimensionless) - Coefficients of polynomial equation used to model second mode shape of tower.

6.13 Format of Output File

NC(1-30) (dimensionless) - Choice of variables to output to files. There are 30 available spaces for output data, ten in each of three files. The list of data available for output is included at the end of this input file for reference use. It is not read by the program.

NCMAX (dimensionless) - Maximum number of variables to output. Not all of the spaces available in output files must be used. If less than 30 columns of output is desired, NCMAX may be set to less than 30. It should not be set to more than 30. If this number is less than 10, only one output file will be created. If this number is less than 20, only two output files will be created.

By varying the values in the array NC( ), the form of the output files can be changed. For example, if the only output desired is time, azimuth angle of the rotor, and teeter angle, then the first three elements of NC would be 0, 13, 9, and NCMAX would be set to 3. Only one output file will be created, and it will have only three columns of data.

6.14 YawDyn/AeroDyn Parameter Input

WAKE (dimensionless) - This flag parameter determines whether the induced velocites (induction factors) will be calculated. (True) Normal iteration for induction factors, (False) Ignore wake. **This parameter should normally be set TRUE.**

ATOLER (dimensionless) - Tolerance (convergence criteria) for iterative solution to determine the induction factor. **A good default value to use is 0.005.** This value may be changed to avoid convergence problems or to speed the calculations.

SWIRL (dimensionless) - This parameter determines whether to calculate the angular or tangential induced velocity a'. (True) include tangential induced velocity a', (False) tangential induced velocity a' = 0. **This parameter should normally be set TRUE.** If the WAKE parameter is set (False) then a' is set to zero independent of this parameter.

DYNINFL (dimensionless) - This flag controls whether a first-order lag is applied to the induction factor. The parameter limits the rate at which the induced velocity can change to simulate the time required for the wake to adjust to a new operating state. A (False) value sets the wake in equilibrium with the blade element forces ("quasi-steady" or equilibrium wake assumption). (True) use dynamic inflow induction lag, (False) use quasi-steady. **At this time it is recommended that a FALSE value be used for the dynamic inflow option.**

WINDFIL (dimensionless) - A flag to indicate the source of wind speed and direction data. (True) read wind file data whose name is enter by the next parameter WNDFILNAME, (False) don't read wind file data. This allows the program to use test data or synthesized time series of wind conditions.

WNDFILNAME (dimensionless) - Wind data file name. This name can be up to 100 characters long and can include the path specification for the file. Leading and trailing spaces are ignored.

TURBLNT (dimensionless) - This flag determines whether to read wind data will be obtained from turbulence files. (True) read turbulence data files for wind input, (False) don't read turbulence data files. The turbulence data files contain wind shear and all three components of windspeed. A (False) flag indicates wind information will be found either in the file WNDFILNAME or other inputed values.

TURBFILE (dimensionless) - Turbulence data file string that determines the filenames where the turbulence data are found. This string is the prefix that is common to all three file names. It can be up to 100 characters in length with the path specification for the files. The filenames must end in u_cmp.dat, v_cmp.dat, and w_cmp.dat. Each file contains one component of the wind vector. Ex. Enter a name awt9ms and the program will look for 3 input files with the name awt9msu_cmp.dat, awt9msv_cmp.dat, and awt9msw_cmp.dat.

The next three integer values control the creation and contents of a file containing blade element aerodynamic data (file 'ELEMENT.PLT'). The blade element data are written by a loop controlled by these integer values.

IPRFRST (dimensionless) - First element to write data.

IPRLAST (dimensionless) - Last element to write data.

IPRINC (dimensionless) - Element increment to write data.

Ex. If you entered 1, 10, 3 for these values, then data for elements number 1,4,7, and 10 will be written to the ELEMENT.PLT file.

SIUNIT (dimensionless) - (True) SI unit system, (False) English unit system. **This must be set to (TRUE) for FLAP_AD.**

VZ (m/s) - Vertical component of wind speed. (This is the z-component of wind speed, thus a positive value is a wind blowing up from the ground.) For flat terrain, this is normally 0, but can be significant in complex terrain. **This value is ignored when WINDFIL or TURBLNT equal TRUE.**

HSHR (dimensionless) - Horizontal wind shear coefficient across the rotor disc. This parameter should normally have a value in the range of -1 to +1. and represents the wind speed at the blade tip on one side of the rotor, minus the wind at the blade tip on the opposite side of the rotor, divided by the hub wind speed. The shear is in the direction perpendicular to the mean, hub-height wind vector (the +y direction when the wind direction is zero). A linear variation of wind speed across the disc is used for shear in the horizontal direction. **This value is ignored when WINDFIL or TURBLNT equal TRUE.**

NOIECEWS (dimensionless) - (True) power law vertical shear used, (False) IEC Extreme wind shear linear vertical shear is used. If WINDFIL is (True), then a value of true also means that the VGD column of that file is an IEC gust velocity. **This flag is ignored when TURBLNT equal TRUE.**

NUMFOIL (dimensionless) - The number of different airfoil tables that will be read to describe the blade elements. A maximum of 20 files can be used.

FOILNM( ) (dimensionless) - Airfoil table file names. Number of airfoil file names must equal number specified by NUMFOIL. The filenames are limited to 30 characters. Trailing and leading blanks in the filename are ignored. Only one filename is entered on each line.

NFOIL (dimensionless) - Airfoil ID number for each element. The number of elements was specified by N1 parameter. If N1 = 12, then there must be 12 ID numbers. If a value of NFOIL =1, then the blade element will use data from the first airfoil file. NFOIL =3, then the blade element will used data from the third airfoil file. Each blade element will have a airfoil data file associated with it.

6.15 Possible Output Quantities

This part of the input file is not used by the program. It is included to facilitate the output specification part of the input.

0) = Time, sec

1) = Blade 1 out-of-plane tip deflection, cm

2) = Blade 1 in-plane tip deflection, cm

3) = Blade 2 out-of-plane tip deflection, cm

4) = Blade 2 in-plane tip deflection, cm

5) = Blade 3 out-of plane tip deflection, cm

6) = Blade 3 in-plane tip deflection, cm

7) = Hub height wind speed, m/s

8) = Hub height wind direction, deg

9) = Teeter angle, deg

10) = Yaw angle, deg

11) = Longitudinal tower top deflection, cm

12) = Lateral tower top deflection, cm

13) = Rotor azimuth angle, deg

14) = Generator azimuth angle, deg

15) = Shaft rotational speed, rpm

16) = Generator rotational speed, rpm

17) = Nacelle tilt angular acceleration, deg/sec2

18) = Nacelle relative tile angle, deg

19) = Nacelle absolute tilt angle, deg

20) = Nacelle tilt angular velocity (deg/s)

21) = Blade 1 out-of-plane bending moment at root, kNm

22) = Blade 1 in-plane bending moment at root, kNm

23) = Blade 2 out-of-plane bending moment at root, kNm

24) = Blade 2 in-plane bending moment at root, kNm

25) = Shaft torque, kNm

26) = Generator torque brake, kNm

27) = Undefined

28) = Undefined

29) = Blade 1 out-of-plane bending moment at 60% radius, kNm

30) = Blade 1 in-plane bending moment at 60% radius, kNm

31) = Rotor torque, kNm

32) = Power, KW

33) = Rotor thrust, kN

34) = Tower yaw moment, kNm

35) = Tower longitudinal pitch moment, kNm

36) = Tower lateral pitch moment, kNm

37) = Shaft bending moment, aligned with blade, kNm

38) = Shaft bending moment, 90 deg from blade, kNm

39) = Generator torque, kNm

40) = Undefined

6.16 References

1. Hansen, A. Craig, “User’s Guide to the Wind Turbine Dynamics Computer Programs YawDyn and AeroDyn for ADAMS®,” University of Utah, June 1996.

7.0 PROGRAM OUTPUT FILES

The program stores four output data files based on calculations from the input files. The output files are named by the user when prompted at the beginning of a run. The name provided by the user is combined with an extension designating the number of the output file. For example, if the user desires to name the output files based on the word "AWT", The program will create three files named AWT.SUM, AWT.OUT, and GFOSUB.OPT.

The first output data file (AWT.SUM) contains the basic input file parameters, and computed frequencies for the blades and tower. The '.OUT' output file contain data chosen by the user in the main input file. The available output variables are shown in Table 7.1.

If the user desires output of other variables not included in Table 7.1, the code must be changed and recompiled. The array variables ZMOTN and ZLOAD are printed directly to the output files and can be changed in Subroutines Motion and Loads. ZMOTN is a one dimensional array that contains 20 displacements and angles. ZLOAD is the same size but contains loading terms. To change the headings printed in the output files, the text fields in Subroutine Setup should be changed.

Note that the power and generator torque will be output as zero in the files when the constant RPM option in the input file is set to zero [i.e., IZD(4) = 0]. This does not mean that the turbine is not capable of generating electricity, but reflects that the generator is not connected to the drive train. Calculations involving power must include IZD(4) options 1, 2, or 3.

The third file has a fixed output name GFOSUB.OPT. It writes blade element geometry data, airfoil data files at the corresponding blade element, and the summary of combined FAST/AeroDyn input parameters.

Table 7.1. Output Variables for ".OUT" File

Index Number		Description
0	' Time '	Time, sec
1	'Bld1out'	Blade 1 out-of-plane tip deflection, cm
2	' Bld1in'	Blade 1 in-plane tip deflection, cm
3	'Bld2out'	Blade 2 out-of-plane tip deflection, cm
4	' Bld2in'	Blade 2 in-plane tip deflection, cm
5	'Bld3out'	Blade 3 out-of-plane tip deflection, cm
6	'Bld3in'	Blade 3 in-plane tip deflection, cm
7	'HH_Wsp'	Hub height wind speed, m/s
8	'HH_Wdir'	Hub height wind direction, deg
9	'Teeter'	Teeter angle, deg
10	' Yaw '	Yaw angle, deg
11	' TwrLng'	Longitudinal tower top deflection, cm
12	'TwrLatr'	Lateral tower top deflection, cm
13	' RtrAzm'	Rotor azimuth angle, deg
14	' GenAzm'	Generator azimuth angle, deg
15	' RotRPM'	Shaft rotational speed, rpm
16	' GenRPM'	Generator rotational speed, rpm
17	'TltAccl'	Nacelle tilt angular acceleration, deg/sec^2
18	'RlTilt'	Nacelle relative tile angle, deg
19	'AbTilt'	Nacelle absolute tilt angle, deg
20	'TltRate'	Nacelle tilt angular velocity (deg/s)
21	' M1ouRt'	Blade 1 out-of-plane bending moment at root, kNm
22	' M1inRt'	Blade 1 in-plane bending moment at root, kNm
23	' M2ouRt'	Blade 2 out-of-plane bending moment at root, kNm
24	' M2inRt'	Blade 2 in-plane bending moment at root, kNm
25	'TODshaf'	Shaft torque, kNm
26	'GQbrake'	Generator torque brake, kNm
27	'Undefin'	Undefined
28	'Undefin'	Undefined
29	'M1ouR60'	Blade 1 out-of-plane bending moment at 60% radius, kNm
30	'M1inR60'	Blade 1 in-plane bending moment at 60% radius, kNm
31	'RotrTrq'	Rotor torque, kNm
32	' Power '	Power, KW
33	'RThrust'	Rotor thrust, KN
34	' TwrYaw'	Tower yaw moment, kNm
35	'TLngPch'	Tower longitudinal pitch moment, kNm
36	'TLatPch'	Tower lateral pitch moment, kNm
37	' Shaft0'	Shaft bending moment, aligned with blade, kNm
38	'Shaft90'	Shaft bending moment, 90 deg from blade, kNm
39	'GenTorq'	Generator torque, kNm
40	'Undefin'	Undefined

8.0 EXAMPLE CASE STUDIES

To provide insight into the operation of the program, sample runs are included for a turbine under steady wind conditions and for turbulent wind conditions. The turbine has two blades, a tilting nacelle, and other specifications given in Tables 8.1, 8.2, and 8.3.

This sample run includes the effects of two-dimensional turbulence, which means that an additional input data file developed with the Veers' Turbulence Code is required. This file as well as the main input file and resulting output files, are included in Appendices A and B. The CD also includes files representative of typical runs.

Table 8.1. Turbine Specifications

Parameter	Specification
	20.3 m/s (45 MPH)
Rotor diameter	27.44 m (90 feet)
Rotor orientation	Downwind
Rotor airfoil	NASA LS(1) 04xx
Tip speed	77 m/s (171.3 MPH)
Rotor RPM	53.3 RPM
Generator type	Induction
Hub Height	42 m (137.8 feet)
Pitch	Fixed
Yaw	Passive
Coning angle	7˚
Natural Frequencies	
Teeter	0.9 Hz
Tower	1.21 Hz
First Flapwise	2.32 Hz
Second Flapwise	6.91 Hz
First Edgewise	~ 4.7 Hz

Table 8.2. Blade Parameters

Radius %	Chord m	Thick Chord t/c	Aero. Twist (deg)	Mass (kg/m)	Flapwise Stiffness ($N\text{-}m^2$)	Struct. Twist (deg)	Edgewise Stiffness ($N\text{-}m^2$)
0.0000	0.772	.26	6.10	90.37	44200000	10.50	117000000
0.0242	0.843	.26	5.85	93.89	43600000	10.44	140000000
0.0606	0.869	.26	5.69	43.91	21000000	10.40	64000000
0.0949	0.960	.26	5.69	46.82	20200000	10.40	79400000
0.1139	0.987	.26	5.39	48.22	18000000	10.20	90700000
0.2182	1.128	.26	4.93	50.78	11700000	9.46	111000000
0.3224	1.142	.26	4.01	44.66	7530000	8.41	96400000
0.4267	1.070	.26	2.88	37.38	4870000	6.32	71500000
0.5309	0.991	.26	1.76	31.32	3050000	4.09	48700000
0.6352	0.899	.20	0.82	25.59	1800000	2.33	28900000
0.7394	0.785	.20	0.25	21.41	938000	1.17	19100000
0.8436	0.655	.20	0.08	16.62	400000	0.48	10100000
0.9479	0.486	.20	0.03	9.68	103000	-0.20	2780000
1.0000	0.399	.20	0.00	3.90	103000	-0.22	2780000

Table 8.3. Tower Parameters

Radius %	Mass kg/m	Longitudinal Stiffness Nm^2	Lateral Stiffness Nm^2
.000	492.86	71900000000.	71900000000.
.119	363.45	51400000000.	51400000000.
.238	343.77	36400000000.	36400000000.
.357	291.85	22500000000.	22500000000.
.476	281.77	12900000000.	12900000000.
.595	266.66	5900000000.	5900000000.
.715	253.23	2150000000.	2150000000.
.834	251.86	1360000000.	1360000000.
.953	248.13	745000000.	745000000.
1.000	248.13	551000000.	551000000.

Upon running the code, the following appears on the computer screen (program text is in plain type, user entry is bold, and explanatory comments are in italics):

```
Enter Name of Input File -> awt.inp
Enter Prefix of Output Files (no extension) -> awt
Select Screen Option:

    Option                                          Number

    Simulation Status Only                                  0
    First Group of Output Quantities                1
    Second Group of Output Quantities               2
    Third Group of Output Quantities                3

              Select Option -> 0
 ------------------------------------------------------------------------------------------------------------

                                                  Blade 1    Blade 2    Tower Top
-------------------------------------------------------------------------------------------------------------

   Weight (kg)                                    441.289    441.289    6540.577

  FIRST BLADE MODE:
   Natural Frequency (Hz)                         1.619      1.619
   Freq. w/ Centrifugal Stiff. (Hz)               2.669      2.669
  SECOND BLADE MODE:
   Natural Frequency (Hz)                         5.212      5.212
   Freq. w/ Centrifugal Stiff. (Hz)               7.829      7.829
  EDGEWISE BLADE MODE:
   Natural Frequency (Hz)                         4.575      4.575
   Freq. w/ Centrifugal Stiff. (Hz)               4.937      4.937
  TOWER

   Tower First Mode Frequency  (Hz)               1.192      1.220

   Tower Second Mode Frequency (Hz)               6.708      6.861


Reading 6x6 grid of 14 mps u-component turbulence data.
 11999 records processed.  Turbulence rate is 20 Hz.
 599.9 seconds total time duration in this turbulence file.

Reading 6x6 grid of 14 mps v-component turbulence data.
 11999 records processed.  Turbulence rate is 20 Hz.
 599.9 seconds total time duration in this turbulence file.

Reading 6x6 grid of 14 mps w-component turbulence data.
 11999 records processed.  Turbulence rate is 20 Hz.
 599.9 seconds total time duration in this turbulence file.
 Timestep:   4.455 of 335.000 seconds.  Completion at 12:18:38 on 05/26/1999.
```

This run did not use a variable speed drive train or variable wind direction. If these options were desired, the appropriate "switches" in the input file should be turned on. In the case of a variable speed

drive train, the user would have to change the variable IZD in the main input file (induction generator, start up, shut down, or variable speed generator).

Another useful feature of the program is the availability of an automatic input file. Because it becomes tedious to type the program inputs with each new run, an automatic input file can be used. To do this, the user must create a text file named USER2.INP. The program automatically looks for this file before calling for the manual input prompts. If the file is present and contains the appropriate information, the user will not have to input any of the information shown in the previous example. A sample automatic input file is shown Appendix A. This file MUST contain nine lines in the correct order shown in Table 8.3. If there are less than nine lines, an error will result and program execution will stop.

Table 8.4. Line-by-Line Description of Automatic Input File

Line	Description
1	Name of main input file
2	Prefix name of output files (e. g. AWT was used in the previous example)
3	Choices of output viewing on screen during run are 0, 1, 2, or 3
4	Name of turbulence input file-only used if ITURB = 1 in main input file
5	Name of variable wind direction input file-only used if IWNDIR and ITURB = 1
6	Name of airfoil look-up data file-only used if IAIRFO = 0
7	Name of binary input file for u-component of 3D turbulence
8	Name of binary input file for v-component of 3D turbulence
9	Name of binary input file for w-component of 3D turbulence

Lines 4-9 will be ignored if their switches are off in the main input file. The program will still read them, but not use them.

9.0 CALCULATED OPERATIONS OF THE AWT-27 USING FAST_AD;

The FAST_AD code has been created by the National Renewable Energy Laboratory by the marriage of the FAST code and AeroDyn aerodynamics subroutines. This code runs rapidly; however, it has not been compared to the test data or otherwise validated. In this paper the AWT-27 two-bladed teetering wind turbine is modeled and results are compared to test data for operation at various wind speeds and with various in-flow conditions. Start-up and shut-down calculations for time history of rotor rpm and torque were made.

9.1 Introduction

During the past year the National Renewable Energy Laboratory (NREL) has produced a new code which is a streamlined version of two existing codes, FAST[1,2] and AeroDyn,[3] which is an aerodynamics subroutine package. This new code, FAST_AD,[4] is used in this study to compare calculated loads to test data for the AWT-27p4, a two-bladed horizontal axis wind turbine. This study deals with modeling the AWT-27p4, start-up and shut-down; and with fatigue loads for various inflow conditions using a variety of delta-3 angles on the teeter hinge.

The streamlined code, FAST_AD, operates considerably faster than the FAST code and is felt to be a useful tool in wind turbine design, design analysis, and certification. Retaining the structural analysis of the FAST code but rearranging some of the kinematics, the hybrid code pushes the simulation ratio, calculation time over real time, closer to unity.

9.2 FAST_AD Code

The dynamic response of a horizontal-axis wind turbine (HAWT) has been modeled in the FAST code using both rigid body and flexible body motion. There are 15 degrees-of-freedom in the system, as shown in Table 9.1. The model accounts for blade flexibility, tower flexibility, yaw and tilt motion of the

nacelle, variations in both rotor and generator speed, blade teetering, and blade bending. By selecting various physical constants, a variety of different configurations may be simulated,

Table 9.1. FAST_AD Degrees of Freedom, 2 Blade Option

Degrees of Freedom	Type of Motion
Nacelle Yaw	Rigid Body
Nacelle Tilt	Rigid Body
Rotor Teeter	Rigid Body
Rotor Angular Velocity	Rigid Body
Shaft Angular Velocity	Rigid Body
Blade 1, Flatwise, 1st Mode	Assumed Mode
Blade 1, Flatwise, 2nd Mode	Assumed Mode
Blade 1, Edgewise, 1st Mode	Assumed Mode
Blade 2, Flatwise, 1st Mode	Assumed Mode
Blade 2, Flatwise, 2nd Mode	Assumed Mode
Blade 2, Edgewise, 1st Mode	Assumed Mode
Tower Windwise Deflection, 1st Mode	Assumed Mode
Tower Windwise Deflection, 2nd Mode	Assumed Mode
Tower Lateral Deflection, 1st Mode	Assumed Mode
Tower Lateral Deflection, 2nd Mode	Assumed Mode

including generator axis tilt, preconed blades, teetering with selected hinge locations, “delta-3" orientation, various restrictions on the teeter angle, selected drive train flexibility and damping, and tower flexibility parameters.

The aerodynamic loading of the blades in the FAST code is determined using modified strip theory with nonlinear lift and drag characteristics. The aerodynamics is driven by a wind model that consists of a deterministic portion made up of mean wind, shear, and tower interference and a stochastic portion consisting of an atmospheric turbulence model including time varying wind direction.

The major loading on the wind turbine blades is due to the aerodynamic forces of lift and drag. The local relative wind speed contains contributions from the local wind, the rigid body motion of the blade due to rotation about the drive shaft, teeter, tilt, and yaw axes, the flexible body motion of the blades and tower, and a contribution due to induction from the wake. The induced velocity is determined using strip theory wherein the local force on the blades due to lift is equated to the momentum flux. The blade force is based on the flow relative to the blade and contains the induced velocity explicitly in the velocity squared term and also contains the induced velocity implicitly in the lift coefficient and in the various trigonometric functions that are used to obtain the component of the blade force in the direction of the momentum flux.

The momentum flux through a segment of the rotor disk in the FAST code is obtained using a momentum equation. Whereas the blade force involves the flow relative to the blade, the momentum flux is determined in an inertial reference frame. The induced velocity appears both explicitly and implicitly in the momentum flux as well as in the blade force so that the induction must be solved for using iteration. A significant amount of computing time is used to determine the local induction at each time step.

In the FAST_AD code, the structural representation and the kinematics are the same as in the FAST code, the major differences in the two codes occurring in the aerodynamics and loading calculation which occur in the AeroDyn portion of FAST_AD. The aerodynamic load calculations made in the FAST_AD code are made in the undeformed, rigid configuration of the wind turbine and the kinematic input to the aerodynamic and loads calculations are determined from rigid body kinematic calculations made in the aerodynamic subroutine. The AeroDyn subroutine is widely used and has undergone continued modification. The so-called skewed wake correction in the AeroDyn subroutine insures the aerodynamic stability in yaw.

The FAST_AD code retains switches for each degree-of-freedom. This feature allows certain actions to be omitted during analysis This is a distinct advantage when examining low frequency events so that the time step may be selected to be rather large and the code run times are minimal.

Although there are 15 degrees-of-freedom in the 2-bladed version of FAST_AD, the fixed maximum number of motions represents a particular limitation of the code. For example, main shaft flexural contributions to rotor/nacelle vibration are not included, and the code user is limited to the degrees-of-freedom which are built into the code.

9.3 Modeling the AWT-27

The AWT-27 wind turbine was tested extensively and has been selected to compare calculated results from the FAST_AD code to field data. The wind turbine, which has two 45-foot (13.7 m) teetering blades, is a fixed pitch, free yaw, downwind machine. The rotor blades employ the S800 series airfoil sections. The specifications for the AWT-27 are summarized in Table 9.2.

Table 9.2. AWT-27 Turbine Specifications

Rated Power	275 kW
Rated Wind Speed	17 m/s
Rotor Diameter	27.2 m
Rotor Type	Teetered – Underslung
Rotor Orientation	Downwind
Rotor Airfoil	S800 series
Tip Speed	77 m/s
Cut-In Wind Speed	6 m/s
Rotor rpm	54 rpm
Generator Type	300 kW, Induction
Gearbox	Planetary, 33.77:1
Hub Height	42 m
Tower	Open – Truss
Pitch	Fixed
Yaw	Passive
Overspeed Control	Tip Vanes
Total Mass on Tower	7074 kg
Coning	7°

The first problem encountered in modeling the AWT-27 was with the tower which was found to have a significant amount of shear deflection. In the FAST and FAST_AD codes, the tower is modeled as an Euler Beam so that some modifications were needed. The codes model each mode as an assumed shape and model the frequency with a second order ordinary differential for each mode. The shear deflection for the tower was incorporated into the code by "tuning" each differential equation with the mass term while retaining the stiffness according to the analysis including shear deflection. Using this approach, both the stiffness and frequency obtained from a finite element analysis were modeled in the code. Specifications concerning mass and stiffness distributions for both the tower and the blades were obtained

from KAMZIN Technology, Incorporated, (KTI) of Seattle, Washington.[5] Shear deflection magnitudes for the blades were small enough that the Euler Beam Model could be used without modification.

The aerodynamics of the blade, that is the lift and drag coefficients as a function of angle of attack were obtained from KTI[5] and initially used without modification. Further investigation revealed that the supplied aerodynamics were compiled several years ago.

During the starting of the rotor, the rotor starts from rest and accelerates to operating rpm. As a consequence, the Reynolds Number of the flow over the blade goes from several hundred thousand to over a million (the blade Reynolds based on chord is about $2\text{-}10^6$ at the blade tip at full speed). The aerodynamics of the airfoils operating below a chord Reynolds Number of a million at high angles of attack has been investigated.[9]

The torque delivered by the generator when acting as a motor during the start-up was modeled as a constant. While a controller was in place to limit generator current during the start-up, the variation of torque as a function of rpm was unknown and the constant value was used until the rotor reached rated slip.

The AWT-27 uses aerodynamic tip brakes during normal and fast stops. The tip vanes, which are parallel to airfoil chord during normal operation, tilt to provide a near flat plate configuration to the on-coming flow. In modeling the tip vanes, the product C_DA was estimated to have a maximum value of 0.7 m^2 during braking and 0.007 m^2 during power producing operation.

Teeter dampers are installed on the AWT-27 and have been modeled in the FAST_AD code using the manufacturer's data. The nonlinear nature of the dampers required writing the specific algorithm into the program.

Modeling the drive train includes the brake, generator/motor and low speed drive shaft. The drive train in the FAST_AD code is modeled as an equivalent drive train.[8] It was found that the low speed shaft dominated the drive-train torsional stiffness and that the rotor and generator armature moments of inertia were, respectively, the largest terms. The characteristics of the brake and motor/generator are given in Table 9.3. The generator is operated as a motor during start-up.

Table 9.3. AWT-27 Drive Train

Component	Remarks
Generator	275 kW, rated slip 1.6% Moment of inertia, 4.4 kg-m^2
Motor	Motoring torque: 400 N·m
Gear Box	Planetary, 99% efficiency
Brake	On high speed shaft, 800 N·m during normal stops, 2400 N·m during fast stops
Low Speed Shaft	Torsional stiffness $0.7 \cdot 10^6$ N·m/rad

The start-up test data shows that there are five distinct phases to the starting process. First, the rotor is not moving and the shaft torque measures the static torque developed by the blade. Second, the brake is released and the rotor and drive train start to rotate. The angular acceleration in this phase was observed to be constant and the torque calculated using the angular acceleration was found to be the same as the measured static torque. The aerodynamic torque developed is largely due to the aerodynamic suction of the leading edge in the high angle-of-attack flow over the blades. In the static case the flow angle is approximately normal to the blades and the angle-of-attack is 90° minus the blade twist angle. The blade twist angle allows the blade normal force to add to the force causing the blades to rotate. For the AWT-27p4, when the blade pitch angle is zero, the static torque is 2/3 due to the chordwise force and 1/3 due to the normal force. The blade chordwise force coefficient is

$$C_t \equiv C_\ell \sin\alpha - C_d \cos\alpha \tag{1}$$

The third phase of the start-up occurs when the generator acts as a motor to increase the rotor rpm. For the AWT-27p4, a controller kept the supplied torque approximately constant. The resulting rotor angular acceleration is constant in this phase indicating that the aerodynamic torque for the rotor is very small. The

chordwise force contribution to the local torque is proportional to $C_t \cos\beta$, where β is the local blade twist angle. Negative values of C_t are required in this angle-of-attack range depending on the blade position. Table 9.4 below gives the range of no net aerodynamic torque at various blade positions.

Table 9.4. Angle-of-Attack Range of Zero Torque Contribution

r/R	α Range
1.0	$64° > \alpha > 26°$
0.8	$69° > \alpha > 32°$
0.6	$74° > \alpha > 40°$
0.4	$79° > \alpha > 50°$

The aerodynamic input data determined from KTI were examined in comparison to the information shown in Table 9.4 and it was concluded that the high angle-of-attack input data was not consistent with Table 9.4. There are many reasons to suspect the input airfoil data. First, the rotor has only three airfoil sections for which test data is available, the S809, the S810 and the S815. The airfoil section between the tip and the 90% station is the S810. In the region between the 90% station and the 70% station, the airfoil sections are interpolated between the S810 and the S809. Between the 70% station and the 35%, interpolation is also used. Inboard of the 35% station, the airfoil section is an extrapolation of the S815 airfoil. Secondly, there is little high angle-of-attack data for the airfoil sections. Third, it is noted that airfoils employed on wind turbines do not exhibit the same type of stall as obtained in two-dimensional wind tunnel tests. This is particularly true of the inboard stations, i.e., the 35% station.

In light of these uncertainties, the high-angle-of-attack input airfoil characteristics were modified to obtain consistency with Table 9.4.

Figures 9.1 thru 9.3 show the static aerodynamic coefficients used in this study. The lift coefficient versus angle-of-attack at various radial stations is given in Figure 9.1. Figures 9.2 and 9.3 give the drag coefficient and chordwise force coefficient respectively. While only the lift and drag coefficients are input to the calculations, the chordwise force coefficient is shown for general background. Using the static airfoil data and a steady wind including shear and tower shadow, the power curve shown in Figure 9.4 was

obtained. Excellent agreement is noted below peak power with divergence between calculated and measured power above peak power.

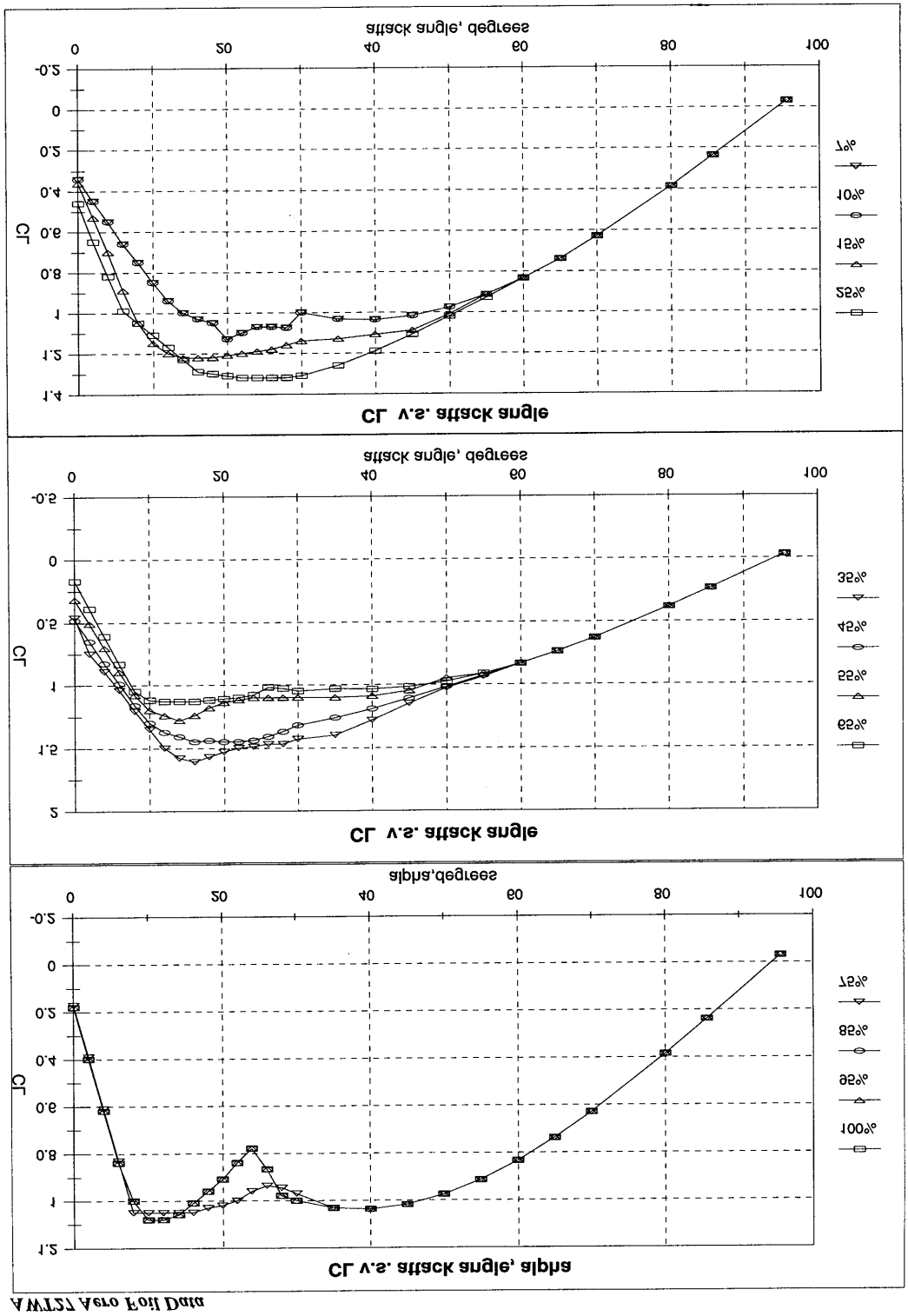

Figure 9.1. Lift Coefficient, CL versus attack angle.

Figure 9. Drag coefficient, CD versus attack angle.

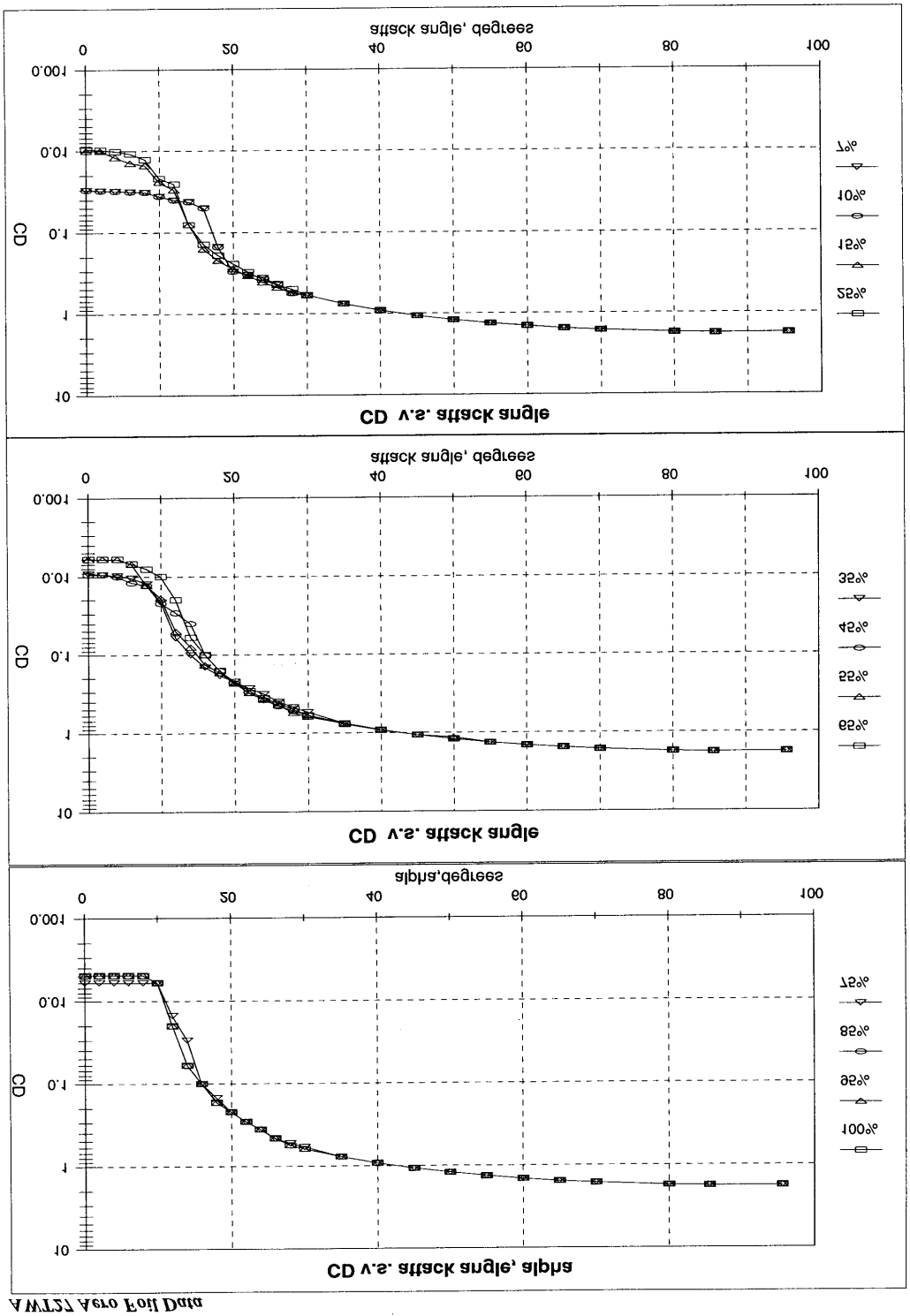

Figure 9.3. Thrust Coefficient, Ct versus attack angle.

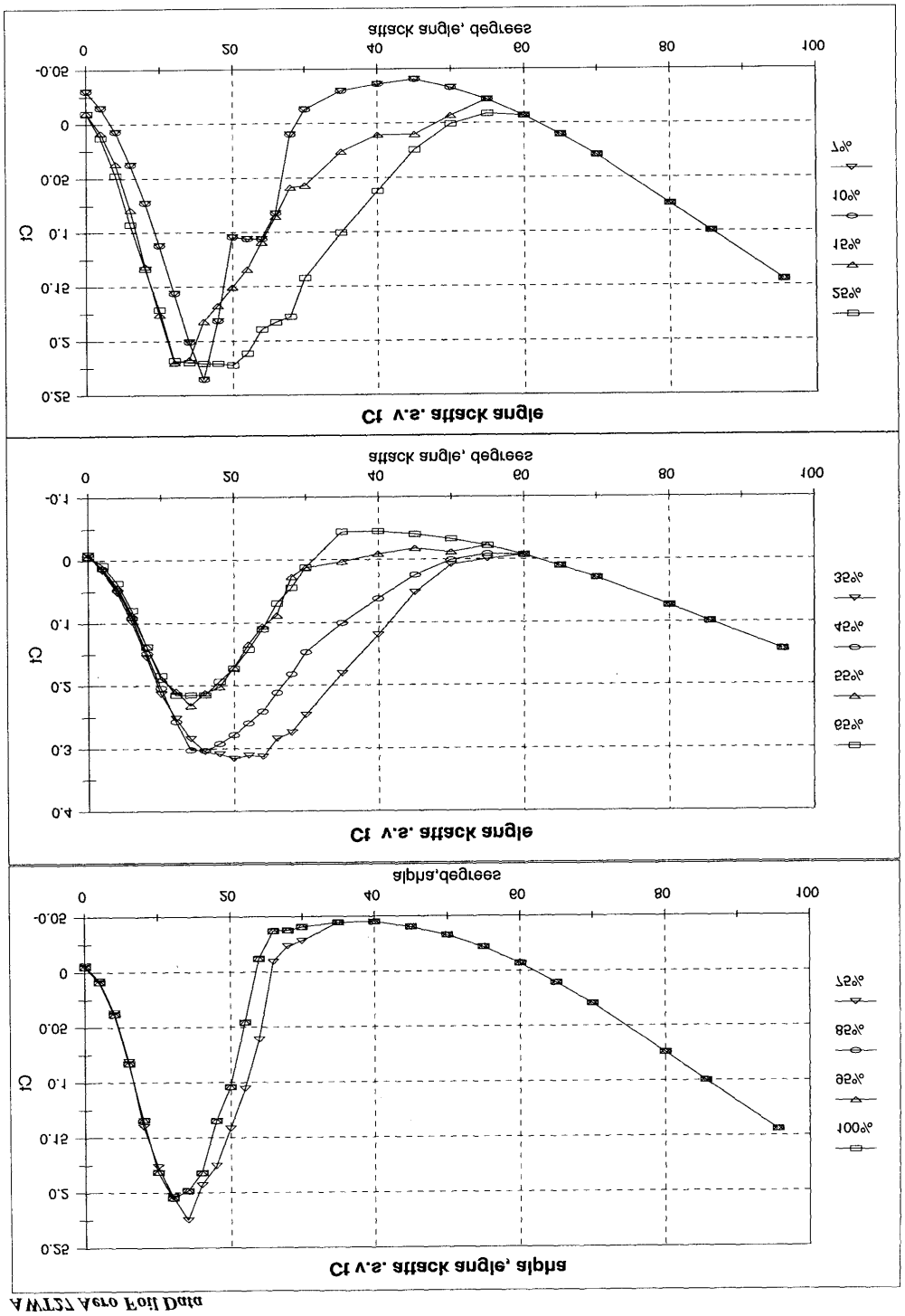

Figure 9.4 Power Curve Comparison between FAST_AD and Field Data.

AWT27 Power Curve

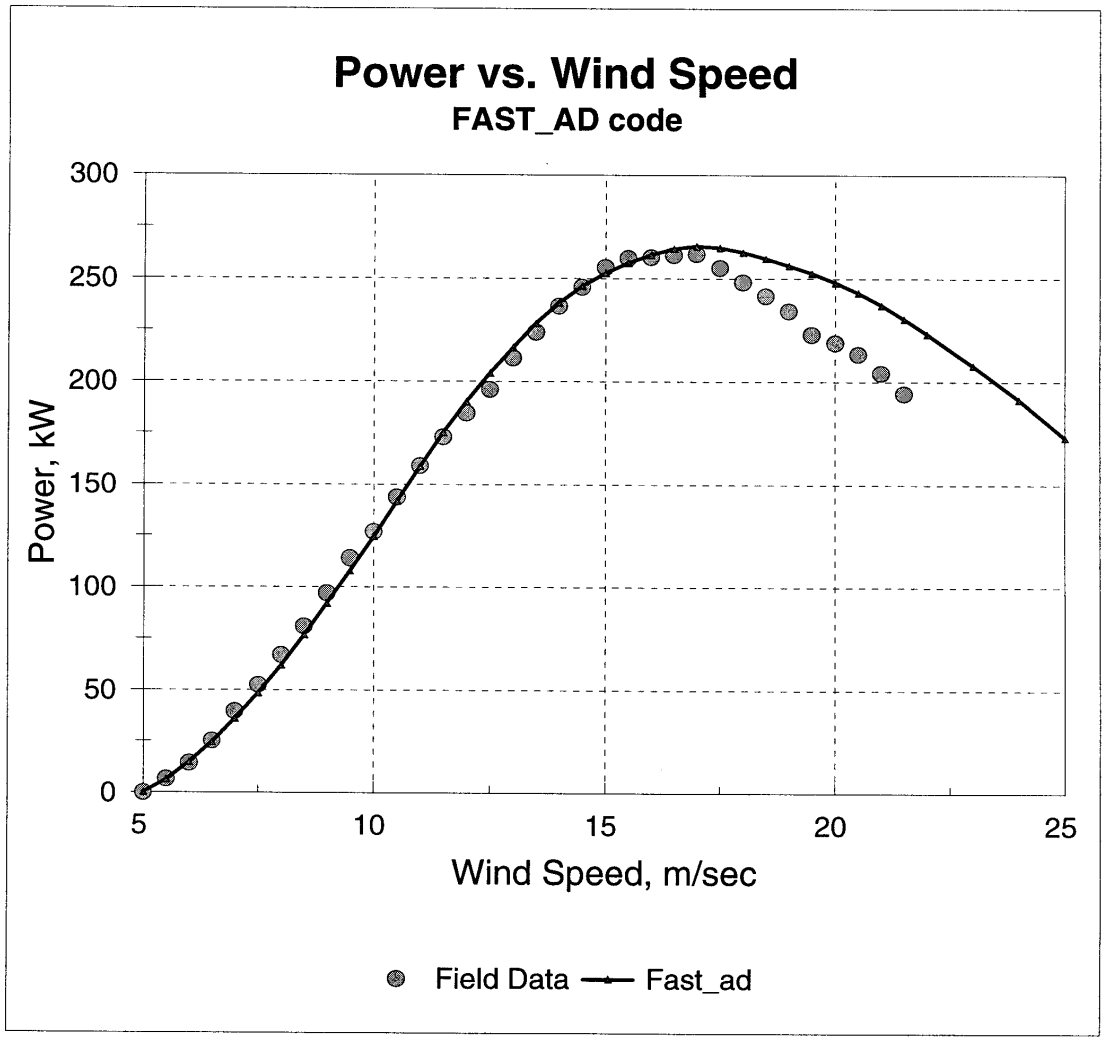

9.4 Simulation of Inflow

The code used to simulate the inflow to the wind turbine was the SNLWIND3D code received from Neil Kelley of the National Wind Technology Center. This code is based on the work done by Paul Veers[6] and is described in Kelly[7]. The application of the code and the selection of options and the value of several parameters was carried out in consultation with Neil Kelley and are reported in Malcolm[10].

The SNLWIND3D program produces three ASCII output files - one for each direction u, v, and w. Each file defines the flow at each time step at each of the spatial array points requested (a 6 by 6 grid was used). Another FORTRAN code was prepared by KTI to read the output from SNLWIND3D and to calculated the characteristics of the flow at the hub. This step allowed further checking of the statistics of the simulated inflow and also allowed direct comparison with the statistics of the field measurements.

This second program was named RSTRESS2 and it calculated the following hub height properties.

- Mean longitudinal velocity
- Standard deviation of each turbulent component
- Mean Reynolds stresses
- Standard deviation of the instantaneous Reynolds stress
- Maximum and minimum values of the three turbulent components and of the instantaneous Reynolds stresses.

This program also outputs the time series of the various quantities at the hub locations so that they were available for plotting or being converted to the frequency domain.

The objective was to select options and parameter values that resulted in characteristics as close as possible to those measured in the field. The parameters finally selected are summarized and the statistical characteristics of the simulated inflows were compared with the field data in Malcolm[10].

The following guidelines were used in selecting the inflow parameters. The normal approach was:

- Specify grid size, time step, time length, rotor diameter, hub height, coherence.
- Specify mean windwise velocity.
- Set the surface roughness to 0.01 m and the wind shear exponent to 0.05 (values reflect the terrain and conform to previous measurements).
- Select the inflow type (SMOOTH, UPWIND, or INTERNAL).
- If the INTRNL category was selected, then a turbine spacing was specified. Normally 14D was used (the only other option was 7D).
- Specify the shear velocity, u*.
- Specify the Richardson stability number, Ri.
- Specify the cross correlations (zero leads to default values). This tends to affect the proximity of one PSD to the other.

Figure 9.5 thru 9.10 give the calculated PSD and frequency histogram of each simulated component on each blade under high wind conditions.

Figure 9.5. PSD and Histogram of Windspeed in u Component (Blade 1).

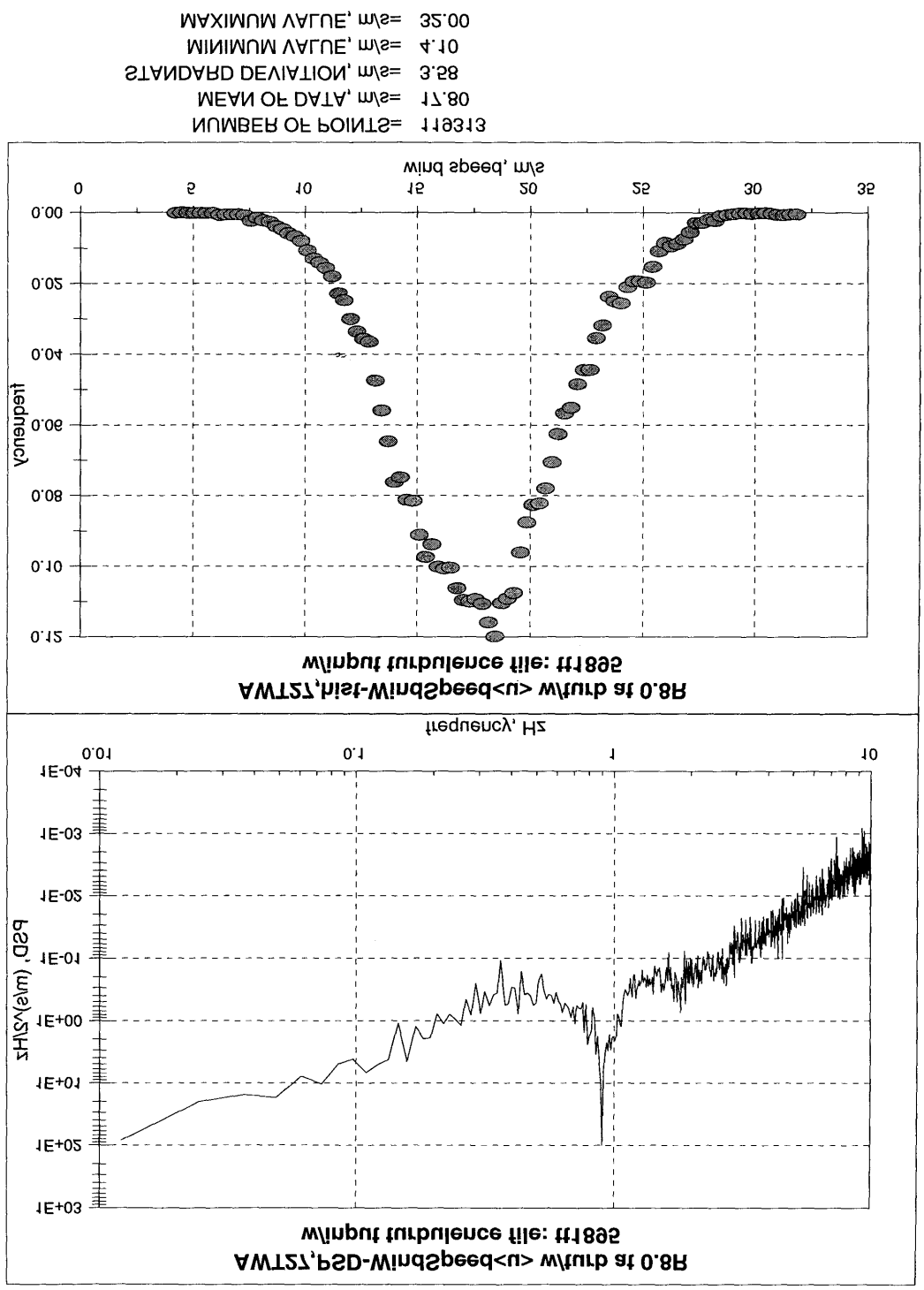

Figure 9.6. PSD and Histogram of Windspeed in v Component (Blade 1).

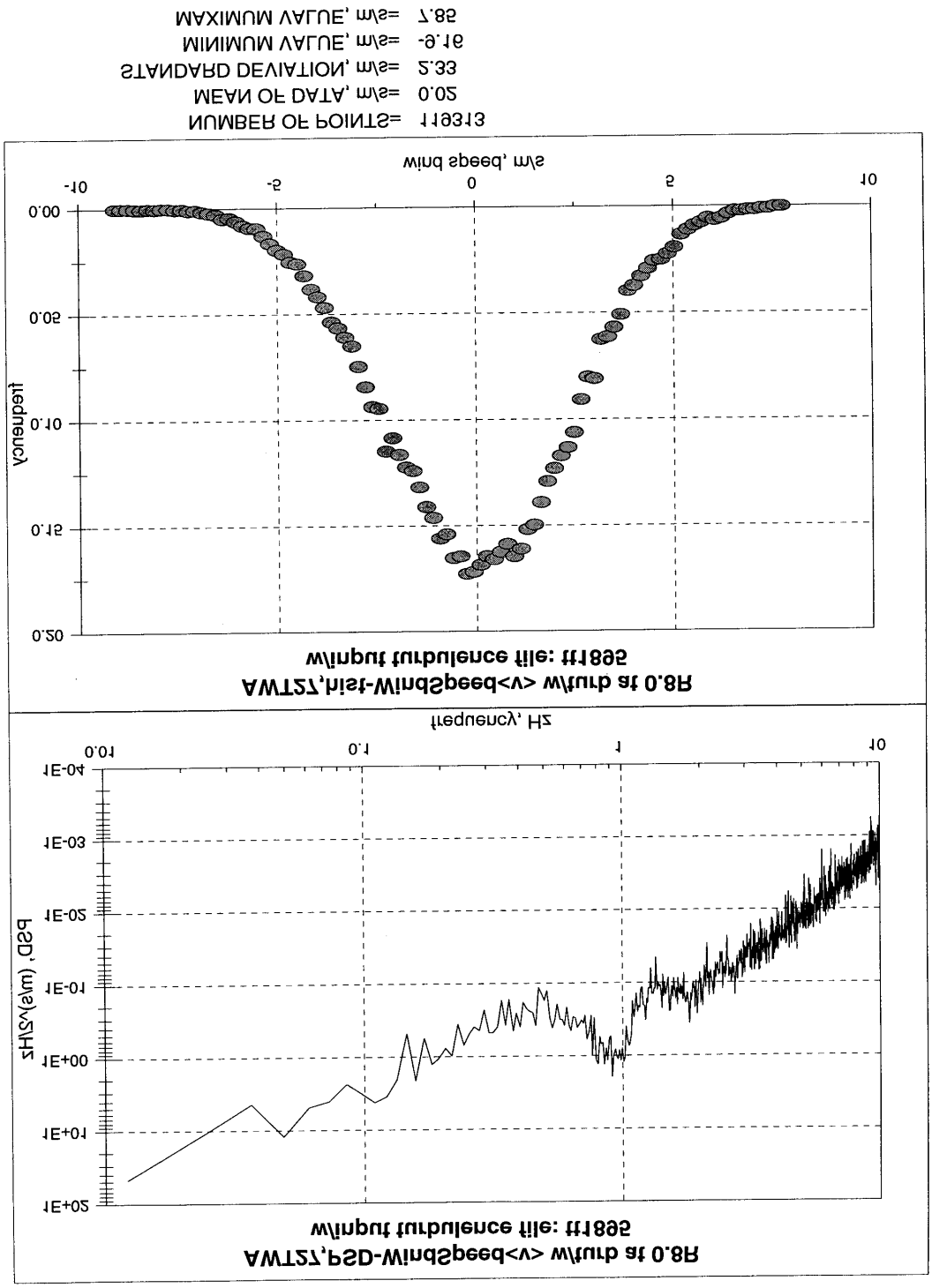

Figure 9.7. PSD and Histogram of Windspeed in w Component (Blade 1).

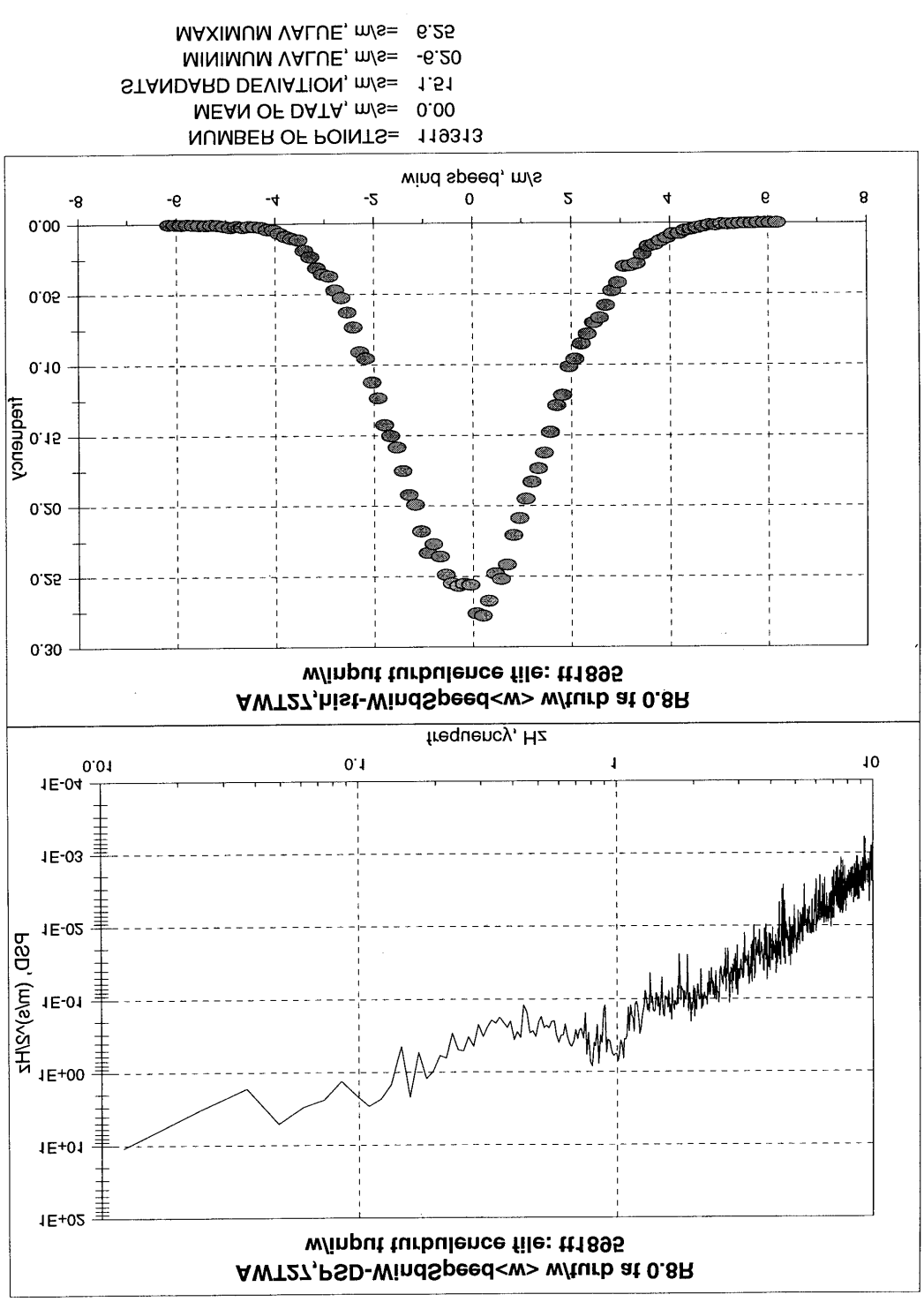

Figure 9.8. PSD and Histogram of Windspeed in u Component (Blade 2).

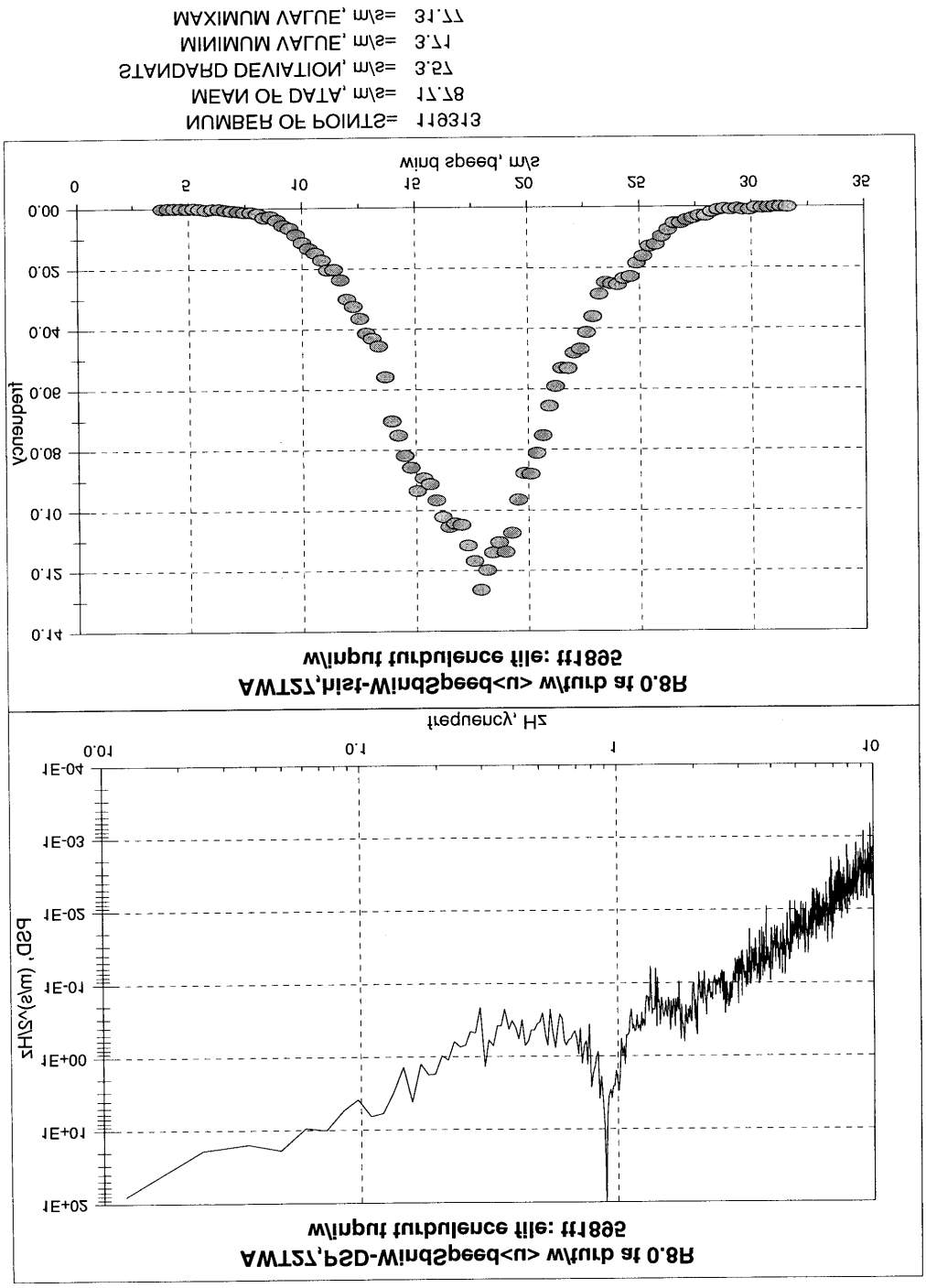

Figure 9.9. PSD and Histogram of Windspeed in v Component (Blade 2).

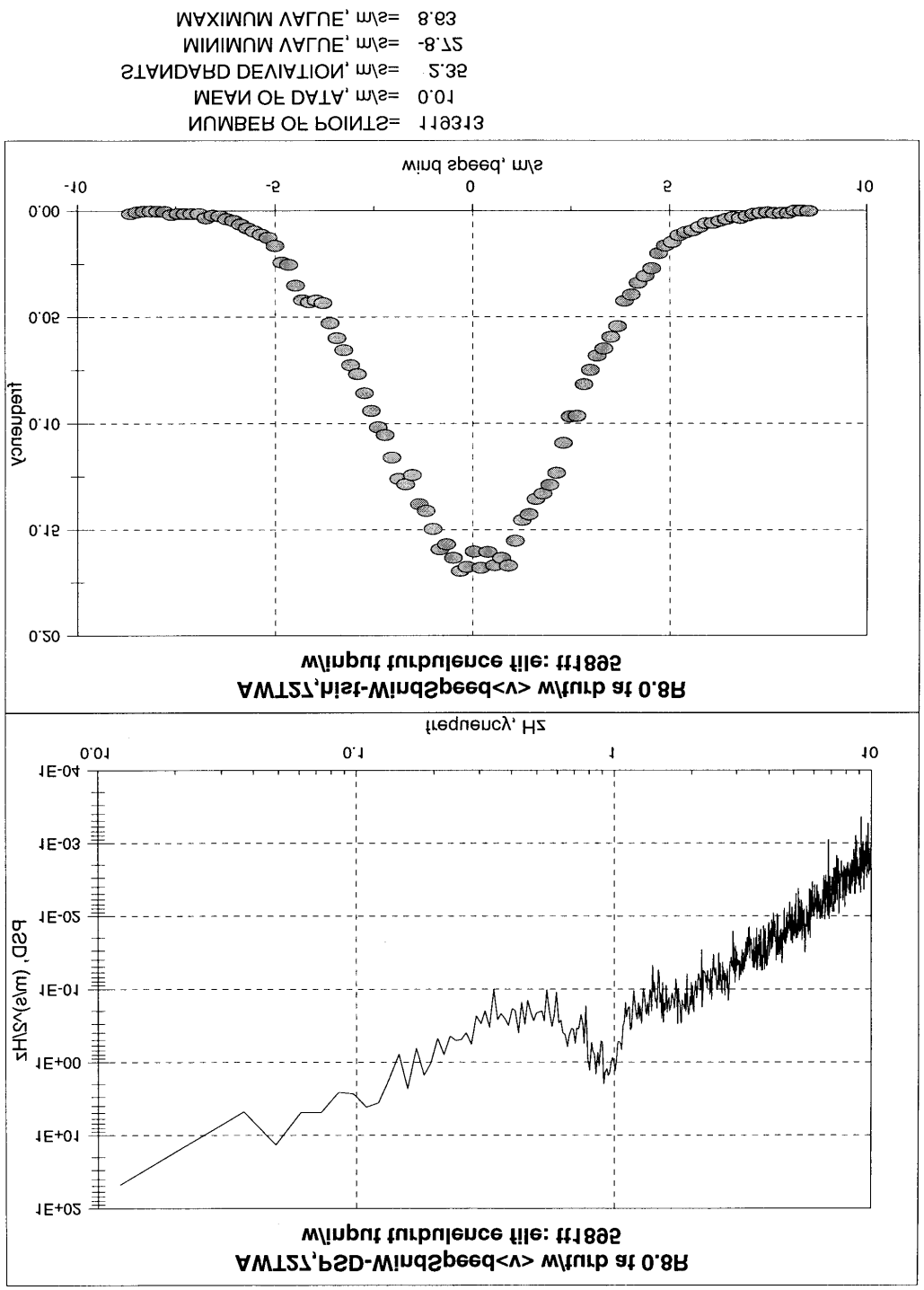

Figure 9.10. PSD and Histogram of Windspeed in w Component (Blade 2).

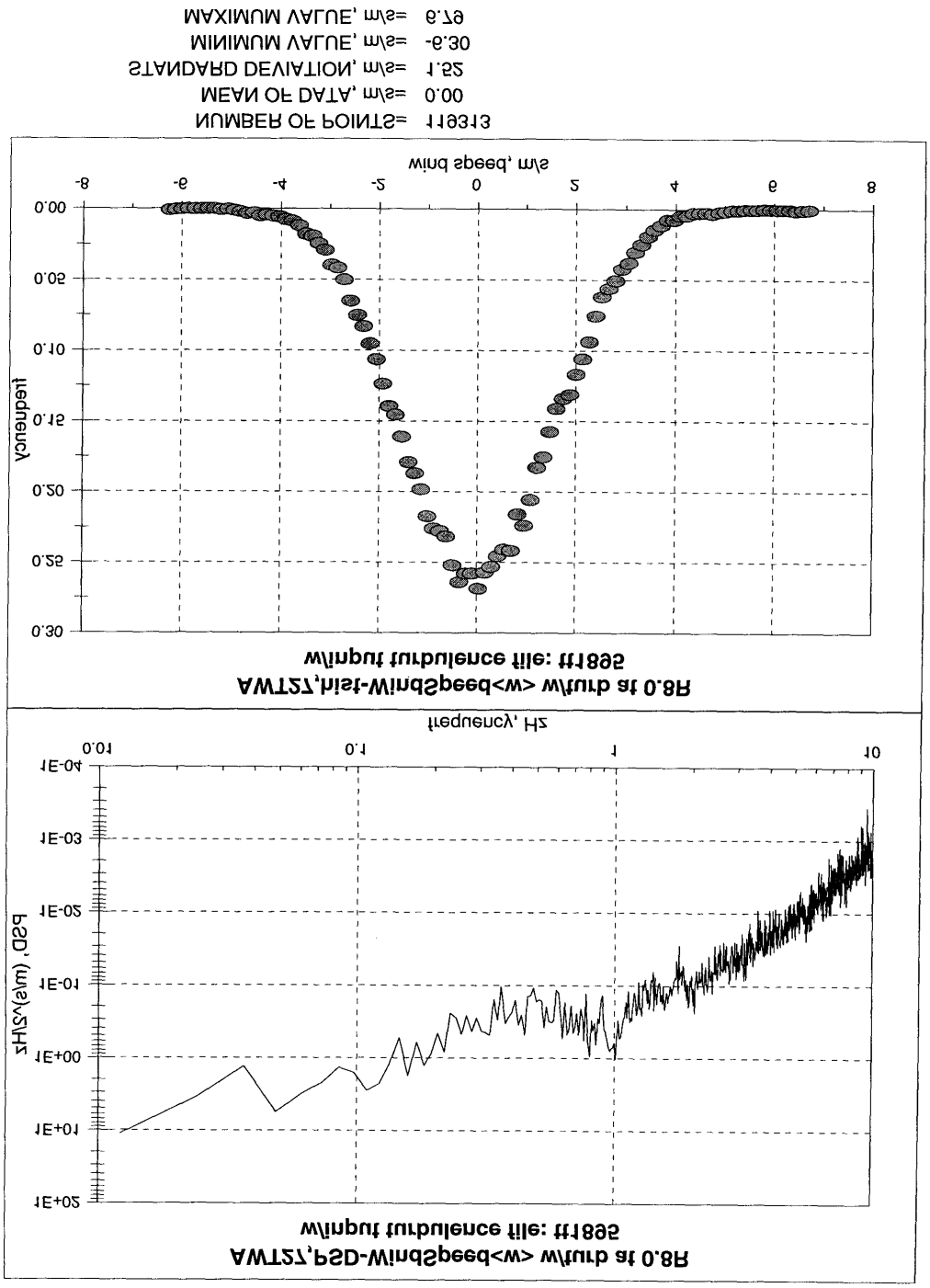

9.5 Results

The following 45 figures (Figures 9.11 thru 9.55) compare rainflow cycle counts calculated using FAST_AD with field data and calculations using the ADAMS code. There are three groups of figures, one group for each δ_3 angle. The delta-three angles are, respectively, zero, -45°, and -30°. Comparisons are made for edgewise bending, flapwise bending, shaft torque, teeter angle, and yaw angle. Limited field data was available for yaw, however some ADAMS calculations were available to compare to FAST_AD results.

A variety of flow conditions were encountered during the tests. For the comparisons these flow conditions are characterized by three different turbulence levels at each of three different wind regimes. Tests were also made at different times of the year since appreciable time spans were required to change the hub (to adjust the delta-three angle) and to acquire test data in each of the flow regimes. In some cases, it was not possible to obtain test data in a particular flow regime, for example in Figure 9.11, there are two blank graphs corresponding to low turbulence operation at low wind speed (9 - 11 m/s) and at high wind speed (16 - 18 m/s). Thus by using blank graphs for cases where no test data are available allows the same format to be used on each page.

Table 9.5 below, summarizes the matrix of flow conditions that were used to compare FAST_AD, ADAMS and test conditions.

Table 9.5 Flow Characterization

		Turbulence Level*	
Wind Speed Range	Low	Medium	High
Low, 9 - 11 m/s	5 - 7.5%	7.5 - 11%	>11%
Medium, 13 - 15 m/s	5 - 7.5%	7.5 - 11%	>11%
High, 16 - 18 m/s	5 - 7.5%	7.5 - 11%	>11%

*** The turbulence level as selected by Malcolm[10] and used for this study is the ratio of the shear velocity calculated from the hub height wind measurements to the mean hub height measured wind speed.**

The test results were obtained between 20 August, 1997 and 17 March, 1998 with the -45° delta-three tests starting on 20 August, the -30° delta-three tests starting on 21 October, and the 0° delta-three tests starting on 1 December, 1997.

Start-up and shut down tests were conducted in the summer of 1995. Figures 9.56 thru 9.58 show a comparison of FAST_AD calculation with test data.

0° Delta-three Cases

Figure 9.11. Rainflow Count of Blade Root Edgewise Bending Moment (low turbulence).

FAST_AD vs. ADAMS & Field Data at low turbulence

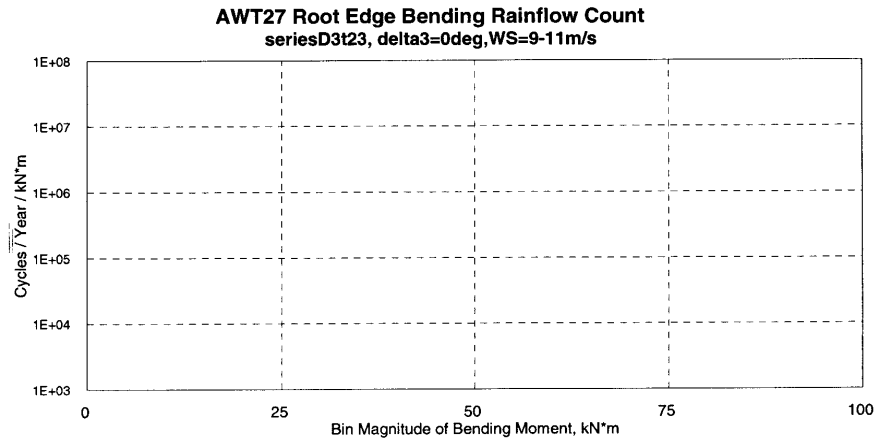

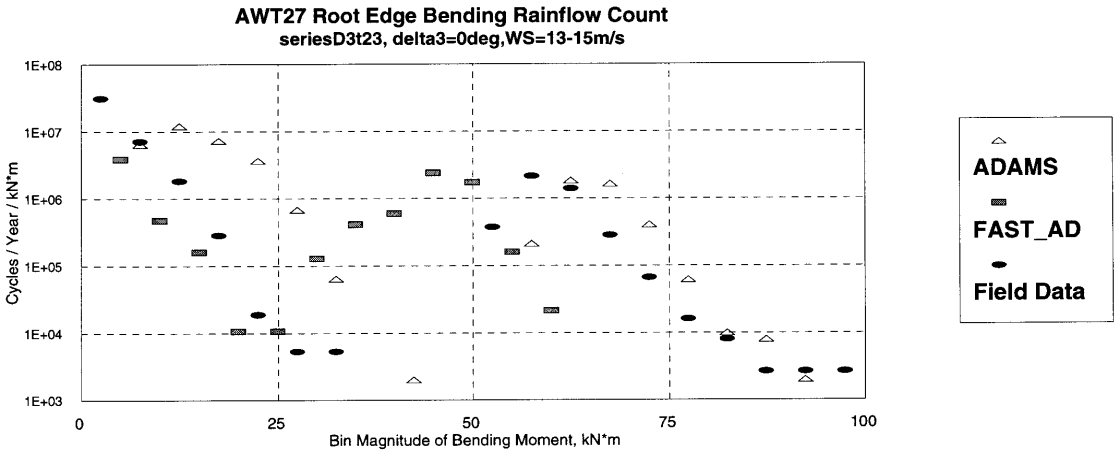

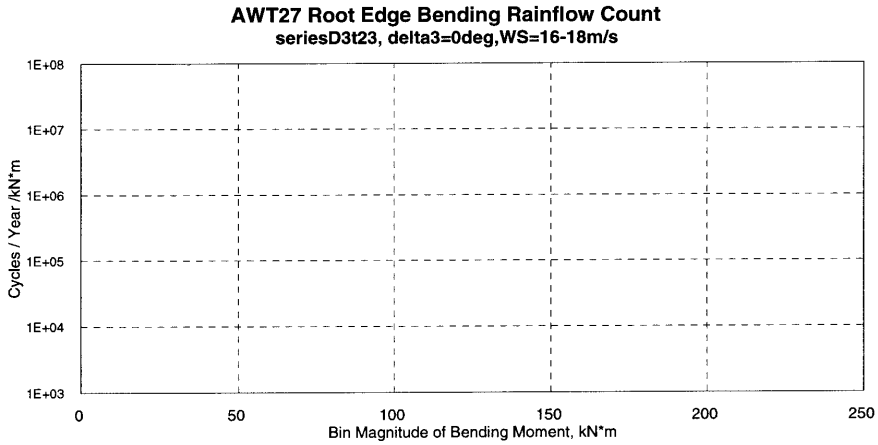

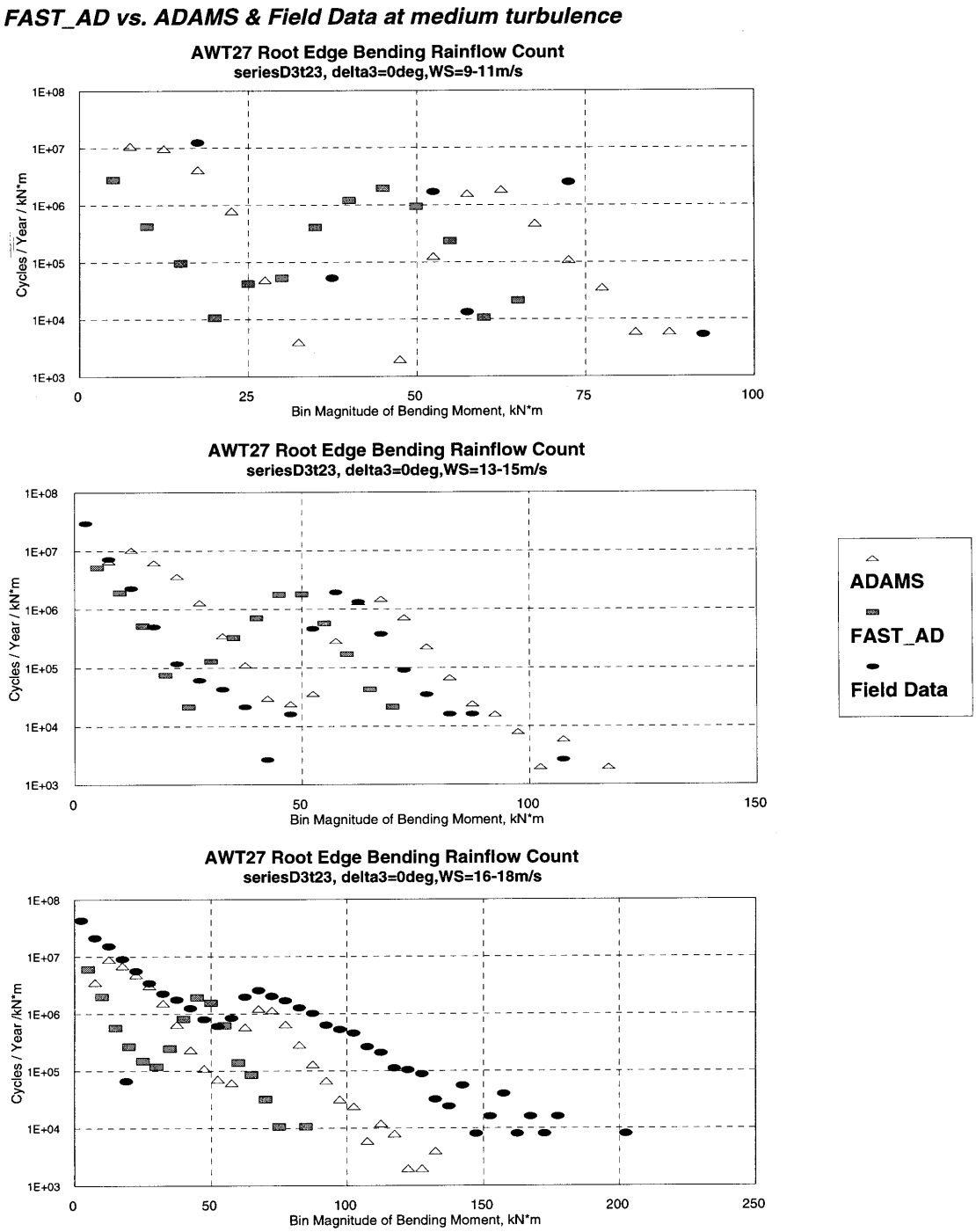

Figure 9.12. Rainflow Count of Blade Root Edgewise Bending Moment (medium turbulence).

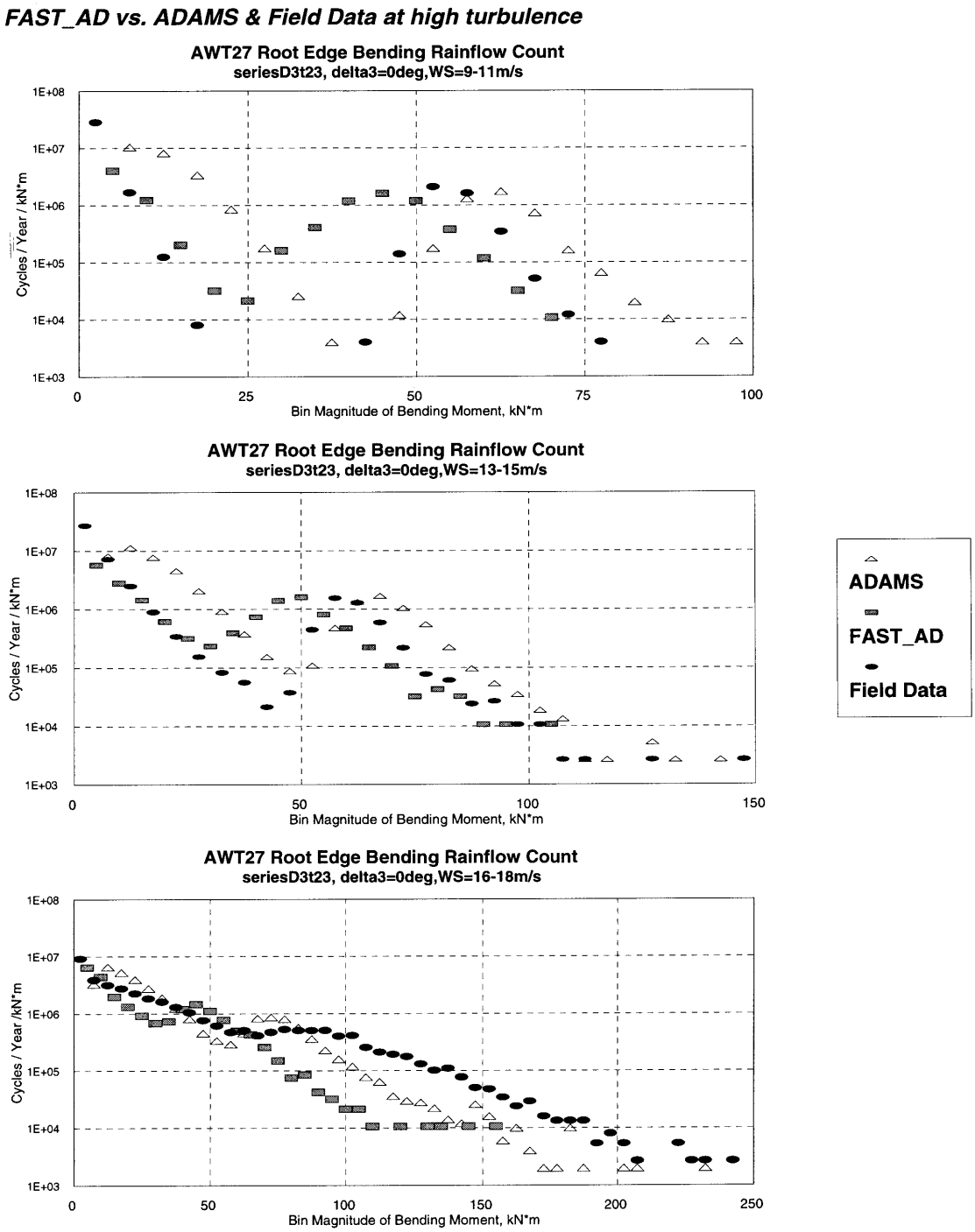

Figure 9.13. Rainflow Count of Blade Root Edgewise Bending Moment (high turbulence).

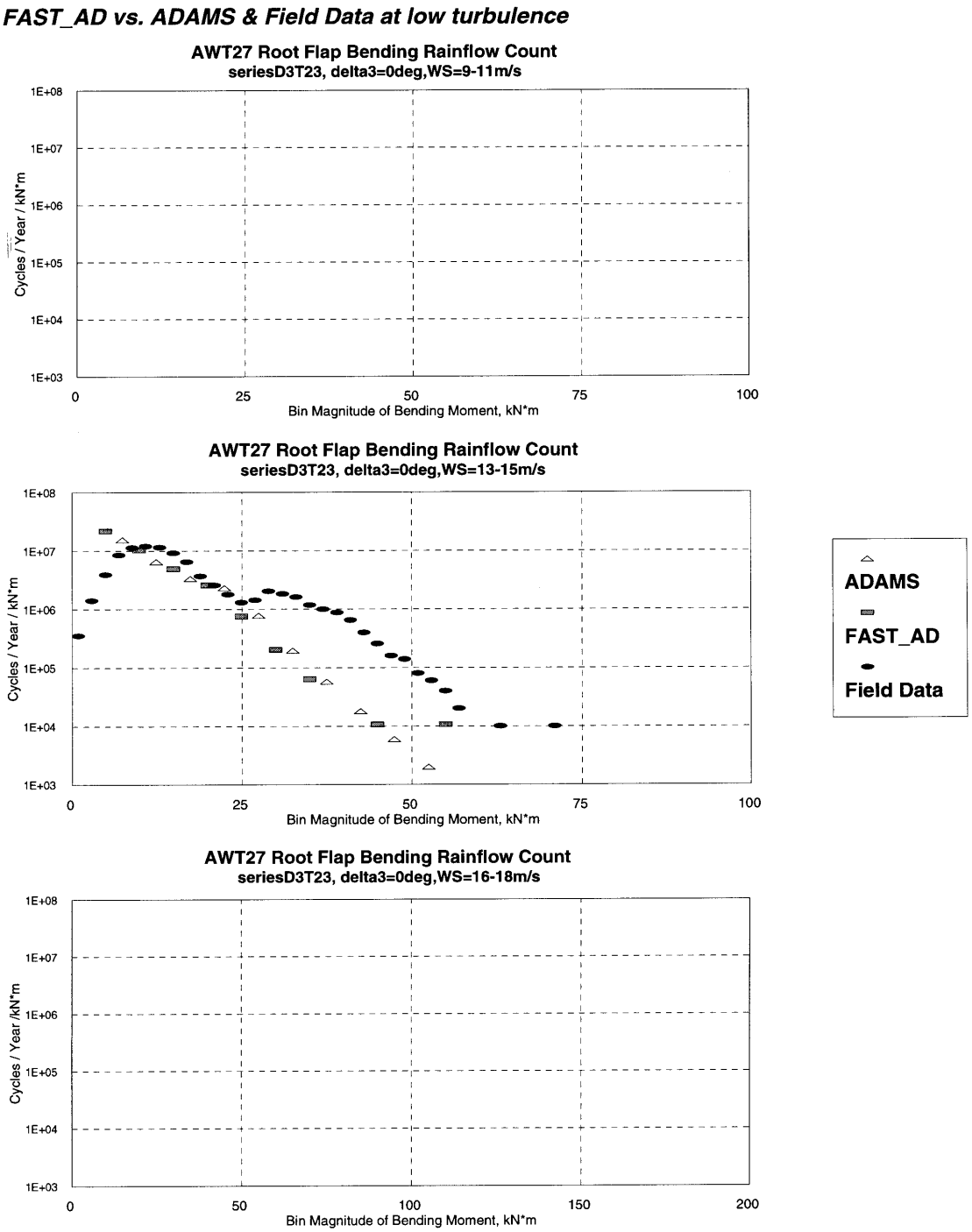

Figure 9.14. Rainflow Count of Blade Root Flapwise Bending Moment (low turbulence).

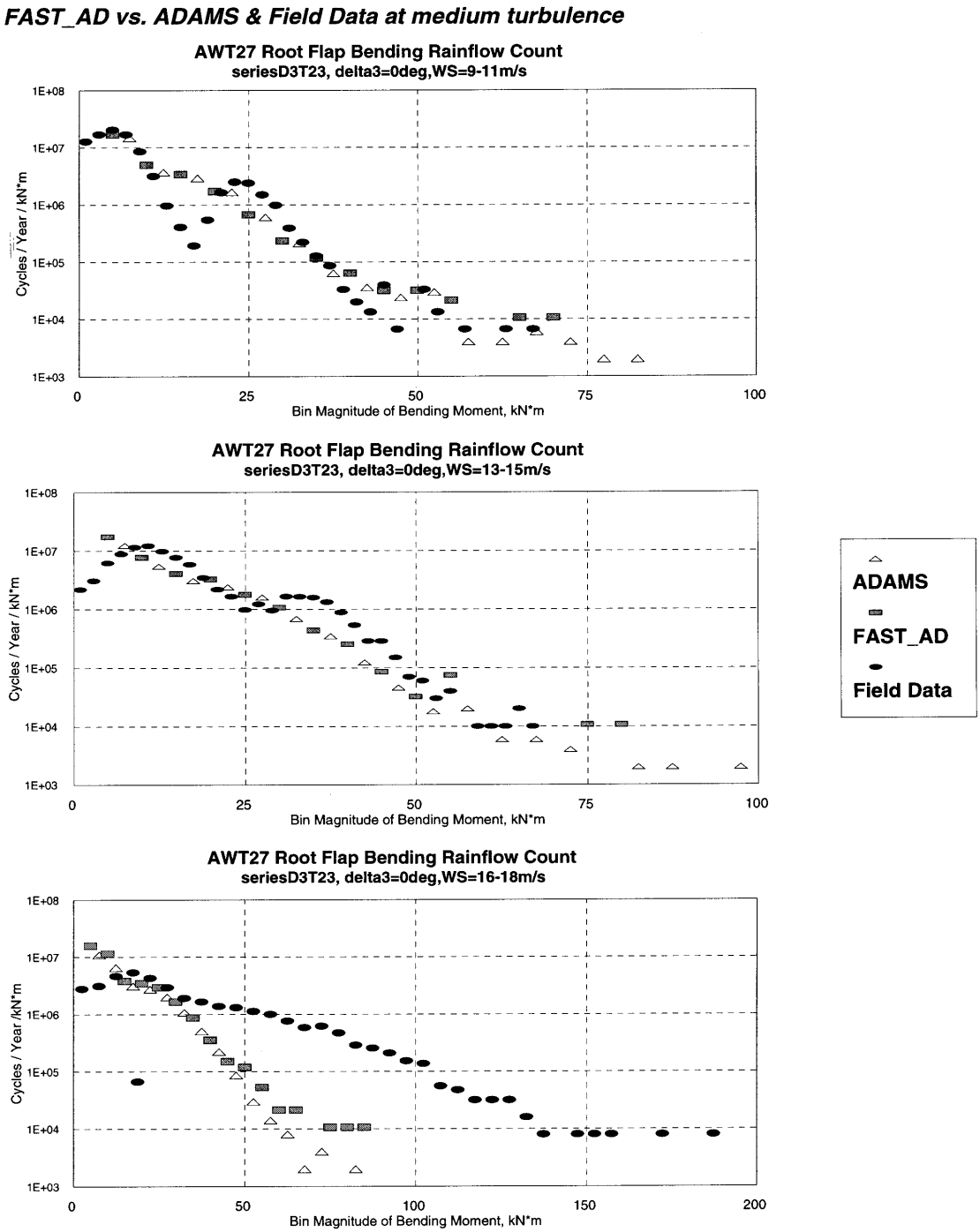

Figure 9.15. Rainflow Count of Blade Root Flapwise Bending Moment (medium turbulence).

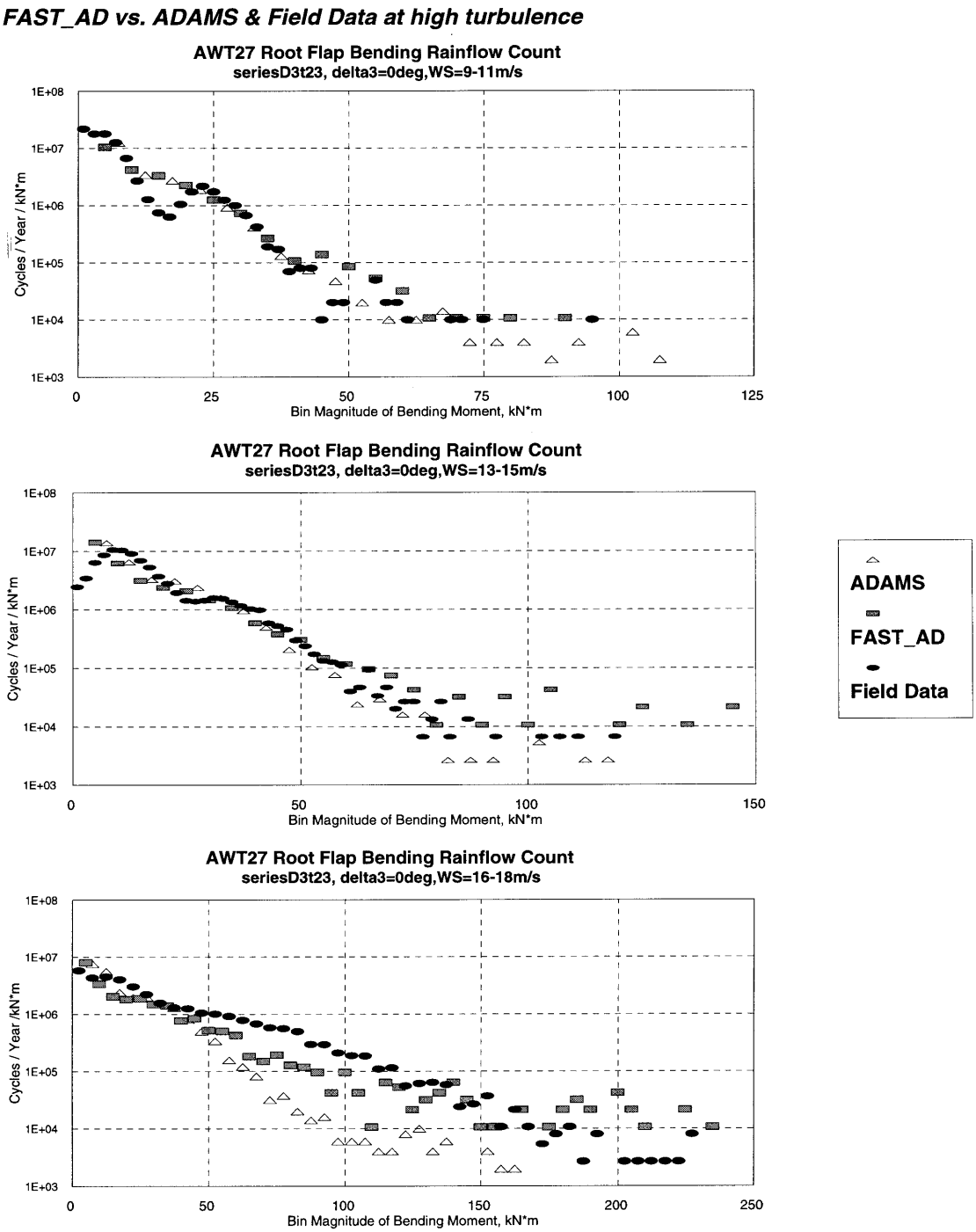

Figure 9.16. Rainflow Count of Blade Root Flapwise Bending Moment (high turbulence).

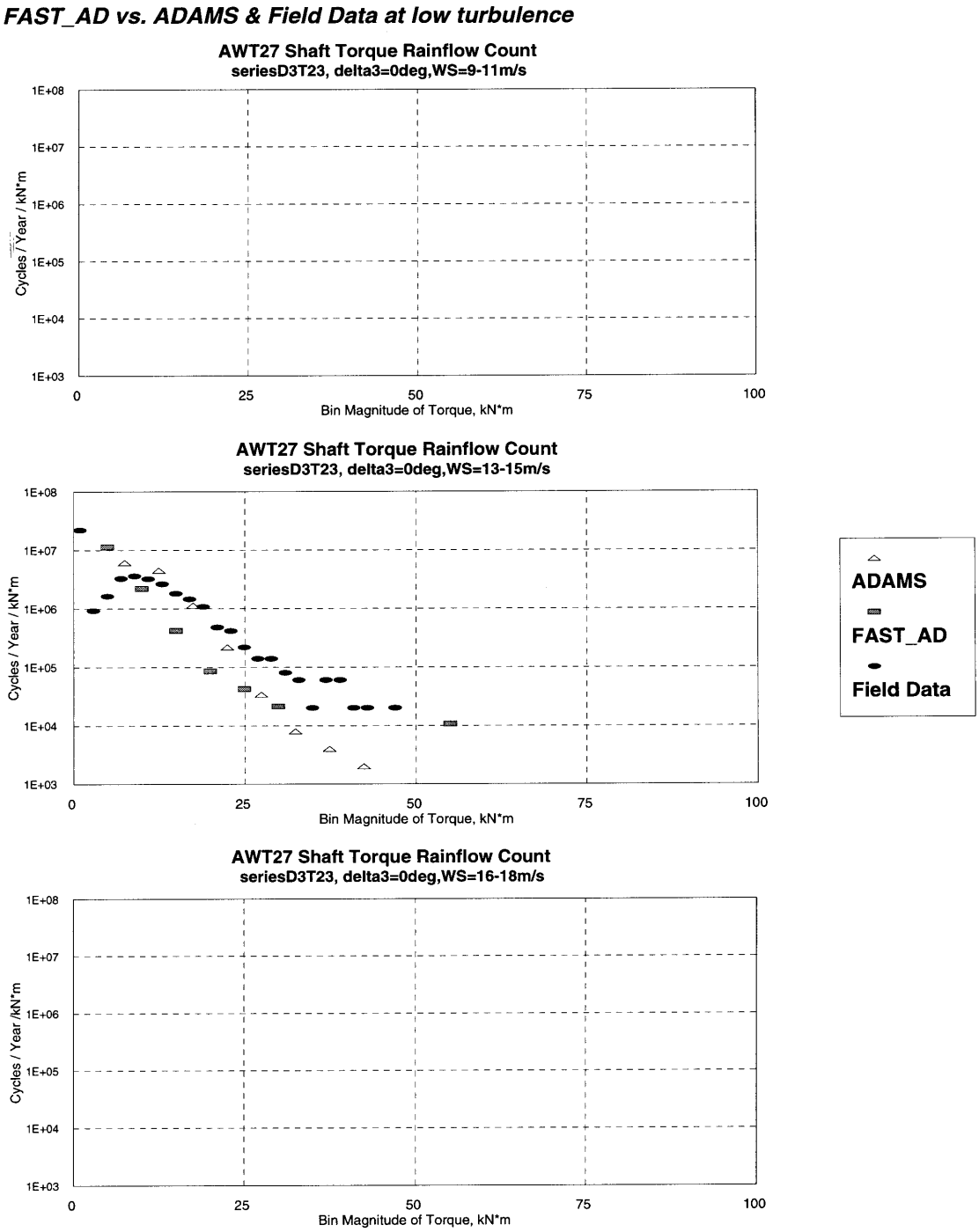

Figure 9.17. Rainflow Count of Shaft Torque (low turbulence).

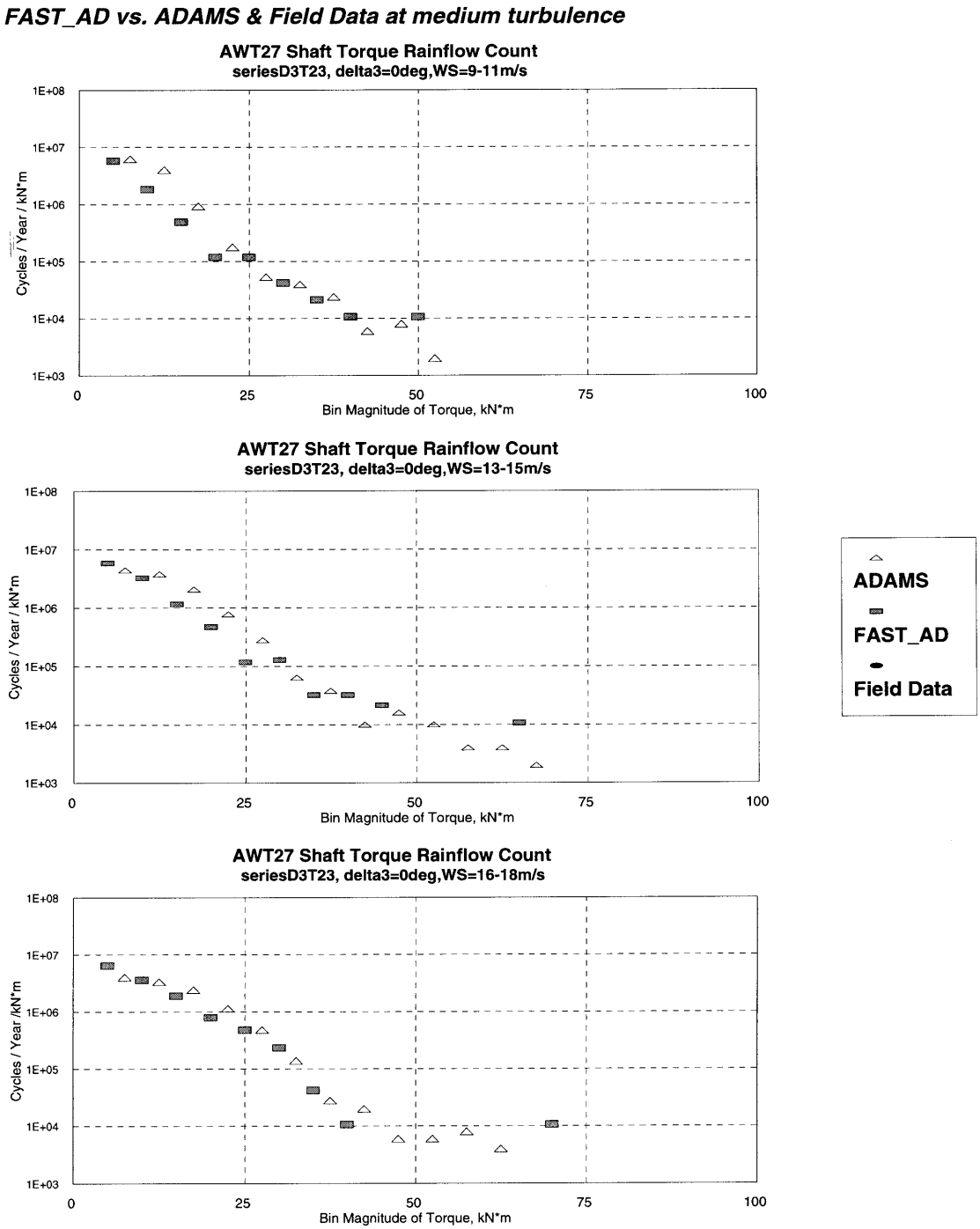

Figure 9.18. Rainflow Count of Shaft Torque (medium turbulence).

Figure 9.19. Rainflow Count of Shaft Torque (high turbulence).

FAST_AD vs. ADAMS & Field Data at high turbulence

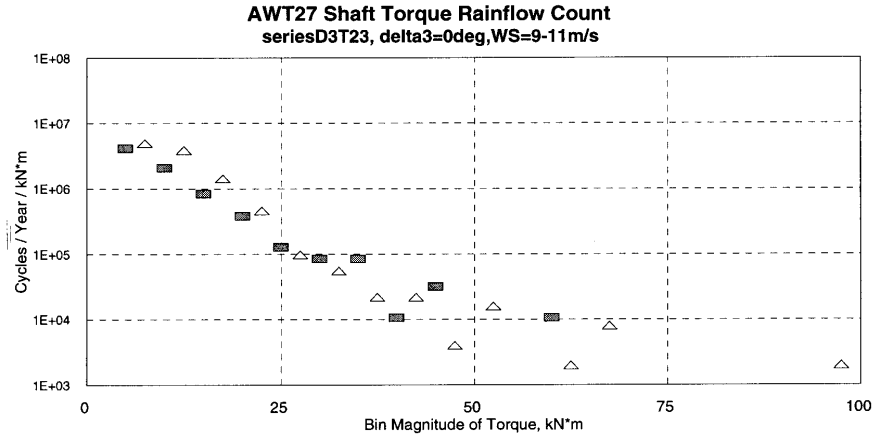

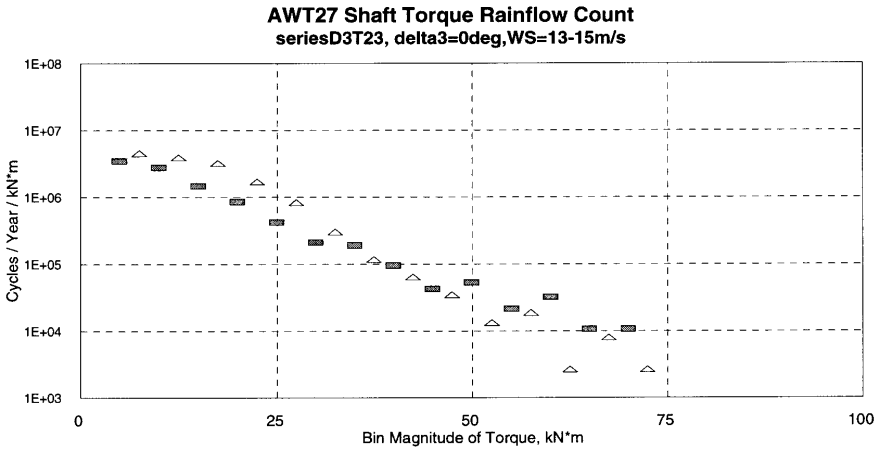

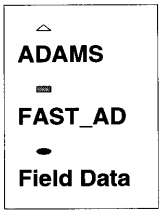

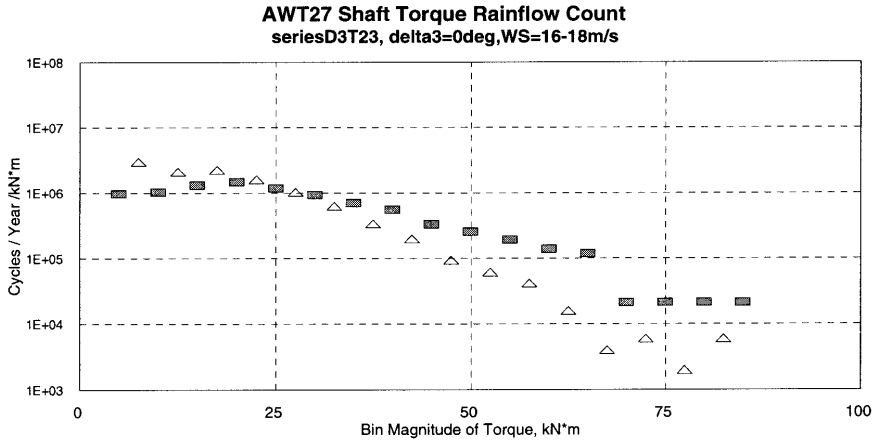

Figure 9.20. Rainflow Count of Teeter Angle (low turbulence).

FAST_AD vs. ADAMS & Field Data at low turbulence

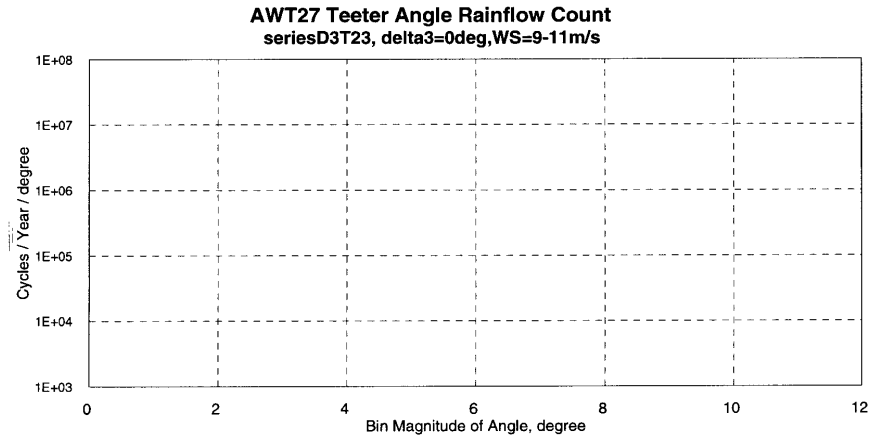

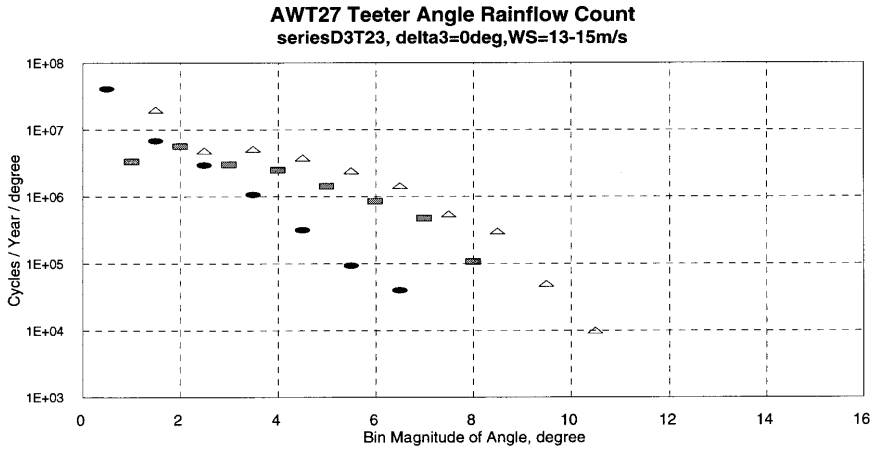

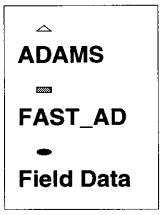

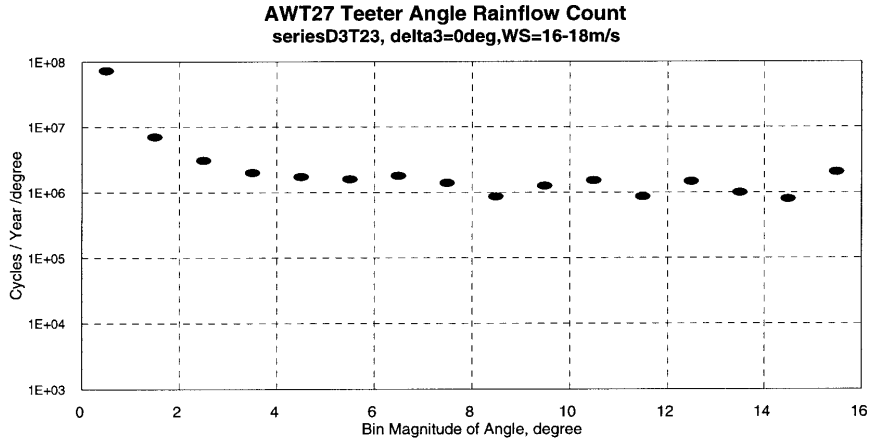

Figure 9.21. Rainflow Count of Teeter Angle (medium turbulence).

FAST_AD vs. ADAMS & Field Data at medium turbulence

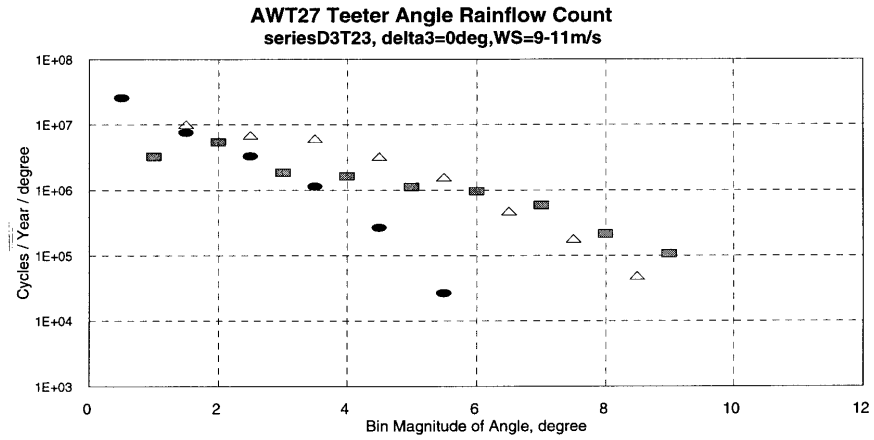

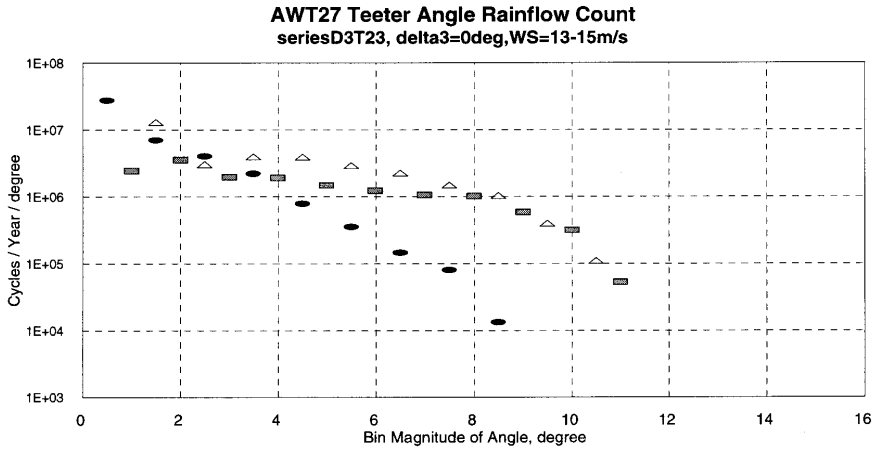

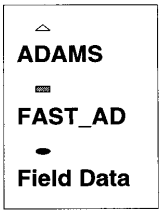

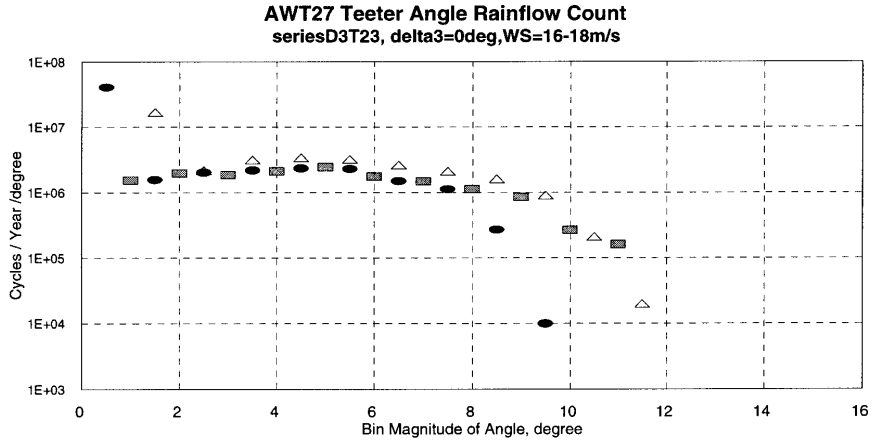

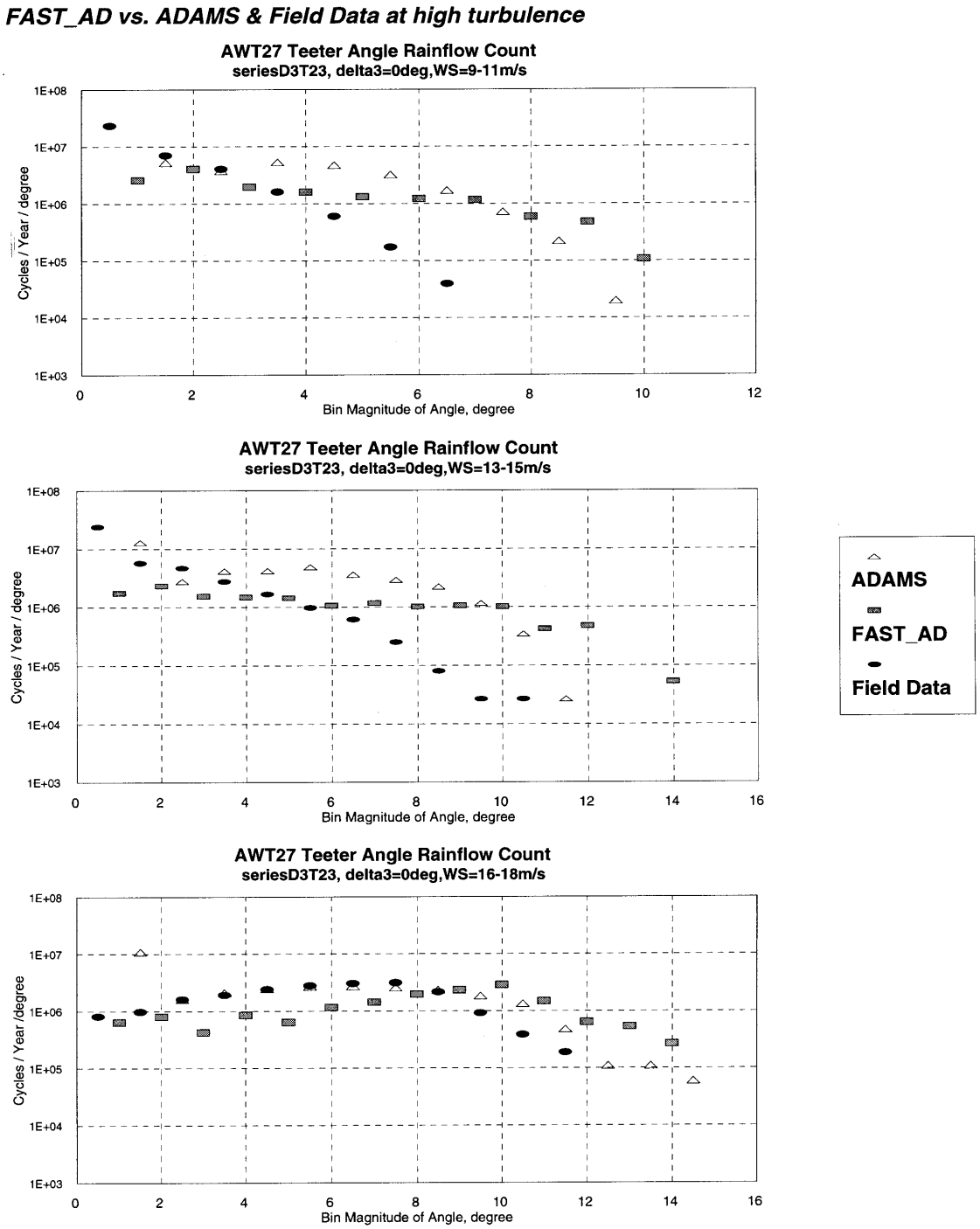

Figure 9.22. Rainflow Count of Teeter Angle (high turbulence).

Figure 9.23. Rainflow Count of Yaw Angle (low turbulence).

FAST_AD vs. ADAMS & Field Data at low turbulence

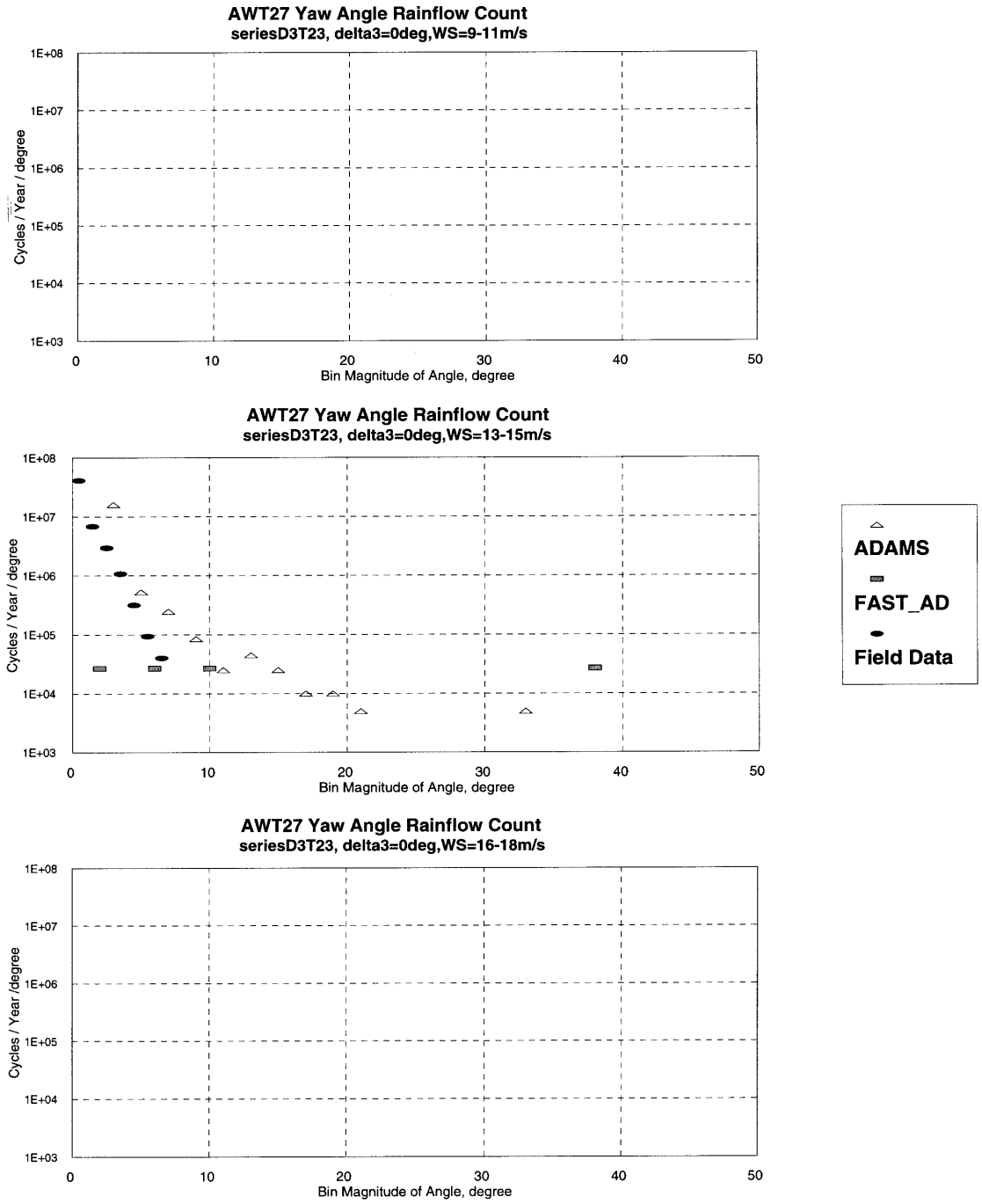

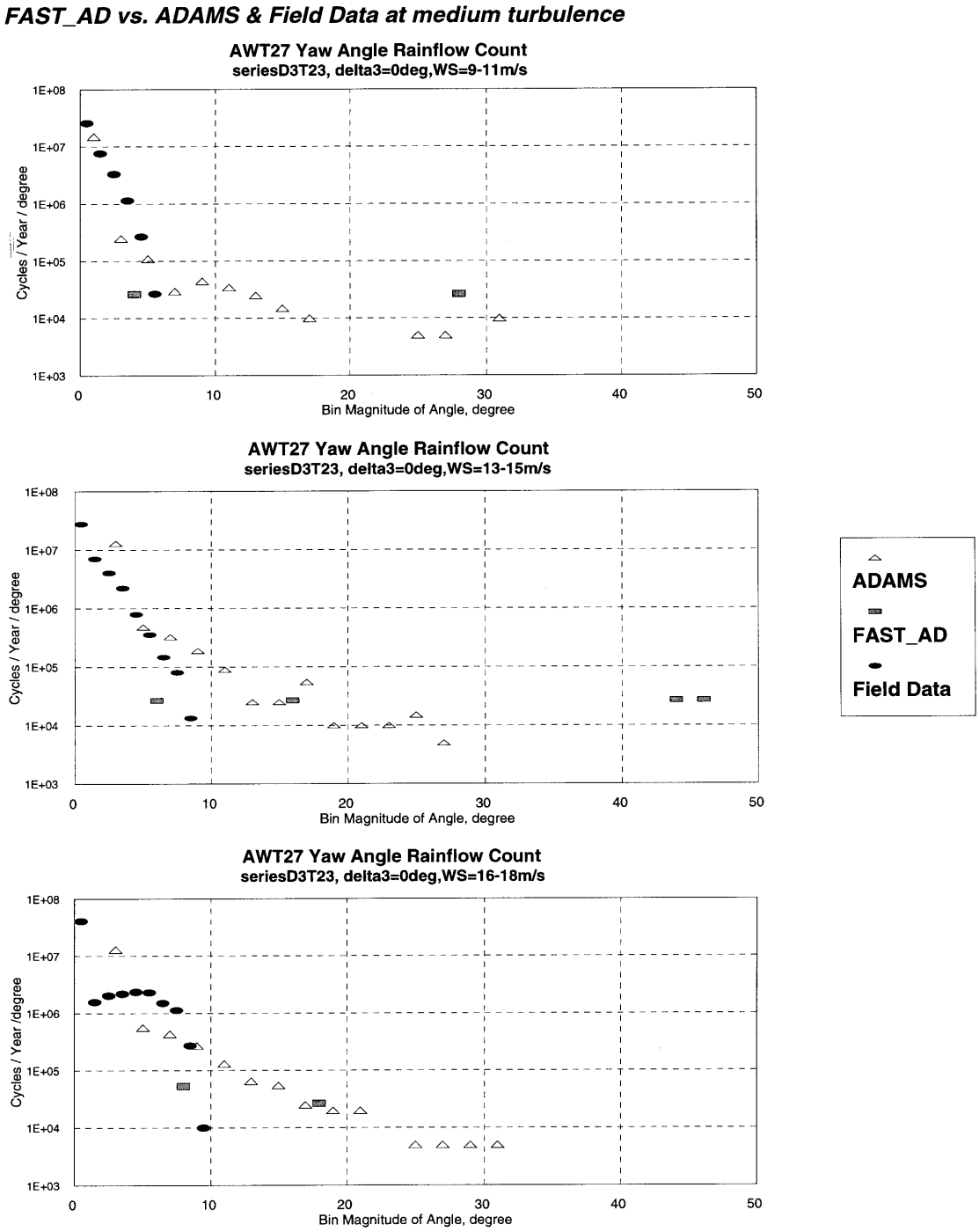

Figure 9.24. Rainflow Count of Yaw Angle (medium turbulence).

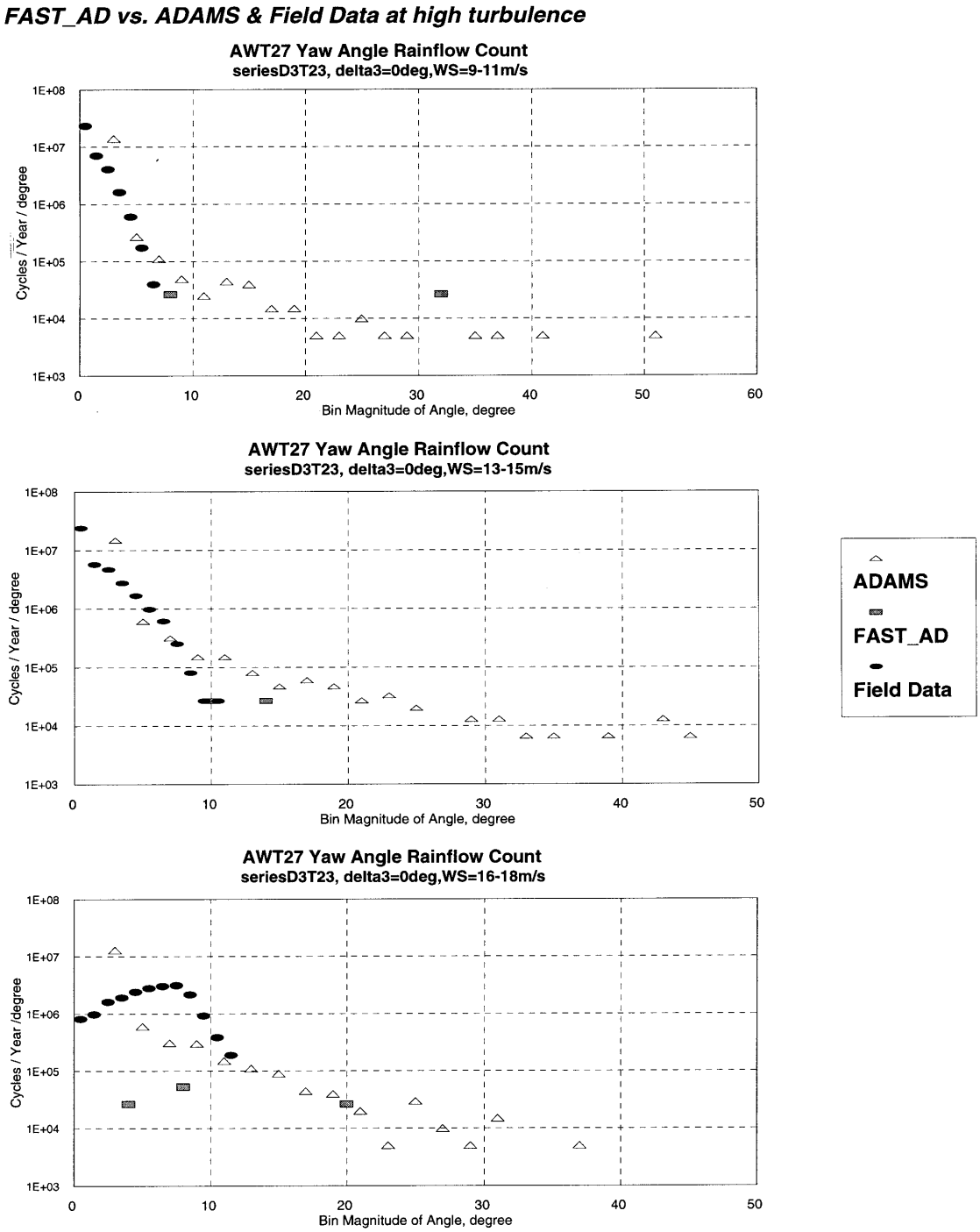

Figure 9.25. Rainflow Count of Yaw Angle (high turbulence).

-45° Delta-three Cases

Figure 9.26. Rainflow Count of Blade Root Edgewise Bending Moment (low turbulence).

FAST_AD vs. ADAMS & Field Data at low turbulence

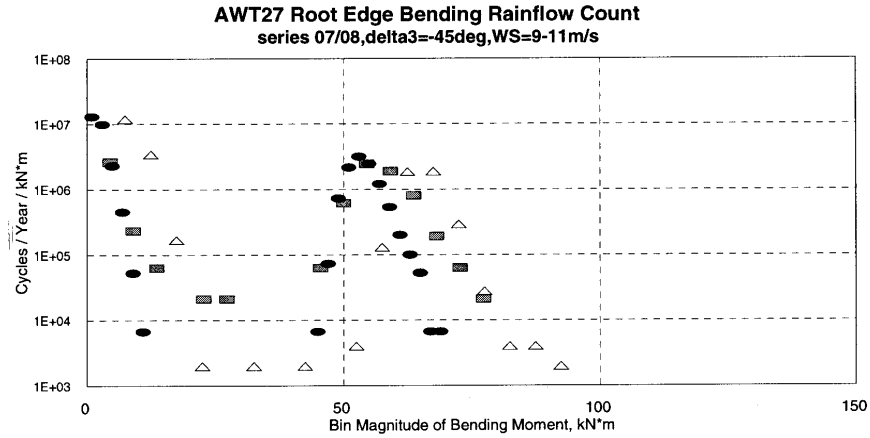

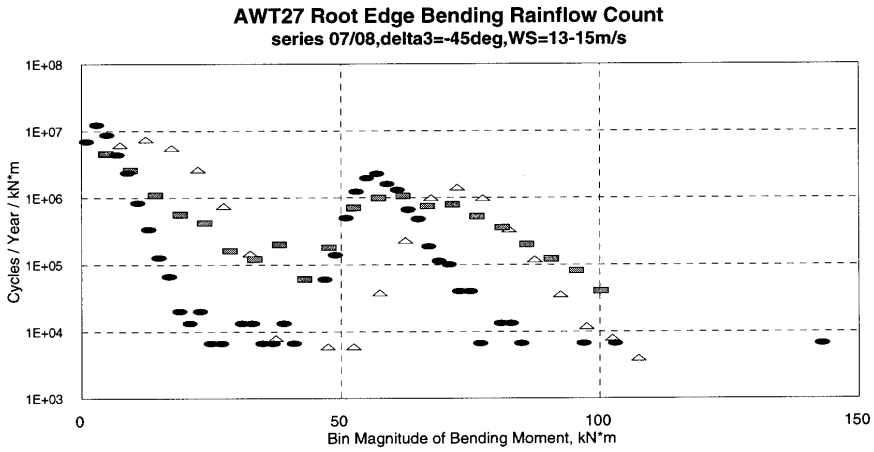

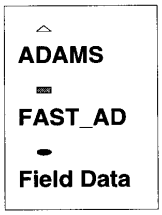

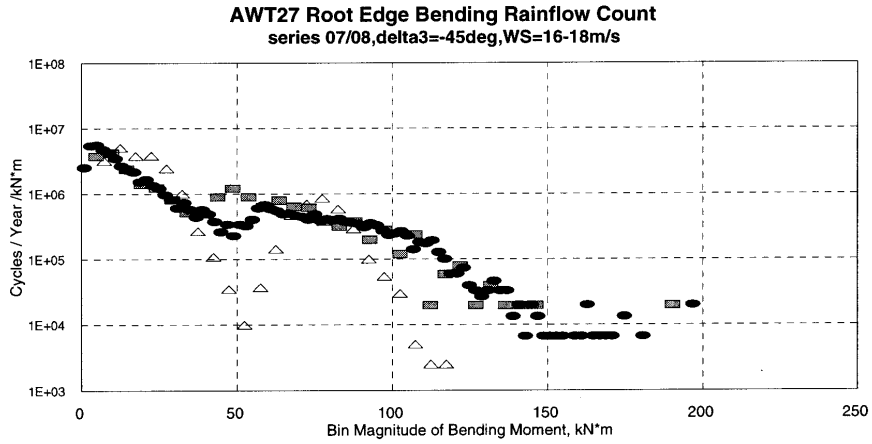

Figure 9.27. Rainflow Count of Blade Root Edgewise Bending Moment (medium turbulence).

FAST_AD vs. ADAMS & Field Data at medium turbulence

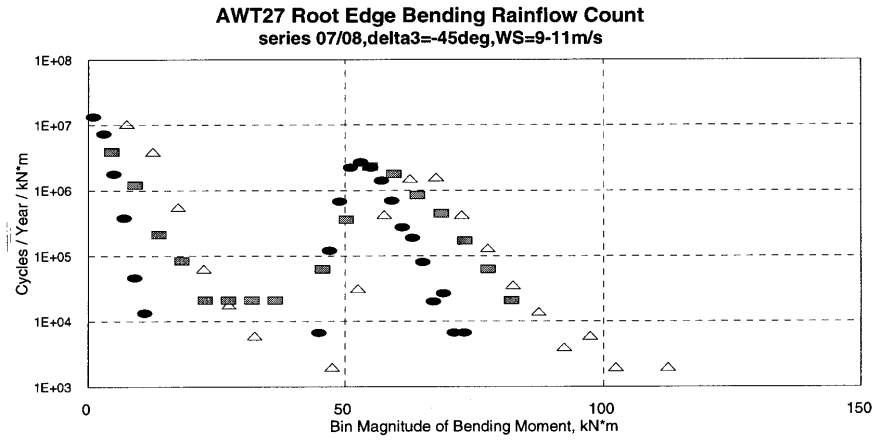

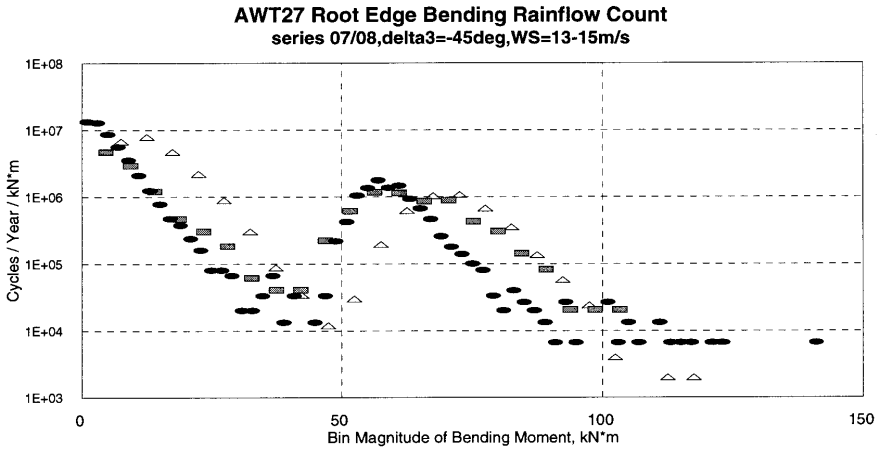

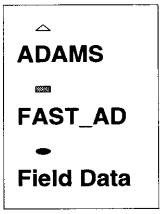

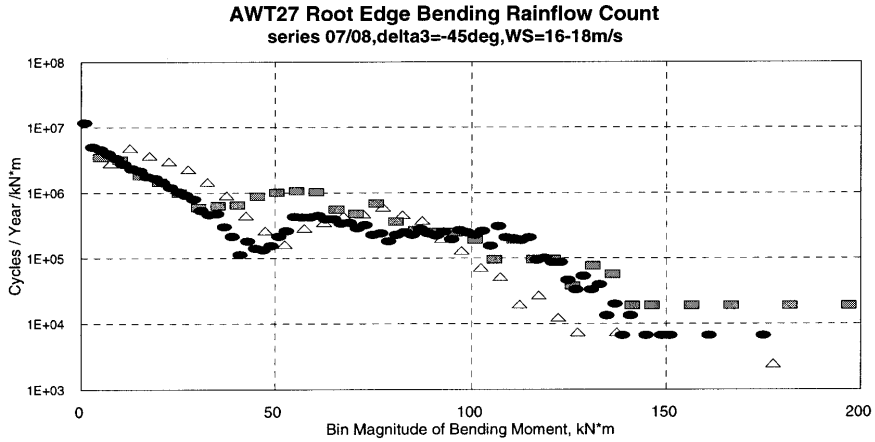

Figure 9.28. Rainflow Count of Blade Root Edgewise Bending Moment (high turbulence).

FAST_AD vs. ADAMS & Field Data at high turbulence

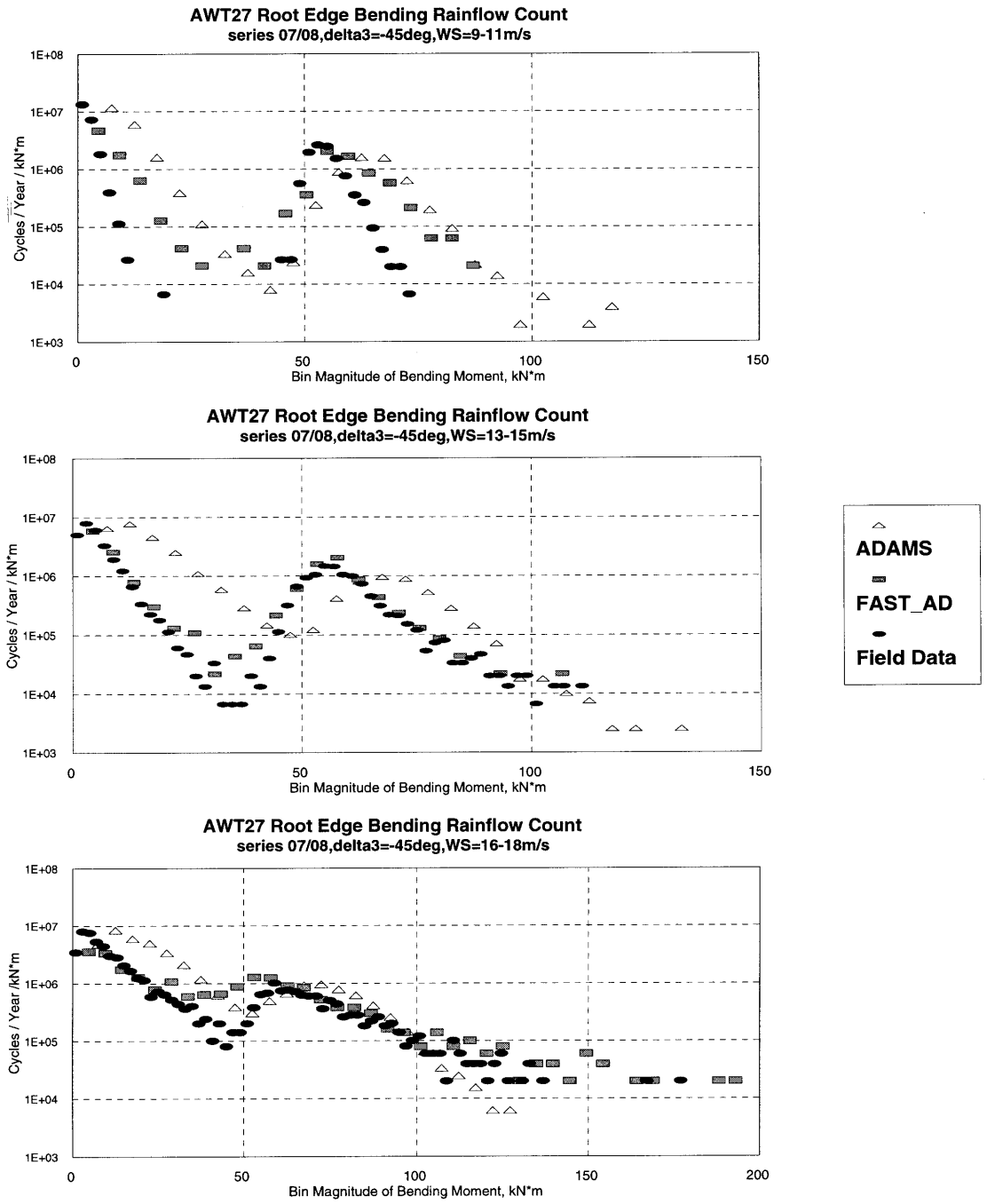

Figure 9.29. Rainflow Count of Blade Root Flapwise Bending Moment (low turbulence).

FAST_AD vs. ADAMS & Field Data at low turbulence

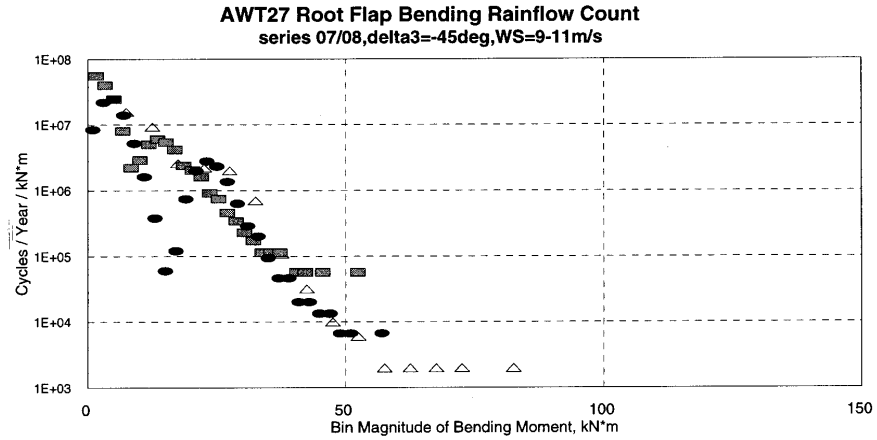

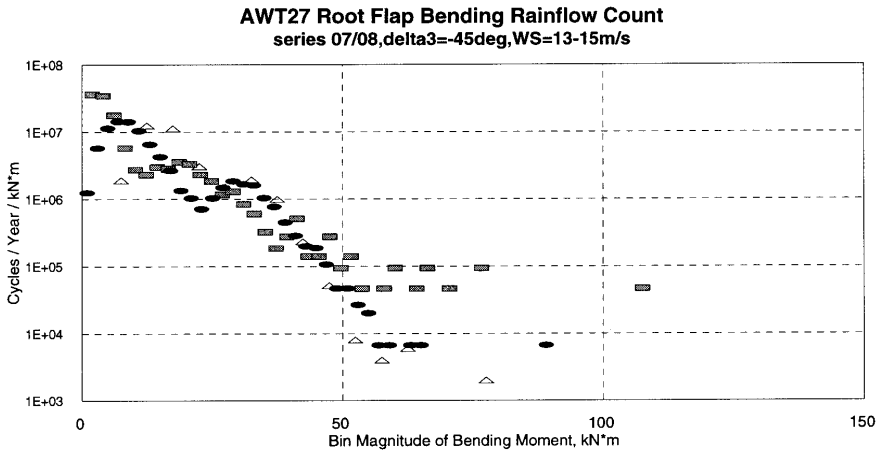

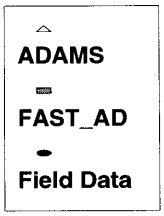

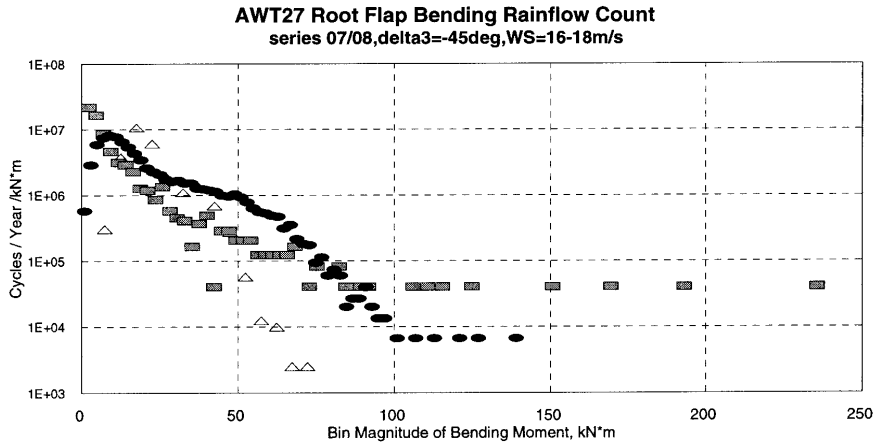

Figure 9.30. Rainflow Count of Blade Root Flapwise Bending Moment (medium turbulence).

FAST_AD vs. ADAMS & Field Data at medium turbulence

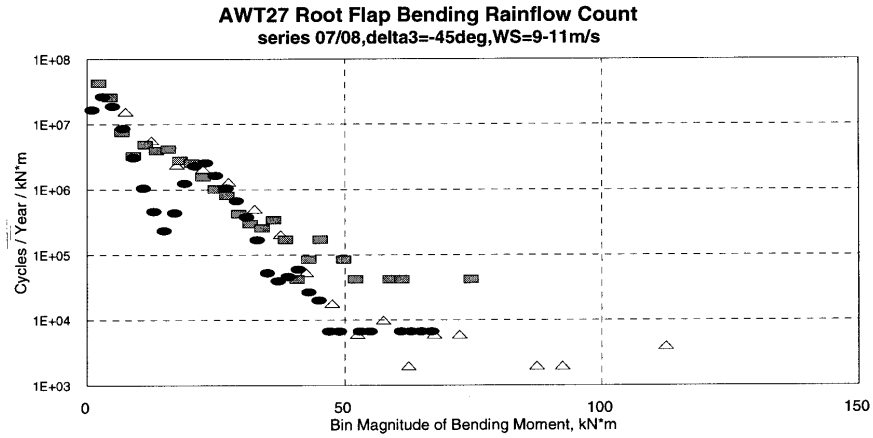

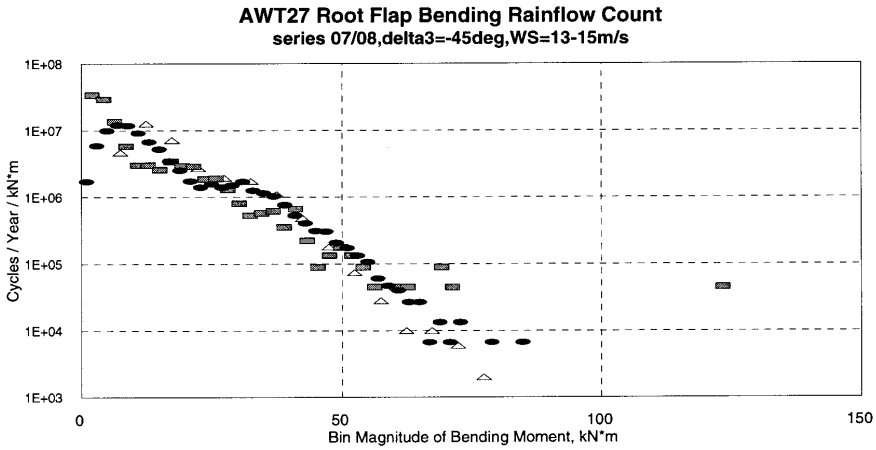

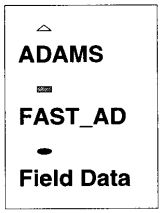

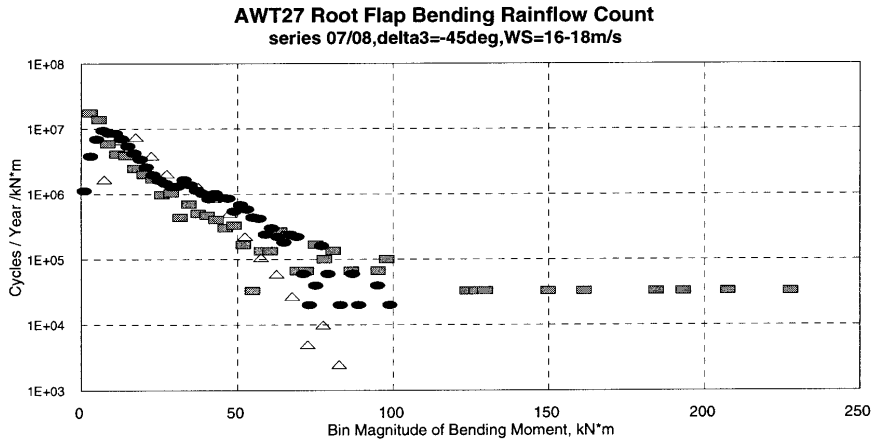

Figure 9.31. Rainflow Count of Blade Root Flapwise Bending Moment (high turbulence).

FAST_AD vs. ADAMS & Field Data at high turbulence

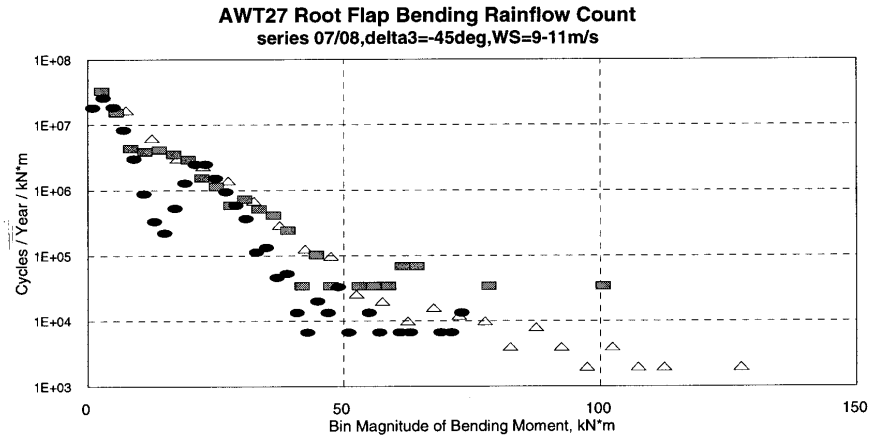

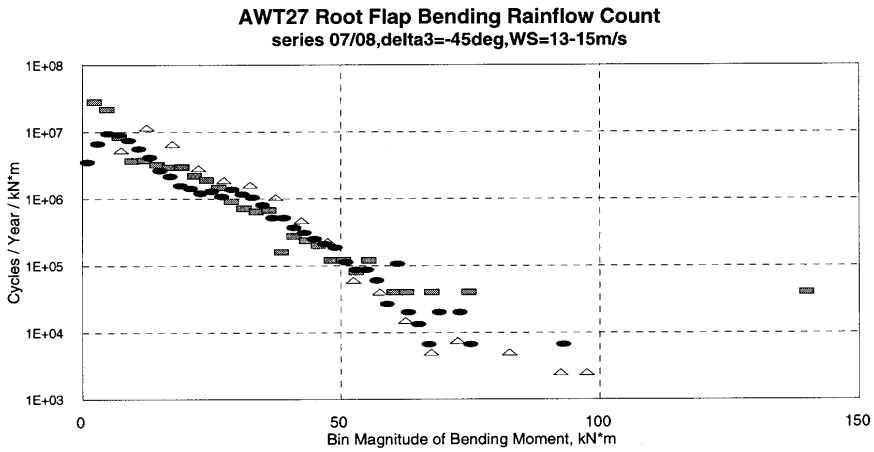

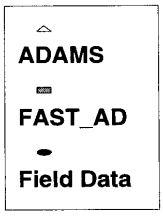

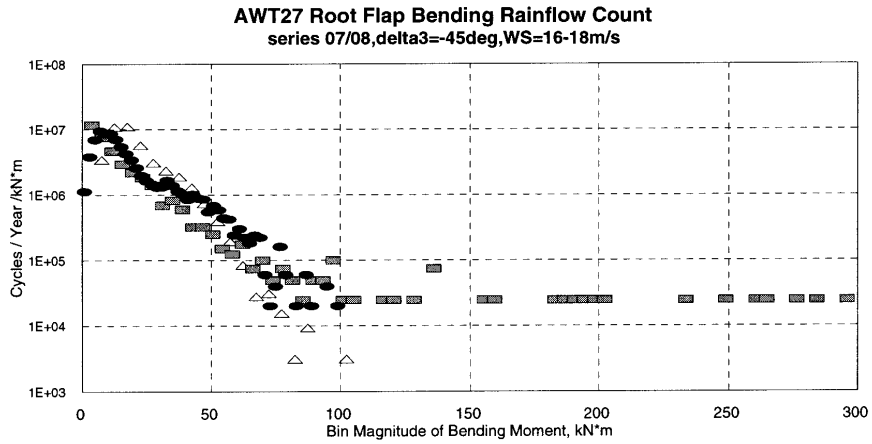

Figure 9.32. Rainflow Count of Shaft Torque (low turbulence).

FAST_AD vs. ADAMS & Field Data at low turbulence

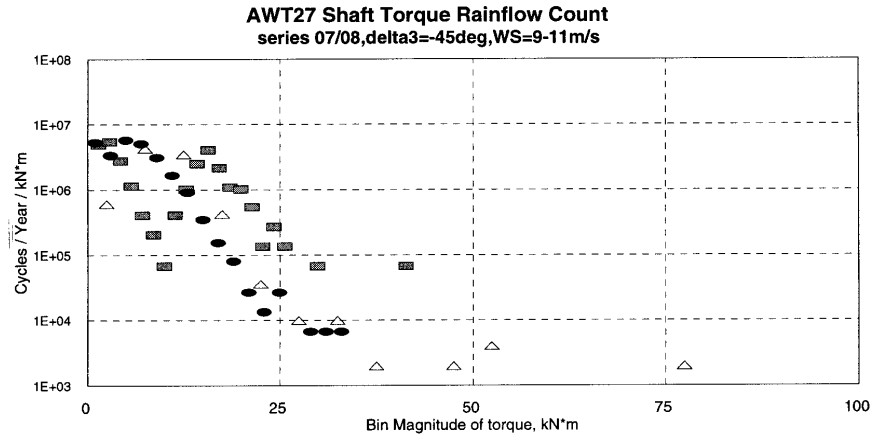

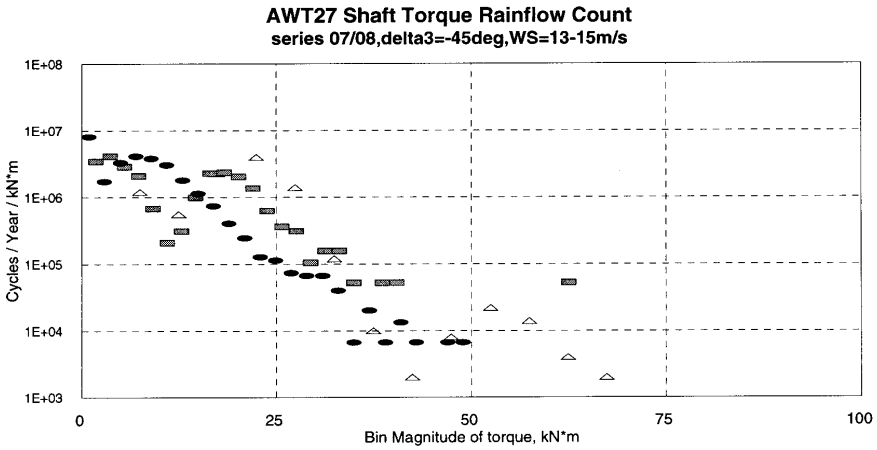

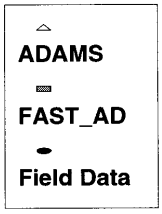

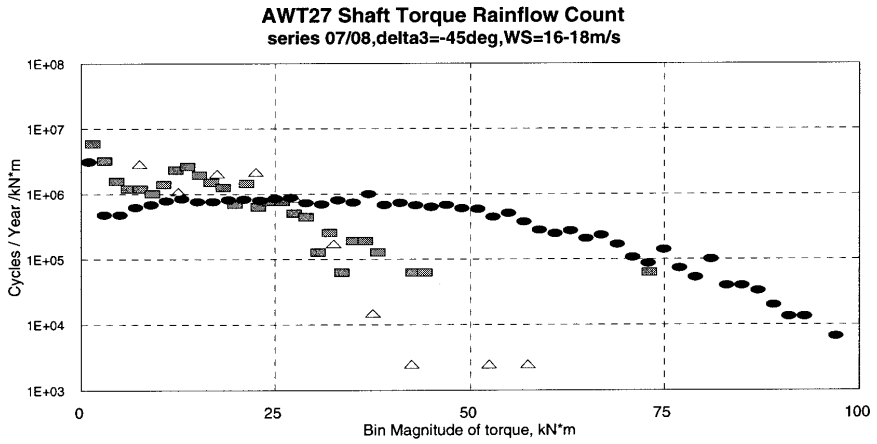

Figure 9.33. Rainflow Count of Shaft Torque (medium turbulence).

FAST_AD vs. ADAMS & Field Data at medium turbulence

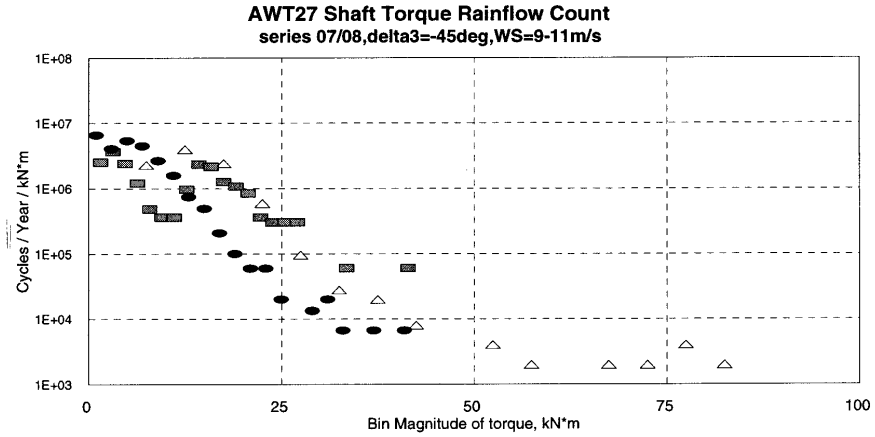

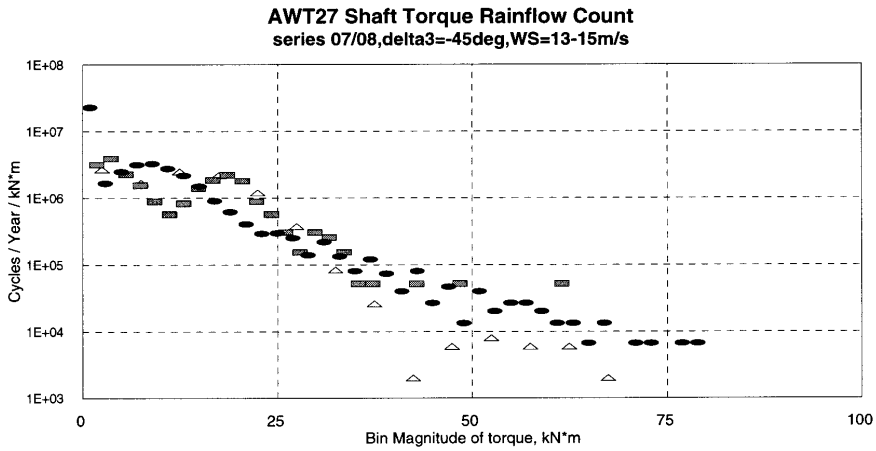

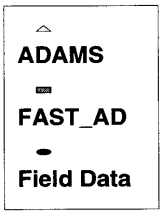

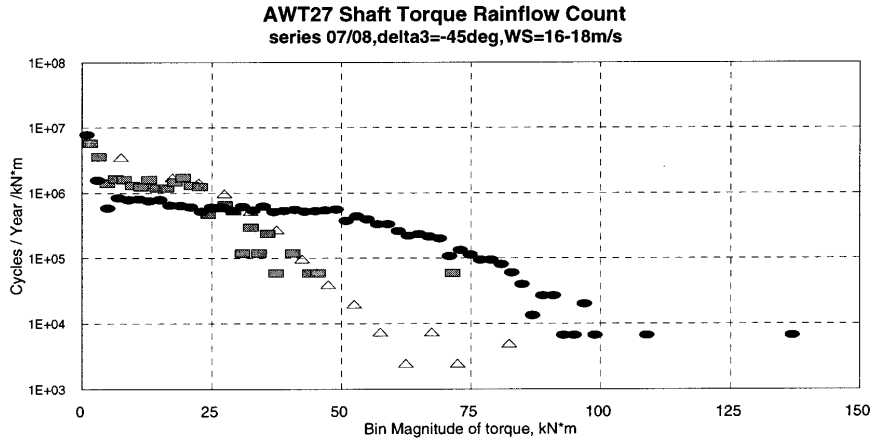

Figure 9.34. Rainflow Count of Shaft Torque (high turbulence).

FAST_AD vs. ADAMS & Field Data at high turbulence

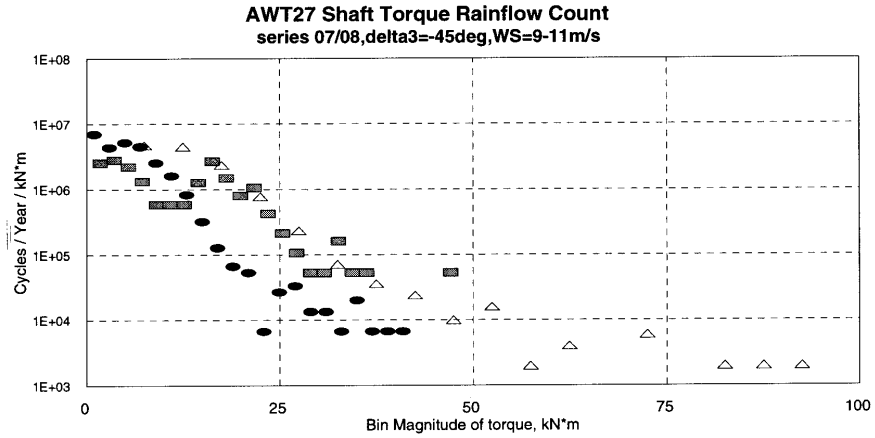

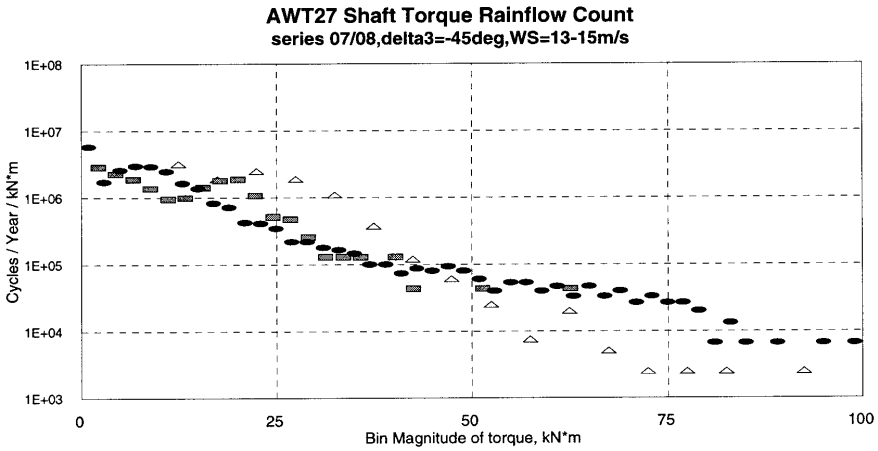

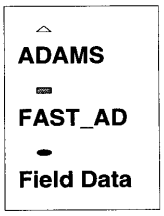

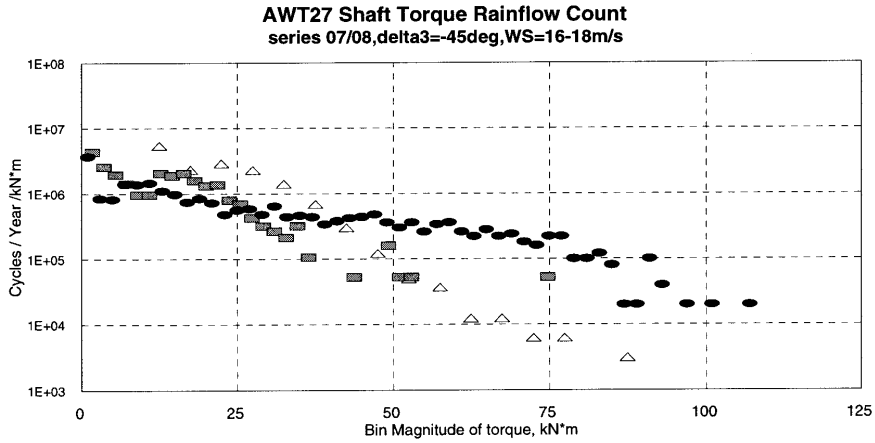

Figure 9.35. Rainflow Count of Teeter Angle (low turbulence).

FAST_AD vs. ADAMS & Field Data at low turbulence

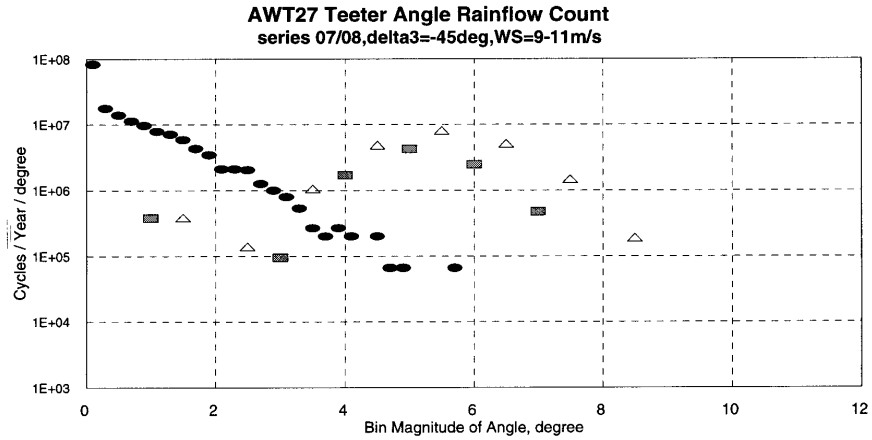

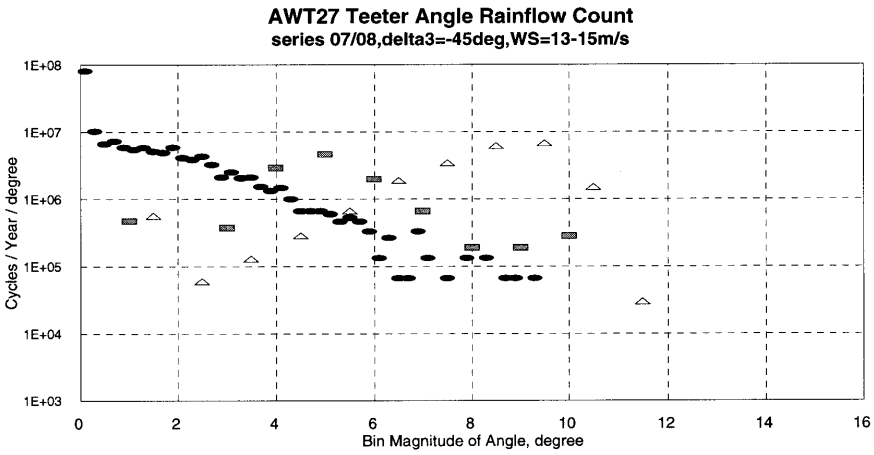

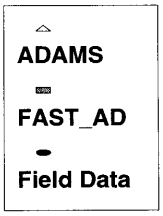

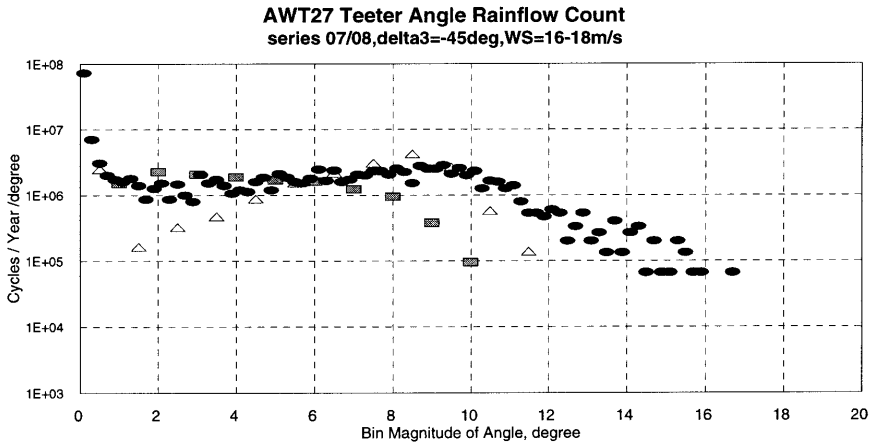

Figure 9.36. Rainflow Count of Teeter Angle (medium turbulence).

FAST_AD vs. ADAMS & Field Data at med turbulence

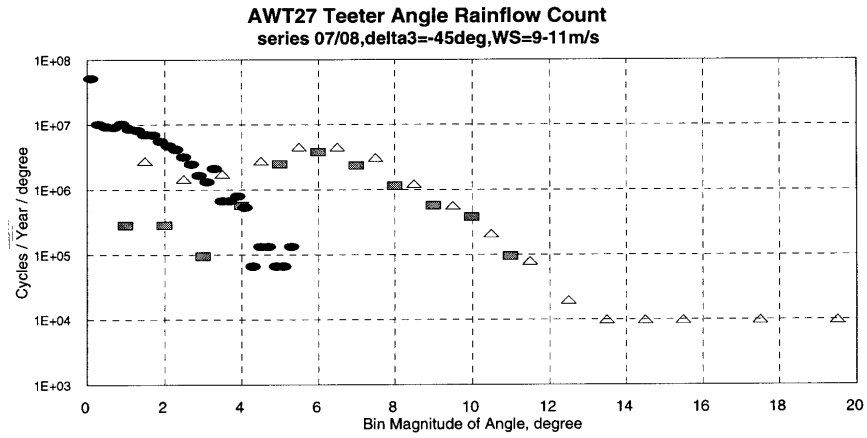

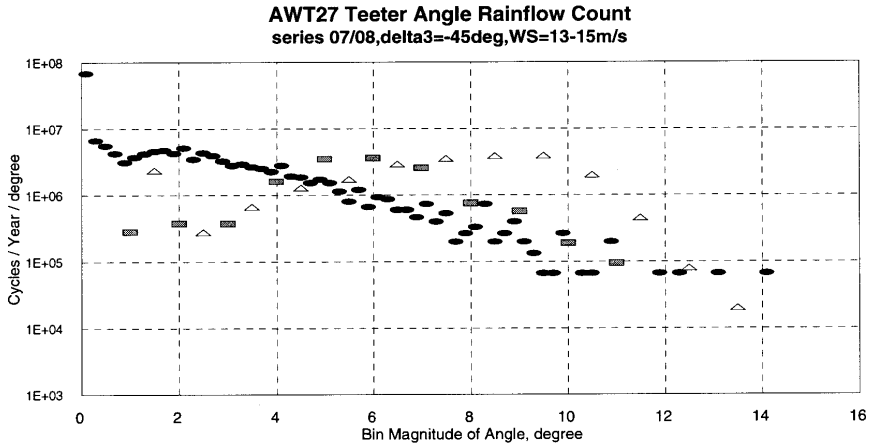

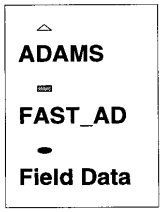

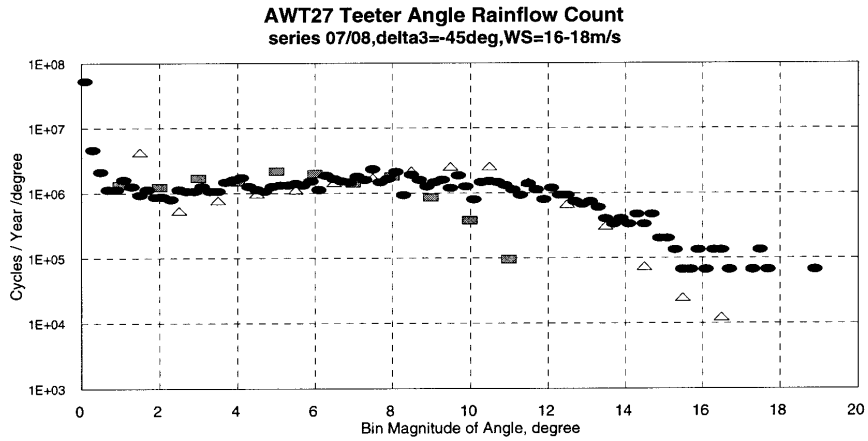

Figure 9.37. Rainflow Count of Teeter Angle (high turbulence).

FAST_AD vs. ADAMS & Field Data at high turbulence

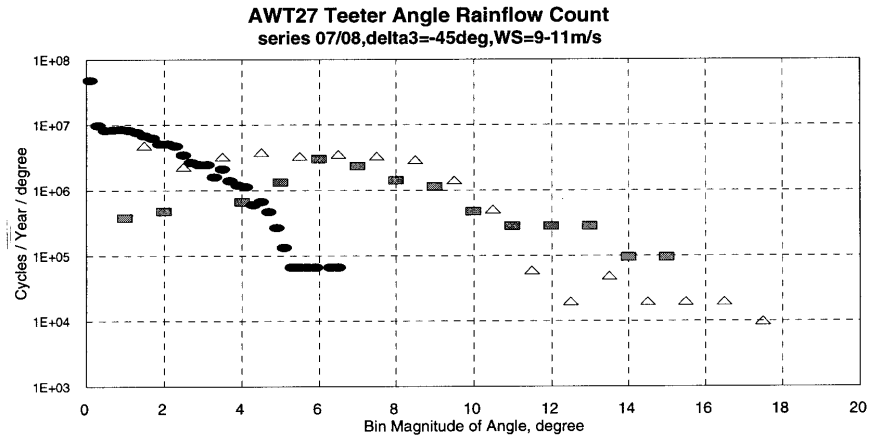

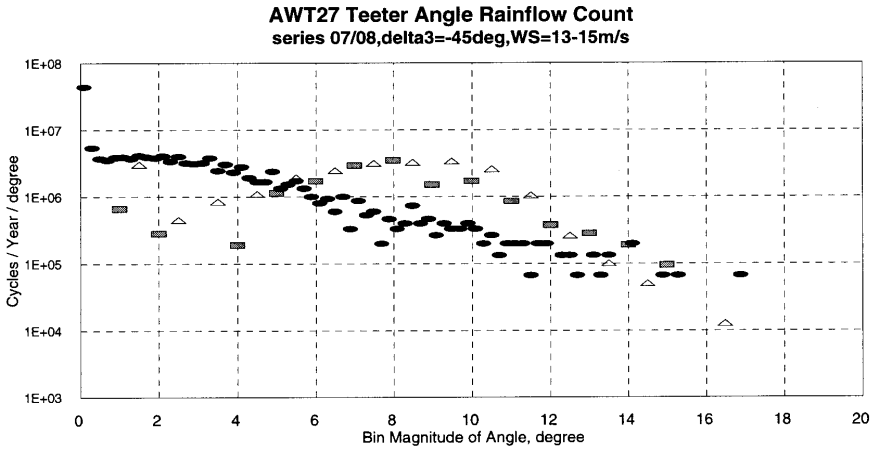

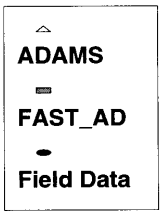

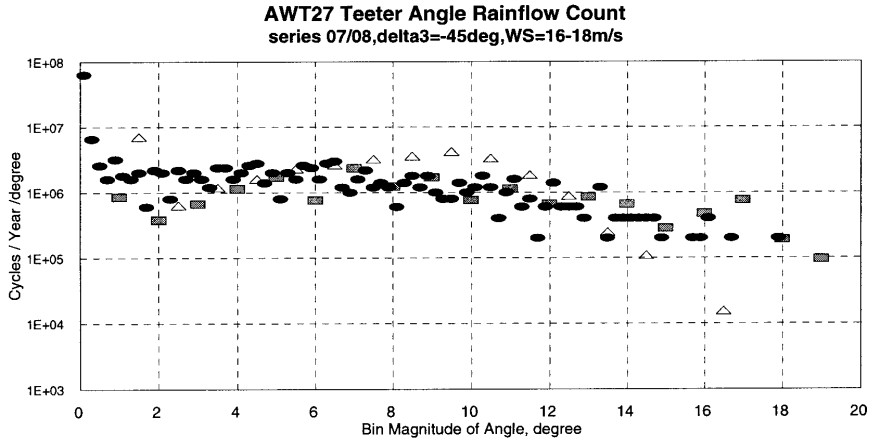

Figure 9.38. Rainflow Count of Yaw Angle (low turbulence).

FAST_AD vs. ADAMS & Field Data at low turbulence

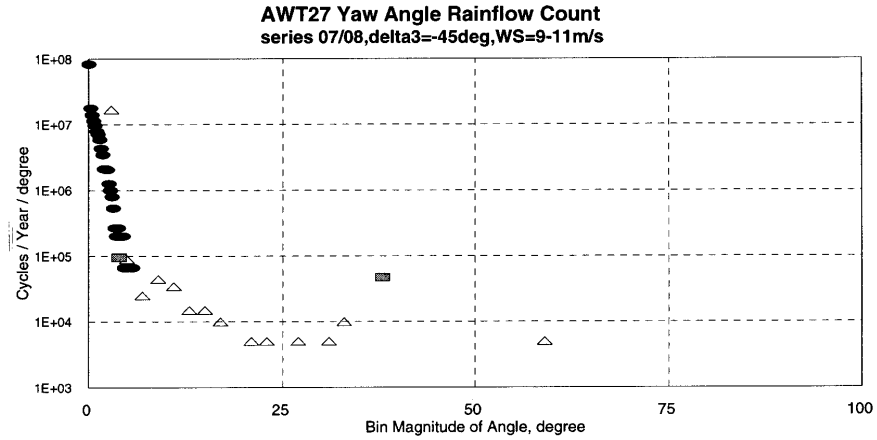

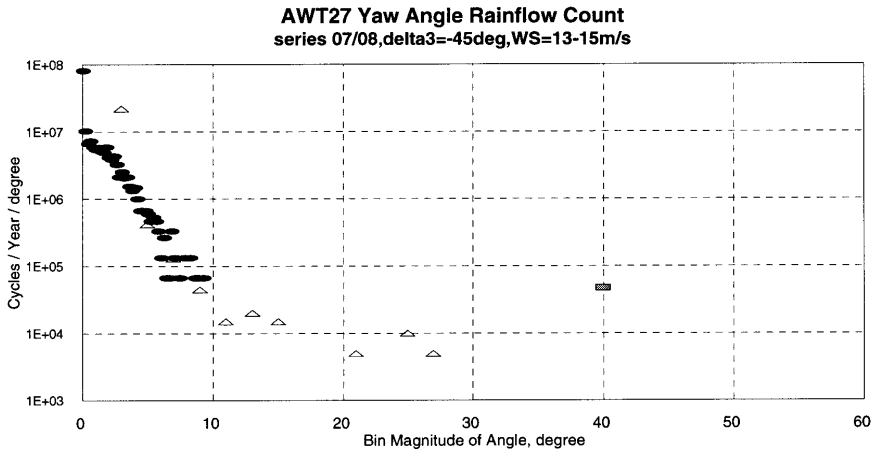

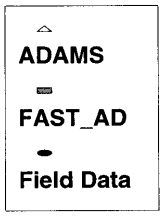

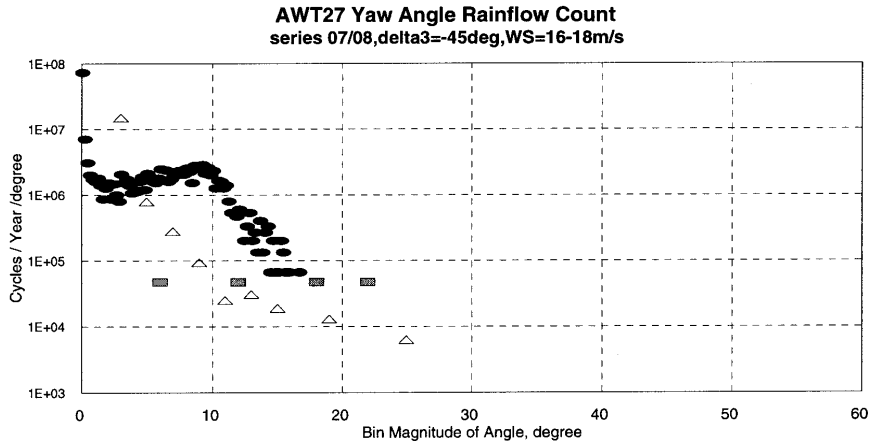

Figure 9.39. Rainflow Count of Yaw Angle (medium turbulence).

FAST_AD vs. ADAMS & Field Data at medium turbulence

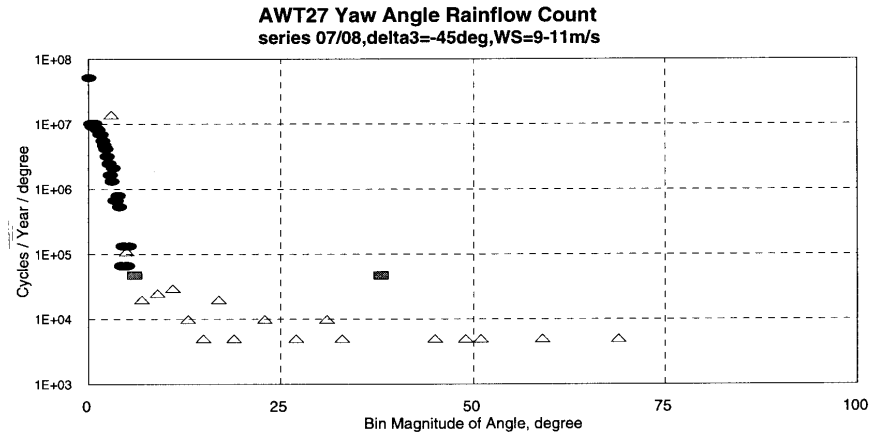

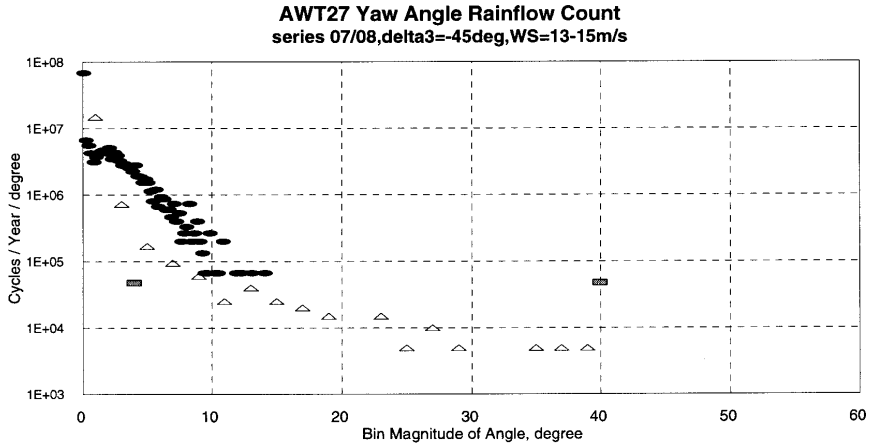

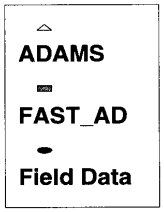

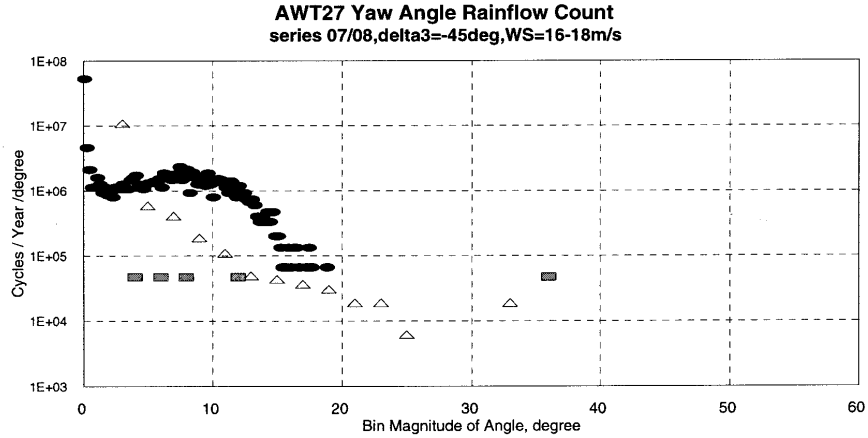

Figure 9.40. Rainflow Count of Yaw Angle (high turbulence).

FAST_AD vs. ADAMS & Field Data at high turbulence

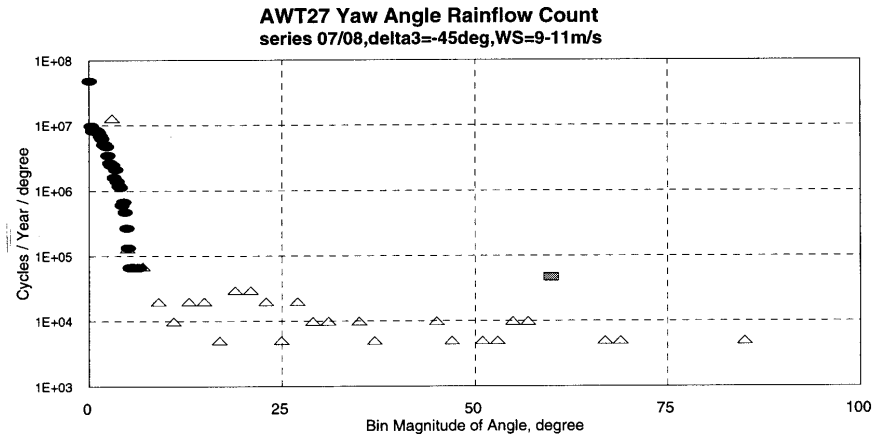

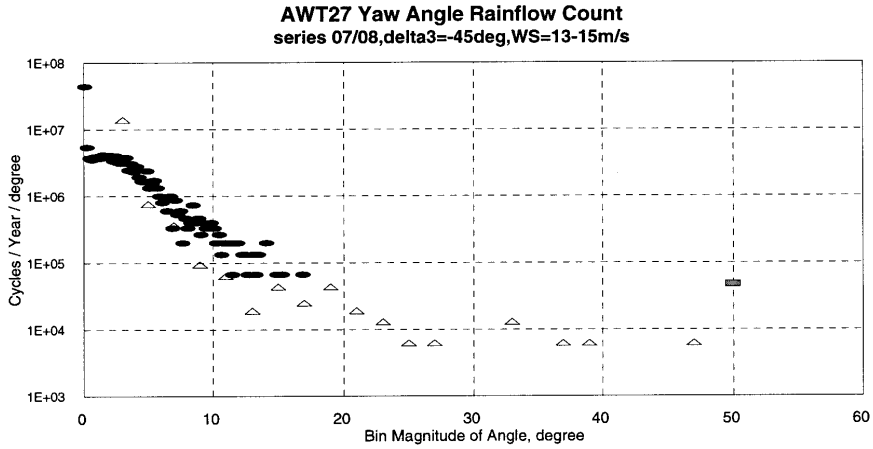

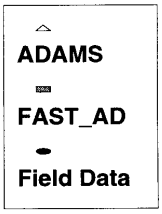

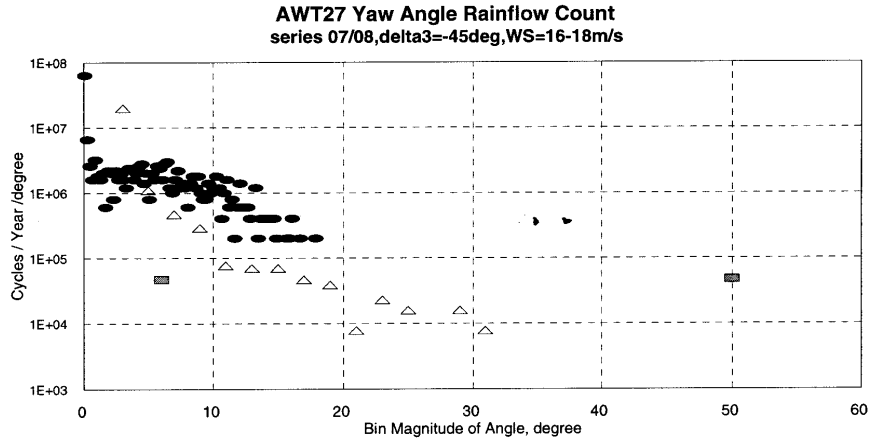

-30° Delta-three Cases

Figure 9.41. Rainflow Count of Blade Root Edgewise Bending Moment (low turbulence).

FAST_AD vs. ADAMS & Field Data at low turbulence

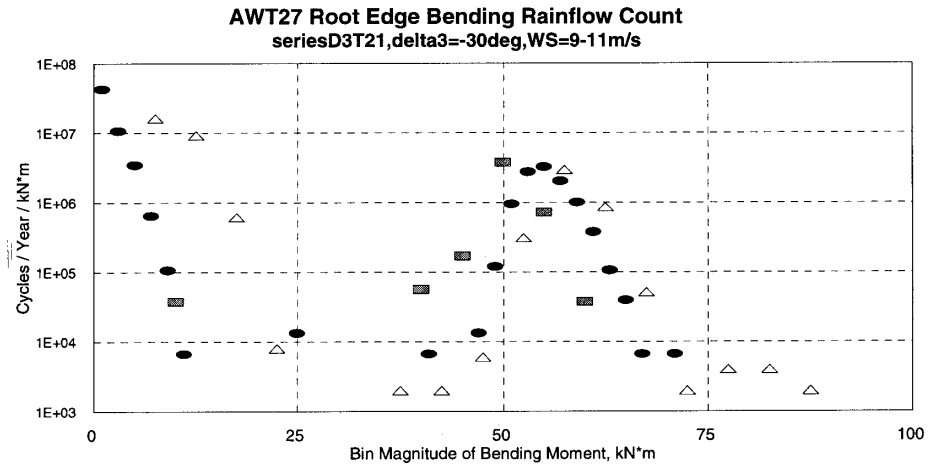

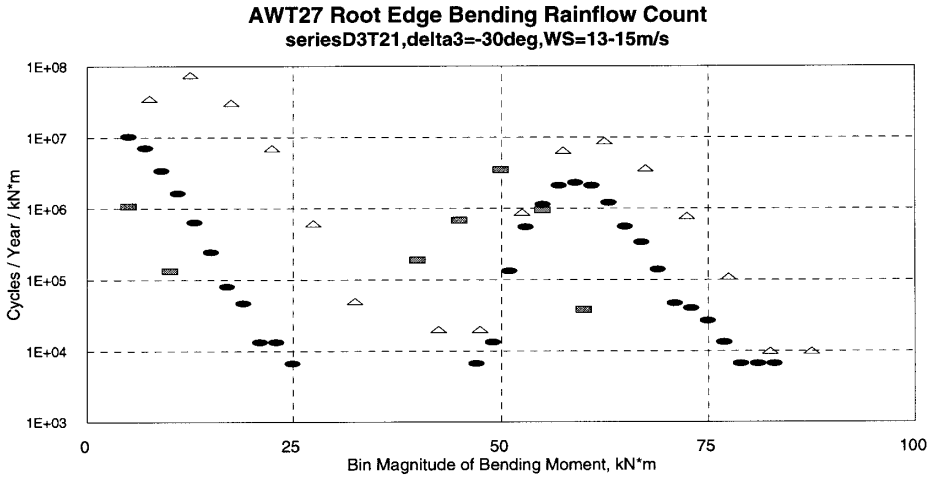

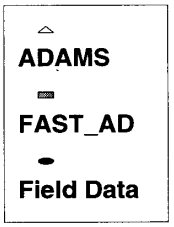

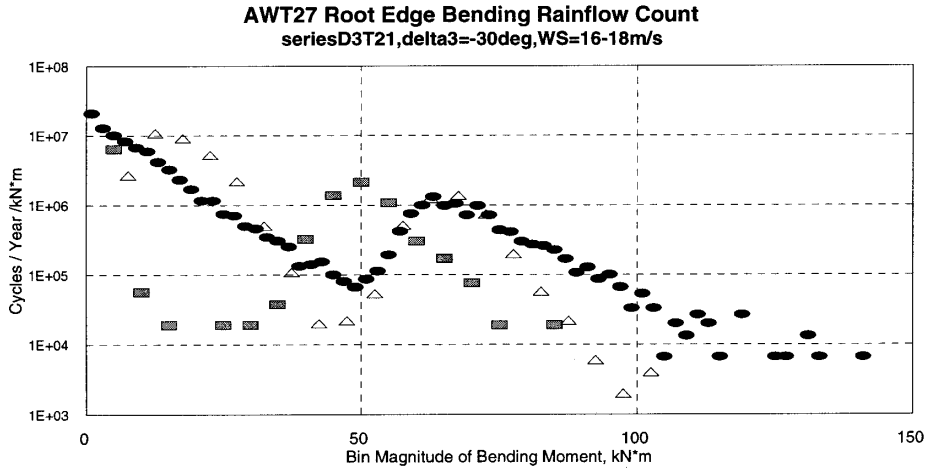

Figure 9.42. Rainflow Count of Blade Root Edgewise Bending Moment (medium turbulence).

FAST_AD vs. ADAMS & Field Data at medium turbulence

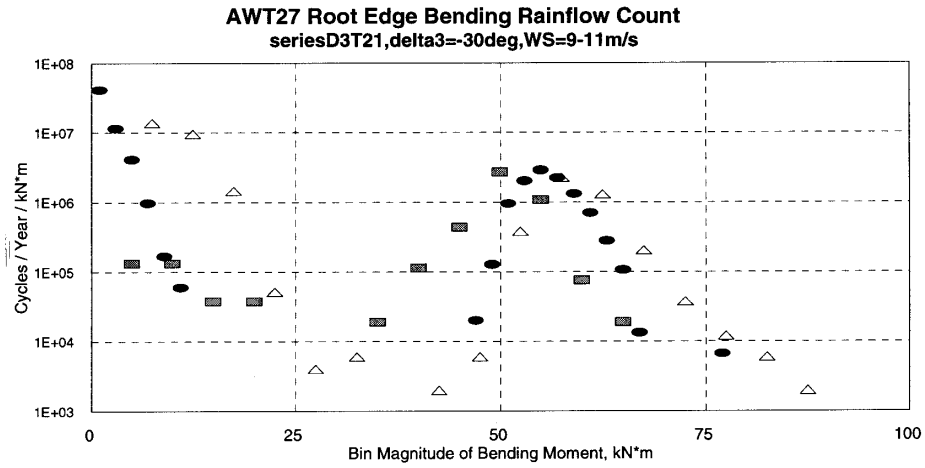

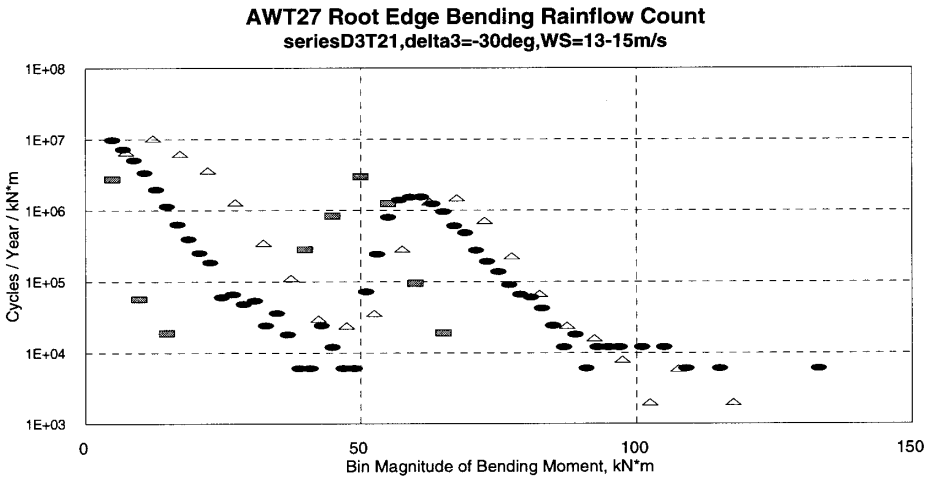

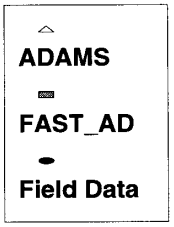

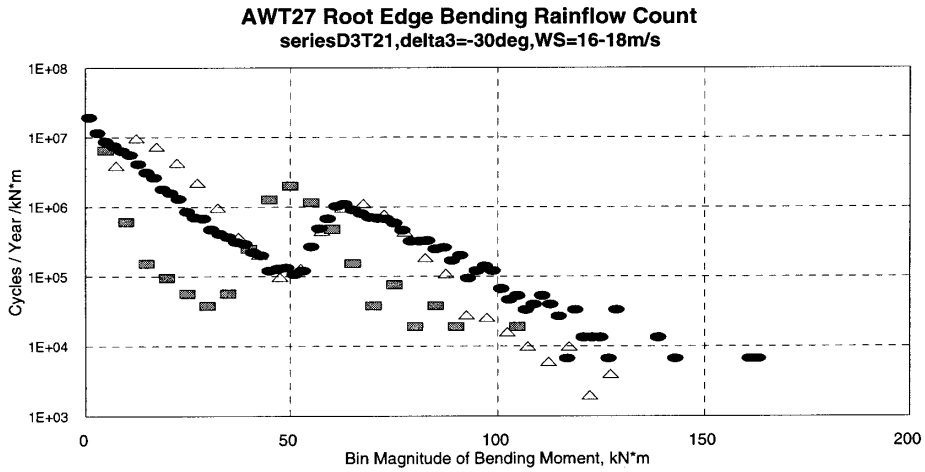

Figure 9.43. Rainflow Count of Blade Root Edgewise Bending Moment (high turbulence).

FAST_AD vs. ADAMS & Field Data at high turbulence

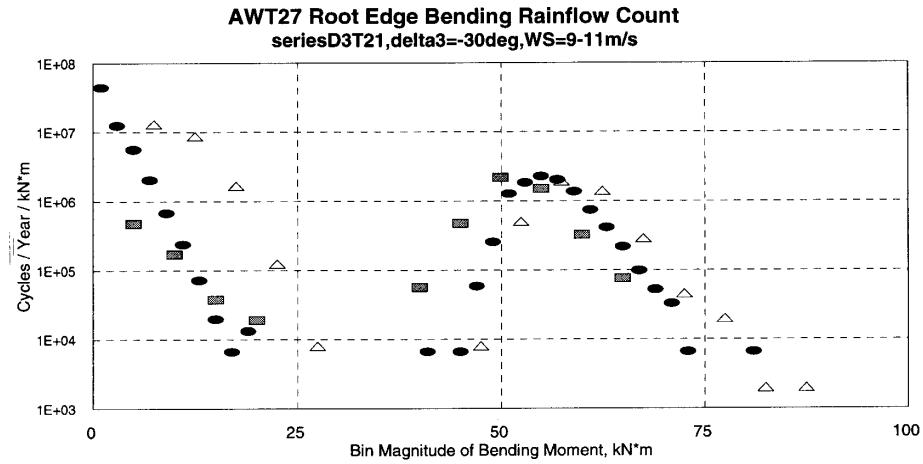

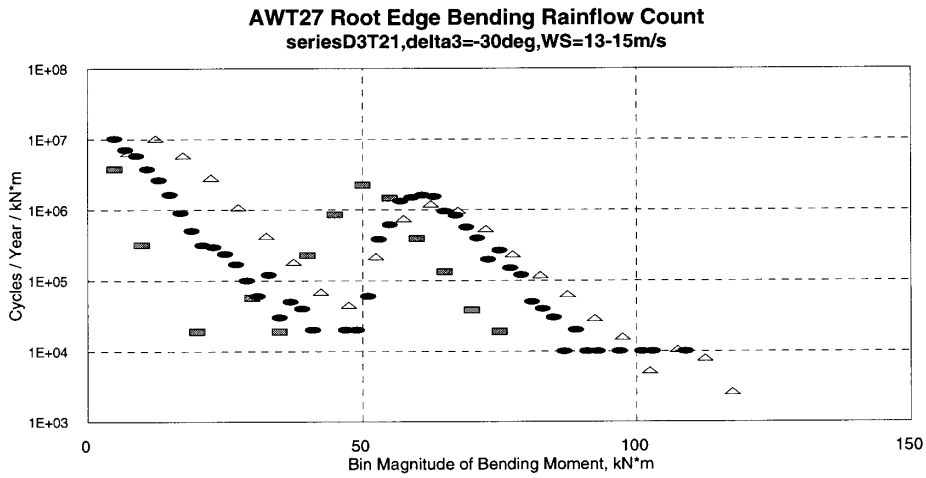

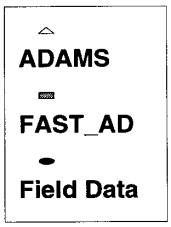

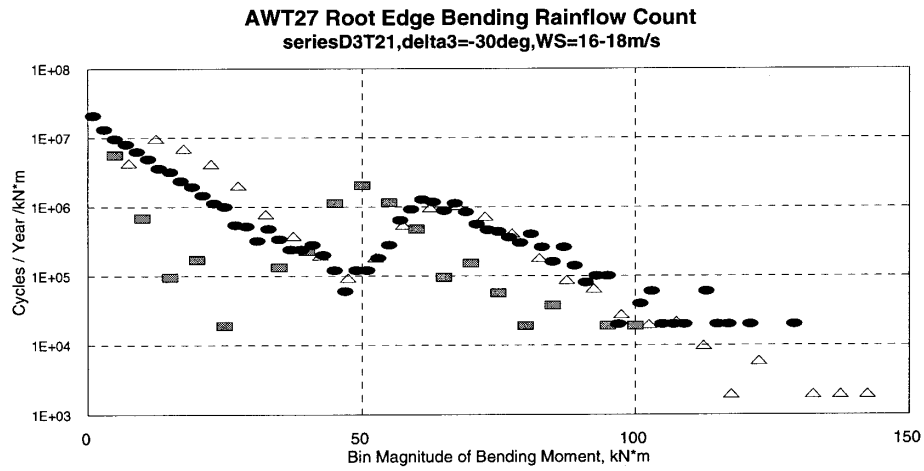

Figure 9.44. Rainflow Count of Blade Root Flapwise Bending Moment (low turbulence).

FAST_AD vs. ADAMS & Field Data at low turbulence

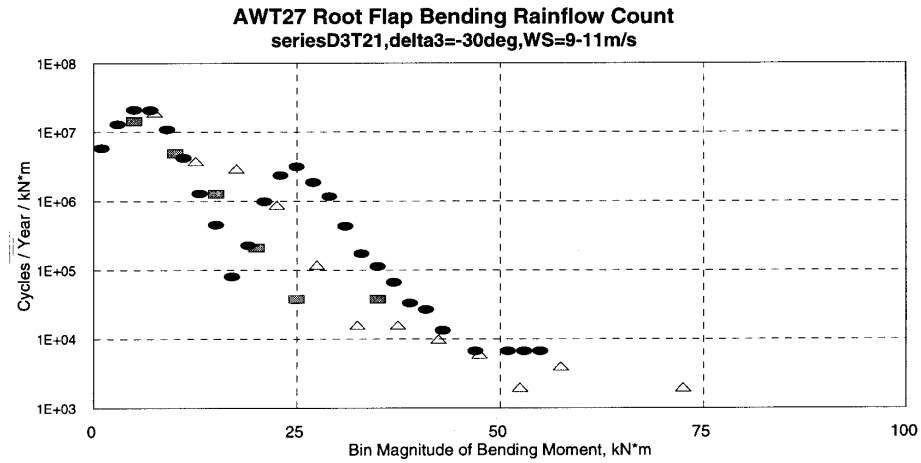

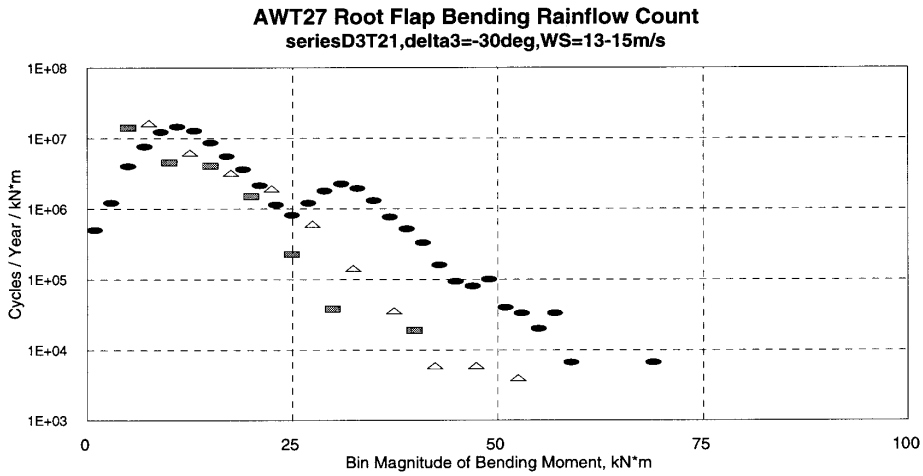

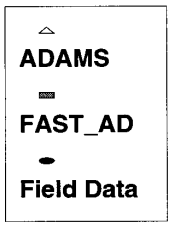

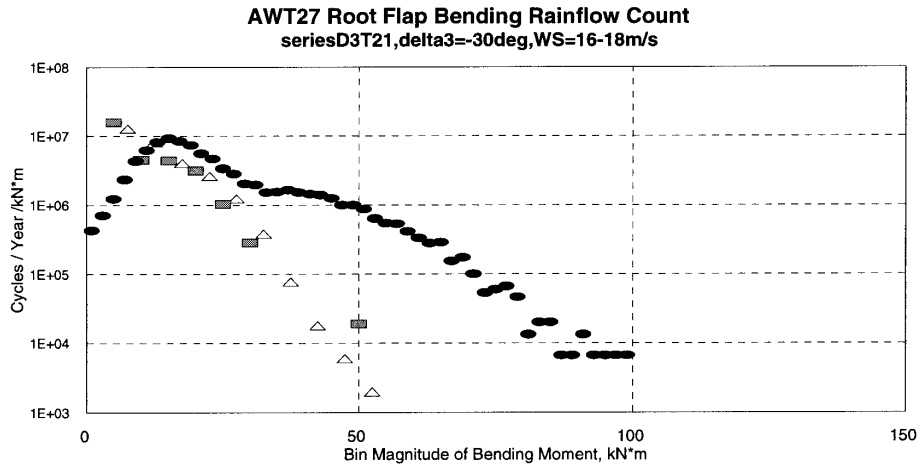

Figure 9.45. Rainflow Count of Blade Root Flapwise Bending Moment (medium turbulence).

FAST_AD vs. ADAMS & Field Data at medium turbulence

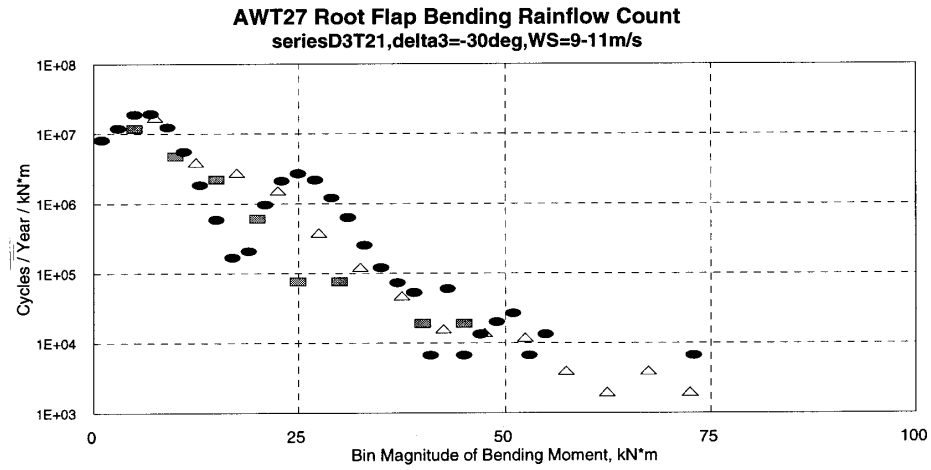

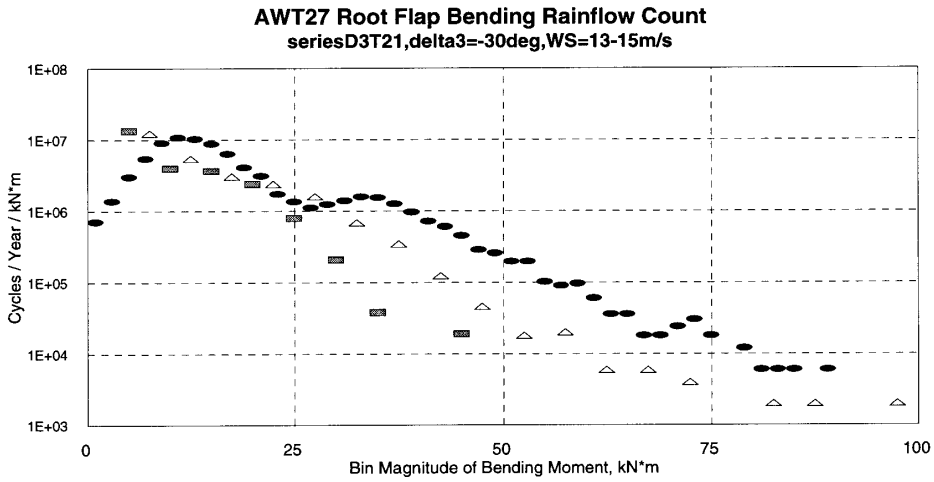

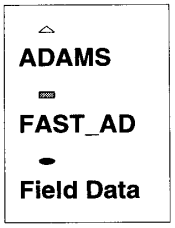

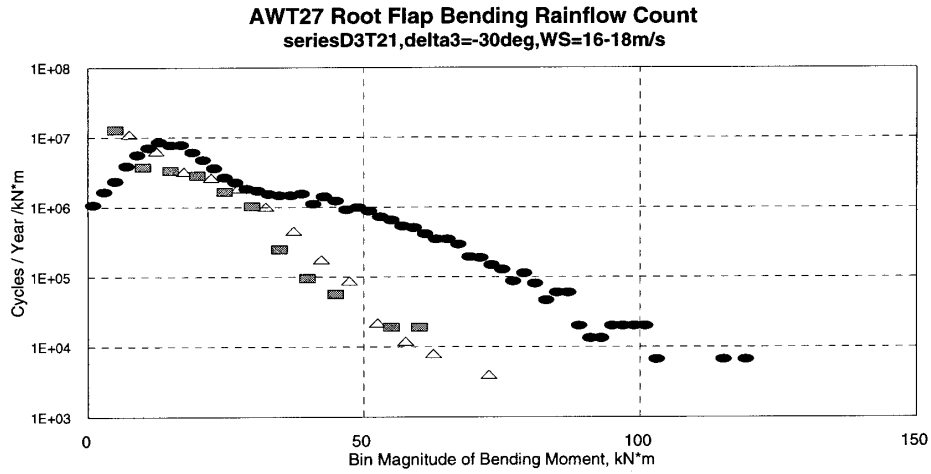

Figure 9.46. Rainflow Count of Blade Root Flapwise Bending Moment (high turbulence).

FAST_AD vs. ADAMS & Field Data at high turbulence

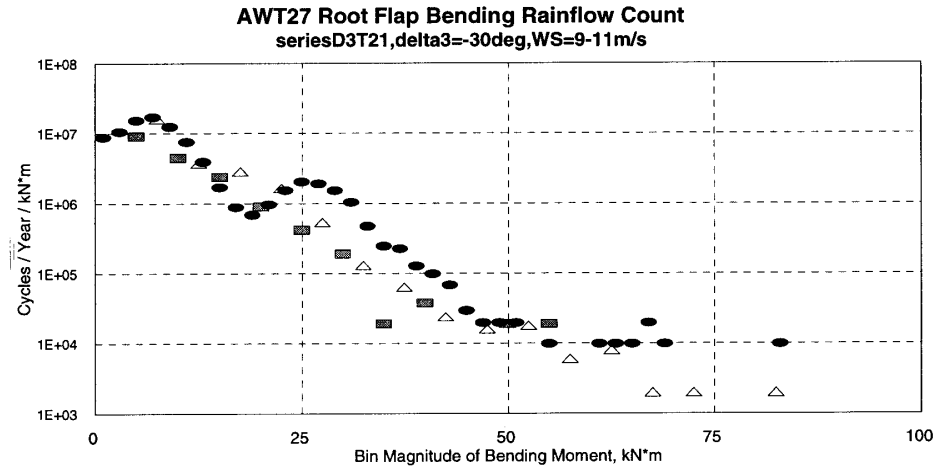

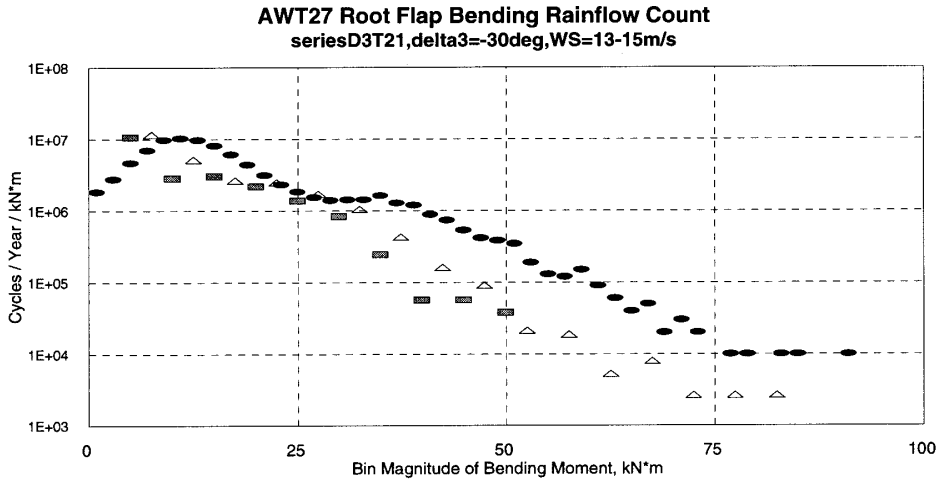

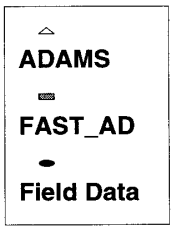

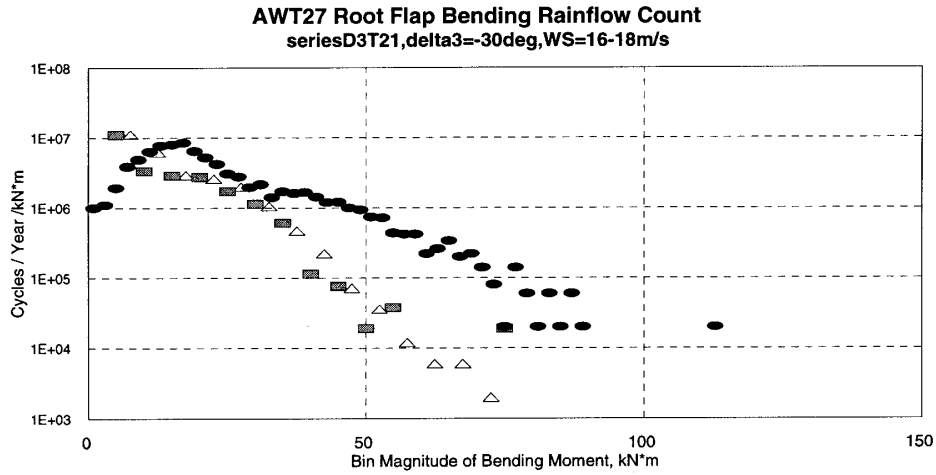

Figure 9.47. Rainflow Count of Shaft Torque (low turbulence).

FAST_AD vs. ADAMS & Field Data at low turbulence

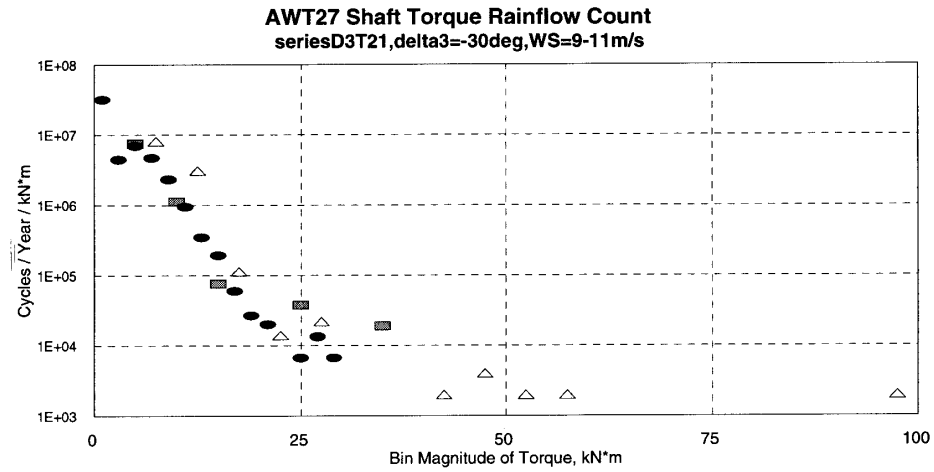

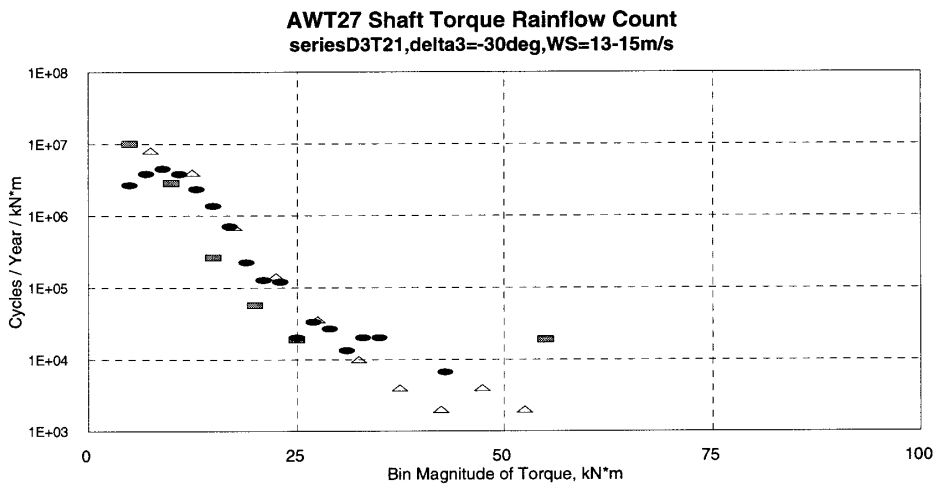

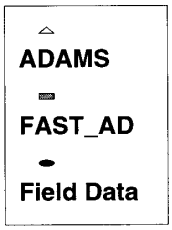

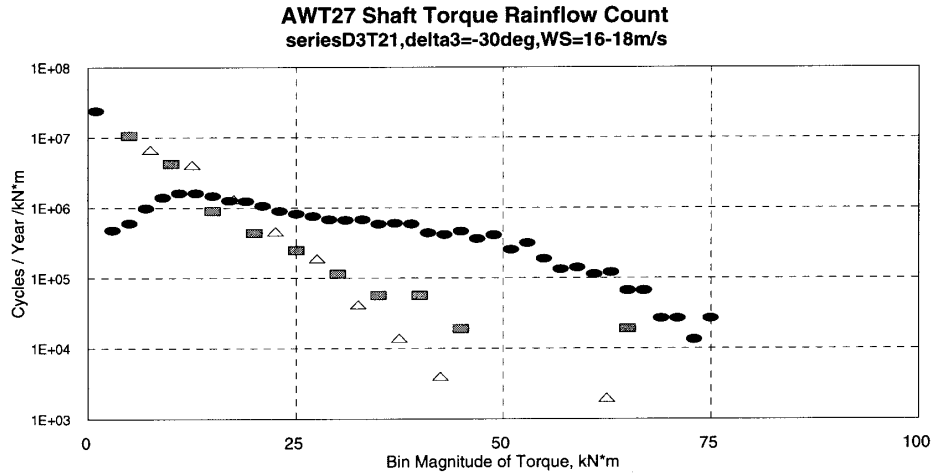

Figure 9.48. Rainflow Count of Shaft Torque (medium turbulence).

FAST_AD vs. ADAMS & Field Data at medium turbulence

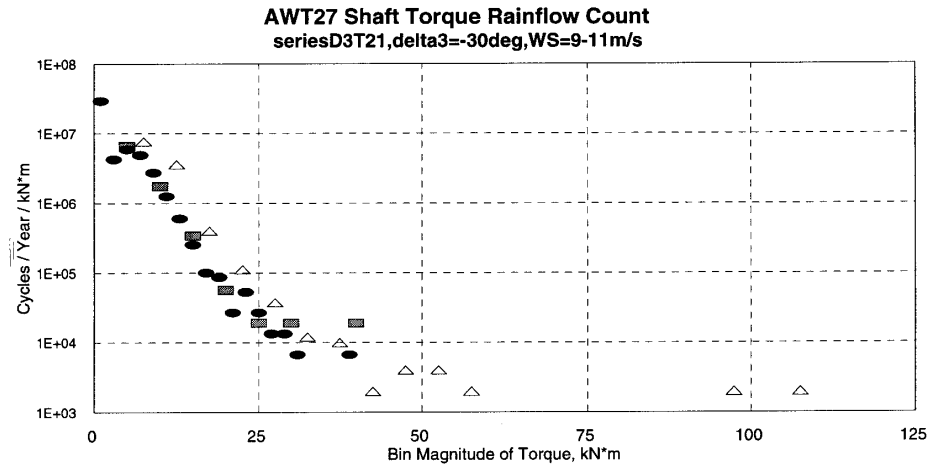

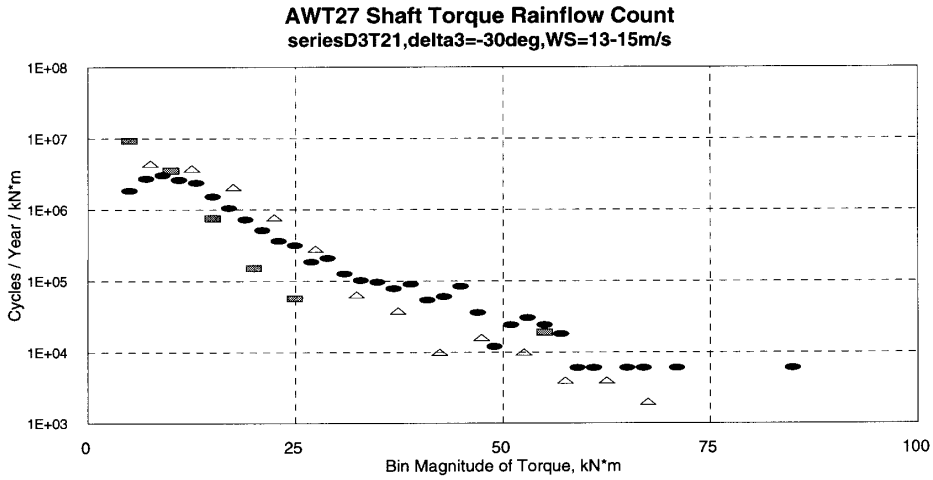

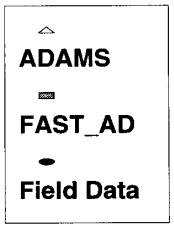

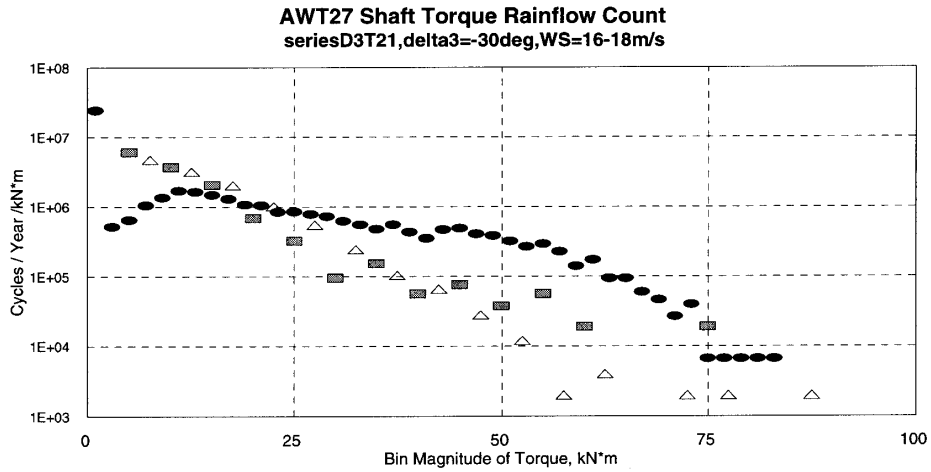

Figure 9.49. Rainflow Count of Shaft Torque (high turbulence).

FAST_AD vs. ADAMS & Field Data at high turbulence

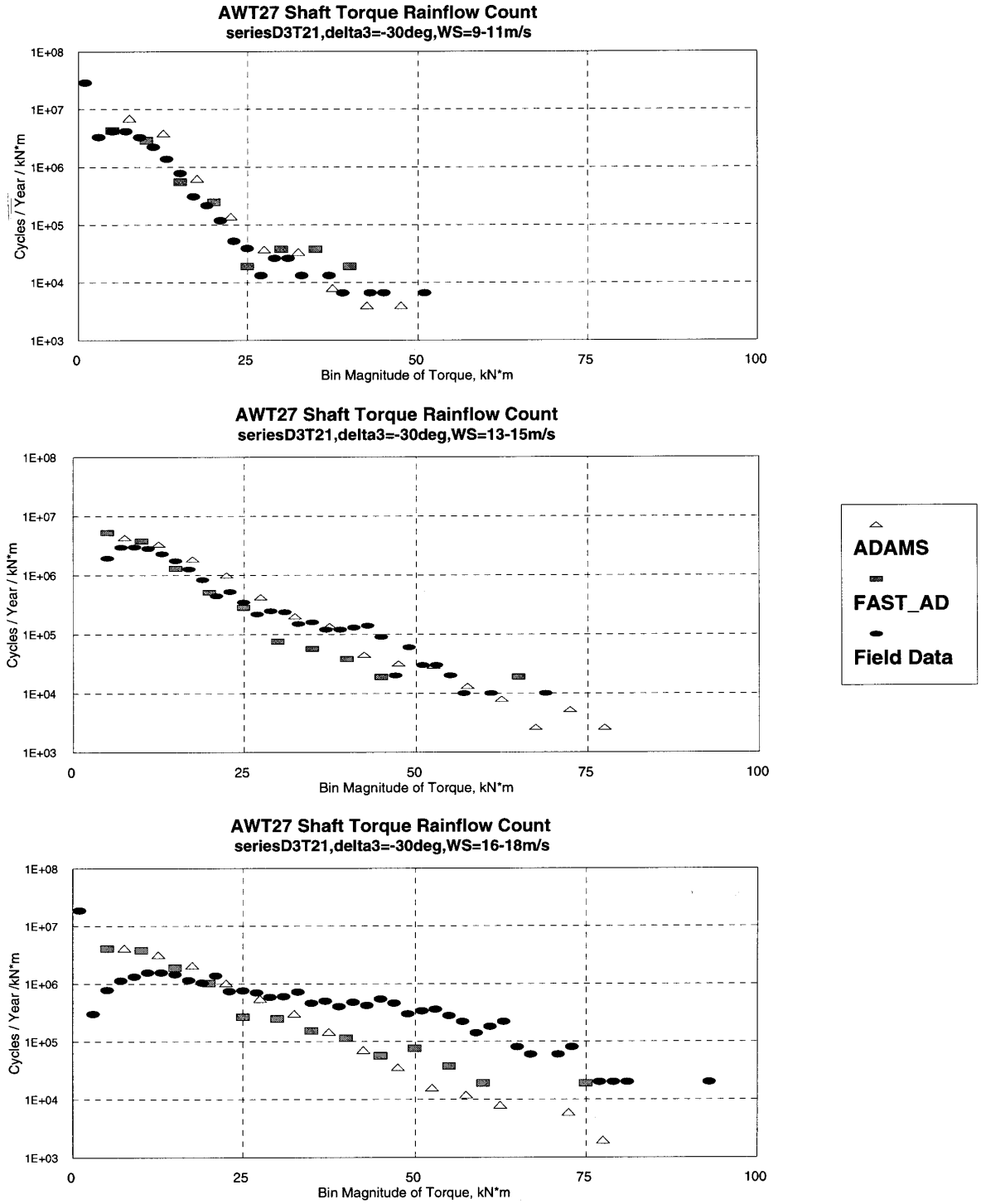

Figure 9.50. Rainflow Count of Teeter Angle (low turbulence).

FAST_AD vs. ADAMS & Field Data at low turbulence

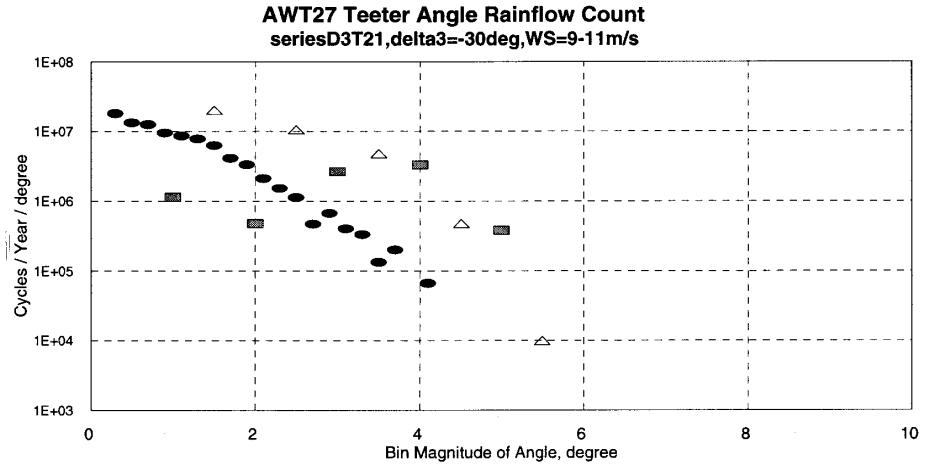

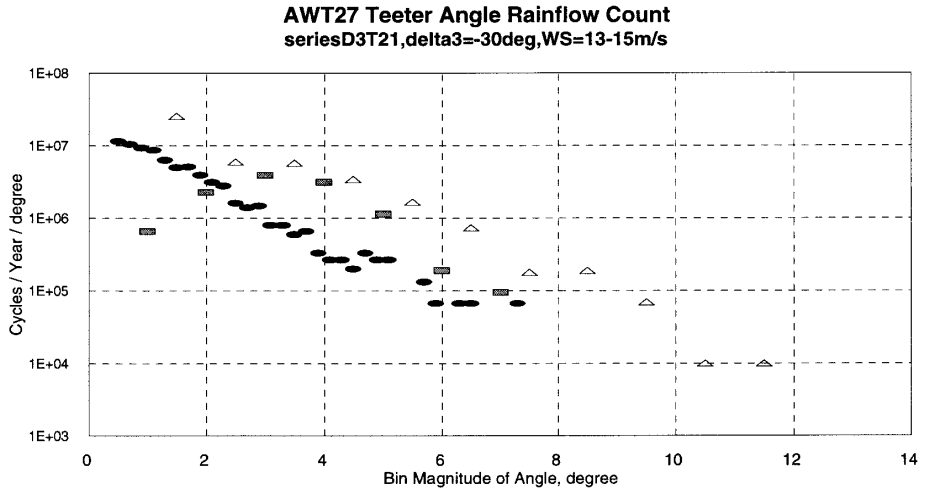

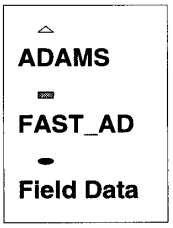

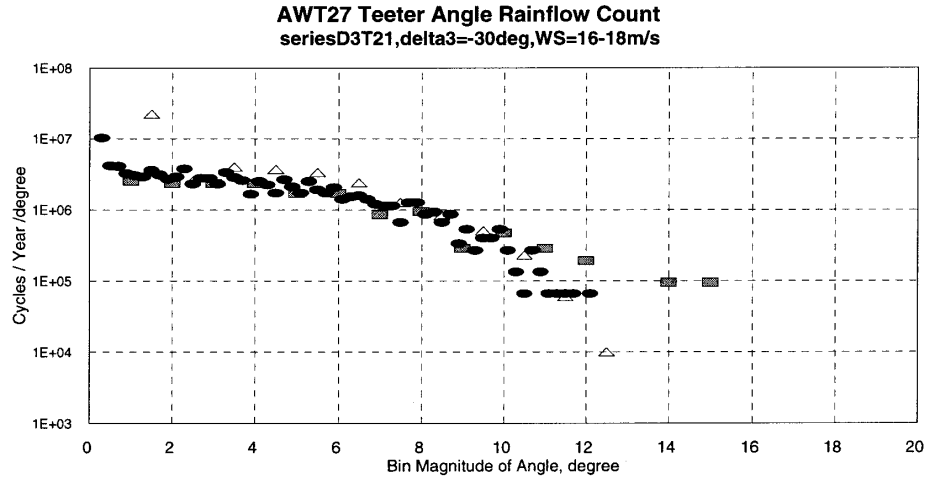

Figure 9.51. Rainflow Count of Teeter Angle (medium turbulence).

FAST_AD vs. ADAMS & Field Data at medium turbulence

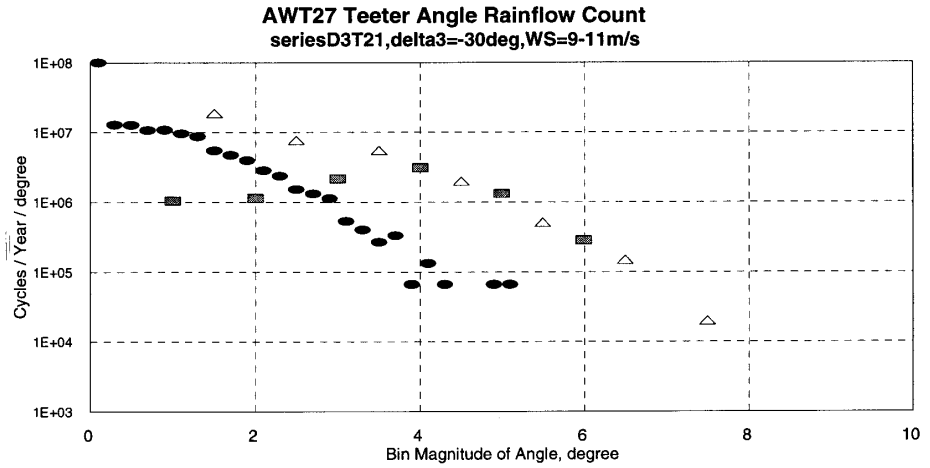

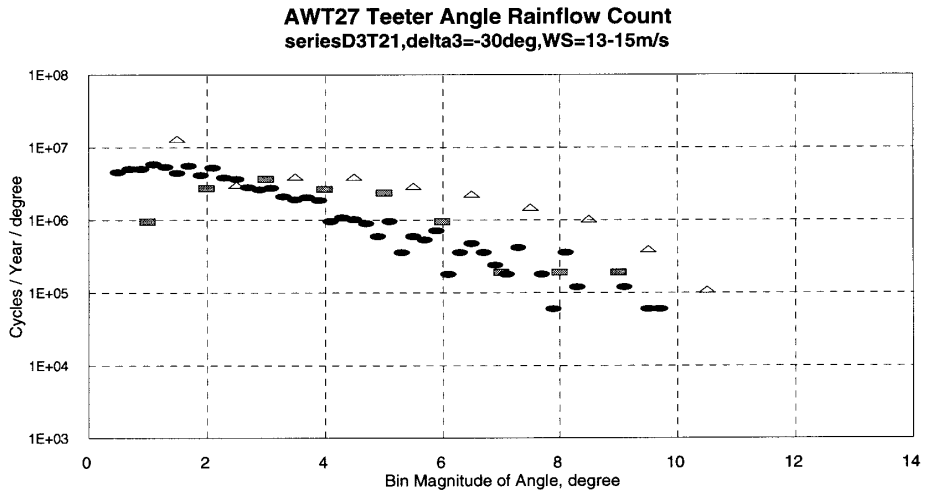

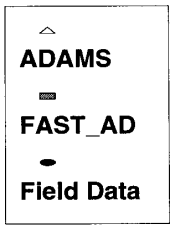

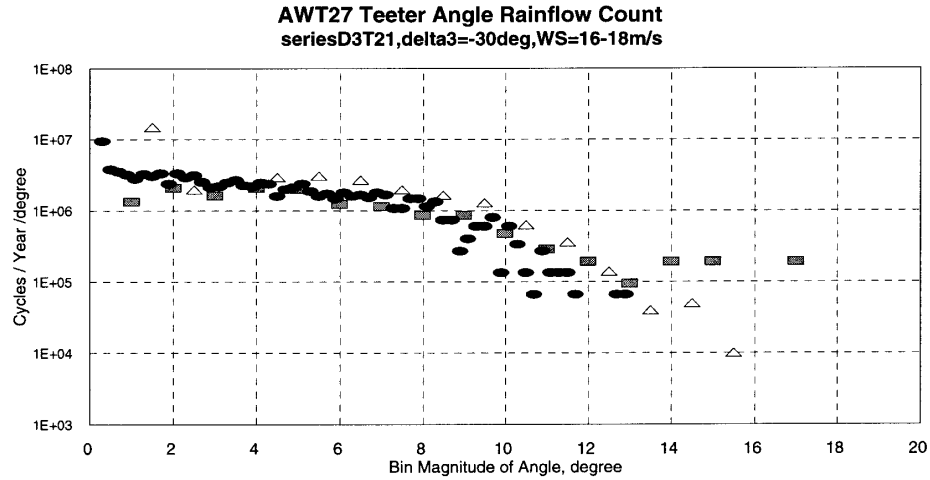

Figure 9.52. Rainflow Count of Teeter Angle (high turbulence).

FAST_AD vs. ADAMS & Field Data at high turbulence

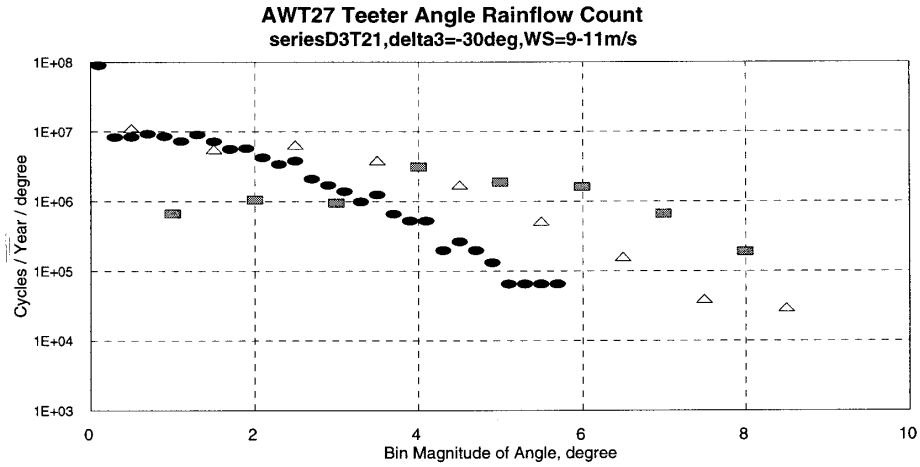

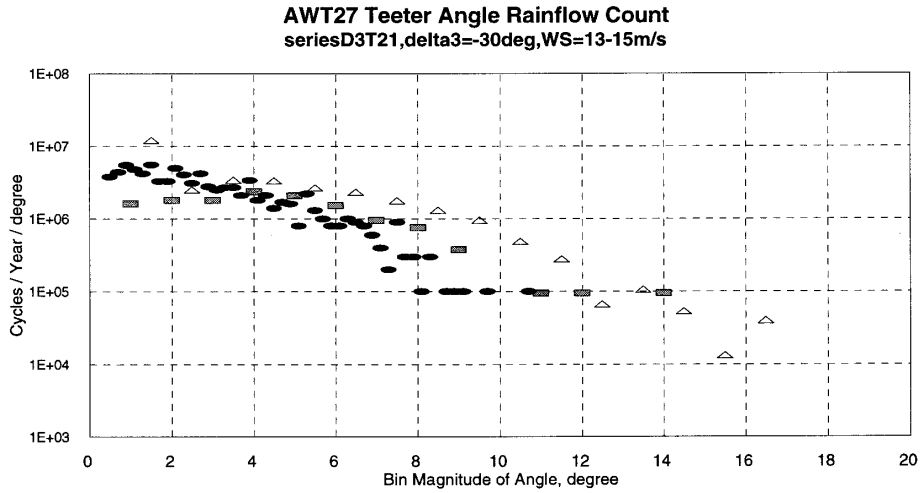

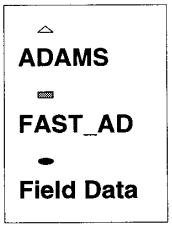

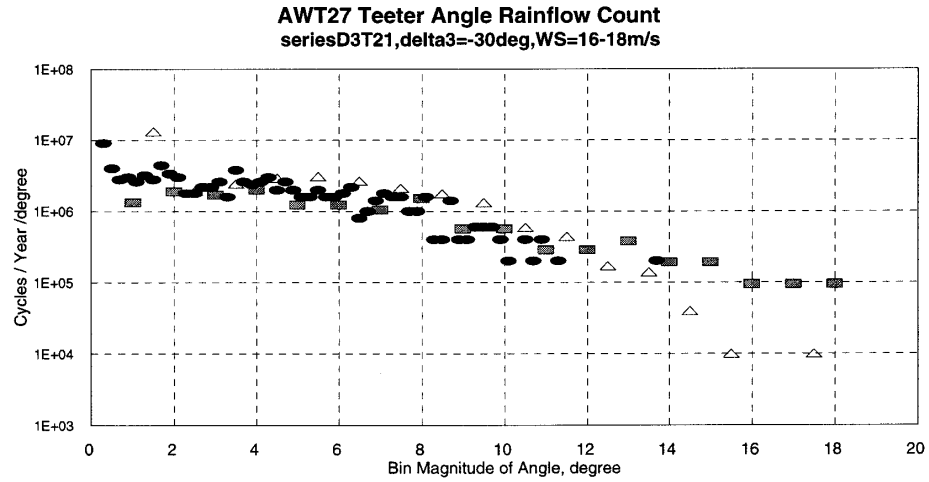

Figure 9.53. Rainflow Count of Yaw Angle (low turbulence).

FAST_AD vs. ADAMS & Field Data at low turbulence

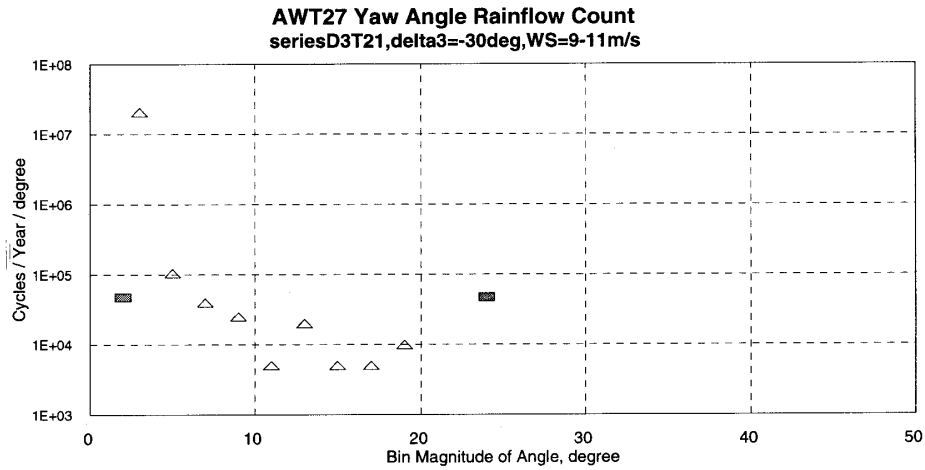

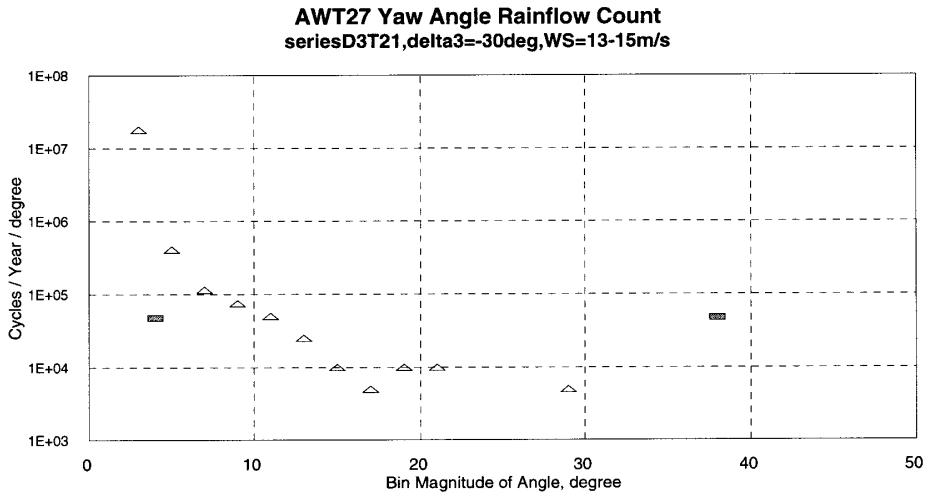

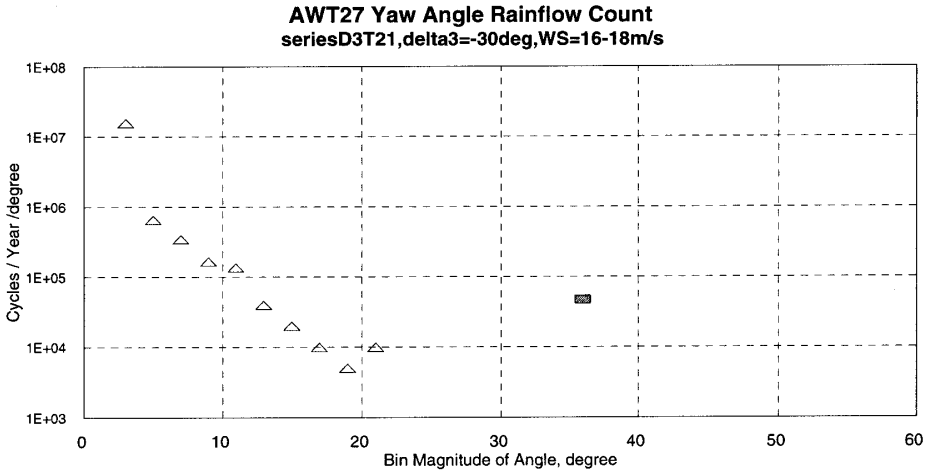

Figure 9.54. Rainflow Count of Yaw Angle (medium turbulence).

FAST_AD vs. ADAMS & Field Data at medium turbulence

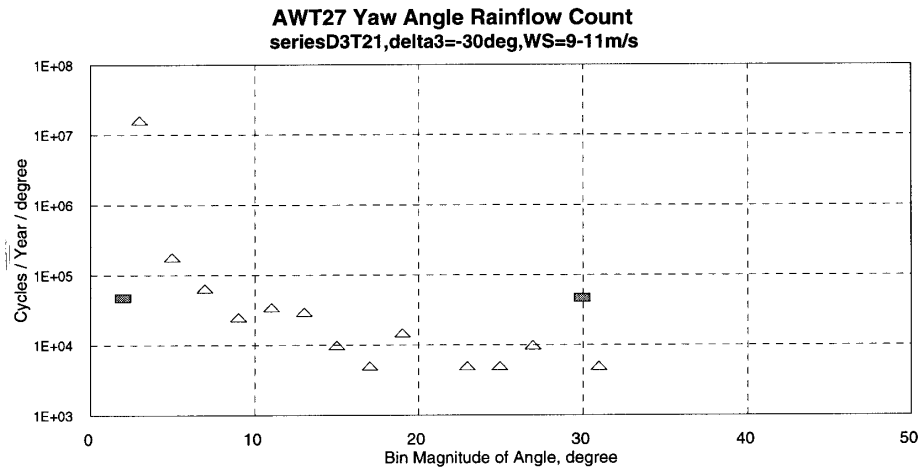

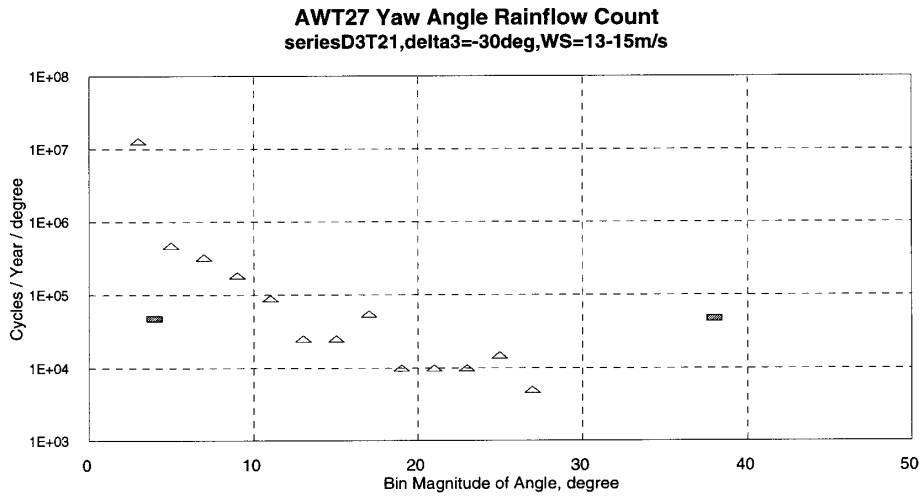

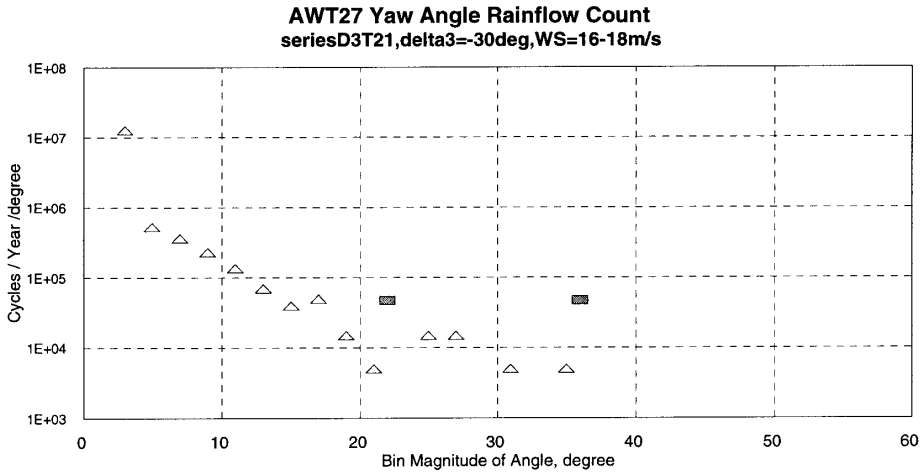

Figure 9.55. Rainflow Count of Yaw Angle (high turbulence).

FAST_AD vs. ADAMS & Field Data at high turbulence

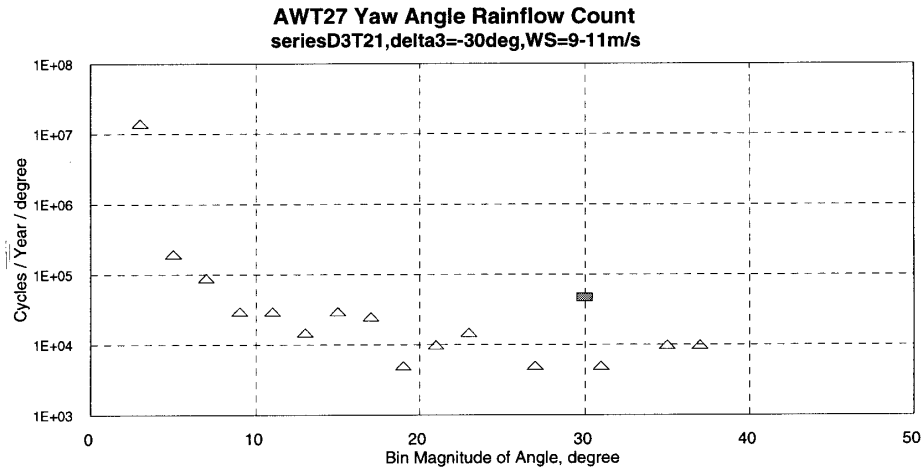

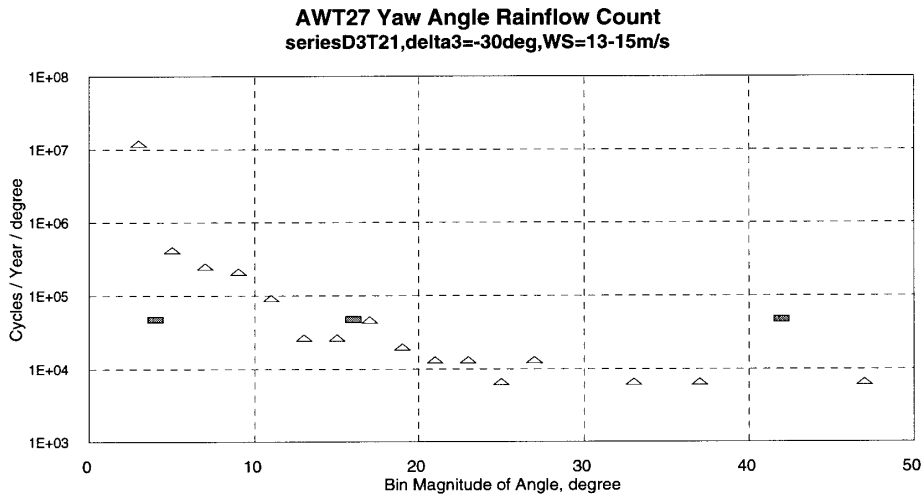

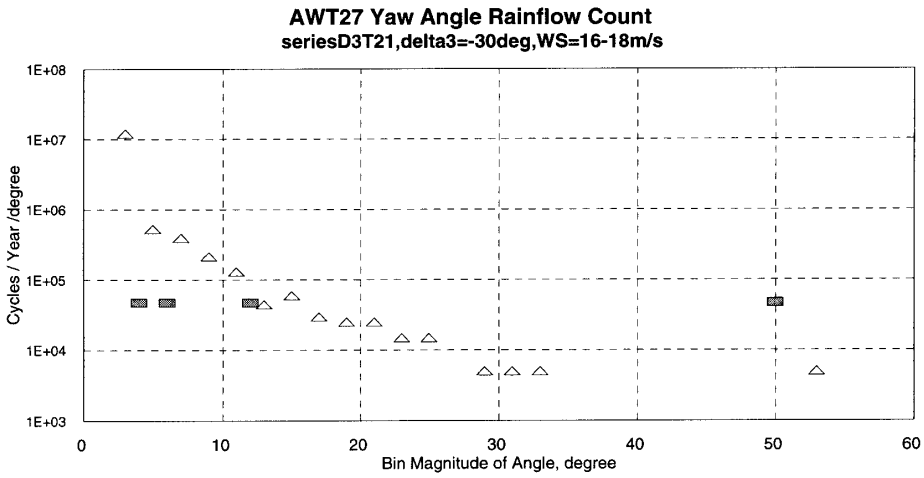

9.6 Discussion

The rainflow cycle counts for root edge bending moment where the delta-three is zero is shown in Figures 9.11 thru 9.13 do not indicate good agreement between test data and the FAST_AD code. The edge bending moment has a large input from the one per revolution gravity moment. The agreement for the root flatwise bending moment is somewhat better although for the case of low turbulence in medium winds (Figure 9.14) and medium turbulence in medium winds (Figure 9.15) agreement is poor.

The rainflow analysis of test data for flatwise bending shows a significant "hump" indicating an input from the gravity moment. The "hump" is about half of the magnitude of the "hump" observed in the edgewise root bending moment. Both FAST_AD and ADAMS failed to predict a "hump" raising the possibility that the calculations failed to account for the location of the axes where the test measurements were made.

The zero degree delta-three wind measurements (series 23) indicated that the mean winds were higher at the 33 meter measurement station than at the 42 meter station. For example, for the high wind case, the mean wind speed measured at 33 meters was 21.5 m/s while the mean hub wind speed was 18.75 m/s. A value of 17.9 m/s was used in the inflow simulations[10]. Positive wind shear was also used. Malcom stated that increasing the tower shadow deficit improved agreement between ADAMS and test data. It is possible that the tower wake deficit was large because of the large free stream wind associated with negative wind shear and not because the shadow was was miss-modeled.

Agreement between FAST_AD and test data for the non-zero delta-three cases was much better than for the zero delta-three case. The wind conditions were more easily simulated for these cases. In particular, attention is called to Figure 9.28, the rainflow cylce count for blade root edgewise bending moment at high wind and high turbulence and Figure 9.31 for the flatwise bending moments.

Finally, the start-up and shut-down of the AWT-27p4 was calculated and shows adequate agreement with test data in Figures 9.56 thru 9.58. Figure 9.56 shows the rotor acceleration history and the low speed shaft torque for the AWT-27p4 during a low wind speed (12.5 m/s) start-up. Both test data and FAST_AD calculations are shown. FAST_AD calculations were made with all degrees of freedom in operation (except the tilt motion, which the AWT-27p4 does not have). Test results show a 5.4 Hertz low speed shaft oscillation while the FAST_AD caculations for the equivalent shaft (virtually the same as

the low speed shaft) show a 5.5 Hertz oscillation. The 5.4 Hertz oscillation is believed to be the natural frequency of the drive train/blade system. No shaft damping was introduced in the FAST_AD calculations. A start-up at higher wind speed is shown in Figure 9.57. The results are qualitatively the same as for the low wind speed case.

The rotor acceleration history calculated using FAST_AD code shows excellent agreement with test data for both the high speed and low speed start-ups. Agreement between test data and FAST_AD calculations for the torque in the low speed shaft is not as good as for the rpm history. As the generator approaches synchronous speed, two spikes are present in the torque. First is a negative spike indicating an increased motoring torque. This increase in the motoring torque is characteristic of an induction motor being operated as a motor. However, in the calculations, the motor torque/speed relation was unknown and our approximation failed to produce a torque spike that was near the magnitude of the negative spike observed. The second spike, associated with rotor overspeed, was also underestimated in the FAST_AD calculations. Since this spike is due to rotor overspeed, the generator must provide too little load on the rotor during this phase. In the calculations, the generator was assumed to provide no load until the rotor reached half of rated slip, an assumption that produced a torque less than half of the observed spike. It was concluded that detailed information concerning the generator electrical equations are necessary to predict the magnitude of the torque spikes.

Whereas in the low speed case illustrated in Figure 9.56, the test data indicates a mean shaft torque of about 43 kN-m, the FAST_AD calculations resulted in shaft torque also near 43 kN-m, which is close to the torque obtained in the long-term power measurements. In a similar manner, the high speed start-up torque history test data shown in Figure 9.57 reaches a mean level near 60 kN-m, which is considerably above the 46 kN-m obtained with FAST_AD (47.4 kN-m from power tests).

Figure 9.56. Rotor RPM and Shaft Torque during Start-up at 12.5 m/s Wind Speed.

(Dark line - FAST_AD simulation, Light line - data)

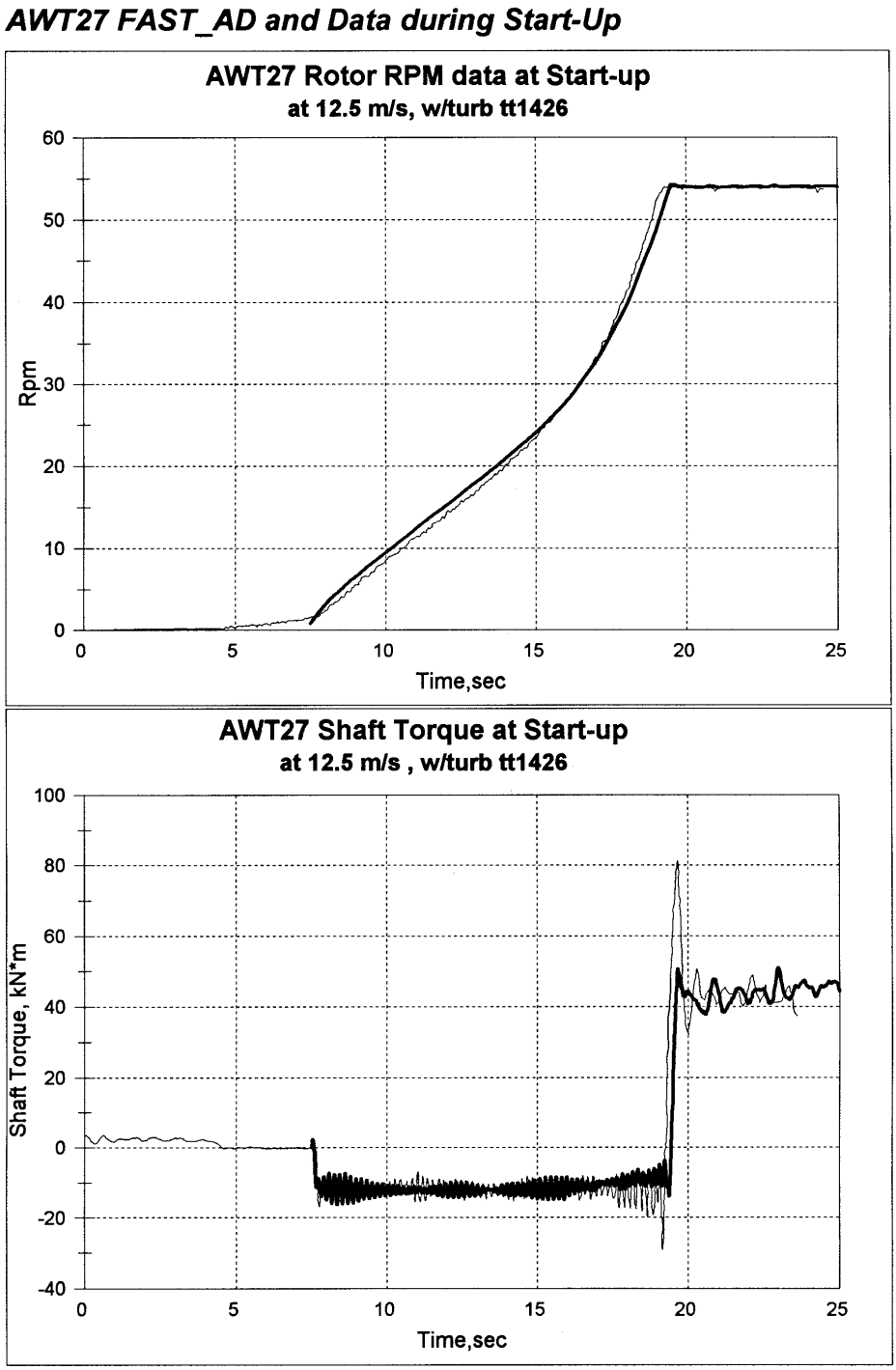

Figure 9.57. Rotor RPM and Shaft Torque during Start-up at 18 m/s Wind Speed. (Dark line - FAST_AD simulation, Light line - data)

AWT27 FAST_AD and Data during Start-Up

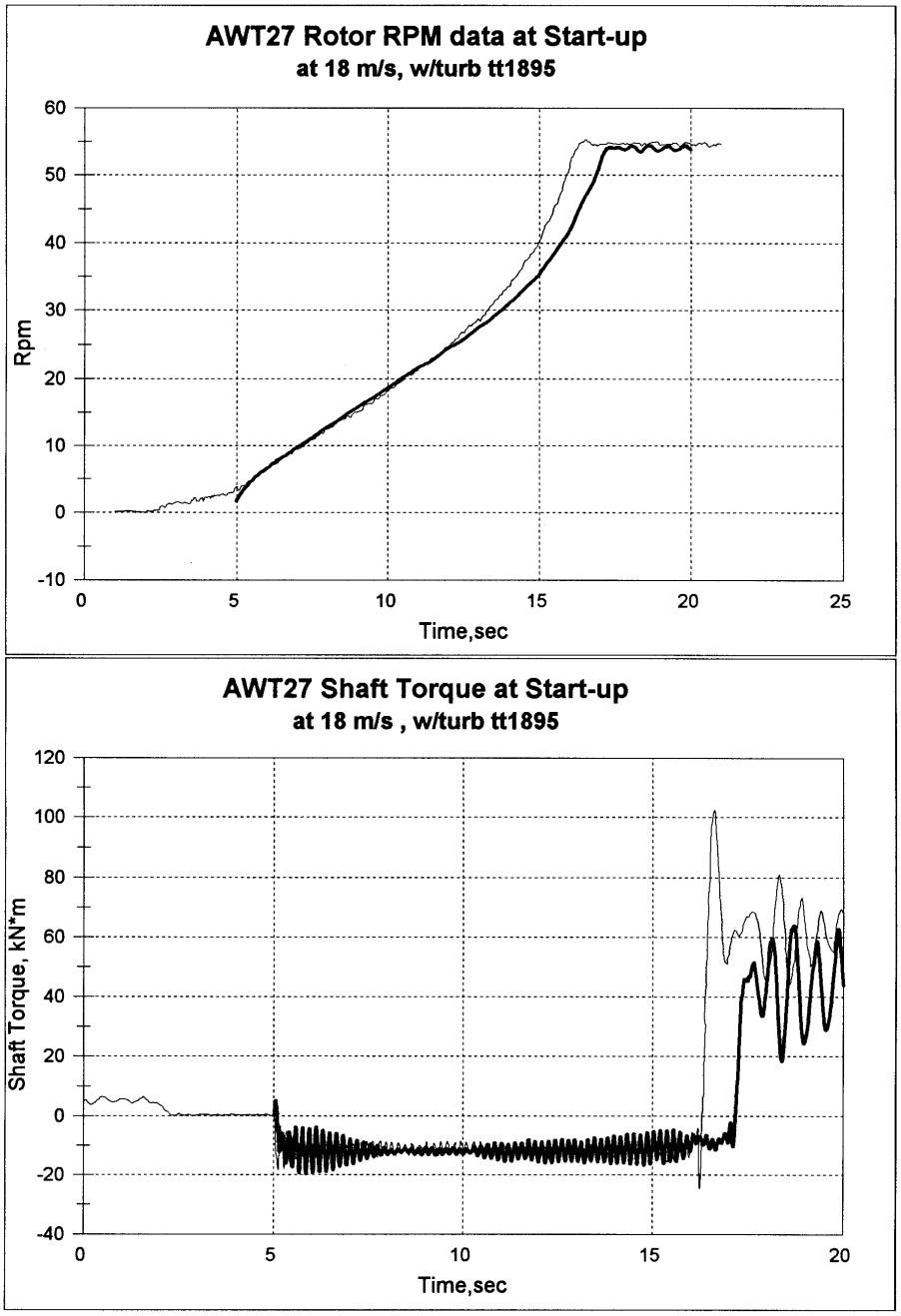

Figures 9.58 shows the time history of rotor angular velocity during a fast stop. During a fast stop, the tip vanes are deployed (we applied the tip vanes over a period of 1 second) and a mechanical brake was applied on the high speed shaft. The brake was applied over a period of 0.4 seconds. Both deployment times were obtained from examination of the test data. In the case of the tip vanes, a spring caused the tip vanes to retract at low rpm; however, our calculations were made with tip vanes deployed during the entire stopping operation. Below 15 rpm, the tip vanes stopping torque was minimal and could be safely ignored.

Figure 9.58. Rotor RPM and Shaft Torque during Fast Stop at 12.5 m/s Wind Speed. (Dark line - FAST_AD simulation, Light line - data)

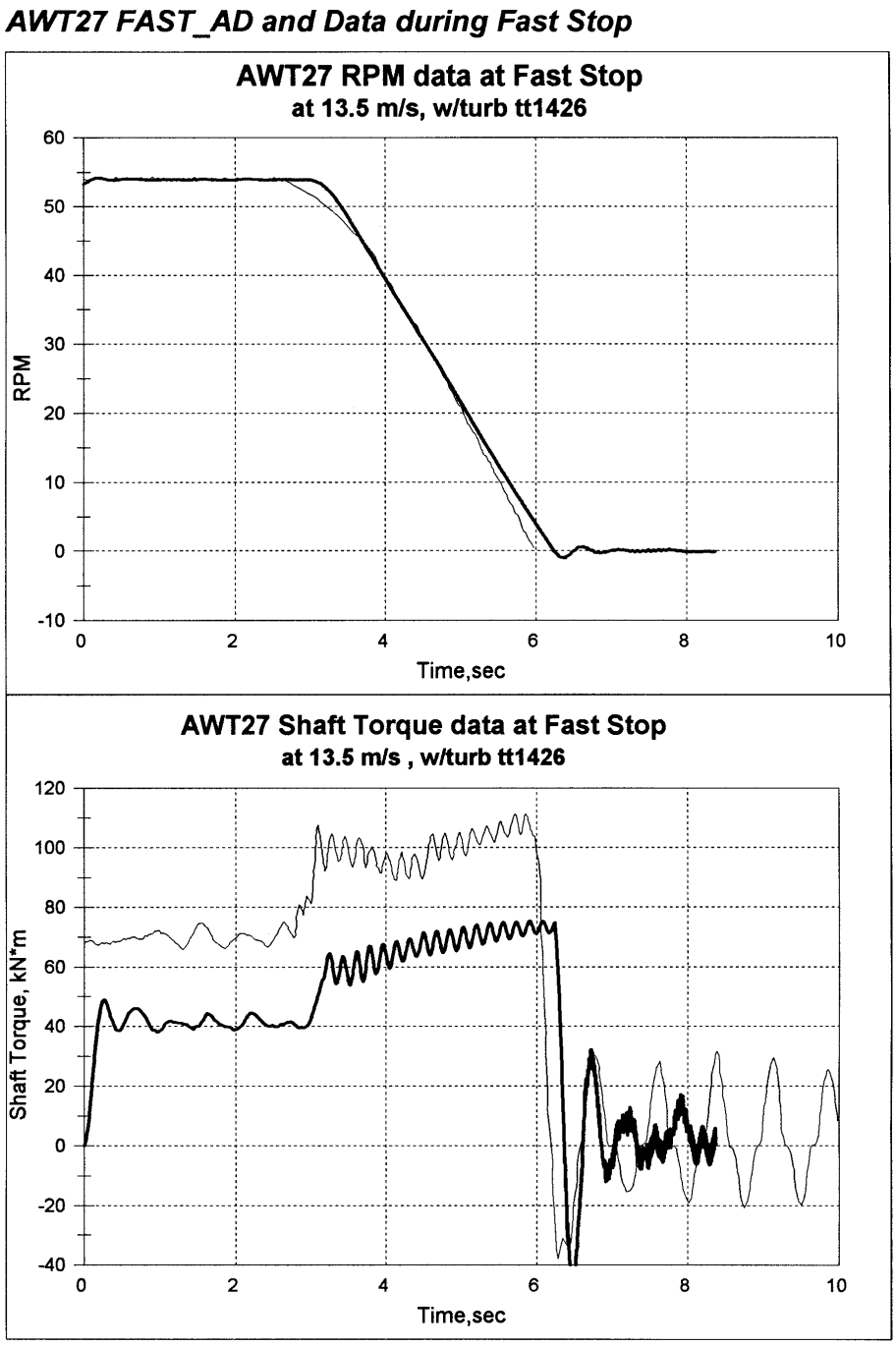

9.7 Acknowledgments

We wish to thank David Malcolm of KAMZIN Technology, Inc., for providing information concerning the AWT-27 characteristics, specification, and description. We also wish to thank Alan Wright of NREL for his leadership and encouragement.

9.8 References

1. Wilson, R.E., Freeman, L.N., and Walker, S.N. "FAST2 Code Validation." *Wind Energy–1995;* January 29-February 1, 1995; Houston, Texas. New York: American Society of Mechanical Engineers; pp. 263-267.

2. Wilson, R.E., Freeman, L.N., Walker, S.N., and Harman, C.R. *FAST Advanced Dynamics Code, Two-Bladed Teetered Hub Version 2.4 User's Manual*. Final Report. Golden, Co: National Renewable Energy Laboratory, March 1996. Work performed by Oregon State University, Corvallis, Oregon.

3. Hansen, A.C. *User's Guide to the Wind Turbine Dynamics Computer Programs YawDyn and AeroDyn for ADAMS®, Version 9.6*. Salt Lake City, UT: University of Utah, June 1996. Prepared for the National Renewable Energy Laboratory under Subcontract No. XAF-4-14076-02.

4. Wright, A.D., Kelley, N.D. and Bir, G.S. *Analysis of a Two-Bladed Flexible Rotor System: Model Development Progress*. AIAA paper no. AIAA-98-0052 presented at the Wind Energy Symposium, AIAA Annual Meeting, Reno, NV, 1998.

5. Malcolm, David. Personal communication.

6. Veers, P.S. *Three-Dimensional Wind Simulation.* SAND 88-0152. Albuquerque, NM: Sandia National Laboratories, 1988.

7. Kelley, N.D. *Full Vector (3-D) Inflow Simulation in Natural and Wind Farm Environments Using an Expanded Version of the SNLWIND (Veers') Turbulence Code*. NREL/TP-442-5225. Golden, Co: National Renewable Energy Laboratory, 1992.

8. Den Hartog, J.D. *Mechanical Vibrations*, fourth edition, McGraw-Hill Book Company, New York, 1956, pp. 29-30.

9. Sheldahl, R.B. and Klimas, P.C. *Aerodynamic Characteristics of Seven Symmetrical Airfoil Sections Through 180-Degree Angle of Attack for Use in Aerodynamic Analysis of Vertical Axis Wind Turbines.* SAND80-2114. Sandia National Laboratories, Albuquerque, NM, March 1981.

10. Malcolm, D.J., *Validation of ADAMS and FAST Codes Final Report.* Prepared for the National Renewable Energy Laboratory by KAMZIN Technology, Seattle, WA under NREL subcontract XCX-8-18213-01, January 1999.

APPENDIX A: CASE STUDY SAMPLE INPUT FILES

This appendix includes the main input file necessary to run the program, as well as the optional input data files required for including the effects of turbulence and variable wind direction. Also included is an example of the automatic input file, awt.inp and airfoil data file.

A.1 Steady Wind

The following is a listing of awt.inp, the input file used to describe the sample horizontal axis wind turbine under steady wind conditions. Detailed descriptions of all inputs are given in Section 6.0.

awt.inp

```
-----------------------------------------------------------------
---- FAST_ADT CODE INPUT DATA FILE -------------------------------------
---- Wind AWT27 W/ COMBINED FAST/AERODYN INPUT          ----
---- Modified 8/07/98, ADW:  added dist blade mass to account for flex.
-------------- FAST/AERODYN GENERAL RUN PARAMETERS ------------------
  0.                    NRSTRT    - NUMBER OF REVOLUTIONS BEFORE TURBULENCE, RECORDING
 10.                    TMAX      - RUN LENGTH (S)
  .005                  DT        - TIME INCREMENT (s)
          0             NTSKIP    - NUMBER OF TIME STEPS TO SKIP FOR OUTPUT (0 = NONE)
-------------- ATMOSPHERIC CONDITIONS --------------------------------
 14.0                   VWIND     - MEAN WIND VELOCITY UPSTREAM AT HUB HEIGHT (m/s)
.143                    ETA       - WIND SHEAR POWER LAW EXPONENT (dim.less)
1.06                    RHO       - AIR DENSITY (kg/m^3)
-------------- DEGREE OF FREEDOM SWITCHES ----------------------------
   1                    IZ(1)     - FIRST FLAPWISE BLADE MODE (YES=1)
   1                    IZ(11)    - SECOND FLAPWISE BLADE MODE (YES=1)
   1                    IZ(13)    - FIRST EDGEWISE BLADE MODE (YES=1)
   1                    IZ(3)     - TEETERED (YES=1)
   1                    IZD(4)    - (0) CONST SPEED (1) IND. GEN. (2) START UP (3) SHUT DOWN
   1                    IZD(15)   - DRIVETRAIN FLEXIBILITY (YES=1)
   0                    IZ(5)     - TILT DEGREE OF FREEDOM (YES=1)
   1                    IZ(6)     - YAW DEGREE OF FREEDOM (YES=1)
   1                    IZ(7)     - FIRST TOWER MODES (YES=1)
   1                    IZ(9)     - SECOND TOWER MODES (YES=1)
   1                    ISHAD     - TOWER SHADOW INCLUDED (YES=1)
   1                    ISHR      - WIND SHEAR INCLUDED (YES=1)
   0                    ITRB2D    - 2D TURBULENCE INPUT (YES=1)
   0                    ITRB3D    - 3D TURBULENCE FIELD (YES=1)...No use at fast_ad
   1                    IDYNST    - DYNAMIC STALL INCLUDED (YES=1)
   0                    IWNDIR    - VARYING WIND DIRECTION FOR 2D TURBULENCE (YES=1)
-------------- INITIAL CONDITIONS ------------------------------------
  0.0                   Z(1)      - BLADE TIP INITIAL FLAPWISE DISPLACEMENT, (meters)
  0.                    Z(13)     - BLADE TIP INITIAL EDGEWISE DISPLACEMENT, (meters)
  0.                    Z(3)      - INITIAL OR FIXED TEETER ANGLE (degrees)
  0.                    Z(4)      - INITIAL AZIMUTH ANGLE FOR BLADE 1 (degrees)
```

```
 53.3                    ZD(4)    - STEADY STATE ANGULAR VELOCITY OF BLADES (RPM)
 0.                      Z(5)     - FIXED OR INITIAL TILT ANGLE (degrees)
 0.                      Z(6)     - FIXED OR INITIAL YAW ANGLE (degrees)
 0.                      Z(7)     - INITIAL LONGITUDINAL TOWER DISPL. (meters)
 0.                      Z(8)     - INITIAL LATERAL TOWER DISPL. (meters)
------------- MACHINE PARAMETERS ------------------------------------
 13.720                  RT          - BLADE TIP RADIUS (meters)
          1.147          RH          - BLADE HUB RADIUS (meters)
          0.             THETA       - BLADE COLLECTIVE PITCH (degrees)
          0.             RRGAP       - LOCATION OF GAP END IN FRACTION OF TIP RADIUS
          0.296          RLU         - UNDERSLING LENGTH (meters)
          0.296          RLUM        - DISTANCE FROM TEETER PIN TO HUB MASS (meters)
  2.433                  DN          - DISTANCE FROM YAW AXIS TO ROTOR / TEETER PIN (meters)
-0.945                   DNM1        - DISTANCE TO NACELLE MASS FROM YAW AXIS c1 (meters)
-0.54                    DNM2        - DISTANCE TO NACELLE MASS FROM YAW AXIS c2 (meters)
          41.99          HH          - HUB HEIGHT ABOVE GROUND LEVEL (meters)
          0.             HS          - TOWER RIGID BASE HEIGHT (meters)
  30.                    DELTA3      - DELTA3 ANGLE (degrees)
  7.                     BETA(1)     - BLADE 1 CONING ANGLE (degrees)
          7.             BETA(2)     - BLADE 2 CONING ANGLE (degrees)
------------- MASS AND INERTIA ------------------------------------
  4908.                  XMNAC       - NACELLE LUMPED MASS (kg)
          750.           XMHUB       - MASS OF HUB (kg)
          12.5           TIPM(1)     - MASS OF TIP BRAKE, BLADE 1 (kg)
          12.5           TIPM(2)     - MASS OF TIP BRAKE, BLADE 2 (kg)
  11880.                 HTINER      - INERTIA OF NACELLE ABOUT TILT AXIS (kg m^2)
  5.                     HSINER      - INERTIA OF GENERATOR (kg m^2)
  13560.                 HYINER      - INERTIA OF NACELLE ABOUT YAW AXIS (kg m^2)
          280.           HINER       - INERTIA OF HUB ABOUT TEETER AXIS (kg m^2)
------------- DRIVETRAIN PARAMETERS -------------------------------
  .99                    ETAGB       - GEARBOX EFFICIENCY (dim.less)
  .94                    ETAGEN      - GENERATOR EFFICIENCY (dim.less)
 54.15                   OMEGR       - RATED SPEED FOR INDUCTION GENERATOR (RPM)
 53.3                    OMEG0       - REFERENCE RPM FOR GENERATOR (RPM)
 478.                    CINGEN      - INDUCTION GENERATOR CONSTANT ((N m)/(r/s))
 33.77                   YN          - GEARBOX RATIO (dim.less)
 46.                     QFL         - FIXED LOSS CONSTANT (N m)
 46.                     QVL         - VARIABLE LOSS CONSTANT (N m)
2400.                    QBRAKE      - MECHANICAL BRAKE TORQUE VALUE (N m)
 400.                    QMOTOR      - MOTOR START-UP TORQUE (GENERATOR SIDE) (N m)
7200000.                             ZKDRV      - DRIVETRAIN TORSIONAL SPRING (N m)/rad
 0.                      CDRV        - DRIVETRAIN TORSIONAL DAMPER (N m)/sec
------------- TOWER PARAMETERS ------------------------------------
  5                      CTWR        - TOWER STRUCTURAL DAMPING IN PERCENT OF CRITICAL (%)
  .140                   EL          - TOWER SHADOW WIDTH / ROTOR RADIUS (dim.less)
  .4                     EPP         - TOWER SHADOW VELOCITY DEFICIT (dim.less)
          1.             TWRMT1      - TOWER MASS TUNER, 1ST MODE (dim.less)
          1.             TWRMT2      - TOWER MASS TUNER, 2ND MODE (dim.less)
          1.             TWRST1      - TOWER STIFFNESS TUNER, 1ST MODE (dim.less)
          1.             TWRST2      - TOWER STIFFNESS TUNER, 2ND MODE (dim.less)
  20                     NXTWR       - NUMBER OF TOWER INCREMENTS (dim.less)
  10                     N2          - NUMBER OF INPUT STATIONS TO SPECIFY TOWER GEOMETRY
  1.20                   AMSTWR      - FACTOR TO ADJUST TOWER MASS (dim.less)
  .65                    STFLNG      - FACTOR TO ADJUST LONGITUDINAL STIFFNESS (dim.less)
  .68                    STFLAT      - FACTOR TO ADJUST LATERAL STIFFNESS (dim.less)
-- RAD ---- MASS -------- LONG STIF ----- LAT STIF -----------------
  %     kg/m        Nm^2        Nm^2
------------- TOWER ------------------------------------------------
          .000,       492.86,          71900000000.,        71900000000.
         .119,        363.45,          51400000000.,        51400000000.
         .238,        343.77,          36400000000.,        36400000000.
         .357,        291.85,          22500000000.,        22500000000.
         .476,        281.77,          12900000000.,        12900000000.
         .595,        266.66,           5900000000.,         5900000000.
```

```
          .715,          253.23,                    2150000000.,              2150000000.
          .834,          251.86,                    1360000000.,              1360000000.
          .953,          248.13,                     745000000.,               745000000.
          1.0,           248.13,                   551000000.,                551000000.
-------------- YAW AND TEETER PARAMETERS ----------------------------
   0.        ZKYAW   - YAW SPRING (N m)/rad
   0.        ZCYAW   - YAW DAMPER (N- m)/rad/sec
   0.       ZKTILT  - TILT SPRING (N m)/rad
   0.        ZCTILT  - TILT DAMPER (N m)/rad/sec
   5.       TILTSTOP1- TILT SOFT STOP ANGLE (degrees)
   6.       TILTSTOP2- TILT HARD STOP ANGLE (degrees)
 1.177E6   QKTSTOP1 - Nacelle soft stop stiffness, N-m/rad
 1.177E8   QKTSTOP2- Nacelle hard stop stiffness, N-m/rad
 0.        COULMB  - COULOMB DAMPING MOMENT, Nm
 3         ITSPDM  - Damper switch:  0 = none, 1 = linear, 3 = user
 0.        CTEET   - TEETER DAMPER (N m)/(rad/s)
  0.       ZKTEET(1)- TEETER SPRING COEFFICIENTS Nm, Nm/rad, Nm/rad^2
  0.       ZKTEET(2)-  teeter moment = ZKT(1) + ZKT(2) * (NET Q3)
  0.      ZKTEET(3)-            + ZKT(3) * (NET Q3)^2
 2.        QCTEET  - ANGLE WHERE TEETER DAMPER BEGINS (degrees)
 19.       QKTEET  - ANGLE WHERE TEETER SPRING BEGINS (degrees)
 8.       TSTOP   - TEETER STOP ANGLE (degrees)
 -------------- BLADE PARAMETERS -------------------------------------
 1.         CBLDF   - BLADE flap STRUCTURAL DAMPING IN PERCENT OF CRITICAL
 1.       CBLDE   - BLADE flap STRUCTURAL DAMPING IN PERCENT OF CRITICAL
 0.007    CDATIPN - DRAG DUE TO TIP BRAKES AT NORMAL OPERATION,CD*AREA
 .9       CDATIPB - DRAG DUE TO TIP BRAKES AT BRAKING, CD*AERA m^2
 1        IAIRFO  - (0) TABLE (1) NASA LS1  (2) NACA 23000 (3) NACAXXXX
 20       NR                - NUMBER OF BLADE INCREMENTS,maxmum=20(dim.less)
14        N1                - NUMBER OF INPUT STATIONS TO SPECIFY BLADE GEOMETRY
 0.45     STFFAC(1) - FACTOR TO ADJUST BLADE 1 STIFFNESS (dim.less)
 0.45     STFFAC(2)    (FLAP)       BLADE 2         (dim.less)
 0.45     STEFAC(1) - FACTOR TO ADJUST BLADE 1 STIFFNESS (dim.less)
 0.45     STEFAC(2)    (EDGE)       BLADE 2         (dim.less)
 1.       AMSFAC(1) - FACTOR TO ADJUST BLADE 1 MASS     (dim.less)
 1.       AMSFAC(2)                BLADE 2         (dim.less)
 1.       CHDFAC(1) - FACTOR TO ADJUST BLADE 1 CHORD    (dim.less)
 1.       CHDFAC(2)                BLADE 2         (dim.less)
 1.       TWIFAC(1) - FACTOR TO ADJUST BLADE 1 TWIST    (dim.less)
 1.       TWIFAC(2)    (AERO)       BLADE 2         (dim.less)
 1.       TWSFAC(1) - FACTOR TO ADJUST BLADE 1 TWIST    (dim.less)
 1.       TWSFAC(2)    (STRUCTURAL)  BLADE 2         (dim.less)
-- RAD ---- CHORD--THICK----AERO - MASS ---- FLAP ----- STRUC---EDGEW. STIFF
  %                    m          t/c                    TWIST      kg/m          STIFF     TWIST          kg/m
-------------- BLADE 1 ----------------------------------------------
 0.0000               0.772      .26                    6.10       90.37         44200000  10.50          117000000

 0.0242               0.843      .26                    5.85       93.89         43600000  10.44          140000000
 0.0606               0.869      .26                    5.69       43.91         21000000  10.40          64000000
 0.0949               0.960      .26                    5.69       46.82         20200000  10.40          79400000
 0.1139               0.987      .26                    5.39       48.22         18000000  10.20          90700000
 0.2182               1.128      .26                    4.93       50.78         11700000  9.46           111000000
 0.3224               1.142      .26                    4.01       44.66         7530000   8.41           96400000
 0.4267               1.070      .26                    2.88       37.38         4870000   6.32           71500000
 0.5309               0.991      .26                    1.76       31.32         3050000   4.09           48700000
 0.6352               0.899      .20                    0.82       25.59         1800000   2.33           28900000
 0.7394               0.785      .20                    0.25       21.41         938000    1.17           19100000
 0.8436               0.655      .20                    0.08       16.62         400000    0.48           10100000
 0.9479               0.486      .20                    0.03       9.68          103000    -0.20          2780000
 1.0000               0.399      .20                    0.00       3.90          103000    -0.22          2780000
-------------- BLADE 2 ----------------------------------------------
 0.0000               0.772      .26                    6.10       90.37         44200000  10.50          117000000

 0.0242               0.843      .26                    5.85       93.89         43600000  10.44          140000000
```

```
0.0606          0.869     .26          5.69     43.91     21000000   10.40     64000000
0.0949          0.960     .26          5.69     46.82     20200000   10.40     79400000
0.1139          0.987     .26          5.39     48.22     18000000   10.20     90700000
0.2182          1.128     .26          4.93     50.78     11700000    9.46    111000000
0.3224          1.142     .26          4.01     44.66      7530000    8.41     96400000
0.4267          1.070     .26          2.88     37.38      4870000    6.32     71500000
0.5309          0.991     .26          1.76     31.32      3050000    4.09     48700000
0.6352          0.899     .20          0.82     25.59      1800000    2.33     28900000
0.7394          0.785     .20          0.25     21.41       938000    1.17     19100000
0.8436          0.655     .20          0.08     16.62       400000    0.48     10100000
0.9479          0.486     .20          0.03      9.68       103000   -0.20      2780000
1.0000          0.399     .20          0.00      3.90       103000   -0.22      2780000
-------------- MODE SHAPES-------------------------------------------
          0.                    PC(1,1) - BLADE MODE 1, COEFF OF X^1
          0.36845     PC(1,2) - BLADE MODE 1, COEFF OF X^2
          0.93899     PC(1,3)          , COEFF OF X^3
         -0.30744     PC(1,4)          , COEFF OF X^4
          0.          PC(1,5)          , COEFF OF X^5
          0.          PC(1,6)          , COEFF OF X^6
          0.          PC(2,1)  - BLADE MODE 2
         -1.30033     PC(2,2)
         -3.32257     PC(2,3)
          5.62290     PC(2,4)
          0.          PC(2,5)
          0.          PC(2,6)
          0.          PC(3,1)  - EDGEWISE MODE 1
          1.43990     PC(3,2)
         -0.70085     PC(3,3)
          0.26095     PC(3,4)
          0.          PC(3,5)
          0.          PC(3,6)
          0.          PC(4,1)  - TOWER MODE 1
   0.4199             PC(4,2)
   0.0541             PC(4,3)
   0.5260             PC(4,4)
          0.          PC(4,5)
          0.          PC(4,6)
          0.          PC(5,1)  - TOWER MODE 2
  -7.8755             PC(5,2)
  -15.8963            PC(5,3)
   24.7696            PC(5,4)
          0.          PC(5,5)
          0.          PC(5,6)
-------------- FORMAT OF OUTPUT FILES ----------
  0       NC(1) = 0
 21        NC(2)
 22        NC(3)
 10        NC(4)
  9       NC(5)
 25        NC(6)
 37        NC(7)
 38        NC(8)
 32        NC(9)
 13        NC(10)
  0       NC(11)
 11        NC(12)
 12        NC(13)
  1       NC(14)
  2       NC(15)
  3       NC(16)
  4       NC(17)
 19        NC(18)
 20        NC(19)
 13        NC(20)
```

```
  0          NC(21)
 29          NC(22)
 30          NC(23)
 35          NC(24)
 36          NC(25)
 39          NC(26)
 26          NC(27)
 31          NC(28)
 33          NC(29)
 13          NC(30)
 10          NCMAX = 30     MAX # COLUMNS TO PRINT
-------------------------------------------------------------
---- BEGIN YAWDYN/AERODYN PARAMETER INPUT -----------------
-------------------------------------------------------------
 TRUE                                  WAKE      - T=Normal iteration for induction factors, F=Ignore wake
 0.005                                 ATOLER    - Tolerance (convergence criteria) for induction factor
 False                                 SWIRL     - Include tangential induced vel?  T-> use a', F-> a'=0
 False                                 DYNINFL   - T=Use dynamic inflow induction lag, F=Quasi-steady
 False                                 WINDFIL   - Read wind data file?: T=YES, F=NO
 ECD_P.WND                             WNDFILNAM - Wind data file name
 False                                 TURBLNT   - Read turbulence files for wind inputs?: T=yes, F=no
 c:\fast_ad\turbs\d3t21\tt1425\        TURBFILE  - Turbulence file name
 1                                     IPRFRST   - First element to write data
 20                                    IPRLAST   - Last element to write data
 5                                     IPRINC    - Write element data increment
 True                                  SIUNIT    - Select units, TRUE= SI, FALSE= English
 0.0                                   VZ        - Vertical component of wind speed (positive up)
 0.0                                   HSHR      - Horizontal wind shear coefficient
 True                                  NOIECEWS  - T=Power Law vertical shear, f= IEC Extreme Wind Shear
 12                                    NUMFOIL   - Number of airfoil tables that will be read
'airfoils\rep7%.dat'
'airfoils\rep10%.dat'
'airfoils\rep15%.dat'
'airfoils\rep25%.dat'
'airfoils\rep35%.dat'
'airfoils\rep45%.dat'
'airfoils\rep55%.dat'
'airfoils\rep65%.dat'
'airfoils\rep75%.dat'
'airfoils\rep85%.dat'
'airfoils\rep95%.dat'
'airfoils\rep100%.dat'                          FOILNM() - Airfoil table file name
1          NFOIL    - Airfoil ID number for each element
2                   (Number of elements = N1)
3                   (Number of elements = N1)
3
4
4
6
6
7
8
9
10
11
12
-------------------------------------------------------------
---- END YAWDYN/AERODYN PARAMETER INPUT -------------------
-------------------------------------------------------------
=============================================================
---- COMMENTS  (The remainder of this file is not used) ----
=============================================================

 POSSIBLE OUTPUT QUANTITIES
```

0) = Time, sec
1) = Blade 1 out-of-plane tip deflection, cm
2) = Blade 1 in-plane tip deflection, cm
3) = Blade 2 out-of-plane tip deflection, cm
4) = Blade 2 in-plane tip deflection, cm
5) = Blade 3 out-of-plane tip deflection, cm
6) = Blade 3 in-plane tip deflection, cm
7) = Hub-height wind speed, m/s
8) = Hub-height wind speed, degrees
9) = Teeter angle, degrees
10) = Yaw angle, degrees
11) = Longitudinal tower top deflection, cm
12) = Lateral tower top deflection, cm
13) = Rotor azimuth angle, deg
14) = Generator azimuth angle, deg
15) = Shaft rotational speed, rpm
16) = Generator rotational speed, rpm
17) = Nac tilt angular accel (d/s^2)
18) = Nac relative tilt angle (deg)
19) = Nac absolute tilt angle (deg)
20) = Nac tilt angular vel (deg/s)
21) = Blade 1 out-of-plane bending moment at root, kNm
22) = Blade 1 in-plane bending moment at root, kNm
23) = Blade 2 out-of-plane bending moment at root, kNm
24) = Blade 2 in-plane bending moment at root, kNm
25) = Shaft torque, kNm
26) = GENERATOR BRAKE
27) = ZMOM
28) = Undefined
29) = Blade 1 out-of-plane bending moment at 60% radius, kNm
30) = Blade 1 in-plane bending moment at 60% radius, kNm
31) = Rotor torque, kNm
32) = Power, KW
33) = Rotor thrust, KN
34) = Tower yaw moment, kNm
35) = Tower longitudinal pitch moment,kNm
36) = Tower lateral pitch moment,kNm
37) = Shaft bending moment, aligned with blade, kNm
38) = Shaft bending moment, 90 deg from blade, kNm
39) = Generator torque, kNm
40) = Undefined

A.2 Turbulent Wind

The input file used to describe the sample horizontal axis wind turbine under turbulent wind conditions uses the same input format as awt.inp except to change the option of TURBLNT in the part of YAWDYN INPUT from “False” to “True”.

```
True      TURBLNT   - Read turbulence files for wind inputs?: T=yes, F=no
```

A.3 3D Turbulence Input Data File

If the 3D turbulence option is used, the program requires three input files, one for each component of the wind. These files are in a binary format to save space. Several steps are taken to create these files. First, Veers Full Field Turbulence code, SNLWIND_3D, is used to generate three components of full field turbulence. The output are three ASCII files - one for each direction: u, v, w. Each file defines the flow at each time step at each of the spatial array points requested (a 6 by 6 grid was used). All three files are ready to be read in by FAST_AD as flows. The first line contains: Hub height wind speed (m/s), time step of 3D turbulence (sec), grid half width (usually the rotor radius, m), and number of grids per side, NGRIDS. This is followed by an array of turbulence data. Because interpolation of this data field is used to get the values of turbulence at the current blade location, the time step of the turbulence data does not need to match the time step of the FAST_AD code run. The files also include wind direction changes, so no wind direction file is necessary.

w_cmp.dat

```
| w-comp |  Y  x  Z  | Grid Resolution | Time-step | Hub Elev | Mean WS |

                6    6      6.000                  0.050      41.99        14.00

Z COORDINATES (M)=

 -15.000  -9.000  -3.000   3.000   9.000  15.000


Y COORDINATES (M)=

 -15.000  -9.000  -3.000   3.000   9.000  15.000


   0.000  -1.979

  -3.473  -1.034  -1.616  -3.268  -2.785  -1.290

   0.302  -1.836  -0.745  -1.194  -0.473  -0.954

  -0.513  -0.521  -2.757  -1.096   0.221  -1.553

  -1.055   0.403  -0.172  -1.000  -1.531  -2.000

   0.050  -0.309   0.095  -0.705  -3.463  -1.978

  -1.394  -0.322  -0.890  -0.275  -1.791   0.238
```

```
 0.050  -0.989
-2.580  -1.777  -1.795  -1.397  -2.509  -1.265
 0.000  -1.169  -1.490  -0.870  -0.300  -0.691
 0.624  -0.463  -1.746  -0.391  -0.726  -1.199
-0.644   0.078  -0.923  -0.667  -1.452  -1.910
-0.103  -0.804   0.266  -0.286  -3.216  -2.194
-1.452  -0.098  -0.547   0.816  -0.489  -0.553

 0.100  -0.986
-2.188  -1.616  -1.390  -0.570  -1.262  -1.327
 0.612  -2.057  -0.396   0.345  -0.567  -1.244
-0.343   0.591  -1.623  -0.829  -1.185  -1.713
-0.049   0.048  -0.398  -0.917  -1.161  -1.916
-0.683   0.710   0.485  -0.852  -2.206  -1.034
-1.384   0.327  -0.144   0.407  -0.001  -1.061

 0.150  -0.620
-0.772  -1.721  -1.200  -1.368  -0.461  -0.092
-0.463  -2.801  -0.498  -0.710  -0.828  -1.090
-0.253   0.213  -1.362  -0.571   0.213  -3.132
 0.367   0.330   0.165  -1.338  -1.636  -1.213
-0.772   0.078   0.610  -1.153  -2.911  -1.120
-1.312  -0.108  -0.235   0.296  -1.081  -1.505

 0.200  -0.992
-1.261  -2.318  -0.840  -0.255  -0.802  -0.827
-0.877  -2.679  -0.811  -0.537  -0.078  -0.899
-0.169   0.233  -0.160  -1.308   0.475  -3.267
 0.196   0.676   0.734  -0.365  -1.865  -0.890
-0.076   0.682   0.725  -0.664  -4.052  -1.115
-2.578  -0.872  -0.903   0.878  -0.144  -1.284
```

A.4 user2.inp Automatic Input File

The following is an example of the automatic input file used to bypass the program's interactive prompts. This file is a time-saving feature useful when making repetitive runs. For a complete explanation of this file, see section three.

```
'awt.inp'        | Name of input file
'awt'            | Prefix of output files
 0               | IAW, choice of output viewing during run
```

The above listing will read a main input file named awt.inp. It will output three files named awt.sum, awt.out, and afosub.opt. The file awt.out will be printed on the computer screen, because IAW = 0. Note that the example automatic input file provided on the CD has been named user2.inp.

A.5 Sample Airfoil Data File

The following is a sample of the airfoil data file format for the 95% blade station. With this file the user can use airfoils not programmed into FAST_AD. Each table in the second section must contain angle of attack (in degrees) and lift and drag coefficients. The fifthteen line begins the sequence which indicates the airfoil data set to use at each station. The first column is the angle of attack. The second column of data is the lift coefficient, and the third column contains the drag coefficient.

```
REP95%.DAT
FROM REP MODEL AERO DATA
1       Number  of  airfoil
0       Table   ID  parameter
12      Stall   angle   (deg)
0       Gormont dynamic stall
0.7     Gormont dynamic stall
0.15    Airfoil thickness ratio
-1.61   Zero    lift    angle
6.308   Cn      slope   for
0.990   Cn      at      stall   of      attack
-0.9    Cn      at      stall   of      attack
0.01    Angle   of      attack
0.0049  Minimum CD      value
-180            -.291   0.9808
-170            0.058   1.0073
-160            0.407   1.0822
-150            0.756   1.1926
-140            0.898   1.3185
-130            0.807   1.4360
-120            0.665   1.5200
-110            0.472   1.5477
-100            0.242   1.5017
-90             0       1.3728
-80             -.242   1.5017
-70             -.472   1.5477
-60             -.665   1.5200
-50             -.807   1.2395
-40             -.898   0.9591
-30             -.856   0.6786
-20             -.708   0.3981
-10             -.559   0.1177
-6              -.500   0.0055
-4              -.273   0.0053
-2              -.047   0.0051
0               0.1802  0.0049
2               0.4000  0.0049
4               0.6198  0.0049
6               0.8396  0.0049
8               1.0000  0.0049
10              1.0800          0.0060
12              1.0800          0.0200
14              1.0600          0.0600
16              1.0100          0.1000
18              0.9600          0.1700
20              0.9100  0.2200
22              0.8400  0.2900
24              0.7800  0.3600
26              0.8670  0.4640
```

28	**0.9790**	**0.5630**
30	**1.0000**	**0.6240**
35	**1.0320**	**0.7770**
40	**1.0370**	**0.9290**
45	**1.0180**	**1.0750**
50	**0.9760**	**1.2140**
55	**0.9140**	**1.3430**
60	**0.8340**	**1.4580**
65	**0.7390**	**1.5590**
70	**0.6300**	**1.6440**
80	**0.3860**	**1.76**
85.6	**0.238**	**1.791**
95.6	**-.03**	**1.787**
105.6	**-.300**	**1.7**
115.6	**-.585**	**1.6**
125.6	**-.751**	**1.5**
135.6	**-.864**	**1.3731**
145.6	**-.902**	**1.2478**
155.6	**-.409**	**1.1278**
165.6	**0.084**	**1.0351**
175.6	**0.578**	**0.9861**
180	**0.291**	**0.9808**

APPENDIX B: OUTPUT FILES

This appendix contains partial listings of output generated from the example cases for the steady wind conditions using awt.inp.

B.1 awt.sum

Below is a complete listing of awt.sum.

```
 Run Parameter File = user2.inp
Input File Name    = awt.inp
Output File Prefix = awt
 ==========================================================================
 Generated by FAST_AD version 2.02, 07/18/97 (Compiled for 2-Blade Analysis)
 ====== Run Title ========================================================

 ---- Wind AWT27 W/ COMBINED FAST/AERODYN INPUT          ----


 Input File Parameters
 ----------------------------------------


Time Step =  .005000 seconds


                Conditions

Mean Wind Velocity = 14.000 m/s
Air Density = 1.060 kg/m^3


                Degrees of Freedom

 Flexible Blades
    Initial Blade Deflection at Tip =    .00 cm
 Teetering Hub
    Initial Teeter Angle =   .00 degrees
 Variable Speed Rotor
 Flexible Shaft
 With Yaw Degree of Freedom
    Initial Yaw Angle =   .00 degrees
 Flexible Tower
    Initial Tower Top Longitudinal Displacement =    .00 cm
    Initial Tower Top Lateral Displacement =    .00 cm
 Tower Shadow Included
    Tower Shadow Width / Rotor Radius =   .140
    Tower Shadow Velocity Deficit =   .400
 Wind Shear Included
    Power Law Exponent =  .143
 Steady Wind, No Turbulence


                Wind Turbine Parameters

Blade Tip Radius = 13.720 m
Hub Radius =  1.147 m
Blade Collection Pitch =       .000 degrees
Location of Gap / Rotor Radius =   .00
```

Undersling Distance = .30 m
Location of Hub CG = .30 m
Distance from Hub to Rotor = 2.43 m
Distance to Nacelle Mass from Yaw Axis = -.94 m
Distance to Nacelle Mass from Yaw Axis = -.54 m
Hub Height Above Ground Level = 41.99 m
Coning Angle Blade 1 = 7.00 degrees, Blade 2 = 7.00 degrees

Blades

Number of Blade Increments = 20
*** ***
Interpolated Parameters for Blade 1

R/RT	CHORD (M)	THICK (t/c)	AERO TW (DEG)	MASS (KG/M)	F-E I (NM^ 2)	STRUCT. TW (DEG)	E-EI (NM^2)
.084	.772	.260	6.10	90.37	.20E+08	.11E+02	.53E+08
.129	.861	.260	5.74	58.46	.12E+08	.10E+02	.39E+08
.175	.967	.260	5.61	47.20	.88E+07	.10E+02	.37E+08
.221	1.036	.260	5.23	49.11	.71E+07	.99E+01	.44E+08
.267	1.103	.260	5.01	50.33	.58E+07	.96E+01	.48E+08
.313	1.132	.260	4.65	48.91	.47E+07	.91E+01	.48E+08
.359	1.139	.260	4.21	45.98	.38E+07	.86E+01	.45E+08
.404	1.123	.260	3.71	42.73	.31E+07	.79E+01	.40E+08
.450	1.088	.260	3.17	39.24	.25E+07	.69E+01	.35E+08
.496	1.052	.260	2.63	36.02	.20E+07	.58E+01	.30E+08
.542	1.014	.260	2.09	33.12	.16E+07	.48E+01	.25E+08
.588	.974	.249	1.59	30.27	.13E+07	.38E+01	.20E+08
.633	.930	.220	1.14	27.52	.10E+07	.29E+01	.16E+08
.679	.883	.200	.74	25.00	.75E+06	.22E+01	.12E+08
.725	.828	.200	.47	22.99	.57E+06	.16E+01	.10E+08
.771	.772	.200	.23	20.92	.40E+06	.11E+01	.82E+07
.817	.709	.200	.15	18.62	.28E+06	.77E+00	.62E+07
.863	.645	.200	.08	16.19	.17E+06	.44E+00	.43E+07
.908	.564	.200	.05	12.87	.11E+06	.11E+00	.28E+07
.954	.482	.200	.03	9.45	.46E+05	-.20E+00	.13E+07
1.000	.399	.200	.00	3.90	.46E+05	-.22E+00	.13E+07

*** ***
Interpolated Parameters for Blade 2

R/RT	CHORD (M)	THICK (t/c)	AERO TW (DEG)	MASS (KG/M)	F-E I (NM^ 2)	STRUCT. TW (DEG)	E-EI (NM^2)
.084	.772	.260	6.10	90.37	.20E+08	.11E+02	.53E+08
.129	.861	.260	5.74	58.46	.12E+08	.10E+02	.39E+08
.175	.967	.260	5.61	47.20	.88E+07	.10E+02	.37E+08
.221	1.036	.260	5.23	49.11	.71E+07	.99E+01	.44E+08
.267	1.103	.260	5.01	50.33	.58E+07	.96E+01	.48E+08
.313	1.132	.260	4.65	48.91	.47E+07	.91E+01	.48E+08
.359	1.139	.260	4.21	45.98	.38E+07	.86E+01	.45E+08
.404	1.123	.260	3.71	42.73	.31E+07	.79E+01	.40E+08
.450	1.088	.260	3.17	39.24	.25E+07	.69E+01	.35E+08
.496	1.052	.260	2.63	36.02	.20E+07	.58E+01	.30E+08
.542	1.014	.260	2.09	33.12	.16E+07	.48E+01	.25E+08
.588	.974	.249	1.59	30.27	.13E+07	.38E+01	.20E+08
.633	.930	.220	1.14	27.52	.10E+07	.29E+01	.16E+08
.679	.883	.200	.74	25.00	.75E+06	.22E+01	.12E+08
.725	.828	.200	.47	22.99	.57E+06	.16E+01	.10E+08
.771	.772	.200	.23	20.92	.40E+06	.11E+01	.82E+07
.817	.709	.200	.15	18.62	.28E+06	.77E+00	.62E+07
.863	.645	.200	.08	16.19	.17E+06	.44E+00	.43E+07
.908	.564	.200	.05	12.87	.11E+06	.11E+00	.28E+07
.954	.482	.200	.03	9.45	.46E+05	-.20E+00	.13E+07
1.000	.399	.200	.00	3.90	.46E+05	-.22E+00	.13E+07

	Blade 1	Blade 2	Tower Top
Weight (kg)	441.289	441.289	1632.577

FIRST BLADE MODE:		
Natural Frequency (Hz)	**1.619**	**1.619**
Freq. w/ Centrifugal Stiff. (Hz)	**2.669**	**2.669**
SECOND BLADE MODE:		
Natural Frequency (Hz)	**5.212**	**5.212**
Freq. w/ Centrifugal Stiff. (Hz)	**7.829**	**7.829**
EDGEWISE BLADE MODE:		
Natural Frequency (Hz)	**4.575**	**4.575**
Freq. w/ Centrifugal Stiff. (Hz)	**4.937**	**4.937**
TOWER		
Tower First Mode Frequency (Hz)	**1.192**	**1.220**
Tower Second Mode Frequency (Hz)	**6.708**	**6.861**

B.2 awt.out

Below is a partial listing of awt.out.

```
Predictions produced by FAST_AD version 2.02, on 05/24/1999 at 22:25:19
---- Wind AWT27 W/ COMBINED FAST/AERODYN INPUT           ----
   Time      M1ouRt     M1inRt      Yaw       Teeter     TODshaf    Shaft0    Shaft90     GenPwr     RtrAzm
  (sec)      (kNm)      (kNm)      (deg)      (deg)       (kNm)     (kNm)      (kNm)       (kW)      (deg)
     .005 -4.774E+00  4.781E+00 -1.144E-04  3.906E-04  9.612E-02 -3.312E-01  1.755E-01  1.645E+01  1.600E+00
     .010  7.283E-01  4.844E+00 -4.693E-04  1.817E-03  4.167E-01 -3.724E-01  1.978E-01  3.678E+01  3.201E+00
     .015 -4.947E+00  5.577E+00 -1.088E-03  4.393E-03  8.966E-01 -5.945E-01  1.417E-01  4.282E+01  4.804E+00
     .020 -5.025E+00  6.535E+00 -2.037E-03  7.767E-03  1.342E+00 -6.264E-01  4.413E-01  4.574E+01  6.407E+00
     .025 -2.991E+00  7.983E+00 -3.217E-03  1.252E-02  2.023E+00 -1.278E+00  4.731E-03  5.401E+01  8.011E+00
     .030 -2.732E+00  9.563E+00 -4.660E-03  1.830E-02  2.641E+00 -1.516E+00  1.504E-01  6.156E+01  9.615E+00
     .035 -2.565E+00  1.119E+01 -6.343E-03  2.508E-02  3.371E+00 -1.858E+00  2.319E-01  6.877E+01  1.122E+01
     .040 -2.259E+00  1.284E+01 -8.229E-03  3.277E-02  4.166E+00 -2.339E+00  2.043E-01  7.673E+01  1.283E+01
     .045 -1.880E+00  1.479E+01 -1.028E-02  4.120E-02  5.010E+00 -2.754E+00  2.959E-01  8.556E+01  1.443E+01
     .050 -1.360E+00  1.670E+01 -1.245E-02  5.014E-02  5.920E+00 -3.172E+00  4.064E-01  9.588E+01  1.604E+01
     .055 -6.751E-01  1.863E+01 -1.467E-02  5.955E-02  6.915E+00 -3.599E+00  5.241E-01  1.083E+02  1.765E+01
     .060  4.946E-02  2.052E+01 -1.687E-02  6.935E-02  8.008E+00 -3.991E+00  6.722E-01  1.225E+02  1.926E+01
     .065  8.509E-01  2.229E+01 -1.897E-02  7.946E-02  9.213E+00 -4.351E+00  8.351E-01  1.378E+02  2.087E+01
     .070  1.715E+00  2.392E+01 -2.089E-02  8.988E-02  1.053E+01 -4.675E+00  1.002E+00  1.535E+02  2.248E+01
     .075  2.613E+00  2.534E+01 -2.254E-02  1.006E-01  1.195E+01 -4.943E+00  1.174E+00  1.686E+02  2.410E+01
     .080  3.540E+00  2.653E+01 -2.386E-02  1.115E-01  1.346E+01 -5.157E+00  1.335E+00  1.823E+02  2.571E+01
     .085  4.495E+00  2.747E+01 -2.476E-02  1.227E-01  1.503E+01 -5.307E+00  1.481E+00  1.940E+02  2.733E+01
     .090  5.468E+00  2.813E+01 -2.520E-02  1.340E-01  1.662E+01 -5.395E+00  1.602E+00  2.035E+02  2.895E+01
     .095  6.460E+00  2.850E+01 -2.511E-02  1.453E-01  1.822E+01 -5.412E+00  1.695E+00  2.109E+02  3.056E+01
     .100  7.475E+00  2.860E+01 -2.447E-02  1.566E-01  1.980E+01 -5.360E+00  1.753E+00  2.166E+02  3.218E+01
     .105  8.501E+00  2.842E+01 -2.326E-02  1.676E-01  2.133E+01 -5.246E+00  1.770E+00  2.215E+02  3.380E+01
     .110  9.546E+00  2.799E+01 -2.148E-02  1.782E-01  2.282E+01 -5.063E+00  1.747E+00  2.263E+02  3.542E+01
     .115  1.059E+01  2.731E+01 -1.915E-02  1.884E-01  2.428E+01 -4.828E+00  1.677E+00  2.317E+02  3.704E+01
     .120  1.164E+01  2.642E+01 -1.629E-02  1.980E-01  2.570E+01 -4.546E+00  1.563E+00  2.382E+02  3.866E+01
     .125  1.268E+01  2.534E+01 -1.295E-02  2.069E-01  2.711E+01 -4.223E+00  1.408E+00  2.457E+02  4.028E+01
     .130  1.372E+01  2.412E+01 -9.197E-03  2.151E-01  2.852E+01 -3.873E+00  1.214E+00  2.541E+02  4.191E+01
     .135  1.476E+01  2.278E+01 -5.100E-03  2.224E-01  2.994E+01 -3.509E+00  9.854E-01  2.629E+02  4.353E+01
     .140  1.579E+01  2.137E+01 -7.424E-04  2.290E-01  3.137E+01 -3.136E+00  7.309E-01  2.713E+02  4.515E+01
     .145  1.681E+01  1.995E+01  3.788E-03  2.349E-01  3.280E+01 -2.778E+00  4.553E-01  2.788E+02  4.678E+01
     .150  1.778E+01  1.854E+01  8.396E-03  2.400E-01  3.421E+01 -2.437E+00  1.688E-01  2.847E+02  4.840E+01
     .155  1.869E+01  1.721E+01  1.299E-02  2.445E-01  3.560E+01 -2.135E+00 -1.202E-01  2.886E+02  5.003E+01
     .160  1.948E+01  1.598E+01  1.747E-02  2.484E-01  3.692E+01 -1.886E+00 -4.026E-01  2.903E+02  5.165E+01
     .165  2.002E+01  1.488E+01  2.174E-02  2.516E-01  3.817E+01 -1.712E+00 -6.704E-01  2.900E+02  5.328E+01
     .170  2.041E+01  1.389E+01  2.570E-02  2.539E-01  3.932E+01 -1.587E+00 -9.132E-01  2.874E+02  5.491E+01
     .175  2.104E+01  1.304E+01  2.928E-02  2.550E-01  4.035E+01 -1.446E+00 -1.117E+00  2.830E+02  5.653E+01
     .180  2.203E+01  1.245E+01  3.239E-02  2.550E-01  4.125E+01 -1.300E+00 -1.270E+00  2.776E+02  5.816E+01
     .185  2.295E+01  1.211E+01  3.499E-02  2.543E-01  4.202E+01 -1.221E+00 -1.378E+00  2.728E+02  5.978E+01
```

B.3 gfosub.opt

Below is a complete listing of gfosub.opt

```
 Finished reading airfoil data file number          1

 Finished reading airfoil data file number          2

 Finished reading airfoil data file number          3

 Finished reading airfoil data file number          4

 Finished reading airfoil data file number          5

 Finished reading airfoil data file number          6

 Finished reading airfoil data file number          7

 Finished reading airfoil data file number          8

 Finished reading airfoil data file number          9

 Finished reading airfoil data file number         10

 Finished reading airfoil data file number         11

 Finished reading airfoil data file number         12

---- Wind AWT27 W/ COMBINED FAST/AERODYN INPUT           ----

  SI UNITS USED FOR INPUT AND OUTPUT
  MEAN WIND SPEED AT HUB             =      14.000000

  PITCHING MOMENTS WERE NOT CALCULATED

  AIR DENSITY                   =        1.060000
  ACCELERATION DUE TO GRAVITY   =        9.810000

  TOWER SHADOW CENTERLINE VELOCITY DEFICIT  =    4.000000E-01
  TOWER SHADOW HALF-WIDTH AT REFERENCE POS. =    9.604000E-01


  ROTOR RADIUS  =      13.720000
  HUB HEIGHT    =      41.990000
  YAW AXIS-TO-HUB DISTANCE   =       2.433000
  NUMBER OF BLADES           =       2.000000
  PRE-CONING ANGLE (DEG)     =       7.000000
  ROTOR TILT ANGLE (DEG)     =   0.000000E+00


  WINDS NOT READ FROM DATA FILE

  TURBULENT WINDS READ FROM FILES WITH
    THE FOLLOWING PREFIX:
    c:\fast_ad\turbs\d3t21\tt1425\

   Read in  6x 6 grid of 14.0 mps (or fps) turbulence data
  11999 records processed with a time step of     .050 sec. per record
```

```
 599.95 sec. total time duration in this turbulence file

  WAKE (INDUCTION FACTOR) WAS CALCULATED IN THIS SIMULATION
  CONVERGENCE TOLERANCE FOR INDUCTION FACTOR =   5.000000E-03

  ANGULAR INDUCTION FACTOR NOT CALCULATED IN THIS SIMULATION

  DYNAMIC INFLOW WAS NOT CONSIDERED IN INDUCTION FACTOR CALCULATION

  TIME INTERVAL FOR AERODYNAMIC CALCULATIONS =    5.000000E-03

  DYNAMIC STALL MODEL WAS USED IN CALCULATIONS

  BEDDOES DYNAMIC STALL PARAMETERS:

 CN SLOPE       6.3080   6.3080   6.3080   6.3080   6.3080   6.3080   6.3080   6.3080   6.3080   6.3080   6.3080
 6.3080
 STALL CN (UPPER) 1.0050   1.0050   1.2700   1.6100   1.9000   1.6500   1.2500   1.1300   1.0500   1.0000    .9900
  .9900
 STALL CN (LOWER) -.9000   -.9000   -.9000   -.9000   -.9000   -.9000   -.9000   -.9000   -.9000   -.9000   -.9000
 -.9000
 ZERO LIFT AOA   -4.0000  -4.0000  -4.0000  -5.0000  -5.0000  -6.0000  -6.0000  -3.5000  -1.5500  -1.6100  -1.6100
-1.6100
 MIN DRAG AOA     .0100    .0100    .0100    .0100    .0100    .0100    .0100    .0100    .0100    .0100    .0100
  .0100
 MIN DRAG COEFF   .0300    .0300    .0100    .0095    .0092    .0094    .0060    .0060    .0059    .0049    .0049
  .0049

    VORTEX TRANSIT TIME FROM LE TO TE       11.000000
    PRESSURE TIME CONSTANT                   1.700000
    VORTEX TIME CONSTANT                     6.000000
    F-PARAMETER TIME CONSTANT                3.000000


 AIRFOIL TABLES USED IN THE ANALYSIS
 ID   FILENAME
  1   airfoils\rep7%.dat
  2   airfoils\rep10%.dat
  3   airfoils\rep15%.dat
  4   airfoils\rep25%.dat
  5   airfoils\rep35%.dat
  6   airfoils\rep45%.dat
  7   airfoils\rep55%.dat
  8   airfoils\rep65%.dat
  9   airfoils\rep75%.dat
 10   airfoils\rep85%.dat
 11   airfoils\rep95%.dat
 12   airfoils\rep100%.dat


  FILE aelement.plt CONTAINS BLADE ELEMENT DATA
     First element printed:           1
     Last element printed:           20
     Printing increment:              5

Blade Element Marker  Rlocal    Pitch    Chord     DR    Airfoil
   2   21         0   13.618     .000     .399     .629     12
   2   20         0   12.994     .029     .482     .629     11
   2   19         0   12.370     .053     .564     .629     11
```

2	18	0	11.746	.077	.645	.629	10
2	17	0	11.122	.151	.709	.629	10
2	16	0	10.498	.233	.772	.629	9
2	15	0	9.874	.466	.828	.629	9
2	14	0	9.250	.739	.883	.629	8
2	13	0	8.626	1.137	.930	.629	8
2	12	0	8.002	1.588	.974	.629	7
2	11	0	7.378	2.092	1.014	.629	7
2	10	0	6.754	2.630	1.052	.629	6
2	9	0	6.130	3.169	1.088	.629	6
2	8	0	5.506	3.711	1.123	.629	6
2	7	0	4.882	4.208	1.139	.629	6
2	6	0	4.258	4.649	1.132	.629	5
2	5	0	3.634	5.010	1.103	.629	4
2	4	0	3.010	5.231	1.036	.629	4
2	3	0	2.386	5.609	.967	.629	3
2	2	0	1.762	5.737	.861	.629	3
2	1	0	1.138	6.100	.772	.629	1
1	21	0	13.618	.000	.399	.629	12
1	20	0	12.994	.029	.482	.629	11
1	19	0	12.370	.053	.564	.629	11
1	18	0	11.746	.077	.645	.629	10
1	17	0	11.122	.151	.709	.629	10
1	16	0	10.498	.233	.772	.629	9
1	15	0	9.874	.466	.828	.629	9
1	14	0	9.250	.739	.883	.629	8
1	13	0	8.626	1.137	.930	.629	8
1	12	0	8.002	1.588	.974	.629	7
1	11	0	7.378	2.092	1.014	.629	7
1	10	0	6.754	2.630	1.052	.629	6
1	9	0	6.130	3.169	1.088	.629	6
1	8	0	5.506	3.711	1.123	.629	6
1	7	0	4.882	4.208	1.139	.629	6
1	6	0	4.258	4.649	1.132	.629	5
1	5	0	3.634	5.010	1.103	.629	4
1	4	0	3.010	5.231	1.036	.629	4
1	3	0	2.386	5.609	.967	.629	3
1	2	0	1.762	5.737	.861	.629	3
1	1	0	1.138	6.100	.772	.629	1

APPENDIX C: MODE SHAPES

This appendix contains instructions for determining the mode shapes for blades and tower. These shape equations are read in as coefficients of a polynomial of the form:

$$\phi(\eta) = C_1\eta + C_2\eta^2 + C_3\eta^3 + C_4\eta^4 + C_5\eta^5 + C_6\eta^6$$

where ϕ is the shape function, η is the dimensionless distance along the flexible beam, and C_1 through C_6 are coefficients specified in the input file. Note that at the fixed end, $\eta = 0$ and $\phi = 0$; and at the free end, $\eta = 1$ and $\phi = 1$. These mode shapes are not arbitrary, but depend on the distribution of mass and stiffness of the flexible body and on its motion.

A separate program, MODES, included with FAST_AD, allows computation of these mode shape coefficients. The program requires one input file, summarized in Table C.1. Note that the form is similar to the input file for the FAST_AD code.

Table C.1. Input File modes.inp

```
   3          N       - NUMBER OF MODES OR COEFFICIENTS (MUST MATCH NN)
  2           p       - ORDER OF FIRST COEFFICIENT
 53.3         ZD(4)   - STEADY STATE ANGULAR VELOCITY OF ROTOR (RPM)
  1           IBODY   - SWITCH:  1 = BLADE, 2 = TOWER
  1           IFLAP   - SWITCH:  1 = FLAPWISE, 2 = EDGEWISE(Default=1)
 13.72 RT     - BLADE TIP RADIUS OR TOWER HEIGHT (M)
 1.147 RH     - BLADE HUB RADIUS OR TOWER RIGID BASE (M)
 12.5         TIPM    - BLADE TIP MASS OR MASS ATOP TOWER (KG)
 14           N1      - NUMBER OF INPUT STATIONS FOR DISTRIBUTED PARAMETERS
 0.45         STFFAC  - FACTOR TO ADJUST STIFFNESS
 1.           AMSFAC  - FACTOR TO ADJUST MASS
0.0000 0.772  .26      6.10  90.37  44200000.0          117000000
0.0242 0.843  .26      5.85  93.89  43600000.0          140000000
0.0606 0.869  .26      5.69  43.91  21000000.0           64000000
0.0949 0.960  .26      5.69  46.82  20200000.0           79400000
0.1139 0.987  .26      5.39   48.22 18000000.0           90700000
0.2182 1.128  .26      4.93  50.78  11700000.0          111000000
0.3224 1.142  .26      4.01  44.66   7530000.0           96400000
0.4267 1.070  .26      2.88  37.38   4870000.0           71500000
0.5309 0.991  .26      1.76  31.32   3050000.0           48700000
0.6352 0.899  .20      0.82  25.59   1800000.0           28900000
0.7394 0.785  .20      0.25  21.41    938000.0           19100000
0.8436 0.655  .20      0.08  16.62    400000.0           10100000
0.9479 0.486  .20      0.03   9.68    103000.0            2780000
1.0000 0.399  .20      0.00   3.90    103000.0            2780000
```

The first two parameters indicate what type of polynomial will be produced. The first parameter, N, indicates how many mode shapes to compute and, more importantly, how many coefficients will be used. The second parameter, P, indicates the order of the first coefficient. For example, the combination of N = 2 and P = 4 produces a coefficient for the polynomial $\phi(\eta) = C_4\eta^4 + C_5\eta^5$. The remaining coefficients are forced to be zero. Note that N must match the parameter NN in the code, and to change it from a hardwired value of NN = 3 the code must be recompiled.

The mode shapes for the blades are affected by the centrifugal stiffening as the rotor turns, so the code also reads in ZD(4), the rotational speed of the rotor in RPM. The switch IBODY indicates whether a blade (1) or the tower (2) is to be considered. The switch IFLAP indicates if either flapwise (1) or edgewise motion (0) is considered. The next two parameters give the length of the flexible part of the body. For a blade, RT is the tip radius and RH is the hub radius. For the tower, RT will be the hub height (HH in FAST_AD) and RH will be the base height (HS in FAST_AD). The parameter TIPM should be the mass of the blade's tip brake or the total mass on top of the tower, including nacelle and rotor. The parameter N1 indicates how many lines of data for the distributed parameters should be read in. The stiffness and mass can be adjusted using the factors STFFAC and AMSFAC. The final portion of the table is a list of the characteristics distributed along the flexible body. The first column is the normalized location, the second column is lineal density, and the final column is stiffness. The same values as those read in the FAST_AD code are used.

The code produces one output file which lists the frequencies and mode shapes computed for the data given, shown in Table C.2. These frequencies are estimates and may not agree exactly with the frequencies estimated or demonstrated by the FAST_AD code.

The code uses a method which assumes the shape functions are made up of the individual terms of the polynomial specified. For example, if P = 4 and N = 2, the shape functions are a combination of the functions $\varphi_1 = \eta^4$ and $\varphi_2 = \eta^5$. These are used to form the following matrices:

$$M_{ij} = \int_o^R \mu\, \varphi_i\, \varphi_j\, dr + M_{TIP}$$

$$K_{ij} = \int_o^R EI \frac{d^2 \varphi_i}{d\bar{r}^2} \frac{d^2 \varphi_j}{d\bar{r}^2}\, dr$$

$$C_{ij} = \int_o^R \left\{ M_{TIP}\, R + \int_r^R \mu\, (s + RH)\, ds \right\} \frac{d\varphi_i}{d\bar{r}} \frac{d\varphi_j}{d\bar{r}}\, d\bar{r} \qquad i,j = 1 \ldots N$$

Table C.2. Output File MODES

3	**Number of Modes**
2	**Order of First Coefficient**
53.300000	**Rotor RPM**
13.720000	**Blade Radius**
12.500000	**Tip Mass**
4.500000E-01	**Stiffness Multiplier**
1.000000	**Mass Multiplier**

Mode Number:

	1	**2**	**3**
Frequencies			
	4.94113	**18.53466**	**46.39703**
Mode Shapes			
1	**.00000**	**.00000**	**.00000**
2	**.88684**	**-.59381**	**.27567**
3	**-.43298**	**.80054**	**-.79676**
4	**.16136**	**-.08084**	**.53775**
5	**.00000**	**.00000**	**.00000**
6	**.00000**	**.00000**	**.00000**

where μ is the lineal density, EI is the stiffness, M_{TIP} is the mass at the free end, and r is the position along the flexible body from the fixed end at 0 to the free end at R which is the length between RH and RT (RT-RH). For the blades which have centrifugal stiffening, these matrices are combined to give the matrix

$$[K + \Omega_o^2 (C + M \sin\theta)]^{-1} [M]$$

$$q = p / 2 \quad \text{for edgewise}$$
$$q = 0 \quad \text{for flapwise}$$

which has eigenvalues (frequencies) and eigenvectors (mode shapes). The final coefficients are normalized so that $\varphi|_{TIP} = 1$.

For the tower, the M and K matrices are similar and C becomes

$$C_{ij} = \int_{o}^{H} \left\{ M_{TOP} + (R - \bar{x})\mu \right\} \frac{d\varphi_i}{d\bar{x}} \frac{d\varphi_j}{d\bar{x}} dx$$

where M_{TOP} is the mass atop the tower.

These matrices are used to form:

$$[K - gC]^{-1} [M]$$

which has eigenvalues (frequencies) and eigenvectors (mode shapes).